

## **Improving Construction Progress Monitoring Using BIM and 3D Reconstruction Technologies**

**Noaman Akbar Sheik**

Doctoral dissertation submitted to obtain the academic degree of  
Doctor of Engineering Technology

### **Supervisors**

Prof. Greet Deruyter, PhD\* - Honorary Prof. Peter Veelaert, PhD\*\*

- \* Department of Civil Engineering  
Faculty of Engineering and Architecture, Ghent University
- \*\* Department of Telecommunications and Information Processing  
Faculty of Engineering and Architecture, Ghent University

May 2024



ISBN 978-94-6355-832-7

NUR 950, 956

Wettelijk depot: D/2024/10.500/37

## **Members of the Examination Board**

### **Chair**

Prof. Hennie De Schepper, PhD, Ghent University

### **Other members entitled to vote**

Prof. Alain De Wulf, PhD, Ghent University

Abdur Rehman Nasir, PhD, University of Hertfordshire, United Kingdom

Timothy Nuttens, PhD, Agentschap Wegen en Verkeer

David Van Hamme, PhD, Ghent University

Ruben Verstraeten, PhD, Ghent University

### **Supervisors**

Prof. Greet Deruyter, PhD, Ghent University

Honorary Prof. Peter Veelaert, PhD, Ghent University



# Word of Gratitude

This journey toward a PhD would not have been possible without the help of many people. First and foremost, I would like to express my deepest gratitude to my supervisors, without whose unwavering support this would not have been possible. Prof. dr. Greet Deruyter, oh what an outstanding soul! an amazing mentor, a stellar academician, the finest teacher, and a true role model. Her exceptional support and encouragement throughout my research journey have been invaluable which I can't just describe in words. Whenever I found myself in need of help, whether it was related to my research or anything else, she was always there, ensuring I received the utmost guidance and support. In the realm of academia, where the pressures can be overwhelming, the esteemed professor emerged as a beacon of kindness, illuminating my path throughout the entirety of my degree. I am truly fortunate to have had such an amazing supervisor by my side, and I will always remember and appreciate the genuine assistance she graciously provided to me. I am also profoundly grateful to Prof. dr. Peter Veelaert for his excellent mentorship and insightful feedback, which played a key role in my ability to grasp the intricacies of a new research field. As a civil engineer, navigating the computer science aspects of my research was a significant challenge. However, under Professor Veelaert's expert guidance, I was able to overcome these obstacles with ease, as he always provided me with the utmost clarity and direction.

Special thanks to my colleagues at workplace AMRP, who made me feel at home throughout my time with them. I would like to express my heartfelt appreciation to Peter, Annelies, and Karim, who were not only my colleagues but also amazing friends. Peter's superb friendliness and welcoming nature played a pivotal role in promoting a sense of belonging at gatherings and greatly facilitated my social integration in Belgium. Working alongside Peter was a real pleasure, and we even worked together on holidays. His amicable and cool personality is truly remarkable. Annelies, an energetic person with incredible organizational skills, has helped me on several occasions and offered me wise counsel. I will miss the humorous discussion of our research's advancement during the lunch break. I wish her the best of luck in completing her PhD. The same goes for Karim, a true gentleman and wonderful company, who impressed me with his skills and unique way of looking at life. I cherish the time we spent at his home on Thursday evenings playing various card games, having interesting talks and enjoying the delicious cakes he baked. Furthermore, I would also like to acknowledge the efforts of our technical support person, Jurgen, who has always made it a top priority to assist me whenever I have faced a work-related challenge, ensuring my comfort and productivity. In addition, I will miss the engaging conversations and cultural exchanges with Joachim and Tom. I would also

like to thank Tim, Hwachyi, Isabelle, Aamir, Mustafa and Tristan for the enriching meetings, both formal and informal, which have contributed so much to my learning. Without a doubt, I'll carry the memories of my time at AMRP with me into my future endeavors.

I must thank my family members for their heartfelt prayers, never-ending support, and continuous encouragement. I am truly blessed to have my diligent father, Sheikh Muhammad Akbar, along with my ever-supportive mother and caring siblings, who have been a constant source of strength in my life. I want to give a heartfelt shout-out to my lovely wife, my true better half, who has made huge sacrifices throughout my PhD. Due to the demands of my studies, I was only able to visit my home country once after our wedding, when our son Ali was born, and then I had to return quickly. Until now, we have not had the opportunity to meet in person. This has been extremely stressful and challenging for both of us, but I am deeply grateful for her sincere support during this difficult time. I am desperately waiting to be reunited with them.

How can I forget the Pakistani community in Belgium, who have erased any notion that I live in a foreign country. I am immensely grateful to my close friends especially, Hassan, Ali, Jawad, Mustafa, Dilawar, Fakhar, Zeeshan, Asad, Rana, Imad and Hafiz. Their unwavering support in various forms, including financial assistance, consolation, and respect, has been extremely helpful in reducing the stress of my PhD. Next, I would like to mention Mashood, Adeel, Fayyaz, Khalid, Aamir, Imran, and Asif for arranging the amazing trip and memories. Additionally, I would also like to highlight the efforts of Ijlal and Arslan bhai for their outstanding support and guidance during my stay in Gent. These two remarkable people have been like angels, greatly simplifying the expatriate life of Pakistani students like me by providing accurate direction and assistance with accommodations, administrative matters, university-related issues, and organizing various cultural events.

It is important to mention the institutions that are involved in this PhD. I would like to express my gratitude to the Higher Education Commission (HEC), Pakistan for providing financial assistance for the major part of my PhD which played an important role in enabling me to conduct the research and support myself in Belgium. I also want to convey my appreciation to Ghent University for giving me the opportunity, learning environment, and resources that greatly facilitated my PhD research. Personally, I truly appreciate the efforts of the university and its staff.

Last but not least, I would like to thank everyone who has helped me on this journey.

-Noaman Akbar Sheik

# Preface

It seems like only yesterday that I was graduating with a bachelor's degree in civil engineering and starting my career on a construction site, ready to make a name for myself in the industry. I love technology, so when I stepped onto that busy construction site, I could not help but notice how far behind the construction industry was in adopting the latest technologies. As a Planning Engineer, I was faced with the difficult task of manually capturing progress data, which required a great deal of labor, time and was rife with errors. Due to the subjective nature of understanding the progress, disputes between stakeholders frequently arose, which complicated project implementation, especially the progress-based payments. I found myself yearning for a better way, a standardized and automated approach that could transform the traditional monitoring approach and help the industry as a whole. This yearning grew stronger the longer I stayed in the construction field.

Ideas swirled in my mind with the imagination where progress monitoring can be automated and the latest technologies could be used. I remember watching the videos in my spare time where the 3D technologies being utilized for self-driving cars and then speculating on how it could possibly be applied at complex construction sites to detect building objects. During my Master's studies, I came across BIM technology and realized its transformative potential in the construction industry, which utterly captivated and fascinated me. My curiosity was piqued, and I became determined to further explore the potential of the technologies, especially in construction progress monitoring. My path to pursuing a Ph.D. in this area of study was paved by a persistent thought and an unquenchable yearning for improvement that slowly took possession of my being.

This dissertation is a very personal journey that was inspired by my undying faith in the transformative potential of technology. It is not just the result of academic study. It is motivated by a sincere desire to effect change in a construction sector that has been stuck to traditional procedures for far too long. I want to spark a seismic change that will improve the automation, accuracy, efficiency, and collaboration of construction project monitoring.

I hope that my work will inspire fellow researchers, practitioners, and industry leaders to join forces in this noble endeavor, pushing the boundaries and shaping a future where automated construction project monitoring is the norm. Join me in envisioning a future where automated monitoring is seamlessly integrated into construction projects, empowering stakeholders and driving industry transformation. Let the exploration begin.

-Noaman Akbar Sheik  
7<sup>th</sup> July 2023





# Summary

*"If you can't measure it, you can't improve it"*

-Peter Drucker

Although the construction sector is a significant part of the global economy, it evolves slowly. Progress monitoring in the construction process is an example of this slow evolution. Inaccurate progress monitoring, particularly in large projects, can lead to severe financial consequences. Efficient tracking of the construction process allows for early error detection, avoids issues in resource and personnel planning, helps meet predefined deadlines, and consequently, is cost-effective. However, over half of construction projects lag behind schedule, and budget overruns are common. Traditional monitoring practices are time-consuming and labor-intensive, leading to errors, missing information, and low monitoring frequency. An automated and precise method for monitoring construction progress would be a significant advancement, but it is still in its early stages.

Recent developments in 3D data acquisition techniques enable the creation of accurate 3D as-built models of construction sites. Many studies utilize these models for automated progress monitoring through a process known as model-based assessment. This process involves the geometric analysis of as-built models with their corresponding as-planned situations and typically consists of three phases: (1) registration, (2) comparison, and (3) estimation/exchange of progress information. Each of these phases faces a variety of difficulties that make it challenging to be applied practically in the construction industry.

The aim of this study is to facilitate progress monitoring on construction sites using modern technologies, addressing challenges in all three phases.

The first phase of model-based assessment requires the automation of the registration process which involves the alignment of the as-built model with the planned model. The challenges in this phase mainly revolve around the automated extraction and identification of geometric features in both the as-built and as-planned models. This process is currently predominantly manual and relies on the operator's expertise. In this research, the abundant and dominant planar structures in most buildings are leveraged in the registration phase. Two algorithms were developed for this purpose.

The first registration technique directly employs the plane segments extracted from both models. After extraction, plane segments from both models are clustered based on their orientation. Rotational matrices for these clusters are evaluated using a matching cost algorithm to determine the extent of correspondence between elements in the as-built model and the BIM model. Finally, the precise translation vector is determined based on the best-matching planar segments. The accuracy and

robustness of this registration technique were validated using multiple datasets with varying degrees of complexity. One key finding is the reduced impact of noise and outliers in the as-built point clouds on this technique. Moreover, the method is successful in registering as-built scans of partially completed constructions with their BIM models, making it suitable for progress monitoring.

The second registration technique utilizes the corner points, as a point of interest, extracted from previously determined planar segments from building structures. The number of points is first limited through RANSAC-based pairwise assessment of distinctive geometric invariants: distance, angle, rotation, and translation, to find potential congruent points. The transformation of these potential corresponding points is then evaluated to identify the actual pairs. Finally, the transformation parameters resulting in the largest overlap between both models are selected as the most optimal transformation parameters. The accuracy and robustness of this technique were validated using the same datasets as the first technique and yielded comparable results for both completed and under-construction buildings. Both techniques are accurate with low sensitivity to point cloud noise. Although the second technique is slightly more accurate, the first is more suitable for under-construction buildings.

The primary outcome of the research in the first phase is the development of new automated techniques enabling accurate and automatic registration of as-built scans of under-construction buildings with their corresponding BIM models using their geometry

The second phase of model-based assessment involves a geometrical comparison of the as-built model with the as-planned BIM model to determine the as-built completion of the building. The traditional comparison methods yield inaccurate results due to the presence of occlusions in point clouds, lack of a suitable comparable as-planned model, and imprecise detection of the built during the comparison process.

This study explores the comparison process and introduces several improvements to enhance accuracy in three steps. First, semantic time-related information from the IFC-based BIM model is used to sort construction components for processing, determine if a comparison is necessary, and confirm the completion of prior components before proceeding with the comparison. Next, a detection analysis is performed using a ray-tracing technique that utilizes geometrical information from BIM and the location of the laser scanner from the as-built scan. Initially, a revised as-planned model is developed, adapted for a suitable comparison by classifying surfaces based on identified occlusions. The final stage conducts the structural comparison, where an as-built surface is more accurately detected by reducing the errors resulting from occlusions. This is achieved by utilizing the classified revised as-planned model, which estimates not only the surfaces exposed to the scanner but also predicts the non-exposed surfaces, along with surface coverage as an additional parameter.

This improved comparison was evaluated with various datasets to assess performance and potential practical applications in construction progress monitoring. The completion ratio of each construction component based on their accurately detected as-built surface is measured. Additionally, the surface coverage by the scanner of each building component and the corresponding range of the overall predicted completion ratio are identified. Utilizing the amount of surface area of each construction component that would be exposed to the scanner if fully realized allows for a better estimate of the actual progress of the construction process. Collectively, these improvements enable a comprehensive understanding of the achieved building completion and result in a significant improvement in accuracy and reliability compared to existing automated model-based comparison methods.

The third phase of the research focuses on estimating and exchanging progress parameters for effective construction progress monitoring. The emphasis is on leveraging the full potential of the BIM model for the automated, accurate, interoperable, and standardized exchange of progress information among all stakeholders in the construction process, without the use of any third-party external commercial software.

A framework is proposed with a task-oriented approach, using the latest IFC schema to accommodate various types of progress information from the construction site. The goal is to convert this information into progress parameters in the form of relevant IFC entities. The progress information being processed is not limited to time-related schedules only to report the completion of building construction but also includes the cost and any other non-standard progress-related information such as construction comments, inspection notes, additional progress indicators, etc. This framework consists of four phases: (1) the integration of IFC entities based on progress information in BIM model; (2) enrichment of planned values; (3) frequent updating of actual values after their accurate estimation; and (4) reporting all information, including additional progress parameters, in a user-friendly manner.

The method was assessed using multiple BIM models, successfully completing the automated exchange of planned and as-built progress information. The information was translated into IFC entities in a standardized manner, conforming to the IFC hierarchy, and making it accessible via any IFC-based application. Additionally, a web-based application was also developed, that takes advantage of the progress information stored in the IFC-based BIM model to retrieve it for effective reporting and visualization in a user-oriented way. The development of a standardized framework for the automated exchange of progress information using a BIM model is a milestone in model-based construction progress monitoring.

This thesis presents significant improvements in various phases of model-based automated monitoring of construction progress for buildings with an existing BIM model, combined with as-built point clouds obtained through laser scanning. It provides automated registration methods and enhances the traditional comparison process of as-built and as-planned information, including an accurate estimation of

completed construction components. Additionally, a framework was developed for standardized and automatic exchange of progress information. The research results have the potential to significantly reduce project delays and cost overruns for large construction projects.

Although this dissertation offers substantial improvements for construction progress monitoring using 3D laser technology and BIM, there is still a long way to go. The current research is an attempt to support the practical application of modern technology in the construction environment. Future research efforts will focus on further facilitating the monitoring process by addressing the remaining challenges in model-based assessment. Further technological developments in 3D data acquisition, AI, etc., will create new synergies for more efficient construction processes.

# Samenvatting

Hoewel de bouwsector een belangrijk onderdeel is van de wereldeconomie, is dit een sector die slechts traag evolueert. Monitoring van de voortgang van het bouwproces is daar een voorbeeld van. Onzorgvuldige voortgangsmonitoring kan vooral bij grote projecten problematisch zijn en leiden tot zware financiële gevolgen. Efficiënte opvolging van het bouwproces maakt vroegtijdig opsporen fouten mogelijk, vermijdt problemen in de planning van mensen en middelen, helpt om de vooropgestelde termijnen te halen en is bijgevolg kostenbesparend. Nochtans loopt meer dan de helft van de bouwprojecten achter op schema en zijn budgetoverschrijdingen schering en inslag. Een van de voornaamste oorzaken is dat traditionele monitoringpraktijken tijds- en arbeidsintensief zijn, wat aanleiding geeft tot fouten, ontbrekende informatie en een te lage monitoringfrequentie. Een geautomatiseerde en nauwkeurige methode voor het monitoren van de bouwvoortgang zou een grote vooruitgang zijn, maar bevindt zich nog in een beginfase.

Recente ontwikkelingen in 3D data acquisitietechnieken maken het mogelijk om nauwkeurige 3D *as-built* modellen van bouwplaatsen te verkrijgen. Een groot aantal studies maakt gebruik van deze modellen voor geautomatiseerde monitoring van de bouwvoortgang via een proces dat bekend staat als modelgebaseerde beoordeling. Dit proces omvat de geometrische analyse van *as-built* modellen met hun overeenkomstige *as-planned* situatie om voortgangsinformatie te identificeren en bestaat doorgaans uit drie fasen: (1) registratie, (2) vergelijking en (3) schatting/uitwisseling van voortgangsinformatie. Elke fase ondervindt echter nog moeilijkheden, waardoor de praktische toepassing in de bouwsector uitdagend is.

Het doel van deze studie is het vergemakkelijken van voortgangsmonitoring op bouwplaatsen door gebruik te maken van moderne technologieën, waarbij de uitdagingen in de drie fasen worden aangepakt.

De eerste fase in de modelgebaseerde beoordeling houdt de automatisering van het registratieproces in. Hieronder wordt verstaan de uitlijning van het *as-built* model met het geplande model. Uitdagingen die verband houden met deze fase omvatten voornamelijk de geautomatiseerde extractie en identificatie van de geometrische kenmerken van het gebouw in zowel het *as-built* als het *as-planned* model. Dit is vooralsnog een proces dat hoofdzakelijk handmatig gebeurt en waarvan het succes afhankelijk is van de expertise van de operator.

In dit onderzoek wordt de dominante aanwezigheid van een groot aantal vlakke structuren in de meeste gebouwen benut in de registratiefase. Hiertoe werden twee algoritmen ontwikkeld.

De eerste registratietechniek maakt direct gebruik van vlaksegmenten, die geëxtraheerd worden uit beide modellen. Na de extractie worden de vlaksegmenten van beide modellen geclusterd op basis van hun richting. Voor die clusters worden alle mogelijke rotatiematrices bepaald en vervolgens samen met de translatievectoren geëvalueerd op basis van een *matching cost* algoritme om te bepalen in welke mate de elementen uit het *as-built* model overeenkomen met die uit het BIM model. Tenslotte wordt de precieze translatievector bepaald op basis van de best overeenkomende vlaksegmenten.

De nauwkeurigheid en robuustheid van deze registratietechniek werd gevalideerd op basis van meerdere datasets bestaande uit gebouwen met een wisselende graad van complexiteit. Een van de belangrijkste bevindingen is dat het effect van ruis en uitschieters in de *as-built* puntenwolken op deze techniek minimaal is. Bovendien is de methode ook succesvol bij de registratie van *as-built* scans van gedeeltelijk voltooide bouwwerken met hun BIM-model, waardoor ze bruikbaar is voor voortgangsmonitoring.

De tweede registratietechniek maakt gebruik van de hoekpunten die geëxtraheerd worden uit de eerder bepaalde vlaksegmenten. Het aantal punten wordt eerst beperkt via een RANSAC gebaseerde paarsgewijze beoordeling van een aantal onderscheidende geometrische invarianten: afstand, hoek, rotatie en translatie om zo potentiële congruente punten te vinden. Vervolgens wordt de transformatie van die potentiële overeenkomstige punten geëvalueerd om de werkelijke paren te identificeren. Tenslotte worden de transformatieparameters die in de grootste overlapping tussen beide modellen resulteren, geselecteerd als de meest optimale transformatieparameters.

De nauwkeurigheid en robuustheid van deze techniek werden gevalideerd op basis van dezelfde datasets als bij de eerste techniek en gaf vergelijkbare resultaten voor zowel volledige als in aanbouw zijnde gebouwen. Beiden technieken zijn zeer nauwkeurig met een lage gevoeligheid voor ruis in de puntenwolken. Hoewel de tweede iets nauwkeuriger is, is de eerste meer geschikt voor in aanbouw zijnde gebouwen.

Het belangrijkste resultaat van het onderzoek gericht op de eerste fase is de ontwikkeling van nieuwe geautomatiseerde technieken die een nauwkeurige en automatische registratie mogelijk maken van *as-built* scans van in aanbouw zijnde gebouwen met hun overeenkomstige BIM-model door gebruik te maken van hun geometrie.

De tweede fase van de modelgebaseerde beoordeling omvat de geometrische vergelijking van het *as-built* model met het *as-planned* BIM-model om de voortgang van het bouwproces te bepalen. Traditionele vergelijkingsmethoden kunnen onnauwkeurige resultaten opleveren vanwege onder andere oclusies in de puntenwolken, het ontbreken van een geschikt *as-planned* model en onnauwkeurige detectie van de gebouwde delen tijdens het vergelijkingsproces.

Het voorliggend onderzoek verkent het vergelijkingsproces en introduceert een aantal verbeteringen om de nauwkeurigheid te vergroten in drie stappen. Eerst wordt gebruik gemaakt van de semantische tijd gerelateerde informatie van het op IFC gebaseerd BIM-model om de bouwcomponenten te sorteren voor verwerking, vast te stellen of de vergelijking nodig is, en de voltooiing van voorafgaande componenten te bevestigen voordat verder wordt gegaan met de vergelijking. Vervolgens wordt een detectieanalyse uitgevoerd met behulp van een *ray-tracing* techniek die de geometrische informatie van BIM en de locatie van laserscanner van de as-built scan gebruikt. Eerst wordt een herzien *as-gepland* model ontwikkeld dat aangepast is voor een geschikte vergelijking door classificatie van de oppervlakken op basis van de geïdentificeerde oclusies. De laatste fase voert de structurele vergelijking uit waarbij een *as-built* oppervlak nauwkeuriger wordt gedetecteerd omdat het effect van fouten voorkomend uit oclusies wordt geëlimineerd door gebruik te maken van het geclassificeerd herzien *as-gepland* model dat niet alleen de aan de scanner blootgestelde as-built oppervlakken schat, maar ook de niet-blootgestelde oppervlakken voorspelt, samen met de oppervlaktedekking als extra parameter.

Deze verbeterde vergelijking werd geëvalueerd met verschillende datasets om de prestaties en het potentieel voor praktische toepassingen in bouwvoortgangsmonitoring te beoordelen. De voltooiingsratio van elk bouwonderdeel op basis van het nauwkeurig gedetecteerde as-built oppervlak wordt gemeten. Daarnaast wordt de oppervlaktedekking door de scanner van elke bouwcomponent en het overeenkomstige bereik van de algehele voorspelde voltooiingsratio geïdentificeerd. Het benutten van de hoeveelheid oppervlakte van elk bouwonderdeel dat zou blootgesteld zijn aan de scanner als het volledig zou gerealiseerd zijn, laat een beter schatting van de daadwerkelijke voortgang van het bouwproces toe. Dit resulteert in een aanzienlijke verbetering van de nauwkeurigheid en betrouwbaarheid ten opzichte van bestaande geautomatiseerde modelgebaseerde vergelijkingsmethodes.

Uiteindelijk richt de derde fase van het onderzoek zich op de schatting en uitwisseling van voortgangsparameters voor de effectieve monitoring van de bouwvoortgang. Hierbij wordt ingezet op het benutten van het volledig potentieel van het BIM-model voor geautomatiseerde, nauwkeurige, interoperabele, en gestandaardiseerde uitwisseling van voortgangsinformatie tussen alle actoren binnen het bouwproces, zonder het gebruik van externe commerciële software.

Er wordt een kader voorgesteld met een taakgerichte aanpak, waarbij het nieuwste IFC-schema wordt gebruikt om diverse soorten voortgangsinformatie van de bouwplaats te accommoderen. Het doel is om deze informatie om te zetten in voortgangsparameters in de vorm van relevante IFC-entiteiten. De verwerkte voortgangsinformatie beperkt echter zich niet tot tijdschema's voor het rapporteren van de voltooiing van de bouwconstructie. Het omvat ook kosten en andere niet-standaard voortgangsinformatie, zoals bouwopmerkingen, inspectienota's, extra voortgangsindicatoren, etc. Dit kader bestaat uit vier fasen: (1) de integratie van

*native* en *non-native* IFC-entiteiten op basis van de voortgangsinformatie in het BIM-model; (2) verrijking van de geplande waarden; (3) het frequent updaten van de werkelijke waarden na hun nauwkeurige schatting; en (4) het rapporteren van alle informatie, inclusief de aanvullende voortgangsparameters, op een gebruiksvriendelijke manier.

De methode werd gevalideerd met behulp van meerdere BIM-modellen, waarbij met succes de geautomatiseerde uitwisseling van geplande en gerealiseerde voortgangsinformatie werd voltooid. De informatie werd vertaald naar IFC-entiteiten op een gestandaardiseerde manier, waarbij werd voldaan aan de IFC-hiërarchie, en is daardoor ook toegankelijk via elke op IFC-gebaseerde toepassing. Er werd eveneens een web-gebaseerde toepassing ontwikkeld die de voortgangsinformatie uit het IFC-gebaseerde BIM-model gebruikt voor een overzichtelijke en efficiënte rapportage en visualisatie.

De ontwikkeling van een standaardraamwerk voor geautomatiseerde uitwisseling van voortgangsinformatie met behulp van een BIM-model, is een mijlpaal in modelgebaseerde bouwvoortgangsbewaking.

Dit proefschrift presenteert aanzienlijke verbeteringen in verschillende fasen van modelgebaseerde geautomatiseerde monitoring van bouwvoortgang van gebouwen waarvoor een BIM-model bestaat in combinatie met *as-built* puntenwolken bekomen via laserscanning. Het biedt volledig geautomatiseerde registratiemethoden en verbetert het traditioneel vergelijkingsproces van *as-built* en *as-planned* informatie met inbegrip van een accurate schatting van de voltooide bouwcomponenten. Daarnaast werd ook een kader ontwikkeld voor een gestandaardiseerde en automatische uitwisseling van de voortgangsinformatie. De onderzoeksresultaten hebben het potentieel om projectvertragingen en kostenoverschrijdingen aanzienlijk te verminderen voor grote bouwprojecten.

Hoewel deze dissertatie aanzienlijke verbeteringen biedt voor bouwvoortgangsbewaking met behulp van 3D-lasertechnologie en BIM, is er nog een lange weg te gaan. Het huidige onderzoek is een poging om de praktische toepassing van moderne technologie in de bouwomgeving te ondersteunen. Toekomstige onderzoeksinspanningen zullen zich richten op verdere facilitering van het bewakingsproces door de resterende uitdagingen in modelgebaseerde beoordeling aan te pakken. Verdere technologische ontwikkelingen op het vlak van 3D data-acquisitie, AI etc. zullen nieuwe synergiën doen ontstaan ten voordele van efficiëntere bouwprocessen.



# Content

Members of Examination Board .....	v
Word of Gratitude .....	vii
Preface .....	ix
Summary .....	xi
Samenvatting .....	xv
Table of Contents .....	xix
List of Figures .....	xxiii
List of Tables .....	xxix
List of Acronyms .....	xxxi
<b>1. INTRODUCTION .....</b>	<b>1</b>
1.1 Background .....	2
1.1.1 Registration .....	4
1.1.2 Comparison .....	5
1.1.3 Estimation and exchange of progress Information .....	6
1.2 Research Overview .....	9
1.2.1 Research Objective .....	9
1.2.2 Research Questions .....	9
1.2.3 General Workflow .....	10
1.2.4 Out of Scope .....	12
1.3 Outline .....	13
1.4 Study Methodology .....	15
1.5 Scientific Contributions .....	17
1.6 Publications .....	18
1.6.1 Publications in international journals .....	18
1.6.2 Publications in proceedings of international conferences .....	18
1.7 References .....	19

<b>2. REGISTRATION BASED ON PLANE SEGMENTS.....</b>	<b>27</b>
Abstract .....	28
2.1 Introduction .....	29
2.2 Related Work.....	30
2.3 Methodology.....	33
2.3.1 Preprocessing .....	34
2.3.2 Determining the Directions of Clustered Plane Segments .....	35
2.3.3 Calculating the Possible Rotation Matrices .....	38
2.3.4 Identifying the Most Likely Rotation Matrix and Translation Vector .....	39
2.4 Results .....	44
2.5 Discussion.....	49
2.5.1 Time Efficiency.....	49
2.5.2 Registration Accuracy .....	51
2.5.3 Effect of Noise and Occlusion .....	51
2.5.4 Application on Partially Constructed Buildings .....	52
2.5.5 Registration of as-builts scans with other scans of same model .....	53
2.5.6 Limitation.....	55
2.6 Conclusions .....	56
2.7 References.....	58
<b>3. REGISTRATION BASED ON CORNER POINTS .....</b>	<b>63</b>
Abstract .....	64
3.1 Introduction .....	65
3.2 Related Work.....	67
3.3 Methodology.....	71
3.3.1 Overview.....	71
3.3.2 Extracting Corner Points.....	71
3.3.3 Identifying the Potential Matching Corner Points through Geometric Invariants .....	74
3.3.4 Evaluating the Transformations of Potential Matching Corner Points .....	80

3.3.5	Calculating the Most Optimal Transformation from Matching Corner Points/Cluster .....	83
3.3.6	Identifying the Matching Planes from Matching Corner Points (Optional) .....	84
3.4	Results and Discussion .....	84
	Comparison with plane-based registration.....	91
3.5	Conclusions .....	93
3.6	References.....	95
<b>4.</b>	<b>IMPROVING THE CONSTRUCTION PROGRESS MONITORING THROUGH DETECTION ANALYSIS .....</b>	<b>101</b>
	Abstract .....	102
4.1	Introduction .....	103
4.2	Related Work.....	104
4.3	Problem Statement .....	108
4.4	Methodology.....	113
	4.4.1 Preliminary Reasoning.....	114
	4.4.2 Detection analysis.....	117
	4.4.3 As-built Progress Detection .....	124
4.5	Results and Discussion .....	127
4.6	Conclusion .....	137
4.7	References.....	138
<b>5.</b>	<b>EXCHANGING PROGRESS INFORMATION USING IFC-BASED BIM.....</b>	<b>145</b>
	Abstract .....	146
5.1	Introduction .....	147
5.2	Literature Review .....	149
5.3	Methodology.....	152
	IFC schema for progress monitoring.....	153
	5.3.1 Integrating the Progress Entities into IFC-Based BIM.....	155
	5.3.2 Inputting the Planned Progress Information into IFC-Based BIM	164
	5.3.3 Updating the Actual Progress into IFC-Based BIM .....	167
	5.3.4 Reporting the Progress from Updated IFC-Based BIM .....	173

5.4	Result and Discussion.....	177
5.5	Conclusions .....	182
5.6	References.....	184
<b>6.</b>	<b>DISCUSSION AND CONCLUSION.....</b>	<b>189</b>
6.1	Concluding Remarks .....	190
6.2	Discussion.....	194
6.2.1	Boundaries and Limitations .....	194
6.2.2	Directions for Future Research.....	196
<b>7.</b>	<b>APPENDICES .....</b>	<b>201</b>
	Appendix 1: Corner-Point Based Registration Workflow .....	202
	Appendix 2: Corner Point Matching Process Flowchart .....	203
	Appendix 3: Corner Point Matching with Distance and Translation Invariants	204
	Appendix 4: A Conceptual Illustration of Optimal Grid-Based Data Acquisition Analysis.....	205
	Appendix 5: Graphical Representation of Extended Research Methodologies	206
	Appendix 6: UML Representation of IFC Schema for IfcSlab, IfcWall, and IfcTask .....	207
	Appendix 7: Plane-Based Registration Methodology Algorithm.....	208
	Appendix 8: Parallel Plane Segments Clustering Algorithm .....	209
	Appendix 9: Creating Corner points from Plane Segments Algorithm ...	210
	Appendix 10: Corner Point Filtering Algorithm .....	211
	Appendix 11: Geometric Invariants-Based Corner Point Matching Algorithm	212

# List of Figures

**Figure 1.1.** The Sequence of different phases in model-based assessment for construction progress monitoring .....3

**Figure 1.2.** An overview of the workflow employed in the current research .....11

**Figure 1.3.** An overview of chapters in the dissertation .....14

**Figure 2.1.** Overall Methodology.....34

**Figure 2.2.** Workflow for determining the directions of clustered plane segments.35

**Figure 2.3.** Visual representation of (a) model, (b) segmented planar components, and (c) planar segments grouped into clusters. ....36

**Figure 2.4.** Visualization of (a) plane segment from BIM, (b) plane segment from original point cloud, (c) bounding box of plane segment created from the point cloud, and (d) centroid points calculated from the original point cloud (red) and from the bounding box (blue).....37

**Figure 2.5.** Visualization of (a) possible combinations with directions from the clustered plane segments having the same relative angles in the as-built and as-planned model, (b) normal vectors from as-built (yellow) and as-planned (green) models before rotation (c), the alignment of a pair of corresponding normal vectors after the first rotation, and (d) the aligned normal vectors of both models after the final rotation. ....38

**Figure 2.6.** Example of a few rotation matrices and their respective rotational effect on the as-built model against the alignment of the as-planned model, obtained from different possible combinations by aligning the corresponding normal vectors of clustered segments from the as-built (yellow) and as-planned (green) models. ....39

**Figure 2.7.** Visualization of the as-built model (yellow) corresponding to the as-planned model (green), with an incorrect orientation (a,b) and correct orientation (c). The lines connecting the matching segments in all orientations represent the corresponding translation. ....40

**Figure 2.8.** General workflow for the assessment of the plane segments for each rotation matrix.....40

**Figure 2.9.** Representation of all the possible translation vectors  $t_{i,j}$ , are shown with line colors indicating the parallel plane segments from the (a) potential matching planes and (b) matching planes. ....42

**Figure 2.10.** Visualization of the corresponding as-built model (yellow) relative to the as-planned model (green) sorted with rotation matrices having matching costs. ....43

**Figure 2.11.** Visualization of the corresponding models registered with different translation vectors computed from the pairs of the most likely matched plane segments sorted according to their matching costs .....44

**Figure 2.12.** Visualization of BIM (as-planned model) and scan (as-built model) from dataset R1, R2, and R3.....46

**Figure 2.13.** Visualization of the registered as-built (yellow) and as-planned (green) models of (a) dataset S1, (b) dataset S2, (c) dataset S3, (d) dataset R1, (e) dataset R2 and, (f) dataset R3. ....48

**Figure 2.14.** Graph indicating the processing time and RMSE at different voxel sizes ranging from 0.01 to 0.5 m for dataset 1.....49

**Figure 2.15.** Comparison of computation time of the proposed technique when the as-planned model is processed in a mesh form (left) vs. a point cloud form (right). .....50

**Figure 2.16.** Visualization of (a) complete as-planned model, (b) incomplete as-built model with only three plane segments in distinct directions, (c) registered model using translation computed from the centroid of matched segments, and (d) registered model using translation computed from the centroid difference of the complete point cloud.....53

**Figure 2.17.** Visualization of point cloud in different views from (a) scan model 1, and (b) scan model 2. ....54

**Figure 2.18.** Visualization of registered scans in three different views after applying the (a) proposed method with the centroid of plane segments calculated from point clouds (b) proposed method (c) proposed method and then fine registration .....55

**Figure 2.19.** An example visualization the incorrect plane segments extracted in different colors from as-built point cloud of (a) dataset R1 and, (b) dataset R3.....56

**Figure 3.1.** An example of IFC content. ....72

**Figure 3.2.** Extracting the geometric details of building components from IFC to construct their structural mesh model. ....72

**Figure 3.3.** Visualization of (a) a single corner point generated from three parent planes; (b) all the possible corner points generated from a model, including the false points; (c) differentiation of false corner points (red color) from others (green) after verification; and (d) final corner points (green) in the model. ....74

**Figure 3.4.** The processing sequence of geometric invariants to identify the potential matching corner points in a cycle. ....75

**Figure 3.5.** Verification of the relative angles between the parent planes of two potential matching corner points using their normals. ....76

**Figure 3.6.** Visualization of (a) rotation matrices obtained after alignment of the corresponding plane normal in different combinations and, (b) their respective rotation effect on the as-built model relative to an as-planned model. ....77

**Figure 3.7.** Visualization of as-planned model and transformed as-built model with transformations aligning the (a) corresponding plane segments with centroids nearest to each other and, (b) non-corresponding plane segments with centroids relatively far from each other.....78

**Figure 3.8.** The identification of potential matching corner points from the as-built (left) and the as-planned model (right). The edges of the arrow with the same labels [a,b,c,...,y,z] in both models represent the potential matching points.....79

**Figure 3.9.** Potential matching points in the as-built (left model) and as-planned model (right model), clustered according to respective transformation parameters visualized next to them in terms of their corner points and 3D models (a–c). .....81

**Figure 3.10.** An example of neighbor corner points with parallel parent planes. ...82

**Figure 3.11.** Visualization of the corner points from the as-built (yellow) and transformed as-planned model (green) resulting in aligned corner points (blue) according to each cluster transformation (a–c). .....83

**Figure 3.12.** Visualization of as-built (yellow) and as-planned (green) registered according to the different transformation parameters with respective error values in ascending order (a–f). .....84

**Figure 3.13.** Visualization of models for (a) dataset A1 and (b) dataset A2. ....85

**Figure 3.14.** Visualization of as-planned and as-built models for (a) dataset R1 and (b) dataset R2. ....86

**Figure 3.15.** Visualization of registered as-built (yellow) and as-planned (green) models of (a) dataset A1, (b) dataset A2, (c) dataset R1, and (d) dataset R2. ....87

**Figure 3.16.** Graph showing the effect on RMSE of increasing the number of RANSAC iterations.....89

**Figure 3.17.** Visualization of the dataset A2 model with different floors utilized to create incomplete as-built models. ....89

**Figure 3.18.** Visualization of registered incomplete as-built (yellow) with as-planned (green) models according to their respective extracted corner points shown above. ....90

**Figure 3.19.** Visualization of the unsuccessful registration of the dataset with a partially built scan model using the plane-based method. ....92

**Figure 3.20.** Visualization of the successful registration of the dataset with partially built scan model using the plane-based registration method. ....92

**Figure 3.21.** Visualization of (a) Models before registration, (b) Incorrectly registered models, and (c) Corner points of Incorrectly registered models .....93

**Figure 4.1.** Visualization of building with data acquisition instrument placed to scan the wall component (in blue) along with obstacle in (a) 3D view, and (b) top view highlighting the detectable coverage (green), and non-detectable coverage due to building component (yellow) and external occluder (orange). ....109

**Figure 4.2.** Visualization of the: (a) acquired as-built scan colored using scalar fields, (b) as-built scan with corresponding as-planned surface (grey), (c) surface of the actual as-built wall (green) as compared to the as-planned surface (grey), and (d) provides a classification of different surfaces in which the detectable surface is highlighted with green while the occluded surfaces  $[(\sigma) \text{ (Un-detected)}]$  due to building component and external occluder are represented with yellow and orange respectively. ....111

**Figure 4.3.** The overall workflow of the proposed three-stage methodology. ....114

**Figure 4.4.** An example of time-related IFC entities associated with three walls having a sequential relationship with each other in IFC-based BIM model information. ...115

**Figure 4.5.** Visualization of (a) Building 2D plan view and (b) Construction schedule. .... 117

**Figure 4.6.** The 3D visualization of the (a) geometrical model from as-planned BIM, (b) detectable model, (c) classified detectable model. .... 117

**Figure 4.7.** Illustration of different elements involved in a ray casting scene. .... 118

**Figure 4.8.** Flowchart of the detection analysis stage outlining the steps for developing and classifying a detection model. .... 119

**Figure 4.9.** An example of placing the scanner either around the required structure (a-b) or only indoors (d-e) to obtain the respective detectable model (grey) of the required building component (structure) after ray casting simulation. .... 120

**Figure 4.10.** Visualization of (a) detectable coverage of laser scanner from the top view, and (b) classification of building component surfaces into detectable (green) and non-detectable (blue). .... 122

**Figure 4.11.** Illustration of occlusion in as-built scan caused by obstacles in the scene, resulting in occluded point clouds of planar building component. .... 122

**Figure 4.12.** Visualization of (a) detectable coverage of laser scanner from top view in the presence of an external obstacle, and (b) classification of building component surfaces into detectable surface (green) and non-detectable surface (blue) including the occluded surfaces marked in red due to the obstacle. .... 123

**Figure 4.13.** Visualization of obtained detectable model of building component classified with detectable surface (green) and un-detectable surface (in red). .... 124

**Figure 4.14.** Workflow for as-built surface detection. .... 124

**Figure 4.15.** An illustration of removing the most likely error points (red) by cropping the as-built scan of a wall component using a detectable surface bounding box (green) to retain the detected as-built points (black). .... 125

**Figure 4.16.** Surface coverage determination based on 3D points within voxel grids. .... 126

**Figure 4.17.** Visualization of as-built surface detected (blue) on a classified detectable model having detectable surface (green) and un-detectable surface (red). .... 126

**Figure 4.18.** The 3D visualization from the simulated dataset demonstrates the geometrical difference between (a) a 3D model representing actual built components at the site, and (b) a 3D as-built scan model (colorized based on scalar fields) representing the actual conditions at the site according to laser scanner range. .... 128

**Figure 4.19.** 3D visualization of (a) detectable model and (b) Classified detectable model with highlighted detectable surface (green) of the simulated dataset. .... 129

**Figure 4.20.** 3D visualization of surfaces highlighting the as-built (blue) from detectable (green), and un-detectable (red). .... 129

**Figure 4.21.** Estimated and predicted completion ratios for building components and the overall building structure. .... 130



**Figure 4.22.** Progress visualization of building components classified with four different colors (blue, green, orange, red) representing different ranges of respective completion ratio percentages (100-90, 90-70, 70-50, 50-30, 30-0). ..... 130

**Figure 4.23.** 3D Visualization of as-planned BIM and as-built scan for real-time datasets: (a) RT-1 and, (b) RT-2. .... 132

**Figure 4.24.** 3D visualization of classified detectable model obtained for dataset (a) RT-1 and, (b) RT-2. .... 133

**Figure 4.25.** 3D Visualization of as-planned BIM (a) and as-built scan (b) for real-time datasets RT-3. .... 135

**Figure 4.26.** Visualization of the (a) Data acquisition trajectory in plan view and, (b) Classified detectable model representing detectable and non-detectable surfaces, for real-time datasets RT-3. .... 136

**Figure 5.1.** Flowchart of the proposed methodology..... 152

**Figure 5.2.** IFC entities related progress information in hierarchy..... 154

**Figure 5.3.** An example of entities associated with a building component in the IFC-based BIM model. .... 155

**Figure 5.4.** Flowchart of verification step to create an IFC entity based on progress information..... 156

**Figure 5.5.** IFC entities IfcSlab, IfcWall, IfcTask having common attributes based on their hierarchical structure. .... 157

**Figure 5.6.** Structure of IFC-based entities created to include time-related progress information..... 158

**Figure 5.7.** The Structure of IFC-based entities was created to include cost-related progress information. Entities on the left and right sides representing the planned and actual cost information..... 161

**Figure 5.8.** An example of IFC content. .... 168

**Figure 5.9.** Flowchart to estimate the earned value parameters..... 174

**Figure 5.10.** Geometrical visualization of an IFC-based BIM model illustrating various building components. .... 177

**Figure 5.11.** IFC code snippet expressing the newly integrated IFC entities. .... 178

**Figure 5.12.** Retrieval of progress information for the building component (#197) using Python. .... 179

**Figure 5.13.** Building component (#197) highlighted in the exported BIM model, along with its attribute details, viewed in the external software (Open IFC Viewer, version 23.3.0). .... 180

**Figure 5.14.** Visualization of building components using different colors (red, yellow, orange, green, and blue) corresponding to their respective completion ratios (0–30%, 30–50%, 50–70%, 70–90%, and 90–100%) in two different viewpoints. .... 180

**Figure 5.15.** A screenshot of the developed web-based application demonstrating the project-level progress details of the updated BIM model..... 181

**Figure 5.16.** Color-coded visualization of two different BIM models (a,b) highlighting the progress status of their building components: 0–30% (Red), 30–50% (Yellow), 50–70% (Orange), 70–90% (Green), and 90–100% (Blue). .....182

**Figure 7.1.** Overall workflow of Corner-point based registration method detailed in Chapter 3. ....202

**Figure 7.2.** The Flowchart showing the process of identifying potential matches between pairs of corner points from as-built and as-planned models using various geometric invariants. ....203

**Figure 7.3.** Demonstration of distance and translation invariants for matching corner points in as-built (highlighted in yellow) and as-planned (highlighted in green) models. ....204

**Figure 7.4.** A conceptual illustration showing the partitioning of a plane space of model into uniform grids, followed by the detection analysis of the grids with the eventual aim to identify the optimal location for data acquisition. ....205

**Figure 7.5.** Graphical representation highlighting the potential extension of current research methodologies with data acquisition domain, highlighting key parameters utilized in the current study (highlighted in blue) and those critical for future investigations (highlighted in red). ....206

**Figure 7.6.** UML representation of the IFC schema for IfcSlab, IfcWall, and IfcTask. ....207

# List of Tables

<b>Table 1.1.</b> An overview of the research questions discussed in each chapter. ....	14
<b>Table 2.1.</b> Details of simulated datasets. ....	45
<b>Table 2.2.</b> Registration details of all the datasets, including the computation of the correct rotation matrix and identical translation. ....	48
<b>Table 2.3.</b> Details concerning the processing time and accuracy error according to each dataset. ....	50
<b>Table 2.4.</b> Segmented as-built point cloud with different noise levels and voxel sizes. ....	52
<b>Table 3.1.</b> Details of simulated datasets. ....	88
<b>Table 4.1.</b> Summary of results for simulated and real-life datasets.....	134
<b>Table 5.1.</b> Details of planned progress entities. ....	165
<b>Table 5.2.</b> Details of actual progress entities. ....	169
<b>Table 5.3.</b> Details of different reporting types for different categories of progress information.....	176



# List of Acronyms

<b>2D</b>	Two-dimensional
<b>3D</b>	Three-dimensional
<b>4D</b>	Three-dimensional
<b>BIM</b>	Building Information Model
<b>CAD</b>	computer-aided design
<b>CEN</b>	European Committee for Standardization (Comité Européen de Normalisation)
<b>CS</b>	Coordinate System
<b>DIN</b>	German Institute for Standardization (Deutsches Institut für Normung)
<b>DoF</b>	Degrees of freedom
<b>FMP</b>	Fast-matching pruning
<b>PPFH</b>	Fast point feature histograms
<b>GPS</b>	Global Positioning Systems
<b>ICP</b>	Iterative Closest Point
<b>ID</b>	Identifier
<b>IFC</b>	Industry Foundation Classes
<b>ISO</b>	International Organization for Standardization
<b>LoD</b>	Level of detail
<b>NDT</b>	Normal Distribution transformation
<b>PCA</b>	Principal Component Analysis
<b>RANSAC</b>	Random sample consensus
<b>RFID</b>	Radio Frequency Identification
<b>RMSE</b>	Root Mean Square Error
<b>RQ</b>	Research Question
<b>SIFT</b>	Scale-invariant feature transform
<b>SURF</b>	Speeded up robust features
<b>UWB</b>	Ultra-Wideband



---

# 1

---

## 1. INTRODUCTION

## 1.1 Background

The construction industry contributes 10% and 25% of the GDP in developed and developing countries, respectively, and has a significant positive impact on the global economy [1]. For construction practitioners and researchers, the low productivity of the construction industry in comparison to other industries continues to be a significant obstacle [2]. One of the key areas where low productivity has a big impact is monitoring the progress of construction projects, which is a key task in construction processes [3-5]. Numerous studies have indicated the precise and efficient monitoring of under-construction buildings as a key element of successful projects and a necessity for effective project management [6-12]. Despite its importance, over 53% of typical construction projects are behind schedule, and over 66% exceed their budget limits [13,14].

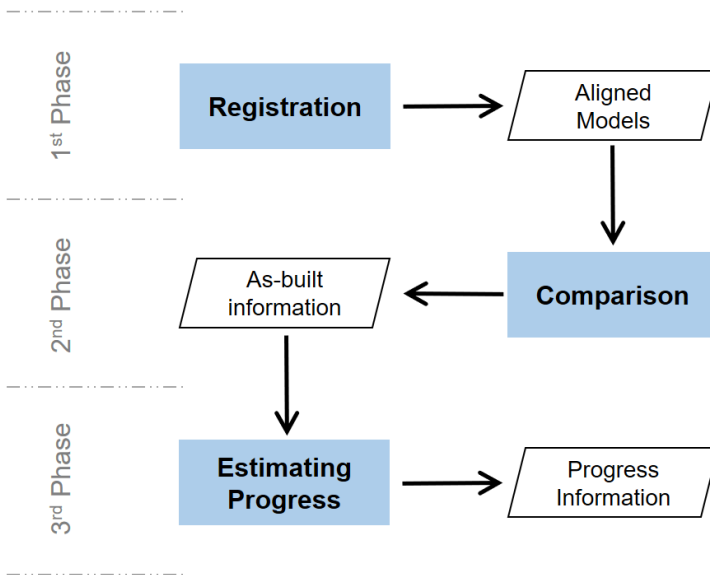
To deliver the project in accordance with the planned specifications, the availability of precise information at the appropriate time is critical for the decision-making process. The exchange of partial or incorrect information can lead to project delays, increased costs, and numerous disputes between stakeholders [15-18]. Generally, large construction projects involve lots of information exchange due to extensive in-progress work activities, hence require some arrangements or practices that ensure the monitoring of these activities [19]. Apart from ensuring that the in-progress work activities are proceeding as planned, the monitoring practices also alert early deviations or non-conformity of these activities from the project goal, allowing the avoidance or mitigation of their undesirable consequences and, eventually saving crucial time and expenses [20-22].

Current practices in construction progress monitoring consist of manual verification of building activities by construction staff in which they walk around the site, making visual observations, and taking extensive physical measurements. Later this site information is manually analyzed with the key information extracted from project drawings, specifications, and construction details to conclude a field progress report that determines how much the ongoing project is progressing technically according to schedule and budget. Overall, this process involves manual data acquisition and extensive processing that requires huge time and resources with prevailing human involvement, ultimately leading to multiple errors inclusive of missing or inaccurate information [23-27]. Therefore, automated and precise alternatives for effective construction progress monitoring are needed, however their development is still in its initial phase and has not achieved the required reliability and efficiency [4,9,28], although this problem it is already acknowledged since the 1960s [29].

Recent advancements in remote sensing technologies have enabled the acquisition of three-dimensional (3D) as-built spatial information from construction sites, and as a result, extensive research is being carried out to make use of these models to improve construction progress monitoring through model-based assessment



methods [9]. These methods infer the building progress through a geometrical assessment to confirm the presence of building components by processing the acquired as-built model with the corresponding as-planned model. The as-built model is a 3D point cloud that represents the actual state of the building and can be acquired through either laser scanning [30-33], image-based reconstruction [8,13,19,23,26,34-36], or integration of both [37-39]. The as-planned model is the design model of the building, which is obtained from a BIM or CAD model in a suitable format. BIM, which stands for Building Information Model, is the major outcome of recent digitalization in the construction industry and represents a virtual model of the building with the ability to store all necessary data, including geometric (graphic) and semantic (non-graphic) information. The model-based assessment methods mainly process the as-built scan and as-planned model to infer the progress information in an automated way and the procedure can be categorized into three different phases, as shown in **Figure 1.1**. In the first phase, it is ensured that both models are accurately aligned with each other with the highest overlap through a technique known as registration while the next core phase performs their geometrical comparison to determine the as-built (completion) information. The last phase precisely processes the obtained as-built information to estimate the standard progress parameters (including time or cost schedule) and enable its seamless exchange with construction stakeholders for effective progress monitoring.



**Figure 1.1.** The Sequence of different phases in model-based assessment for construction progress monitoring

The model-based assessment is facing numerous challenges across all phases, hindering its application in the construction industry. This research focuses on

addressing these challenges by thoroughly investigating each phase to improve construction progress monitoring in an automated way.

### 1.1.1 Registration

The model-based assessment for progress monitoring requires the geometrical alignment of as-built and as-planned models which is achieved through an essential technique known as registration. The precision with which the as-built model is registered with the corresponding as-planned model determines the effectiveness of model-based assessment as the comparison in the lateral phase requires the accurate overlap of models [40]. If the surfaces of the models are too far apart or not accurately located with each other, then the subsequent comparison phase may fail or provide incorrect progress information.

Technically, registration involves the determination of the rotation matrix and translation vector to align the as-built model with the corresponding as-planned model in 3D space. Normally, a coarse-to-fine registration approach is implemented which first performs the coarse (or global) registration to establish the initial alignment of models, followed by fine (or local) registration to obtain the most optimized overlap between the corresponding structures of models [41]. Furthermore, the fine registration is usually implemented with the well-known iterative closest point (ICP) algorithm [42] and its different versions [43-45], which requires the initial alignment of the models. Consequently, the direct implementation of fine registration without a preceding coarse registration is prone to failure [46], further emphasizing the significance and necessity of the coarse registration step. However, a key challenge in coarse registration is the extraction of geometric features from a model, as well as the identification of their corresponding matches in order to determine the required transformation.

Although, registration is a widely explored research area, there is more emphasis on the registration of point clouds than on the registration of point clouds with BIM or mesh models particularly as the latter can be converted into the former [40]. The sampling of BIM/mesh models into point clouds, instead of the direct use of BIM, may affect the accuracy of the geometrical information and result in registration errors [47]. Furthermore, the current registration techniques have specific approaches that employ certain geometrical features, which limits their application to specific scenarios [48].

Generally, building structures have orthogonal geometry with an abundance of dominant planar features, such as floors, roofs, walls, etc. and registration of building structures necessitates leveraging these features. Using these planar-based features, instead of processing a complete point cloud, not only saves computation time, but is also less affected by outlier and noise errors resulting in greater accuracy [48,49]. However, the reliable identification for matching primitives through these planar-based features is still a major challenge [48,50-53]. Furthermore, the registration of

as-built scans with the as-planned BIM for model-based assessment in the context of construction progress monitoring also poses additional challenges. For example, few research is dedicated to challenges in comparing as-built scans obtained from a partial-constructed buildings to its complete model in the as-planned BIM. Apart from that, various errors including noise, occlusions, etc., are commonly present in the as-built scan due to the presence of machinery, materials, and human workers. These errors influence the extraction of geometrical features from the model and pose hurdles for the registration process [54]. Additionally, the building models typically have several self-similar building components such as doors, windows, walls, etc. that may hinder the identification of matching features for registration [40]. Consequent to all these challenges, registration is mostly carried out manually through human input [52], as the available solutions are not reliable enough, especially when dealing with complex point clouds [55]. This illustrates the need for the development of automated model-based registration techniques for construction progress monitoring which is capable of dealing with these challenges in construction environment and accurately align the as-built scan with the as-planned BIM.

It is important to mention here that a BIM model in model-based assessment can act as a most suitable as-planned model due to its ability to facilitate information exchange during various monitoring processes especially for planning schedules, updating ongoing as-built information, visualizing and communicating the progress information to stakeholders [56-58]. However, the previous studies either did not directly use BIM model or manually converted BIM into another format, which conflicts with the automation concept in progress monitoring [4,12,33,58]. Therefore, it is imperative to propose a registration technique in the context of automated construction progress monitoring that leverages the utilization of the BIM model and directly extracts the geometrical details for processing.

### 1.1.2 Comparison

After the registration phase, the comparison of the as-built and as-planned models (also referred to as Scan-vs-BIM comparison) is performed to infer the as-built information through the structural analysis [9,59]. It is the core phase in the model-based assessment that primarily examines the surface geometry of the as-built scan in contrast to the BIM model to estimate the building completion based on surface identification. Technically, the comparison aims to identify the parts of the as-planned surface that are already constructed based on the presence of corresponding as-built points. The results from the model-based assessment are reliable only if the as-built information estimated from the comparison phase is a precise representation of the actual as-built. However, this phase is often subject to several challenges that may compromise the overall reliability of the as-built information obtained. The challenges include but are not limited to the lack of suitable as-planned geometry for comparison, the presence of many errors (notably

the occlusion) in the as-built scan, an inaccurate comparison process. The details of these challenges are given below.

Generally, the as-planned model is directly compared with the corresponding as-built model to find out the surfaces that are built. However, there are always some surfaces from the as-planned model that are completely hidden from data acquisition instruments such as the sandwiched surfaces of beams and roofs. If these surfaces are considered in the comparison then they can increase the inaccuracy in the result. Hence, the as-planned model needs to be revised to include only those surfaces that are possibly exposed to the instrument, presenting a significant challenge in its development. Similarly, the captured as-built scan should truly represent the actually built surface in an ideal case to estimate the accurate as-built information during the comparison process, which is not possible in real life. At a construction site, there is a presence of a range of elements including construction materials, machinery, and humans [12]. However, when acquiring spatial data from the site, these elements become obstacles (or occluders) that create occlusions in the as-built scan. Furthermore, there are cases where the data acquisition instrument is not appropriately positioned or fails to capture the entirety of the as-built surfaces due to pre-existing already built other components acting as obstacles. As a result, the non-exposure of surfaces due to obstacles creates incompleteness in the as-built scan ultimately leading to the estimation of the imprecise as-built information during the comparing process. An example would be an as-built scan of a wall component that is highly affected by occlusion and noise errors. If the wall is nearly completed (e.g. 80%) in reality then the comparison may inaccurately estimate its completion around half (e.g. 55%) mainly due to errors in its as-built scan. This inaccurate estimation arises from the surface of the component not being fully exposed to the data acquisition instrument due to the other components and occlusion at the site. Hence, it is a big challenge for the instrument to capture all the as-built surfaces. Apart from that, the errors in the traditional comparison process should be identified for improvement eventually to effectively detect the as-built surface. Collectively, all these challenges create a difference between the actual and the estimated progress, thus limiting the application of model-based assessment in the construction industry and demands addressing this inaccuracy in the comparison phase [60-63].

Currently, there is no study addressing these issues or providing a solution to improve the accuracy and reliability of the comparison process. Therefore, the comparison process needs to be explored to accurately identify the as-built surface while integrating the potential improvements to increase the accuracy of progress results.

### 1.1.3 Estimation and exchange of progress Information

To monitor the progress of the construction projects in an automated way, accurate and up-to-date progress information is required in accordance with standard forms

commonly used in construction. The traditional method may not be a suitable fit for automated progress monitoring due to the time-consuming and labor-intensive nature of collecting and processing the information and may result in inaccurate and incomplete information [23,25,63-66]. Even though there is advancement in developing automated progress monitoring systems, there remains a challenge in terms of automation, accuracy, standardization, and interoperability [56]. The need for an automated solution that facilitates the exchange of progress information from the construction site between the stakeholders while ensuring the utilization of standardized parameters and user-friendly reporting.

In model-based assessment, the progress information obtained from the comparison phase includes the completion ratio (or percent completion) of building components which indicates the extent to which the components are built. For effective construction progress monitoring, this information has to be translated in terms of schedule, cost, or other benchmarks. For example, if a specific wall has reached a completion ratio of 80% from 50%, it will necessitate respective adjustments to the actual schedule (actual duration, actual start and finish date) and existing cost information upon further processing to reflect the actual conditions. Furthermore, it is crucial that the automated processing system adheres to industry-standardized parameters to ensure accurate and consistent processing of information. Similarly, it should also have the ability to report updated information along with the additional progress indicators in a user-friendly and comprehensive way to the stakeholders.

Recently, BIM became popular in construction projects due to its ability to act as a digital representation of a building that encompasses comprehensive and accurate information about geometry and other semantic information [12,56,57,60,63,67,68]. According to studies, BIM has a transformative influence on the design, construction, and operation of buildings, serving as a valuable collection of information to enhance these processes [69-72]. BIM-enabled digital planning and construction have the capability to reduce cost by 13% to 21% during construction, and 10% to 17% during operation [73,74]. The adoption of BIM has facilitated effective project management with improved communication, collaboration, and project control [12,75-77]. Despite the advantages of BIM, its full potential for progress monitoring, and reporting has not yet been reached [78]. The effective exchange and management of information throughout the entire construction process is a significant challenge in this regard and demands the exploration of BIM for communication, especially for current research in which the BIM model is being employed as the as-planned model in all phases of model-based assessment.

The major challenges involved in the utilization of BIM at the construction site include the time-consuming and laborious updating process to integrate the as-built information [56,79], and issues in interoperability between different phases and stakeholders [80,81]. Furthermore, BIM dependence on particular software renders

the information inaccessible once dissociated from it, resulting in inefficiencies in building management as well as reliance on specific vendor tools [67,82].

IFC is a globally established standard for BIM data exchange, that allows the information transfer between different software applications used in construction industry. It is defined by IFC schema which is built on the EXPRESS language and designed to be open and non-proprietary, providing a uniform approach for data transfer specifications. Therefore, BIM software applications with the certification can transform their BIM models into the standardized IFC model, enabling enhanced interoperability and fostering collaboration among diverse stakeholders within the construction industry. [69,83]. The major limitations associated with the IFC schema include the incomplete linkage of modeled elements with semantics and the potential loss of information during conversion into the IFC file format [63,84,85]. However, it continues to be improved with extensive deployment in relevant areas of construction projects such as energy consumption [86,87], project performance evaluation [88], virtual construction [89,90], data standards for facility management classes [91], etc. Furthermore, there are some studies that utilized the IFC-based BIM in the context of progress monitoring [12,56,58], however, there is a clear gap in exchanging progress information using the latest IFC schema particularly to integrate all types of information including time-related schedule, cost and any other information such as a textual note or additional progress indicators.

For effective progress monitoring in automated model-based assessment, there is a need for research that is focused on IFC-based BIM updating to provide a comprehensive solution for exchanging any kind of possible progress information.

## 1.2 Research Overview

### 1.2.1 Research Objective

The objective of this research is to analyze the model-based assessment in the domains of registration, comparison and progress exchange, with the ultimate goal of improving automated construction progress monitoring.

### 1.2.2 Research Questions

The following research questions (RQs) arises based on the above-mentioned research objective, which urges the investigation of the model-based assessment phases for construction progress monitoring.

- RQ 1.** How can BIM be utilized effectively to extract the different types of information for construction progress monitoring?

Model-based assessment with a BIM model employed as an as-planned model requires the direct and automated extraction of information from it, which is a major challenge as outlined in the first research question (RQ 1). The utilization of BIM in the different phases of model-based assessment demands the resolution of certain issues, such as: How can the geometrical information from the BIM model be accurately taken out and processed to develop its 3D model? How the other semantic information related to progress can be retrieved from BIM for its different applications in construction progress monitoring?

- RQ 2.** How can the structural features of the building geometry be exploited for registration of partial as-built scans with the IFC-based as-planned BIM in a construction environment, specifically tailored for progress monitoring of under-construction building structures in model-based assessment?

The second research question (**RQ 2**) describes the registration issue that may rises for the alignment of the error-prone as-built scan with their BIM model due to the non-identification of matching primitives in their structural models. This demands the response to a few challenges i.e. what are the possible discriminatory and distant primitives that can be extracted from building structures? How these primitives can be identified and matched from both models for registration, especially for the error-prone and incomplete as-built scan acquired from the construction site? How the geometrical information can be directly extracted from the BIM model to ensure accuracy and automation in model-based assessment?

- RQ 3.** What are the challenges involved in the geometrical comparison of as-built scans obtained from ongoing building construction with the corresponding as-planned BIM model to estimate the as-built completions, and how can the accuracy and reliability of the overall process be improved?

The third research question (**RQ 3**) deals with the challenges associated with the comparison process that analyzes the geometry of registered models to estimate the precise progress information. The main focus is to explore the comparison process with the aim to detect the accurate as-built completions of building components, eventually improving the process. It also analyzes how the geometrical and semantic information from the BIM model can contribute to the improvement of comparison. How the inaccuracies resulting from the error-prone as-built can be minimized and addressed? In addition, how the comparison process can be revised to accommodate the reduction of errors during as-built surface detection? The inaccuracy resulting from both models and the comparison itself requires a detailed investigation to propose improvements.

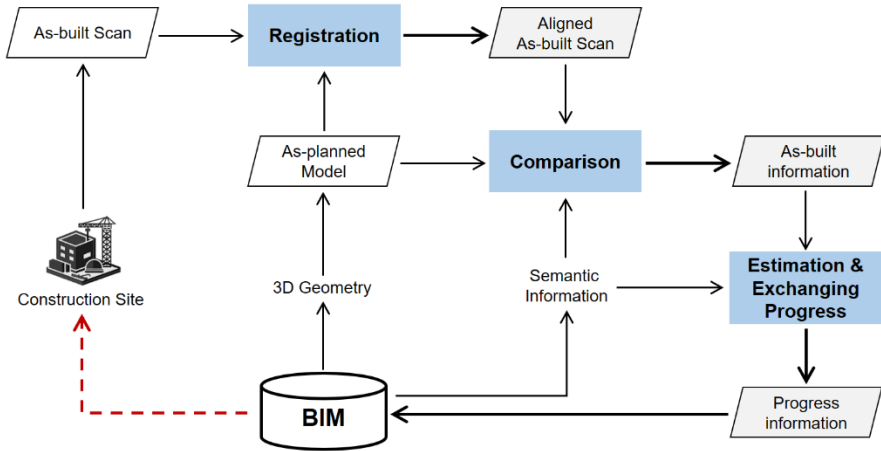
**RQ 4.** How the as-built completion information can be efficiently translated into progress information and then exchanged in an effective and efficient way? And how can BIM be employed for information exchange to integrate, update and report progress information including time, cost, and other additional information obtained at the construction site?

The last research question (**RQ 4**) reveals the challenges related to the utilization of IFC-based BIM as an information exchange tool. How the progress information including the time, cost, and other customized information such as site comments, progress variables, etc., can be integrated into BIM in a standardized framework for frequent updating? How to interpret the as-built completion information of building components from the site into progress variables for standardized processing? How the latest IFC schema can be exploited for automated updating and user-friendly reporting of progress information in the context of construction progress monitoring?

### 1.2.3 General Workflow

The research aims to improve automated construction progress monitoring through model-based assessment involving the as-built scan and BIM model of buildings. The research focuses on three key areas: registration, comparison, and progress estimation & exchange. The general workflow pertaining to these areas is shown in **Figure 1.2**. The goal is to explore innovative methods and tools that enhance the accuracy, efficiency, and reliability in these key areas of construction progress monitoring using automated systems. The study incorporates proficient use of BIM in every phase to leverage the additional information stored in it to achieve higher quality and precise assessments.





*Figure 1.2.* An overview of the workflow employed in the current research

In the first phase, the registration of models is performed to transform the coordinates of the as-built scan so that it can attain maximum overlap with the as-planned BIM. The plane-based features of buildings are employed to perform the registration between the inaccurate as-built scan and as-planned BIM model models. Two different methods based on the discriminative primitives and matching approach are proposed. These methods process the BIM model by extracting the geometrical information through the IFC schema to develop the respective as-planned 3D model. The first method makes direct use of plane-based features to identify the matching correspondence using a directional and translational assessment through a matching cost algorithm. Similarly, the second method employs the corner points developed from these planes as discriminatory primitives and identifies their matching through a series of distinct variants. As both methods utilize different geometrical characteristics, they offer certain advantages and limitations. This variety of methods proves beneficial, catering to particular requirements and situations.

After registration, the comparison of the aligned models is performed in the second phase. The study advances the accuracy of the traditional comparison process through the identification of possible errors by analyzing BIM model, as-built scan, and as-built detection approach. The process is improved by utilizing the geometrical and semantic information extracted from IFC-based BIM and processed through different stages including reasoning measures, detection analysis, and as-built progress identification. It not only identifies the errors to accurately estimate the progress of each building component but also computes the additional parameters that help to understand the as-built information and predict the total progress against the uncertainties.

In the third and last phase, a comprehensive solution is provided to estimate and exchange the progress information using IFC-based BIM. A four-stage method is detailed that integrates the relevant progress entities according to the progress information and then updates their planned and actual values. The integrated progress information is further handled to allow user-friendly reporting as well as the computation of additional progress indicators. This method is designed to perfectly fit the automated progress monitoring using model-based assessment in which the same BIM model is also leveraged for registration and comparison.

By comprehensively investigating the challenges in registration, comparison, and progress estimation & exchange, this research seeks to contribute to the advancement of automated construction progress monitoring by proposing innovative techniques and advancements. The research outcomes aim to improve project management practices, facilitate decision-making processes, and ultimately increase productivity in the construction industry.

#### 1.2.4 Out of Scope

As the research topic focused on construction progress monitoring of buildings is inherently expansive. This section addresses certain aspects that fall beyond the scope of the specific.

The dissertation investigates the different phases of model-based assessment in which the as-built and as-planned models are analyzed with each other to infer the progress information. The previous studies may have utilized different types of as-planned models such as CAD models or mesh models, however, the current research study focuses on BIM models as they support automation and significant improvements in each phase. Although, the CAD or mesh models can also be utilized by adopting the methodology accordingly. Similarly, the as-built model includes the 3D point cloud that is either acquired from a laser scanner, through reconstruction of 2D images, or integration of both. The current study, particularly in the registration and comparison phases, is performed on laser-scanned as-built models. Although the image reconstructed as-built model can also be utilized in the current research, however, it may affect the accuracy of obtained results correspondingly.

The registration methods focus on building structures having dominant planar geometry as most buildings have the majority of planar structures. However, there are exceptions as well as certain buildings possess non-planar or curved components. In such cases, the methods may not work if they do not find enough plane segments in both models. Furthermore, the registration techniques are dependent on plane segments, the plane segments from the as-built scans are extracted through RANSAC-based plane segmentation in which the segments are estimated randomly through numerous iterations. Hence, the segmented plane may change slightly each time, thus also marginally impacting the registration accuracy.

The current research is not focused on the plane extraction technique; therefore, it relies on the already available efficient RANSAC-based segmentation technique.

The method proposed for the comparison phase identifies the accurate completion ratio by processing the building components. The method is designed to be efficient; however, it may experience high computation times for large datasets including the buildings model with hundreds of components that are being processed for the first time. The underlying reason is that the proposed methodology precisely identifies the surface completion of each building component. The intended prioritizing of the accuracy over efficiency may not affect the overall computation time, as it has no impact on the progress monitoring of already processed building components because the progress monitoring requires the regular processing of models over time. Similarly, the method also handles the occlusion in the scan models due to 1) other building components that are already built and, 2) the presence of other external objects placed at the scene. The method presented successfully identified the occlusion for the first type for simulated and real-life datasets. Although, a solution for the second type of occlusion was proposed and validated for simulated datasets, however, it required some advancement for its successful application on real-life datasets, which is another extensive research domain; hence, it is planned for the future.

Currently, there is an absence of standardized datasets that can be used to benchmark the results of model-based assessment techniques. This limitation may be attributed to the scarcity of extensive research in this particular research domain. Ideally, standard datasets should include diverse models comprising scans and their corresponding BIM models completely enriched with semantic planning information, particularly the time-related data of building components and their construction sequences. As the practical application of model-based assessment techniques is still in its early stages and not yet fully developed, the availability of adequate data for testing remains limited. However, it is important to acknowledge that the current thesis primarily focuses on investigating and proposing improvements to construction-based assessment processes for automated progress monitoring. While the lack of standardized datasets is acknowledged, the research within this thesis was conducted within the scope of available resources and data. The main goal is still the advancement of model-based assessment techniques for automated progress monitoring while recognizing the need for further research and standardization in this emerging field.

### 1.3 Outline

This dissertation is composed of a several research publications that were produced within the scope of this PhD. The complete list of publications is provided in Section 1.6 . These publications offer a comprehensive and integral overview of the research performed. Similarly, significant research contributions are achieved through the

current research study, which are also described in Section 1.5 . **Figure 1.3** provides an overview of the main chapters of the dissertation, excluding the first (introduction) and last (conclusion) chapters. As evident from the figure, each chapter corresponds to a specific phase of model-based assessment and is arranged according to their sequence.



**Figure 1.3.** An overview of chapters in the dissertation

The overview of the remainder of this dissertation is provided with an explanation of how the different chapters are linked together. **Table 1.1** indicates how the different research questions are being addressed in each chapter. These chapters are also briefly summarized in next section according to the research questions that are highlighted in Section 1.2.2 . It is pertinent to mention that the same consistent model is being employed throughout the methodologies section in all chapters, serving as the fundamental framework for demonstrating their approaches. This model acts as the cornerstone, providing a cohesive and unified foundation for the demonstration of different methodologies.

**Table 1.1.** An overview of the research questions discussed in each chapter.

	Ch. 2	Ch. 3	Ch. 4	Ch. 5
RQ 1		✓		
RQ 2	✓	✓		
RQ 3			✓	
RQ 4				✓

## 1.4 Study Methodology

The objective of this research was to improve construction progress monitoring by analyzing the model-based assessment in the research domain of registration, comparison and progress information exchange. Each chapter presents innovative methods and tools aimed at improving accuracy, efficiency, and reliability across the key phases of model-based construction progress monitoring. Chapter 2 and 3 focus on registration issues, while chapter 4 examines the comparison stage. Additionally, the chapter 6 explores the progress exchange mechanism. The goal of this comprehensive approach is to provide a deeper understanding of progress monitoring processes and facilitate more effective decision-making in construction projects. A brief summary of all chapters is as follow:

The chapter 2 addresses the registration issue by adopting a novel approach that directly utilizes the plane segments in the building geometry to robustly determine the most accurate registration parameters in three stages. Initially, the plane parameters are extracted from the building model through plane segmentation and then they are clustered according to their directions to get the nominal directions of models. In the second stage, the nominal directions obtained from both models are then further processed to determine the possible rotation matrices. These matrices are then assessed in the last stage based on a computation framework that measures the correspondence through a matching cost algorithm, deploying a minimization process. The framework performs the directional and translational assessment to identify the correct rotation matrix and translation vector.

The next chapter also deals with the registration challenge by proposing another unique method that makes use of evident and distinct corner points in the building structures for registration of the as-built scan of under-construction buildings with as-planned BIM. Similar to the previous registration plane-based approach this method also employs the building plane segments but only to create the corner points as points of interest for matching. It mainly consists of four stages. The first stage extracts the corner points from the models by finding the possible intersection points obtained from any three non-parallel plane segments. Later the potential matching corner points are identified in the subsequent stage by pruning the extracted corner points using different geometric matching invariants related to distance, angle, rotation, and translation. In the third stage, transformation parameters obtained from potential matching points are evaluated to find the cluster with the correct transformations. In the end, the most optimal transformation among the correct transformations is identified that gives the maximum overlapping of surfaces. This chapter also compares the corner-based registration method with the previously proposed plane-based method for the registration of building models presenting the merits and the limitations.

Chapter 4 delves into the comparison stage with the aim to improve the procedure by introducing new measures. These new measures not only increase the accuracy of comparison but also provide additional progress parameters to get important insights and a comprehensive understanding of progress information, exceeding the limitation of traditional comparison. The proposed methodology focuses on identifying the possible errors and identifies the detected as-built component by leveraging the planned information and analyzing the geometrical surfaces of models. The proposed methodology detailed in this chapter consists of three main stages: preliminary reasoning, detection analysis, and as-built progress detection. The first stage involves the reasoning measures to reduce the progress error based on the sequencing and time-related schedule of building components by extracting the semantic information from BIM models through the IFC schema. Later, detection analysis is performed that first develops a detection model from the BIM model for more conformable comparison and then classifies its surfaces by identifying the occlusion. In the end, as-built progress is accurately estimated by considering the possible errors during comparison and then predicting the non-exposed surfaces as-built surfaces. These advancements in the improved comparison provide accurate as-built progress information with additional parameters.

Chapter 6 describes the exchange of information during the complete process of construction progress monitoring by providing a comprehensive framework. It outlines the process of effectively communicating progress information to a BIM model through a task-based systematic approach, ensuring efficient and accurate progress monitoring. A detailed methodology is provided that includes the four stages to perform the exchange of progress information with the BIM model using the latest IFC-based schema. The IFC entities to accommodate the progress information are integrated into the BIM model in the first stage while their corresponding values for planned progress are inputted in the second stage. A separate third stage, designed to facilitate the frequent incorporation of actual progress, enriches the BIM model with the latest actual progress. In the end, the retrieval of progress information to report the construction progress monitoring is carried out. The approach not only identifies the standard progress parameters but also incorporates the estimation of additional progress indicators, such as earned value analysis, to provide valuable insights. The methodology is well explained and supplemented with the required IFC modification algorithm, values estimation, and the relevant IFC hierarchy of entities. In addition to incorporate standard progress information such as time-related schedules or costs, the framework also facilitates the integration of supplementary semantic progress information that might not align with the predefined IFC entities such as additional progress parameters, textual comments, etc. If the native IFC entity supports it, all the information is stored within it; otherwise, a designated property set is assigned to accommodate the information. In the end, a web-based application was also developed to report the construction

progress with additional progress indicators including earned values in an efficient and human-friendly way.

The last chapter of the dissertation presents the summary of the contributions made throughout the study, discusses the limitations and offers valuable suggestions for further research in the future.

## 1.5 Scientific Contributions

The challenges to improve the automated construction progress monitoring through different phases of model-based assessment are presented in section 1.2.2 . The remaining sections of this dissertation address these challenges for which a brief outline is provided in section 1.3 . A concise list detailing the main research contributions made in this dissertation is presented below:

- **Outcome 1:** Proposed two different novel methods based on building geometry to perform the automated registration of as-built scan with the as-planned BIM.
  - Methods are based on two evident geometric features of buildings: planes and corner points
  - Directly extract the Geometry of the as-planned model directly from BIM using the IFC schema
  - Works accurately for the as-built scan of under-construction buildings
- **Outcome 2:** Improved the traditional comparison process for under-construction buildings to infer their accurate as-built information
  - Evaluation of progress information through reasoning measures based on time-related schedule and components execution sequencing information extracted from BIM model
  - Develops a revised model from an as-planned model representing a compatible surface for its comparison with the as-built model
  - Classify the as-built scan surface based on the errors and coverage
  - Accurately detects the exposed as-built surface and also predicts the non-exposed as-built surface.
- **Outcome 3:** developed a comprehensive BIM-based progress monitoring framework to enable the automated estimation and exchange of progress information effectively between different stakeholders and the construction site.
  - Comprehensive methodology with a task-based approach
  - Introduced the algorithms to integrate the relevant IFC entities using the latest IFC4.x schema.
  - Enables the integration of progress information

- Not only integrate the time-related information but also the cost as well as any other non-standardized information including the site inspection notes, delay reasons, additional progress indicators, etc.
- Also computes the additional progress indicators including earned value analysis
- Allows the reporting of construction progress in a user-friendly way

## 1.6 Publications

The findings of this PhD research have been published in scientific journals and international conferences. The following list is the research publications produced during the PhD research.

### 1.6.1 Publications in international journals

Followings are the research articles published in high-impact international journals factors with A1 ratings.

1. Sheik, N. A., Deruyter, G., & Veelaert, P. (2022). Plane-based robust registration of a building scan with its BIM. *Remote Sensing*, 14(9), 1979. <https://doi.org/10.3390/rs14091979>
2. Sheik, N. A., Veelaert, P., & Deruyter, G. (2022). Registration of Building Scan with IFC-Based BIM Using the Corner Points. *Remote Sensing*, 14(20), 5271. <https://doi.org/10.3390/rs14205271>
3. Sheik, N. A., Veelaert, P., & Deruyter, G. (2023). Exchanging Progress Information Using IFC-Based BIM for Automated Progress Monitoring. *Buildings*, 13(9), 2390. <https://doi.org/10.3390/buildings13092390>

### 1.6.2 Publications in proceedings of international conferences

Followings are the research articles published in international conferences proceedings with C1 rating.

1. Sheik, N. A., Deruyter, G., & Velaerts, P. (2022). Automated Registration of Building Scan with BIM through Detection of Congruent Corner Points. In *The 7th International Conference on Smart City Applications (Vol. 48, pp. 179-185)*. Copernicus GmbH.
2. Sheik, N. A., Deruyter, G., Veelaert, P., & De Wulf, A. (2022). A first step towards automatic construction progress monitoring. In *XXVII FIG Congress 2022*.



## 1.7 References

1. Kim, M.J.; Chi, H.-L.; Wang, X.; Ding, L. Automation and robotics in construction and civil engineering. *Journal of Intelligent & Robotic Systems* **2015**, *79*, 347.
2. Abdel-Wahab, M.; Vogl, B. Trends of productivity growth in the construction industry across Europe, US and Japan. *Construction management and economics* **2011**, *29*, 635-644.
3. Alizadehsalehi, S.; Yitmen, I. A concept for automated construction progress monitoring: technologies adoption for benchmarking project performance control. *Arabian Journal for Science and Engineering* **2019**, *44*, 4993-5008.
4. Pučko, Z.; Šuman, N.; Rebolj, D. Automated continuous construction progress monitoring using multiple workplace real time 3D scans. *Advanced Engineering Informatics* **2018**, *38*, 27-40.
5. Ibrahimkhil, M.; Shen, X.; Barati, K. Enhanced Construction Progress Monitoring through Mobile Mapping and As-Built Modeling. In Proceedings of ISARC. Proceedings of the International Symposium on Automation and Robotics in Construction; pp. 916-923.
6. Bosché, F. Automated recognition of 3D CAD model objects in laser scans and calculation of as-built dimensions for dimensional compliance control in construction. *Advanced engineering informatics* **2010**, *24*, 107-118.
7. Navon, R. Research in automated measurement of project performance indicators. *Automation in Construction* **2007**, *16*, 176-188.
8. Zhang, X.; Bakis, N.; Lukins, T.C.; Ibrahim, Y.M.; Wu, S.; Kagioglou, M.; Aouad, G.; Kaka, A.P.; Trucco, E. Automating progress measurement of construction projects. *Automation in Construction* **2009**, *18*, 294-301.
9. Rebolj, D.; Pučko, Z.; Babič, N.Č.; Bizjak, M.; Mongus, D. Point cloud quality requirements for Scan-vs-BIM based automated construction progress monitoring. *Automation in Construction* **2017**, *84*, 323-334.
10. Arditi, D.; Gunaydin, H.M. Total quality management in the construction process. *International Journal of Project Management* **1997**, *15*, 235-243.
11. Zhang, C.; Arditi, D. Automated progress control using laser scanning technology. *Automation in construction* **2013**, *36*, 108-116.
12. Golparvar-Fard, M.; Pena-Mora, F.; Savarese, S. Automated progress monitoring using unordered daily construction photographs and IFC-based building information models. *Journal of Computing in Civil Engineering* **2014**, *29*, 04014025.
13. Han, K.; Degol, J.; Golparvar-Fard, M. Geometry-and Appearance-Based Reasoning of Construction Progress Monitoring. *Journal of Construction Engineering and Management* **2017**, *144*, 04017110.
14. Bevan, M.; Steve, J. LCI National Webinar: Preliminary findings from national project performance research. 2016.
15. Matthews, J.; Love, P.E.; Heinemann, S.; Chandler, R.; Rumsey, C.; Olatunji, O. Real time progress management: Re-engineering processes for cloud-based BIM in construction. *Automation in Construction* **2015**, *58*, 38-47.

16. Akinsiku, O.E.; Akinsulire, A. Stakeholders Perception of the Causes and Effects of Construction Delays on Project Delivery. *Journal of Construction Engineering and Project Management* **2012**, *2*, 25-31.
17. Chan, A.P.; Chan, A.P. Key performance indicators for measuring construction success. *Benchmarking: an international journal* **2004**, *11*, 203-221.
18. Love, P.E.; Zhou, J.; Sing, C.-p.; Kim, J.T. Documentation errors in instrumentation and electrical systems: Toward productivity improvement using System Information Modeling. *Automation in Construction* **2013**, *35*, 448-459.
19. Golparvar-Fard, M.; Peña-Mora, F.; Savarese, S. Automated Progress Monitoring Using Unordered Daily Construction Photographs and IFC-Based Building Information Models. *Journal of Computing in Civil Engineering* **2015**, *29*, 04014025, doi:10.1061/(asce)cp.1943-5487.0000205.
20. Han, K.K.; Golparvar-Fard, M. Automated monitoring of operation-level construction progress using 4D BIM and daily site photologs. In Proceedings of Construction Research Congress 2014: Construction in a Global Network; pp. 1033-1042.
21. Omar, T.; Nehdi, M.L. Automated Data Collection for Progress Tracking Purposes: A Review of Related Techniques. In Proceedings of International Congress and Exhibition " Sustainable Civil Infrastructures: Innovative Infrastructure Geotechnology"; pp. 391-405.
22. Fang, J.; Li, Y.; Liao, Q.; Ren, Z.; Xie, B. Construction Progress Control And Management Measures Analysis. *Smart Construction Research* **2018**.
23. Golparvar-Fard, M.; Savarese, S.; Peña-Mora, F. Interactive Visual Construction Progress Monitoring with D4 AR—4D Augmented Reality—Models. In Proceedings of Construction Research Congress 2009: Building a Sustainable Future; pp. 41-50.
24. Braun, A.; Tuttas, S.; Borrmann, A.; Stilla, U. A concept for automated construction progress monitoring using BIM-based geometric constraints and photogrammetric point clouds. *Journal of Information Technology in Construction (ITcon)* **2015**, *20*, 68-79.
25. Omar, H.; Dulaimi, M. Using BIM to automate construction site activities. *Building Information Modelling (BIM) in Design, Construction and Operations* **2015**, *149*, 45.
26. Tuttas, S.; Braun, A.; Borrmann, A.; Stilla, U. Acquisition and consecutive registration of photogrammetric point clouds for construction progress monitoring using a 4D BIM. *PFG—journal of photogrammetry, remote sensing and geoinformation science* **2017**, *85*, 3-15.
27. Wei, W.; Lu, Y.; Zhong, T.; Li, P.; Liu, B. Integrated vision-based automated progress monitoring of indoor construction using mask region-based convolutional neural networks and BIM. *Automation in Construction* **2022**, *140*, 104327.
28. Khairadeen Ali, A.; Lee, O.J.; Lee, D.; Park, C. Remote Indoor Construction Progress Monitoring Using Extended Reality. *Sustainability* **2021**, *13*, 2290.

29. Solihin, W.; Eastman, C. Classification of rules for automated BIM rule checking development. *Automation in construction* **2015**, *53*, 69-82.
30. Bosche, F.; Haas, C.T. Automated retrieval of 3D CAD model objects in construction range images. *Automation in Construction* **2008**, *17*, 499-512.
31. Kim, C.; Son, H.; Kim, C. Automated construction progress measurement using a 4D building information model and 3D data. *Automation in construction* **2013**, *31*, 75-82.
32. Tang, P.; Huber, D.; Akinici, B.; Lipman, R.; Lytle, A. Automatic reconstruction of as-built building information models from laser-scanned point clouds: A review of related techniques. *Automation in construction* **2010**, *19*, 829-843.
33. Turkan, Y.; Bosche, F.; Haas, C.T.; Haas, R. Automated progress tracking using 4D schedule and 3D sensing technologies. *Automation in Construction* **2012**, *22*, 414-421, doi:10.1016/j.autcon.2011.10.003.
34. Fathi, H.; Dai, F.; Lourakis, M. Automated as-built 3D reconstruction of civil infrastructure using computer vision: Achievements, opportunities, and challenges. *Advanced Engineering Informatics* **2015**, *29*, 149-161, doi:10.1016/j.aei.2015.01.012.
35. Golparvar-Fard, M.; Pena-Mora, F.; Savarese, S. Monitoring changes of 3D building elements from unordered photo collections. In Proceedings of Computer Vision Workshops (ICCV Workshops), 2011 IEEE International Conference on; pp. 249-256.
36. Golparvar-Fard, M.; Peña-Mora, F.; Savarese, S. Automated progress monitoring using unordered daily construction photographs and IFC-based building information models. *Journal of Computing in Civil Engineering* **2012**, *29*, 04014025.
37. Brilakis, I.; Lourakis, M.; Sacks, R.; Savarese, S.; Christodoulou, S.; Teizer, J.; Makhmalbaf, A. Toward automated generation of parametric BIMs based on hybrid video and laser scanning data. *Advanced Engineering Informatics* **2010**, *24*, 456-465.
38. El-Omari, S.; Moselhi, O. Integrating 3D laser scanning and photogrammetry for progress measurement of construction work. *Automation in construction* **2008**, *18*, 1-9.
39. Shahi, A.; Aryan, A.; West, J.S.; Haas, C.T.; Haas, R.C. Deterioration of UWB positioning during construction. *Automation in Construction* **2012**, *24*, 72-80.
40. Bueno, M.; Bosché, F.; González-Jorge, H.; Martínez-Sánchez, J.; Arias, P. 4-Plane congruent sets for automatic registration of as-is 3D point clouds with 3D BIM models. *Automation in Construction* **2018**, *89*, 120-134.
41. Dong, Z.; Liang, F.; Yang, B.; Xu, Y.; Zang, Y.; Li, J.; Wang, Y.; Dai, W.; Fan, H.; Hyyppä, J. Registration of large-scale terrestrial laser scanner point clouds: A review and benchmark. *ISPRS Journal of Photogrammetry and Remote Sensing* **2020**, *163*, 327-342.
42. Besl, P.J.; McKay, N.D. Method for registration of 3-D shapes. In Proceedings of Sensor fusion IV: control paradigms and data structures; pp. 586-606.

43. Yang, J.; Li, H.; Jia, Y. Go-icp: Solving 3d registration efficiently and globally optimally. In Proceedings of Proceedings of the IEEE International Conference on Computer Vision; pp. 1457-1464.
44. Pavlov, A.L.; Ovchinnikov, G.W.; Derbyshev, D.Y.; Tsetserukou, D.; Oseledets, I.V. AA-ICP: Iterative closest point with Anderson acceleration. In Proceedings of 2018 IEEE International Conference on Robotics and Automation (ICRA); pp. 3407-3412.
45. Tazir, M.L.; Gokhool, T.; Checchin, P.; Malaterre, L.; Trassoudaine, L. CICIP: Cluster Iterative Closest Point for sparse–dense point cloud registration. *Robotics and Autonomous Systems* **2018**, *108*, 66-86.
46. Li, J.; Hu, Q.; Ai, M. GESAC: Robust graph enhanced sample consensus for point cloud registration. *ISPRS Journal of Photogrammetry and Remote Sensing* **2020**, *167*, 363-374.
47. Anil, E.B.; Tang, P.; Akinci, B.; Huber, D. Assessment of the quality of as-is building information models generated from point clouds using deviation analysis. In Proceedings of Three-Dimensional Imaging, Interaction, and Measurement; p. 78640F.
48. Zong, W.; Li, M.; Zhou, Y.; Wang, L.; Xiang, F.; Li, G. A Fast and Accurate Planar-Feature-Based Global Scan Registration Method. *IEEE Sensors Journal* **2019**, *19*, 12333-12345.
49. Pavan, N.L.; dos Santos, D.R.; Khoshelham, K. Global Registration of Terrestrial Laser Scanner Point Clouds Using Plane-to-Plane Correspondences. *Remote Sensing* **2020**, *12*, 1127.
50. Theiler, P.; Schindler, K. Automatic registration of terrestrial laser scanner point clouds using natural planar surfaces. *ISPRS Annals of Photogrammetry, Remote Sensing and Spatial Information Sciences* **2012**, *3*, 173-178.
51. Xu, Y.; Boerner, R.; Yao, W.; Hoegner, L.; Stilla, U. AUTOMATED COARSE REGISTRATION OF POINT CLOUDS IN 3D URBAN SCENES USING VOXEL BASED PLANE CONSTRAINT. *ISPRS Annals of Photogrammetry, Remote Sensing & Spatial Information Sciences* **2017**, *4*.
52. Zhang, D.; Huang, T.; Li, G.; Jiang, M. Robust algorithm for registration of building point clouds using planar patches. *Journal of Surveying Engineering* **2012**, *138*, 31-36.
53. He, W.; Ma, W.; Zha, H. Automatic registration of range images based on correspondence of complete plane patches. In Proceedings of Fifth international conference on 3-D digital imaging and modeling (3DIM'05); pp. 470-475.
54. Bassier, M.; Vergauwen, M.; Poux, F. Point Cloud vs. Mesh Features for Building Interior Classification. *Remote Sensing* **2020**, *12*, 2224.
55. Hattab, A.; Taubin, G. 3D rigid registration of cad point-clouds. In Proceedings of 2018 International Conference on Computing Sciences and Engineering (ICCSE); pp. 1-6.
56. Hamledari, H.; McCabe, B.; Davari, S.; Shahi, A. Automated schedule and progress updating of IFC-based 4D BIMs. *Journal of Computing in Civil Engineering* **2017**, *31*, 04017012.

57. Hamledari, H.; Rezazadeh Azar, E.; McCabe, B. IFC-based development of as-built and as-is BIMs using construction and facility inspection data: Site-to-BIM data transfer automation. *Journal of Computing in Civil Engineering* **2017**, *32*, 04017075.
58. Son, H.; Kim, C.; Kwon Cho, Y. Automated schedule updates using as-built data and a 4D building information model. *Journal of Management in Engineering* **2017**, *33*, 04017012.
59. Bosché, F.; Ahmed, M.; Turkan, Y.; Haas, C.T.; Haas, R. The value of integrating Scan-to-BIM and Scan-vs-BIM techniques for construction monitoring using laser scanning and BIM: The case of cylindrical MEP components. *Automation in Construction* **2015**, *49*, 201-213.
60. Braun, A.; Tuttas, S.; Borrmann, A.; Stilla, U. Improving progress monitoring by fusing point clouds, semantic data and computer vision. *Automation in Construction* **2020**, *116*, 103210.
61. Meyer, T.; Brunn, A.; Stilla, U. Change detection for indoor construction progress monitoring based on BIM, point clouds and uncertainties. *Automation in Construction* **2022**, *141*, 104442.
62. Pexman, K.; Lichti, D.D.; Dawson, P. Automated Storey Separation and Door and Window Extraction for Building Models from Complete Laser Scans. *Remote Sensing* **2021**, *13*, 3384.
63. Kavaliuskas, P.; Fernandez, J.B.; McGuinness, K.; Jurelionis, A. Automation of Construction Progress Monitoring by Integrating 3D Point Cloud Data with an IFC-Based BIM Model. *Buildings* **2022**, *12*, 1754.
64. Braun, A.; Tuttas, S.; Borrmann, A.; Stilla, U. A concept for automated construction progress monitoring using bim-based geometric constraints and photogrammetric point clouds. *J. Inf. Technol. Constr.* **2015**, *20*, 68-79.
65. Carrera-Hernández, J.; Levresse, G.; Lacan, P. Is UAV-SfM surveying ready to replace traditional surveying techniques? *International journal of remote sensing* **2020**, *41*, 4820-4837.
66. Abd-Elmaaboud, A.; El-Tokhey, M.; Ragheb, A.; Mogahed, Y. Comparative assessment of terrestrial laser scanner against traditional surveying methods. *Int. J. Eng. Appl. Sci* **2019**, *6*, 79-84.
67. Yang, B.; Dong, M.; Wang, C.; Liu, B.; Wang, Z.; Zhang, B. IFC-based 4D construction management information model of prefabricated buildings and its application in graph database. *Applied Sciences* **2021**, *11*, 7270.
68. Erdélyi, J.; Honti, R.; Funtík, T.; Mayer, P.; Madiev, A. Verification of Building Structures Using Point Clouds and Building Information Models. *Buildings* **2022**, *12*, 2218.
69. Petronijević, M.; Višnjevac, N.; Praščević, N.; Bajat, B. The extension of IFC for supporting 3D cadastre LADM geometry. *ISPRS International Journal of Geo-Information* **2021**, *10*, 297.
70. Bortoluzzi, B.; Efremov, I.; Medina, C.; Sobieraj, D.; McArthur, J. Automating the creation of building information models for existing buildings. *Automation in Construction* **2019**, *105*, 102838.

71. Mihindu, S.; Arayici, Y. Digital construction through BIM systems will drive the re-engineering of construction business practices. In Proceedings of 2008 international conference visualisation; pp. 29-34.
72. Ghaffarianhoseini, A.; Tookey, J.; Ghaffarianhoseini, A.; Naismith, N.; Azhar, S.; Efimova, O.; Raahemifar, K. Building Information Modelling (BIM) uptake: Clear benefits, understanding its implementation, risks and challenges. *Renewable and sustainable energy reviews* **2017**, *75*, 1046-1053.
73. Söbke, H.; Peralta, P.; Smarsly, K.; Armbruster, M. An IFC schema extension for BIM-based description of wastewater treatment plants. *Automation in Construction* **2021**, *129*, 103777.
74. Gerbert, P.; Castagnino, S.; Rothballer, C.; Renz, A.; Filitz, R. Digital in engineering and construction. *The Boston Consulting Group* **2016**, 1-18.
75. Eastman, C.; Teicholz, P.; Sacks, R.; Liston, K.; Handbook, B. A guide to building information modeling for owners, managers, designers, engineers and contractors. *BIM handbook* **2011**, *2*, 147-150.
76. Arayici, Y.; Aouad, G. Building information modelling (BIM) for construction lifecycle management. *Construction and Building: Design, Materials, and Techniques* **2010**, *2010*, 99-118.
77. Succar, B. Building information modelling framework: A research and delivery foundation for industry stakeholders. *Automation in construction* **2009**, *18*, 357-375.
78. Azhar, S.; Khalfan, M.; Maqsood, T. Building information modeling (BIM): now and beyond. *Australasian Journal of Construction Economics and Building, The* **2012**, *12*, 15-28.
79. Lopez, R.; Chong, H.-Y.; Wang, X.; Graham, J. Technical review: Analysis and appraisal of four-dimensional building information modeling usability in construction and engineering projects. *Journal of Construction Engineering and Management* **2016**, *142*, 06015005.
80. Li, C.Z.; Xue, F.; Li, X.; Hong, J.; Shen, G.Q. An Internet of Things-enabled BIM platform for on-site assembly services in prefabricated construction. *Automation in construction* **2018**, *89*, 146-161.
81. Deng, Y.; Gan, V.J.; Das, M.; Cheng, J.C.; Anumba, C. Integrating 4D BIM and GIS for construction supply chain management. *Journal of construction engineering and management* **2019**, *145*, 04019016.
82. Vieira, R.; Carreira, P.; Domingues, P.; Costa, A.A. Supporting building automation systems in BIM/IFC: reviewing the existing information gap. *Engineering, Construction and Architectural Management* **2020**.
83. 16739-1; I. Industry Foundation Classes (IFC) for data sharing in the construction and facility management industries—Part 1: Data schema. **2018**.
84. Noardo, F.; Wu, T.; Ohori, K.A.; Krijnen, T.; Stoter, J. IFC models for semi-automating common planning checks for building permits. *Automation in Construction* **2022**, *134*, 104097.
85. Koo, B.; Shin, B. Applying novelty detection to identify model element to IFC class misclassifications on architectural and infrastructure Building

- Information Models. *Journal of Computational Design and Engineering* **2018**, *5*, 391-400.
86. Lam, K.; Wong, N.; Shen, L.; Mahdavi, A.; Leong, E.; Solihin, W.; Au, K.; Kang, Z. Mapping of industry building product model for detailed thermal simulation and analysis. *Advances in Engineering Software* **2006**, *37*, 133-145.
  87. Ma, Z.; Teng, M.; Ren, Y. Method of extracting static data for building energy consumption monitoring from BIM. *J. Harbin Inst. Technol* **2019**, *51*, 187-193.
  88. Xu, Z.; Wang, X.; Xiao, Y.; Yuan, J. Modeling and performance evaluation of PPP projects utilizing IFC extension and enhanced matter-element method. *Engineering, Construction and Architectural Management* **2020**, *27*, 1763-1794.
  89. Zhang, J.; Yu, F.; Li, D.; Hu, Z. Development and implementation of an industry foundation classes-based graphic information model for virtual construction. *Computer-Aided Civil and Infrastructure Engineering* **2014**, *29*, 60-74.
  90. Zhang, J.; Guo, J.; Wang, S.; Xu, Z. Intelligent facilities management system based on IFC standard and building equipment integration. *Qinghua Daxue Xuebao/Journal of Tsinghua University* **2008**, *48*.
  91. Yu, K.; Froese, T.; Grobler, F. A development framework for data models for computer-integrated facilities management. *Automation in construction* **2000**, *9*, 145-167.





---

# 2

---

## 2. REGISTRATION BASED ON PLANE SEGMENTS

*This chapter is an adapted version from the following original publication:*

Sheik, N. A., Deruyter, G., & Veelaert, P. (2022). Plane-based robust registration of a building scan with its BIM. *Remote Sensing*, 14(9), 1979. <https://doi.org/10.3390/rs14091979>

**Sheik, N. A.**, Deruyter, G., Veelaert, P., & De Wulf, A. (2022). A first step towards automatic construction progress monitoring. In XXVII FIG Congress 2022.

## Abstract

The registration of as-built and as-planned building models is a pre-requisite in automated construction progress monitoring. Due to the numerous challenges associated with the registration process, it is still performed manually. The research study described in this chapter proposes an automated registration method that aligns the as-built point cloud of a building to its as-planned model using its planar features. The proposed method extracts and processes all the plane segments from both the as-built and the as-planned models, then—for both models—groups parallel plane segments into clusters and subsequently determines the directions of these clusters to eventually determine a range of possible rotation matrices. These rotation matrices are then evaluated through a computational framework based on a postulation concerning the matching of plane segments from both models. This framework measures the correspondence between the plane segments through a matching cost algorithm, thus identifying matching plane segments, which ultimately leads to the determination of the transformation parameters to correctly register the as-built point cloud to its as-planned model. The proposed method was validated by applying it to a range of different datasets. The results proved the robustness of the method both in terms of accuracy and efficiency. In addition, the method also proved its correct support for the registration of buildings under construction, which are inherently incomplete, bringing research a step closer to practical and effective construction progress monitoring.

**Keywords:** BIM; point cloud, registration, buildings, automated, 3D model.

## 2.1 Introduction

Numerous studies indicate the precise monitoring of the as-built status of constructions as a critical component of the building process [1-3]. Good monitoring practices not only assure adequate project management, but also allow for the early detection of deviations from, or nonconformity with, the design, thus providing the opportunity to remediate in an early stage to save both time and money [4-6]. Notwithstanding the significance of effective monitoring, the current methods of monitoring progress involve manual data collection and processing, which are time consuming and labor intensive with a dominant human presence, thus entailing several flaws, such as missing or inaccurate information [7-9]. Although the construction industry demands timely and accurate progress monitoring through an automated approach, the development of automated progress monitoring is still at an early stage and has not yet reached the desired efficiency and reliability [10-12].

With the advancement in remote sensing technologies to acquire three-dimensional (3D) data from construction sites, a vast body of research dedicated to improving (or automating) construction monitoring through model-based assessment methods is emerging. In these methods, the actual state of the building in the form of an as-built model is compared to the as-planned model. In most cases, the as-built spatial information is captured in the form of point clouds obtained through image-based 3D reconstruction [3,7,13-17], laser scanning [18-21], or the integration of both techniques [22-24], whereas the as-planned or design information originates from a building information model (BIM) that is converted into a point cloud or another suitable format. Before the comparison, the as-built model is geometrically aligned with the as-planned data through an essential technique known as registration. The effectiveness of model-based assessments depends on the accuracy of the registration of the as-built with the as-planned model. Normally, registration techniques can be classified as either coarse or fine registration. The fine registration of point clouds is commonly achieved through iterative closest point (ICP)-based algorithms [25-28]. However, directly applying this type of registration is likely to fail, because it requires an initial alignment, achieved through a coarse registration. While there is a variety of literature available providing automated solutions for different environments and applications, coarse registrations are mostly performed manually through human involvement, because although they may work relatively well when applied to simple corresponding point clouds or certain scenarios, the probability of failure is quite high given more intricate point clouds [29]. In addition, the presence of working equipment or objects at building construction sites increases the likelihood of noise, occlusions, and missing data in the as-built model, which often limits the effectiveness of the registration. Furthermore, almost always, the as-built model of a completed building is used as input for the registration, and only limited research has been conducted on the registration problem focusing on the alignment of an incomplete building with its as-planned model. As a result, the registration of building models for progress monitoring remains a challenge.

Therefore, instigating research on registration systems that can accurately align a partially completed as-built model will expand the applicability of automated model-based assessment methods for the progress monitoring of buildings under construction.

The current chapter deals with the research related to registration challenge. It proposes a new method to automate the registration of as-planned and as-built building models by particularly leveraging their planar geometry in a highly robust and efficient way, leading to an accurate registration of both models, even if the built structure is not fully completed. First, the possible rotations are determined based on the directions obtained from the clustered plane segments of both building models. Then, the matching segments are estimated in both models based on the geometric details of individual plane segments. Finally, these matching segments are used to identify the most likely rotation and translation the as-built model must be subjected to in order to be fully aligned with the as-planned model.

In Section 2, a literature overview on registration problems is given. Then, the main concept and a detailed explanation of the proposed technique are provided in Section 3. Section 4 describes the experiments along with the results. Section 5 discusses the results of the experimental evaluation of the method. Finally, Section 6 concludes the discussion based on the results and major findings.

## 2.2 Related Work

Registration is an extensively studied research problem, with most efforts dedicated on the registration of two or more point clouds and less on the registration of point clouds with BIM/mesh models, as the latter can be transformed into the former [30]. BIM/mesh are the artificially prepared building models that are utilized for structural comparison with the scan point cloud after registration. Nevertheless, the sampling of BIM/mesh models can deteriorate the precision of the geometrical information and thus introduce registration errors [31]. Similarly, errors, including noise, occlusion, etc., in the scan point cloud also affect the precision of directly extracted geometrical information [32], and thus challenge the geometrical procedures of registration.

The registration problem of point clouds can be reduced to finding the rotation matrix and translational vector to transform the coordinate system (CS) of one point cloud into the CS of the other, thus aligning both point clouds. A rigid transformation has six degrees of freedom (DoF) referring to three translations and three rotation angles in the three-dimensional (3D) space. Often, a coarse-to-fine strategy is applied, meaning that a coarse registration is applied first to get an initial alignment, followed by a fine registration to achieve the utmost correspondence between the matching areas. Directly applying the fine registration without an initial alignment is likely to fail [33].

The registration process can be classified into two major categories: point-based and feature-based approaches. Point-based approaches use corresponding point pairs in both clouds and do not require complex processing algorithms [34,35]. Random sample consensus (RANSAC), proposed by Bolles et al. [36], is extensively used to identify corresponding points. It is an iterative method, where in each iteration, a random selection of sample points is performed in the corresponding point clouds, after which the transformation is calculated to detect the number of inliers. In the end, the transformation with the largest number of inliers is considered to be the most likely and final transformation [37,38]. Another widely used point-based method is the iterative closest point (ICP) algorithm [25], which is based on a strategy where point-to-point distances between the corresponding points in overlapping parts are minimized through iteration. To improve the original ICP algorithm in terms of a weighting strategy, error metric formulation, correspondence building, and outlier rejection, a large number of ICP variants have been proposed [34]. Furthermore, the 4-point congruent sets (4PCS) and their variants make use of coplanar sets of four congruent points with an affine invariant ratio between point clouds through iteration to find correspondences [39-41]. Generally, iterative methods similar to ICP or 4PCS have been proven to be computationally expensive if a good initial alignment is not attained. However, the computation time can be largely reduced if only key points are processed instead of all the points as an alternative solution [42]. The methods that employ this solution include scale-invariant feature transform (SIFT) key points [43,44], virtual intersecting points [45], difference-of-Gaussian (DoG) key points [39], fast point feature histograms (FPFH) key points [46], and semantic feature points [47]. Although all these point-based methods demonstrate the ability to register point clouds, they are still very sensitive to noise, occlusions, differences in the point density of the two point clouds, and scene complexity. Furthermore, these methods also face difficulties in registering large point clouds.

Compared to point-based approaches, feature-based approaches are less affected by noise or outliers, because the registration is based on identified features extracted from the point clouds. These features are geometric primitives formed by lines [48-51], curved surfaces [52], or planes [35,42,53-56]. A lack of these features can result in the failure of these methods; however, man-made structures usually contain an abundance of planar features. Registration using planar features only, instead of whole point clouds, not only reduces the needed computation power but also significantly increases the overall accuracy due to the decreased influence of noise and outliers [34,57]. To apply plane-based registration, the plane segments are first extracted from both point clouds, after which the correspondence between the extracted planes is computed to identify the conjugate/matching planes. To extract the plane segments from the point clouds, frequently used segmentation techniques are RANSAC segmentation [58-60], dynamic clustering [61], Hough transform [62], region growing [63], and voxel-based growing [35]. The quality of the extracted

segments affects the efficiency of plane-based methods. Furthermore, if the normal vectors from a plane are biased, this will eventually lead to the identification of incorrect conjugate/matching planes [42]. To determine the correspondence between the extracted plane segments, discriminative geometric primitives, known as descriptors, are used. This procedure is still challenging due to the lack of reliable and distinct descriptors. Furthermore, a high number of similar planar surfaces extracted from large point clouds increases the difficulty of finding matching/conjugate planes. Therefore, defining descriptors to identify the distinct planes also becomes a challenge. As a consequence, some researchers prefer to manually identify the conjugate/matching planes [64], although research aimed at efficiently solving this problem in an automated environment is ongoing. He et al. [65] determined the matching planes using an interpretation tree based on plane attributes, such as area, normal angle, and centroid. Dold et al. [54] used the area, bounding box, boundary length, and mean intensity value of the planes to identify matching pairs. Brenner et al. [66] proposed the intersection angles formed by a set of three planes to find the matching local geometry in the other point cloud, while Theiler et al. [45] deployed the virtual intersection point of planes as a key point with the help of specialized descriptors to find the matching points for the registration. Xu et al. [35] used a set of three planes that formed 3D virtual corner points and then estimated a coordinate frame using their normal vectors to find their matching set of planes. Similarly, Pavan and dos Santos [67] introduced a global refinement to evade the iterative method using the local consistency of planes. Geometric constraints formed by planes were employed along with similarities in plane properties to identify the correspondence between the planes. Xu, Boerner, Yao, Hoegner and Stilla [42] applied the 4PCS strategy on pairs of voxelized planed patches from both corresponding point clouds to find the 4-plane congruent sets for registration. Recently, Pavan, dos Santos and Khoshelham [57] performed plane-based registration by proposing a global closed-form solution via a graph-based formulation to find plane-to-plane correspondences. All these methods were proposed for the registration of different scans, mostly for urban scenes. Compared to these scans, the registration involved in the model-based assessment of buildings has unique challenges, because the registration is typically performed between a scan-based point cloud and the design model of a building. These challenges include the self-similarities of building components, such as walls or floors, lack of completeness of as-built data, symmetrical geometry of buildings, and occlusion due to objects or machinery present at the construction site during as-built data acquisition [30].

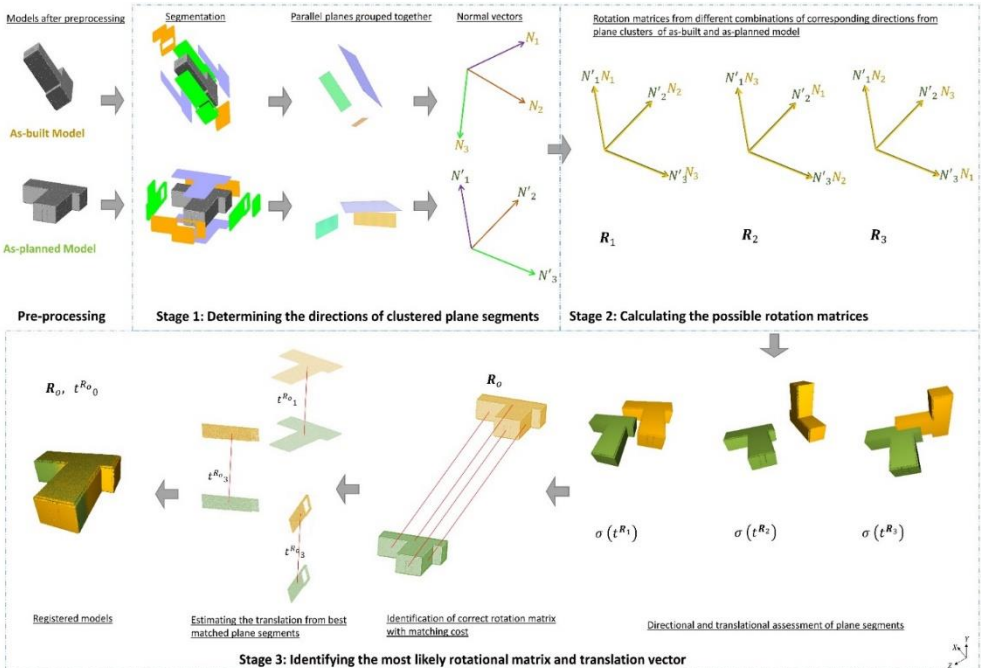
As mentioned before, coarse registration is often applied manually through an n-point approach that requires picking at least three pairs of matching points in both models [1,16,68]; there are few research efforts that propose solutions for automated registration in the context of the progress monitoring of buildings. For example, Kim et al. [69] applied a coarse-to-fine strategy for the registration of the

scanned point cloud to the design model of the building in which principal component analysis (PCA) [70] was used as coarse registration, while LM-ICP [71] was applied as fine registration. In the coarse registration, the rotation was computed from the bases formed by the principal components of both models, and the translation was calculated from the centroids of the models. However, this method assumes that the principal components of both models have the same global directions with congruent centroids, which is only possible if both models are exactly the same. Therefore, this method is not applicable in real-life scenarios involving occlusions, noise, or missing data, which are typical of as-built point clouds of incomplete buildings. Similarly, Chen et al. [72] used a column-based scan registration in which the first columns are detected by projecting the point clouds on a heat map through a rule-based detection scheme. After that, a RANSAC-based strategy that randomly selects two columns from each point cloud in each iteration and calculates the transformation parameters by matching those two columns was applied. Later, all the columns were transformed based on these transformation parameters, and an alignment score based on correctly placed columns was obtained. In the end, the transformation with the highest score was finalized. This method only provides good results for buildings that possess a substantial number of columns. Bueno et al. [30] adapted the 4PCS algorithm that randomly selects the set of four planar patches as candidates for 4-plane bases in which the first three planes are not pair-wise parallel and the fourth plane is not co-planar to any of the other three planes. This method computes the possible transformations based on 4-plane congruent sets and then evaluates these transformations using a two-step support method. In the end, the method clusters the transformations and gives a ranked list of the top five. In this study, three simulated datasets and two real datasets were tested. For the simulated dataset, the correct transformation parameters were ranked first, while for the real datasets the correct transformation parameters were ranked second. Except for Bueno et al. [30], none of the above-mentioned studies address the problem of the incompleteness of data that is typical for buildings in the construction phase. This observation demonstrates the need for research on registration methods in the case of progress monitoring.

### 2.3 Methodology

Generally, buildings have dominant planar geometric features, such as walls or floors, of which a large number are parallel to each other. By clustering the planar structures based on their orientation, nominal clusters—each containing a set of parallel planar structures—can be created to represent the main directions of the building. A typical building has a minimum of three clusters, where one cluster represents parallel floors and roofs, and the others act as walls. In the case of non-horizontal roofs or non-perpendicular walls, the total number of clusters increases. Normally, the as-built models of the building exhibit the same overall geometry as the as-planned model; thus, comparing the directions of the nominal clusters from both models offers an opportunity to determine the possible rotation matrices.

**Figure 2.1** illustrates the general workflow of our method. In the first stage (**Figure 2.1**, Stage 1), the directions of the nominal clusters of parallel plane structures are determined. In the second stage, the possible rotation matrices are calculated based on at least three matching directions (**Figure 2.1**, Stage 2). Finally, in the third stage, the most likely rotation matrix and translation vector are identified (**Figure 2.1**, Stage 3). A pseudo-code outlining the procedural stages for implementing the proposed methodology is presented in Appendix 6 while the detailed explanation of each stage is provided in the following sections.



**Figure 2.1.** Overall Methodology

### 2.3.1 Preprocessing

Data from corresponding as-built and as-planned building models may not be in their best form for comparison; therefore, preprocessing can be necessary as an initial stage, to ensure the geometric parameters of both models can be compared efficiently, thus assuring a robust and accurate registration.

A 3D as-built point cloud acquired through laser scanning is generally dense and accurate; however, it contains noise and outliers which may limit the overall reliability of the registration. Therefore, the point cloud needs to be cleaned completely beforehand through computer algorithms, such as the tensor voting algorithm [73,74]. Furthermore, as high point densities increase the computation time, it can be necessary to down-sample the point cloud using octree-based voxelization. The voxel size must be chosen in function of the desired level of detail

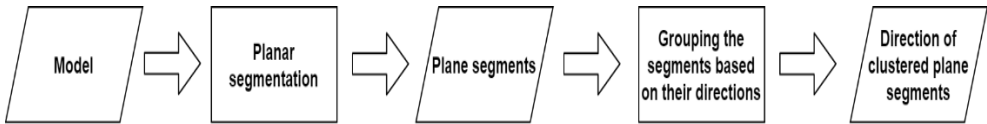


because although the computation time benefits from a larger voxel size, this also causes a loss of detail.

The as-planned model, often a BIM design, can be represented in a triangulated mesh format that contains accurate geometric information, including the vertices and normal values of each building plane. Most researchers convert BIM into a point cloud format for compatibility reasons with the as-built point cloud. However, this practice results in a loss of detail in the as-planned model, which, in turn, causes a loss of accuracy and augments the processing time in later stages. Therefore, it is better to process the as-planned model in a mesh format. A detailed procedure to translate the geometrical information from the IFC-based BIM to construct their structural mesh model is detailed in section 3.3.2.

### 2.3.2 Determining the Directions of Clustered Plane Segments

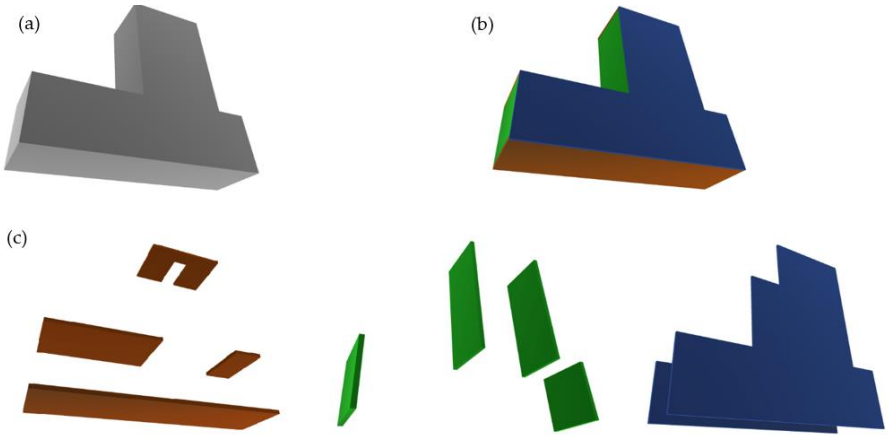
Calculating the direction of clustered plane segments in both the as-planned and as-built models involves two steps, as shown in **Figure 2.2**. In the first step, the model, represented by **Figure 2.3a**, is segmented to extract all of its plane segments (**Figure 2.3b**), which are then clustered based on their orientation in the second step (**Figure 2.3c**). The similar normal values of the plane segments in each cluster act as the directions of the model.



**Figure 2.2.** Workflow for determining the directions of clustered plane segments.

#### 2.3.2.1 Planar Segmentation

The as-built point cloud is first segmented into planar segments with 3D points  $(x,y,z)$  and normal vector  $\mathbf{n}(a,b,c)$  at a distance 'd' from the origin satisfying the plane equation:  $ax + by + cz + d = 0$ , which is performed through RANSAC segmentation. During the segmentation, coplanar segments are handled as one large segment. For extracting the plane structures in the as-planned model, the meshes are split based on their face connectivity.



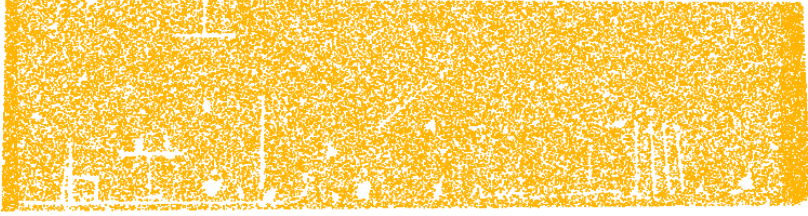
**Figure 2.3.** Visual representation of (a) model, (b) segmented planar components, and (c) planar segments grouped into clusters.

The as-built point cloud may include outliers and occlusions due to the presence of objects in the scene during scanning. On the one hand, to reject outliers, the plane segments are ordered in a hierarchy based on their surface area, where the largest plane segment is ranked first. Only the dominant planes in both models are retained by rejecting the smaller segments based on the suitable threshold expressed as a certain percentage of the area of the largest plane. On the other hand, occlusions have an effect on the determination of the plane centroids, which will be used for calculating the translations in a later stage. For example, the surface coverage of matching plane segments from the as-planned and as-built models, as shown in **Figure 2.4a,b**, respectively, are slightly different due to the occlusions in the as-built point cloud. This problem is mitigated by creating an axis-aligned bounding box of each plane segment in the as-built and BIMs, thus allowing the similar representation of the geometrical shapes in both models (**Figure 2.4a,b**). The example in **Figure 2.4c** shows the bounding box created from the occluded plane segment (**Figure 2.4b**). The centroid calculated from the bounding box is located closer to the center; hence, it is more accurate than the centroid calculated from the occluded point cloud (**Figure 2.4d**).

(a)



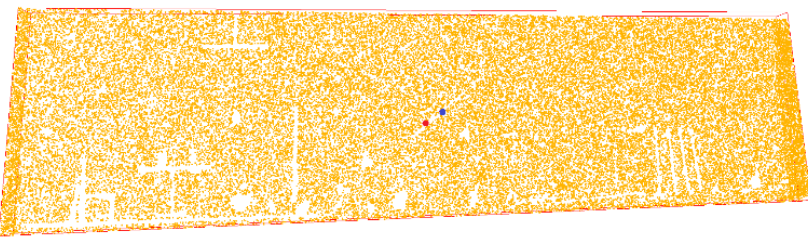
(b)



(c)



(d)



**Figure 2.4.** Visualization of (a) plane segment from BIM, (b) plane segment from original point cloud, (c) bounding box of plane segment created from the point cloud, and (d) centroid points calculated from the original point cloud (red) and from the bounding box (blue).

### *2.3.2.2 Clustering the Plane Segments*

After extracting all the plane segments and determining their geometrical parameters, parallel planes are grouped together into clusters based on their normal vectors. To avoid the failure of the clustering process caused by inaccuracies in the segmentation, a suitable tolerance is introduced in the direction of the normal

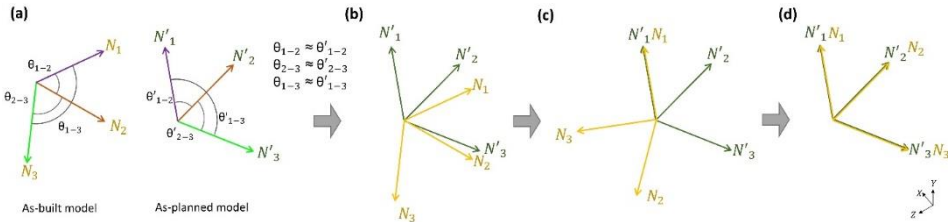
vectors. The direction of a cluster is defined as the weighted average of the normal vectors according to Equation (1):

$$\mathbf{n}_g = \frac{\sum_{i=1}^t \mathbf{n}_i s_i}{\sum_{i=1}^t s_i} \quad (1)$$

In Equation (1),  $\mathbf{n}_g$  is the weighted normal of a cluster of parallel plane segments,  $\mathbf{n}_i$  represents the normal vector of each segment,  $s_i$  is the area of the plane segment  $i$ , and  $t$  is the total number of parallel segments in the cluster. A pseudocode describing the program designed to cluster parallel plane segments is provided in Appendix 7.

### 2.3.3 Calculating the Possible Rotation Matrices

The rotation matrix is calculated from the directions of the plane clusters in both models. First, all the possible combinations of the three plane cluster directions in both models (as-built and as-planned) are made and the angles between the cluster directions in each combination are calculated. Then, for each combination in the as-built model, these angles are compared to all possible combinations within the as-planned model. Combinations with the same angles are withheld. While comparing the angles, a suitable tolerance is applied to account for slight inaccuracies in the directions. **Figure 2.5a** demonstrates an example of a combination with corresponding cluster directions in both models having the same angles.



**Figure 2.5.** Visualization of (a) possible combinations with directions from the clustered plane segments having the same relative angles in the as-built and as-planned model, (b) normal vectors from as-built (yellow) and as-planned (green) models before rotation (c), the alignment of a pair of corresponding normal vectors after the first rotation, and (d) the aligned normal vectors of both models after the final rotation.

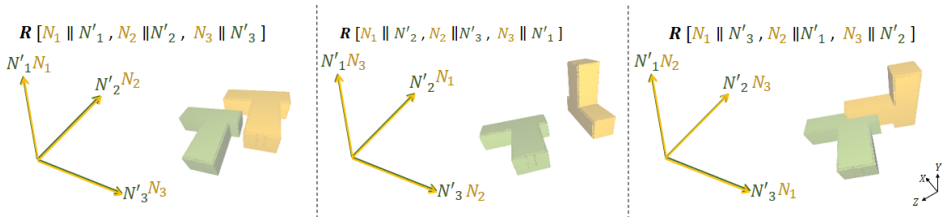
In the next step, for the combinations that were withheld previously, the rotation matrices are determined in two phases. First, the first pair of normal vectors of the as-built and the as-planned models, as shown in **Figure 2.5b**, are aligned with each other by rotating the normal vector of the as-built model around the perpendicular axis, as shown in **Figure 2.5c**. Then, the other normal vectors of the as-built model are simultaneously aligned with their corresponding normal vectors by rotating them about the axis defined by the first rotated normal vector, as shown in **Figure 2.5d**.

The rotation is performed by the Rodriquez rotation formula, given in Equation (2), with an input of the axis of rotation ( $k$ ) and angle ( $\vartheta$ ), given in Equation (3).

$$R(k, \vartheta) = I + k \sin\vartheta + k^2(1 - \cos\vartheta) \quad (2)$$

$$k (k_x, k_y, k_z) = \begin{bmatrix} 0 & -k_z & k_y \\ k_z & 0 & -k_x \\ -k_y & k_x & 0 \end{bmatrix} \quad (3)$$

In the case of the occurrence of corresponding combinations with unique angles between their cluster directions, these clusters can automatically be regarded as being the clusters with matching plane segments. In this ideal scenario, the rotation matrix calculated from these corresponding clusters represents the correct orientation of the as-built model with the as-planned model. However, this ideal scenario seldom occurs, as most buildings have an orthogonal geometry with many parallel structural components. This reduces the number of possible distinct angles between plane clusters; hence, the number of possible rotation matrices ( $R_1, R_2, \dots, R_r$ ) increases substantially. Some rotations resulting from different combinations of the directions of the two models are shown in **Figure 2.6**.



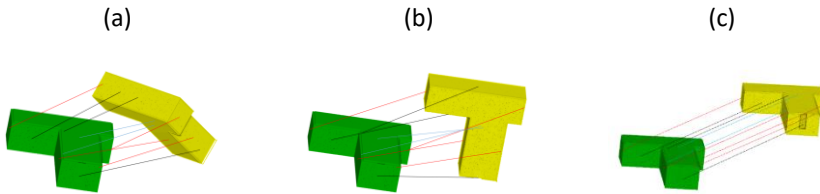
**Figure 2.6.** Example of a few rotation matrices and their respective rotational effect on the as-built model against the alignment of the as-planned model, obtained from different possible combinations by aligning the corresponding normal vectors of clustered segments from the as-built (yellow) and as-planned (green) models.

### 2.3.4 Identifying the Most Likely Rotation Matrix and Translation Vector

Only one of the calculated rotation matrices will lead to the correct orientation of the as-built to the as-planned model. To identify this most likely rotation matrix (and translation vector), a computational framework is proposed here based on the principles that if two models with a similar geometric structure are correctly oriented then:

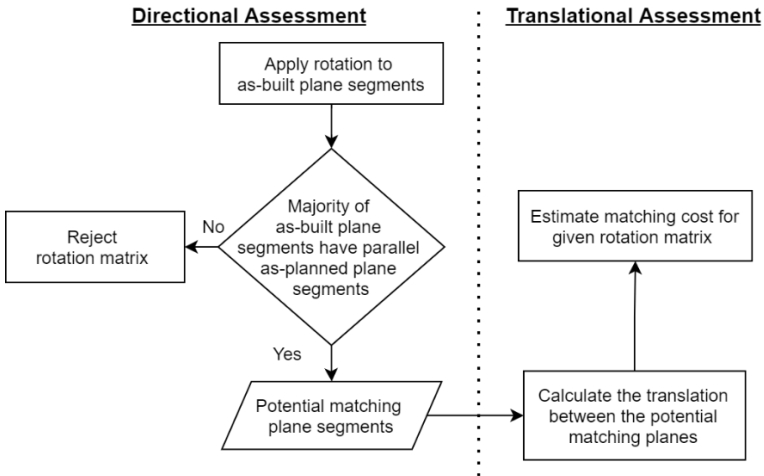
1. Matching plane segments between the two models should be parallel to each other.
2. The translation between the models should be the same for all matching planar segments.

**Figure 2.7** shows a few examples with different orientations of the as-built model relative to the as-planned model to depict how the direction and translation between the matching plane segments can be different if the models are not correctly aligned. Based on this, all the possible rotation matrices are evaluated to identify the rotation matrix offering the most likely alignment. The identification process is performed by assessing the individual plane segments of both models based on their directions and translations for each rotation matrix by computing a matching cost. The details of this calculation are explained below.



**Figure 2.7.** Visualization of the as-built model (yellow) corresponding to the as-planned model (green), with an incorrect orientation (a,b) and correct orientation (c). The lines connecting the matching segments in all orientations represent the corresponding translation.

For each rotation matrix, first a preliminary assessment of the directions of the plane segments from both models is performed to either discard the rotation matrix, because it is an unlikely candidate, or to continue by computing the total matching cost based on potential matching planes. The assessment workflow is shown in **Figure 2.8**.



**Figure 2.8.** General workflow for the assessment of the plane segments for each rotation matrix.

#### 2.3.4.1 Directional Assessment

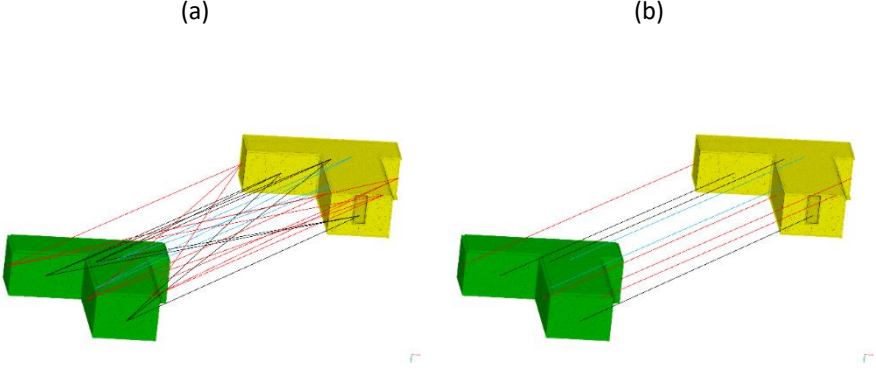
For each rotation matrix, all the plane segments from the as-built model are rotated, after which each rotated plane segment is paired with all the as-planned plane segments. For each pair, the angle between the planes is computed using their normal vector. Pairs of plane segments that are not parallel to each other are rejected, leaving only those pairs with parallel plane segments. If for the majority of the as-built plane segments no parallel plane segments from the as-planned model are found, it is obvious that this particular rotation matrix must be rejected from the list of possible matrices. If, on the other hand, the majority of as-built plane segments have several parallel plane segments in the as-planned model, then the rotation matrix is further scrutinized by considering the pairs of parallel plane segments in the corresponding models as the potential matching plane segments. By lowering the number of rotation matrices based on the directional scrutiny of plane segments, the overall computation time is reduced substantially.

#### 2.3.4.2 Translational Assessment

Once a rotation matrix is accepted, a matching cost that combines the rotation with the most likely translation is computed. For a particular rotation matrix  $R$ , all possible translation vectors  $t^R_{i,j}$  that map a centroid of a plane segment ' $i$ ' of the as-built model onto the centroid of a plane segment ' $j$ ' of the as-planned model are considered. Let  $C_i$  and  $C_j$  denote the centroids of these planes calculated from their bounding boxes earlier in stage 1. Provided the two planes are almost parallel after rotation, the translation vector  $t^R_{i,j}$  for this pair is defined as:

$$t^R_{i,j} = C_j - RC_i \quad (4)$$

The translation vectors determined between all the potential pairs of matching planes for dataset 1 are shown in **Figure 2.9a**. From this set of all possible translation vectors, the most likely translations are selected, as shown in **Figure 2.9b**. Because of noise in the as-built point cloud, the occlusions in some of the as-built plane segments, and small errors in the alignment, plane segments that are supposed to match may still define slightly different translations. Therefore, a minimization process is proposed by allocating a cost to each possible translation vector, which takes into account that some segments may be incomplete or not aligned correctly.



**Figure 2.9.** Representation of all the possible translation vectors  $\mathbf{t}_{i,j}$ , are shown with line colors indicating the parallel plane segments from the (a) potential matching planes and (b) matching planes.

Depending on the translation, each plane segment from the as-built model may have more than one potential matching plane from the as-planned model. Therefore, the assumption is made that the most likely match is the one for which the distance between the centroids is minimal. Let  $\mathbf{t}^R_o$  denote a possible translation and  $\mathbf{R}$  represent one of the rotation matrices. For a particular plane segment 'i' from the as-built model, the most likely matching plane segment of the as-planned model is then  $j = \operatorname{argmin}_j \|\mathbf{t}^R_o - \mathbf{t}^R_{i,j}\|$ . That is, from all possible translation vectors that map the centroid of segment 'i' onto one of the centroids of the as-planned model, the one closest to the proposed translation  $\mathbf{t}^R_o$  is chosen. The total matching cost, as a function of  $\mathbf{t}^R_o$  and  $\mathbf{R}$ , is then defined as:

$$\sigma(\mathbf{t}^R_o) = \frac{\sum_{i=1}^m \left( \min_j \|\mathbf{t}^R_o - \mathbf{t}^R_{i,j}\|^2 \right)}{m} \quad (5)$$

The most likely translation  $\mathbf{t}^R_o$  for rotation matrix  $\mathbf{R}$  is found by minimizing the above total matching cost over a finite set of translation vectors. To further simplify the computation, it is also assumed that the optimal translation vector  $\mathbf{t}^R_o$  will be close to one of the translation vectors  $\mathbf{t}^R_{i,j}$ :

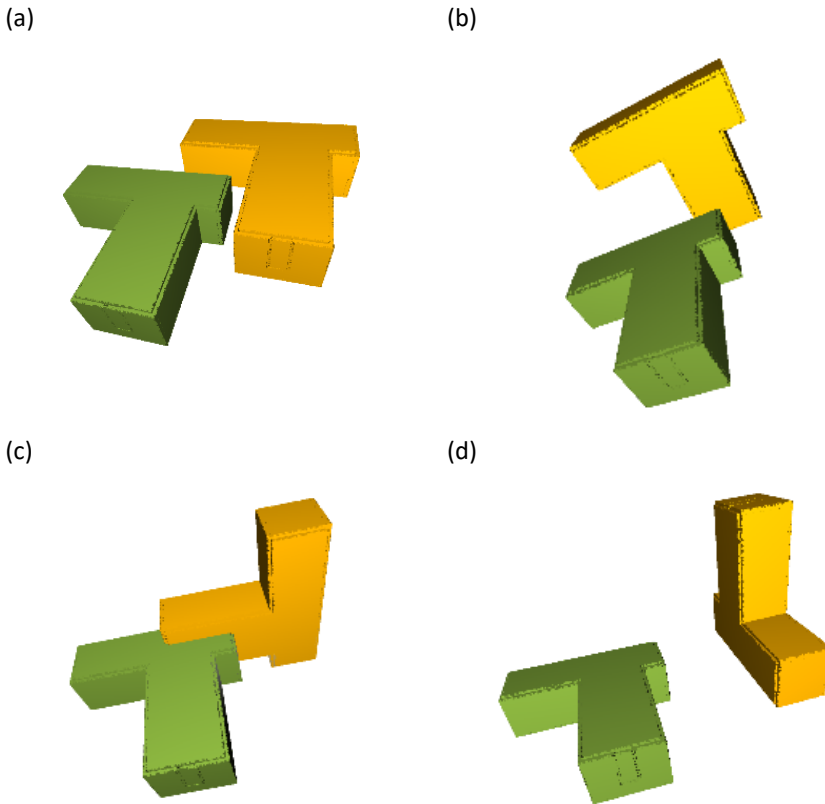
$$\mathbf{t}^R_o \approx \mathbf{t}^R_{p,q} : (p,q) = \operatorname{argmin}_{(i,j)} \sigma(\mathbf{t}^R_{i,j}) \quad (6)$$



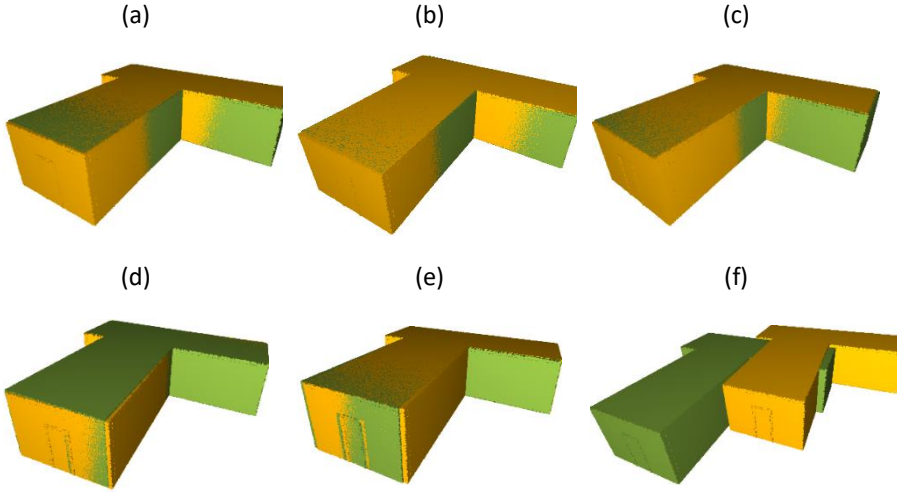
Similarly, the most likely rotation matrix  $R_o$  is also identified from a finite set of pre-filtered rotation matrices.

$$R_o = \underset{R}{\operatorname{argmin}} \sigma(t^{R_o}) \quad R \in \{R_1, R_2, R_3, \dots, R_r\} \quad (7)$$

Hence, the matching cost ensures that the most likely rotation matrix, as compared to other matrices, is measuring the matching of all the corresponding plane segments of both models, as shown in **Figure 2.10**. Similarly, it also confirms the most likely translation is determined from the potential pair of matching plane segments that is offering the maximum overlap of all the matching plane segments, as shown in **Figure 2.11**. To further improve the registration, fine registration using ICP can be performed in the end, if required.



**Figure 2.10.** Visualization of the corresponding as-built model (yellow) relative to the as-planned model (green) sorted with rotation matrices having matching costs( $\sigma$ ): **a)**  $\sigma(t^{R_1_o})=0.4304$ , **b)**  $\sigma(t^{R_2_o})=4.8754$ , **c)**  $\sigma(t^{R_3_o})=5.0401$  and, **d)**  $\sigma(t^{R_4_o})=5.5786$ .



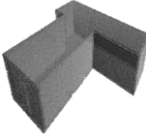

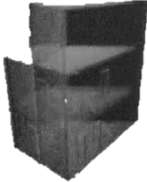



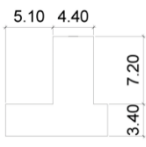
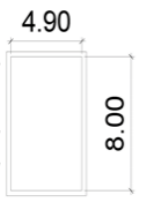
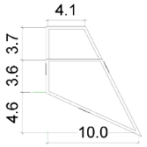

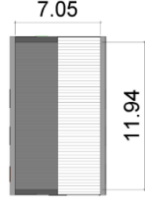

**Figure 2.11.** Visualization of the corresponding models registered with different translation vectors computed from the pairs of the most likely matched plane segments sorted according to their matching costs( $\sigma$ ): **(a)**  $\sigma(t^{R_{0_1}})=0.4304$ , **(b)**  $\sigma(t^{R_{0_2}})=0.4361$ , **(c)**  $\sigma(t^{R_{0_3}})=0.4423$ , **(d)**  $\sigma(t^{R_{0_4}})=0.4448$ , **(e)**  $\sigma(t^{R_{0_5}})=0.4783$  and, **(f)**  $\sigma(t^{R_{0_6}})=0.5874$ .

## 2.4 Results

The proposed method was validated by tests on different datasets, including both simulated and real-life datasets that were different from each other in terms of their architectural shape, the number of planes, and the number of 3D points in their as-built model. The simulated data were used to validate the theoretical framework, while the real-life datasets helped in understanding the practical difficulties and limitations of the proposed method in real building projects.

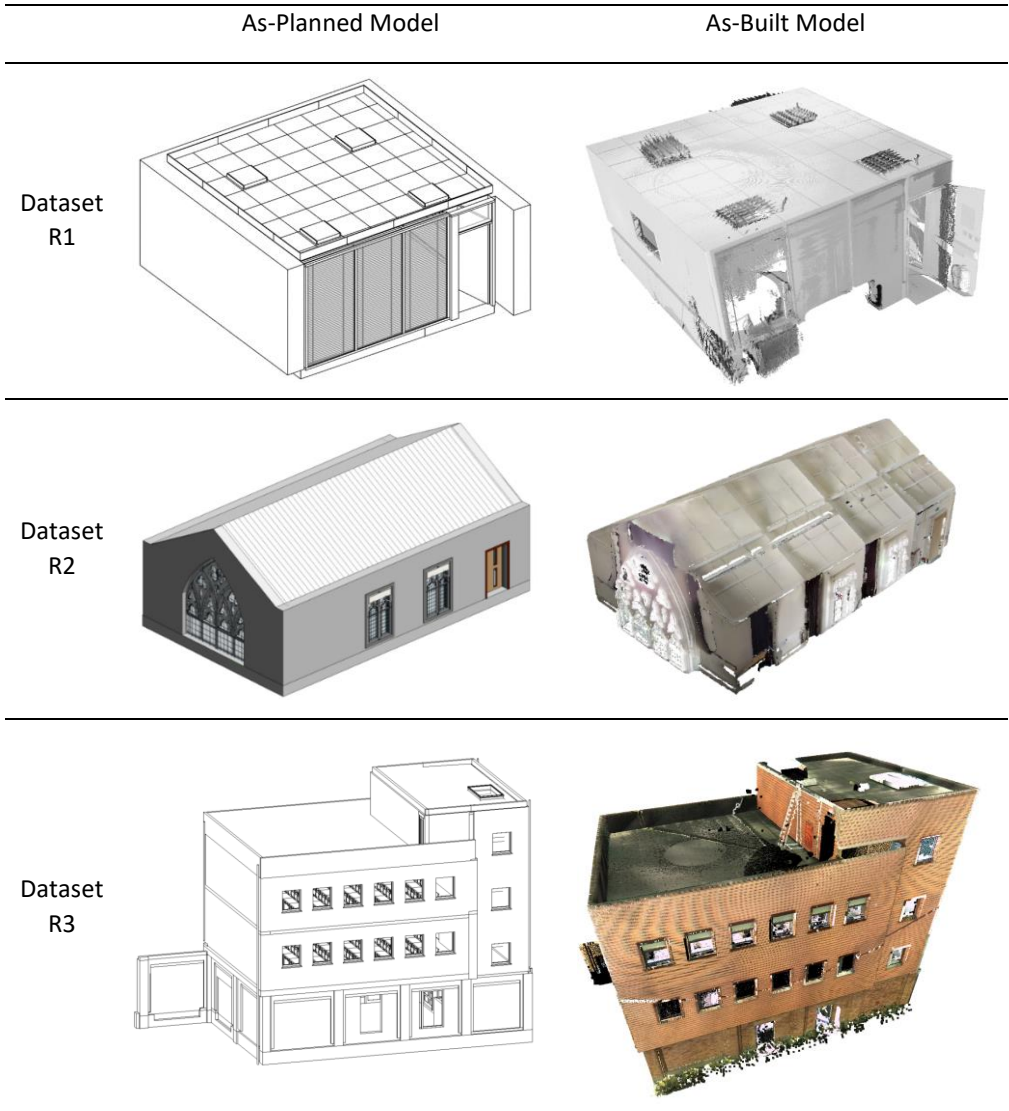
For the simulated datasets (S1, S2, and S3), the as-built model was derived from the as-planned model with random transformation. The registration of the as-built model with its original model allowed us to analyze the proposed method without any influence of factors including noise, outliers, or missing information. The real-life case studies (datasets R1, R2, and R3) were carried out to test the validity of the proposed method using laser scan data for the as-built model together with the BIM model of the same existing building.

*Table 2.1.* Details of simulated datasets.

	Dataset S1	Dataset S2	Dataset S3	Dataset R1	Dataset R2	Dataset R3
3D view of as-built model						
Dimensions from top view (m)						
Height (m)	3	27	9	2.55	5.21	14.6
Area per floor (m <sup>2</sup> )	69	Each floor: 39.2	1st and 2nd floor: 56 3rd floor: 38.8	18.7	84.2	1st, 2nd, and 3rd floor: 200 4th floor: 75
No. of plane segments	9	14	9	6	6	10
No. of 3D points in the as-built model	1,000,006	2,485,913	1,364,741	79,537,667	3,580,303	64,773,370

The real-life dataset R1 represents a point cloud scan of office space acquired using a Faro Focus 120 scanner. It comprises around seventy nine million 3D points and includes six plane segments structurally. Similarly, dataset R2 constitute an indoor point cloud scan, acquired by laser scanner, capturing the architectural details of a building hall with a distinctive gabled roof structure. It contains nearly 3.5 million 3D points, covering an area of 84.2 square meters per floor, and features six plane segments. The last dataset R3 is a point cloud scan of four-storey structure captured

with terrestrial laser scanner. A comprehensive collection effort involving 53 scans yielded a densely populated dataset exceeding 500 million points. This dataset has previously been utilized in studies referenced as [75,76]. The geometric details of all the datasets are presented in **Table 2.1**, and the real-life datasets R1, R2, and R3 are shown in more detail in **Figure 2.12**.

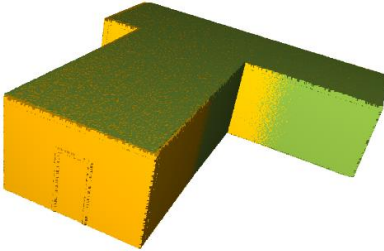


**Figure 2.12.** Visualization of BIM (as-planned model) and scan (as-built model) from dataset R1, R2, and R3.

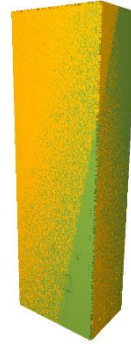
All the datasets, both simulated and real, were successfully registered using the proposed method. **Figure 2.13** shows the registration results for all the datasets,

while the respective processing details of the registration are listed in **Table 2.2**. The reported results were obtained by initially down-sampling the as-built cloud points during preprocessing using a voxel size of 0.2 m. Similarly, plane segmentation was performed using RANSAC with the number of iterations limited to 3000. Furthermore, because the directions of the plane segments can be slightly faulty due to the presence of noise in the point cloud, a suitable tolerance level according to the datasets was set for the normal values of plane segments during the process of clustering to determine the directions of clustered plane segments. All the processing was conducted on a laptop with an Intel i7-8850H CPU with 16 GB RAM and the proposed method was implemented in the Python language. The proposed method was further analyzed in terms of processing time and accuracy to evaluate its performance and explore its limitations.

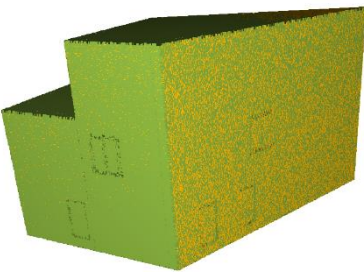
(a)



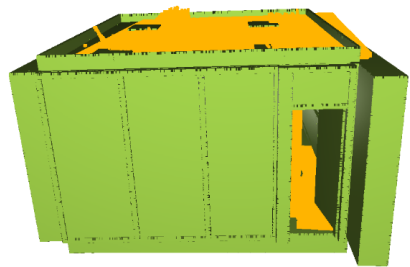
(b)



(c)

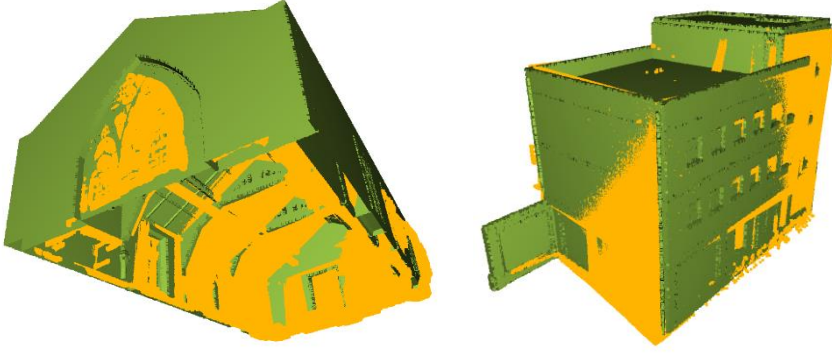


(d)



(e)

(f)



**Figure 2.13.** Visualization of the registered as-built (yellow) and as-planned (green) models of (a) dataset S1, (b) dataset S2, (c) dataset S3, (d) dataset R1, (e) dataset R2 and, (f) dataset R3.

**Table 2.2.** Registration details of all the datasets, including the computation of the correct rotation matrix and identical translation.

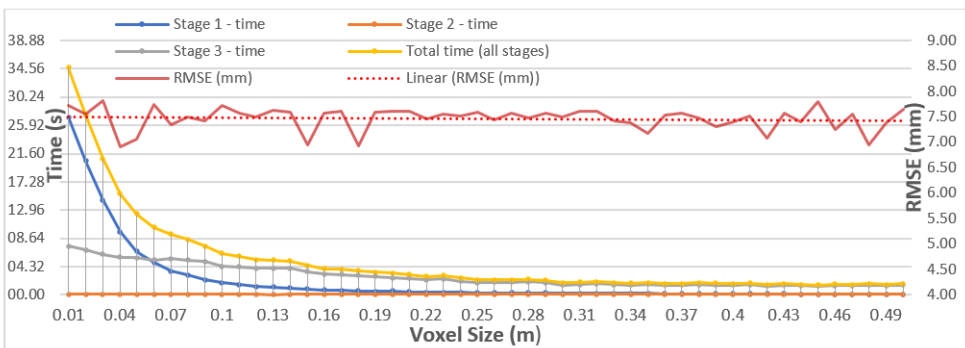
	Dataset No.	Dataset S1	Dataset S2	Dataset S3	Dataset R1	Dataset R2	Dataset R3
	No. of plane segments	9	14	9	6	6	10
No. of directions from plane segment clusters	3	3	5	3	4	4	
Processing time (s)	3.18	47.43	15.48	3.96	5.01	23.92	
RMSE (mm)	7.186	9.278	8.792	18.119	23.205	17.781	
Matching cost	According to each possible rotation $(R_1, R_2, R_3, \dots, R_r)$	<b>0.430</b>	<b>1.787</b>	<b>0.825</b>	<b>2.214</b>	<b>1.866</b>	<b>3.471</b>
	$\sigma(t^{R_1}_o)$	4.875	15.984	3.588	4.742	4.053	8.281
	$\sigma(t^{R_2}_o)$	5.040	20.721	4.350	4.985	5.095	16.335
	$\sigma(t^{R_3}_o)$	5.578	21.571	4.522	5.383	7.047	19.784
	According to the translation of matching plane segments	<b>0.430</b>	<b>1.787</b>	<b>0.825</b>	<b>2.214</b>	<b>1.866</b>	<b>3.471</b>
	$\sigma(t^{R_0_1})$	0.436	1.795	0.825	2.235	1.876	3.503
	$\sigma(t^{R_0_2})$	0.442	1.797	0.830	2.290	2.090	3.571
	$\sigma(t^{R_0_3})$	0.444	1.800	0.855	2.477	2.364	3.864
	$\sigma(t^{R_0_4})$						

## 2.5 Discussion

### 2.5.1 Time Efficiency

The time efficiency of the proposed technique was analyzed in detail. First, the effect of voxel size on processing time was examined. Generally, a decrease in voxel size increased the size of the point cloud, which in turn increased the processing time. However, an increase in voxel size induces a loss of detail, leading to a possible decrease in the registration accuracy. Hence, a compromise must be found. Therefore, the processing time of the different processing stages (illustrated in **Figure 2.14**), as well as the overall registration accuracy, were analyzed with a range of different voxel sizes for dataset S1. The results are shown in **Figure 2.14**, where it can be observed that the overall processing time of the method significantly increased once the voxel size was lowered to 0.1m. The time complexity of the proposed technique is  $O(\log n)$ , where  $n$  equals the voxel size in a grid. When the computation time was analyzed per processing stage, it was clear that the overall processing time was not affected by stage 2, while the processing time of stage 3 increased approximately linearly with a decreasing voxel size, and the computation time in stage 1 increased significantly once the voxel size dropped under 0.1 m. This major increment in computation can be attributed to the plane segmentation of the as-built point cloud that is performed using RANSAC segmentation, which estimates the plane from the voxelized points in numerous iterations. Therefore, the voxel size should be chosen to be between 0.1 m and 0.5 m to ensure the success of the proposed method and limit the significant increment in processing time.

To gain insight into the influence of different parameters on the computation time, the overall processing time of all the datasets was further analyzed at a voxel size of 0.2 m, as shown in **Table 2.3**. As could be expected, the total number of plane segments was the determining factor influencing the processing time in stages one and three.

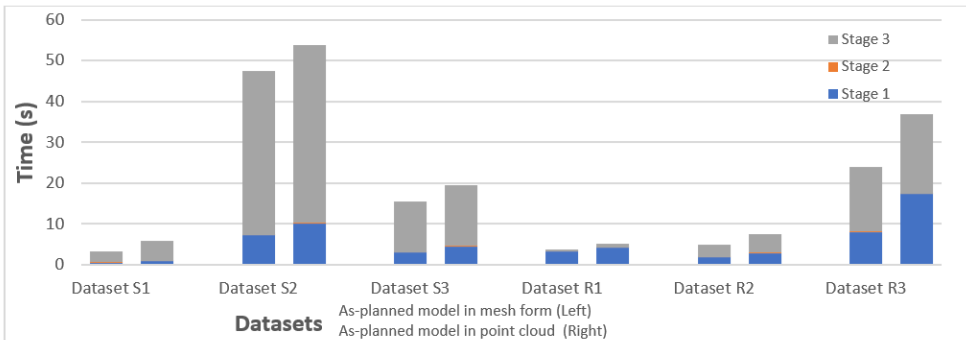


**Figure 2.14.** Graph indicating the processing time and RMSE at different voxel sizes ranging from 0.01 to 0.5 m for dataset 1.

**Table 2.3.** Details concerning the processing time and accuracy error according to each dataset.

Dataset No.	Processing Time				Error		
	Step 1	Step 2	Step 3	Total Time	RMSE	$\epsilon_R$	$\epsilon_t$
	(s)	(s)	(s)	(s)	(mm)	(°)	(mm)
Dataset S1	0.52	0.08	2.58	3.18	7.186	0.007	29.164
Dataset S2	7.19	0.07	40.17	47.43	9.278	0.007	40.961
Dataset S3	2.99	0.09	12.40	15.48	8.792	0.005	35.385
Dataset R1	3.23	0.07	0.39	3.69	18.119	0.027	94.267
Dataset R2	1.82	0.08	3.11	5.01	23.205	0.020	190.482
Dataset R3	8.1	0.08	15.74	23.92	17.781	0.021	107.142

As the proposed method processes the as-planned model from BIM directly into the triangulated mesh instead of the point cloud, the total processing time of the proposed technique was also analyzed by processing the as-planned model in both triangulated mesh and point cloud form. It was found that extracting the geometric parameters directly from the triangulated mesh of the as-planned model instead of converting it into a point cloud had a positive impact on the overall computation time, as shown in **Figure 2.15**. This is due to the fact that the required plane parameters (such as the normal of a plane) can be extracted directly from the mesh model, while in the case of the point cloud, these parameters are calculated from the 3D points of plane segments, which increases the processing time.



**Figure 2.15.** Comparison of computation time of the proposed technique when the as-planned model is processed in a mesh form (left) vs. a point cloud form (right).



### 2.5.2 Registration Accuracy

The accuracy of the proposed method was evaluated by comparing the transformed as-built model to the ground truth model. The ground truth model is the as-planned model and the fine registered as-built model for simulated and real-life datasets, respectively. According to Figure 2.14, the voxel size did not affect the registration accuracy in terms of RMSE. As the root mean square error (RMSE) is not only an effective indicator of registration accuracy [34], the rotation error (in degrees) and translation error (in mm) for each dataset were also calculated, using Equations (8) and (9), respectively.

$$\epsilon_R = |\theta^{GT} - \theta^T| \quad (8)$$

$$\epsilon_t = || \mathbf{t}^{GT} - \mathbf{t}^T || \quad (9)$$

In Equation (8),  $\theta^T$  and  $\theta^{GT}$  denote the respective quaternion rotation angles of the transformed model and the ground truth, whereas  $\mathbf{t}^T$  and  $\mathbf{t}^{GT}$  represent the respective translation vectors of the transformed model and the ground truth in Equation (13). The results of the evaluation metrics are listed in **Table 2.3**; they indicate a good accuracy of the proposed method, however this does not mean that the method has relatively higher accuracy over other methods. This is because the proposed method is a coarse registration method that aims to roughly align the models. The registration accuracy of these roughly aligned models is later achieved through fine registration techniques such as ICP. From the results, it is evident that building structures with an overall simple geometry and fewer planes had relatively higher accuracy. The accuracy in terms of rotation was high in all datasets. This is inherent to the proposed method due to the accurate normal values of plane segments. The normal values of plane segments obtained from the mesh surfaces in the as-planned model are error-free, and the normal values from the as-built model are determined through RANSAC plane estimation with a high iteration value. Furthermore, the proposed method computes the weighted average for parallel segments to ensure a minimal influence of inaccurately extracted normal values, if any.

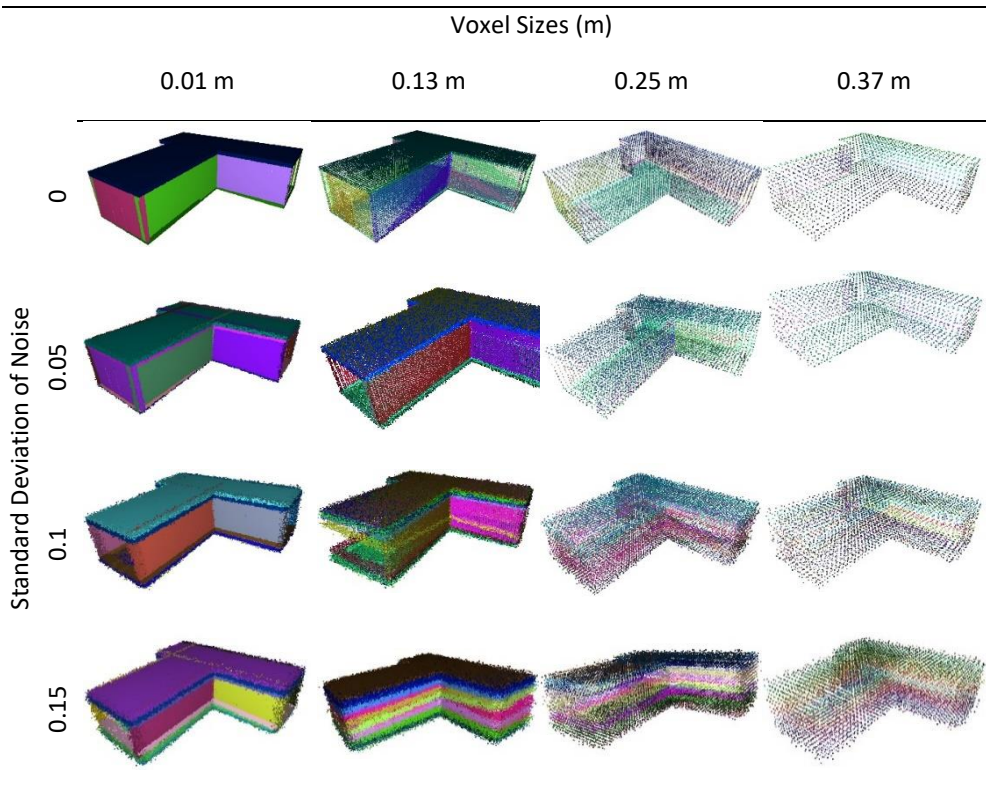
It should be noted that the proposed method depends on plane segments extracted randomly from the as-built model by means of RANSAC plane estimation, and the registration parameters may change slightly each time the proposed method is applied, thus also slightly impacting the resulting registration accuracy. However, these minor changes can be covered by fine registration through an ICP algorithm, if required.

### 2.5.3 Effect of Noise and Occlusion

The effect of noise on the success ratio along with different voxel sizes was also analyzed. It was observed that the voxel size influenced the planar segmentation stage in the proposed method, as a greater voxel size decreased the number of 3D

points in the model. If the amount of 3D points is too low, the planar segmentation may extract inaccurate plane segments from the model, which affects the results of the proposed technique. The presence of noise in the point cloud may hinder the detection of plane segments, thus also attributing to the possible failure of the proposed technique, although this can be solved by decreasing the voxel size. **Table 2.4** illustrates different point cloud models of dataset 1 having Gaussian noise with a variance of zero and a standard deviation ranging from 0 to 0.15. Planar segmentation was performed on these point clouds after down-sampling them with voxel sizes from 0.01 to 0.37 m. It was evident that a higher voxel size enabled the extraction of accurate plane segments, even in the presence of strong noise, for the success of the proposed method.

*Table 2.4.* Segmented as-built point cloud with different noise levels and voxel sizes.

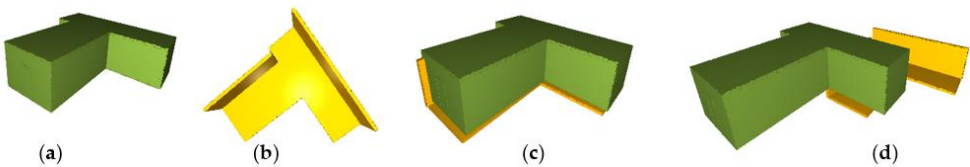


#### 2.5.4 Application on Partially Constructed Buildings

To investigate the registration success of partially constructed as-built models with their as-planned model for automated construction progress monitoring, the proposed method was evaluated using as-built models with different combinations of missing planes simulating different stages of completion. During testing, it was found that the proposed method worked successfully if the necessary conditions were met. These conditions include: (i) as-built models with an overall

unsymmetrical structure should have at least three planes in distinct directions and (ii) the size of most plane segments should correspond highly to their matching segments in the as-planned model. The presence of at least three planes in distinct directions assures that the correct rotation matrix will be calculated in the second stage along with other possible rotation matrices. Similarly, matching plane segments with high geometrical correspondence improve the identification of matching plane segments in the third stage.

Generally, the building models met these two conditions, and even a scan of a small typical building had plane segments in three distinct directions with a point cloud covering the walls for the most part. In the worst scenario, with a major missing part in the point clouds, the registration can further be improved through ICP registration. **Figure 2.16** shows an example of a modified simulated model of dataset 1 with an as-planned model (**Figure 2.16a**) and an as-built model (**Figure 2.16b**) with just three plane segments that were successfully registered through the proposed method. In this example, all three plane segments of the as-planned model had different directions and were identical in size to their corresponding segments. Similarly, it is also evident that the proposed method accurately calculated the translation based on matching planes even if the major part of the model was missing, as compared to the traditional technique based on the centroid of whole models, as shown in **Figure 2.16c,d**.

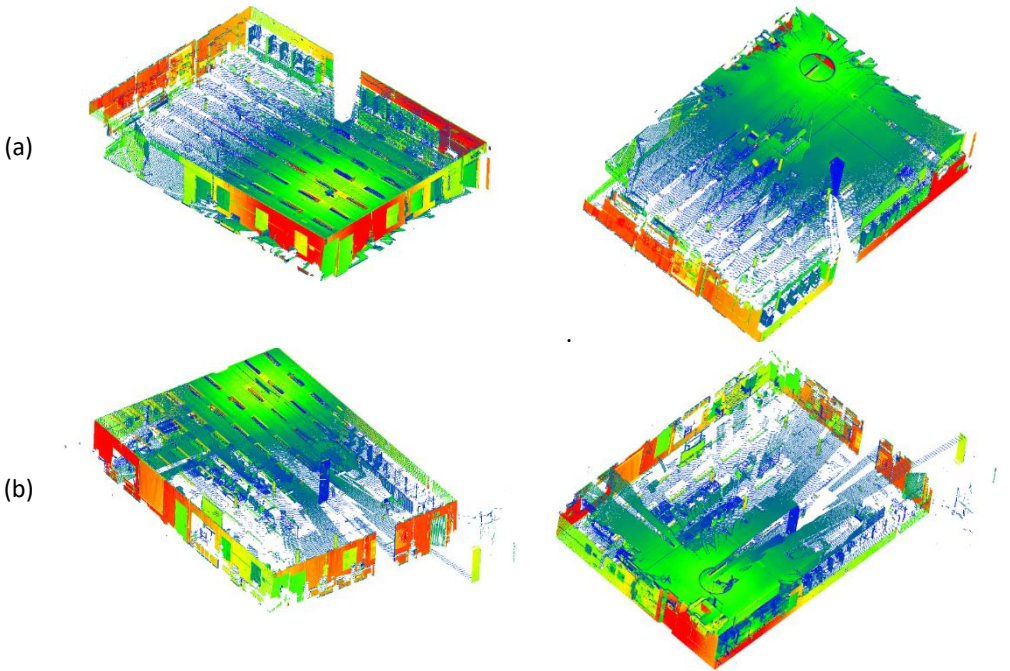


**Figure 2.16.** Visualization of (a) complete as-planned model, (b) incomplete as-built model with only three plane segments in distinct directions, (c) registered model using translation computed from the centroid of matched segments, and (d) registered model using translation computed from the centroid difference of the complete point cloud.

### 2.5.5 Registration of as-builts scans with other scans of same model

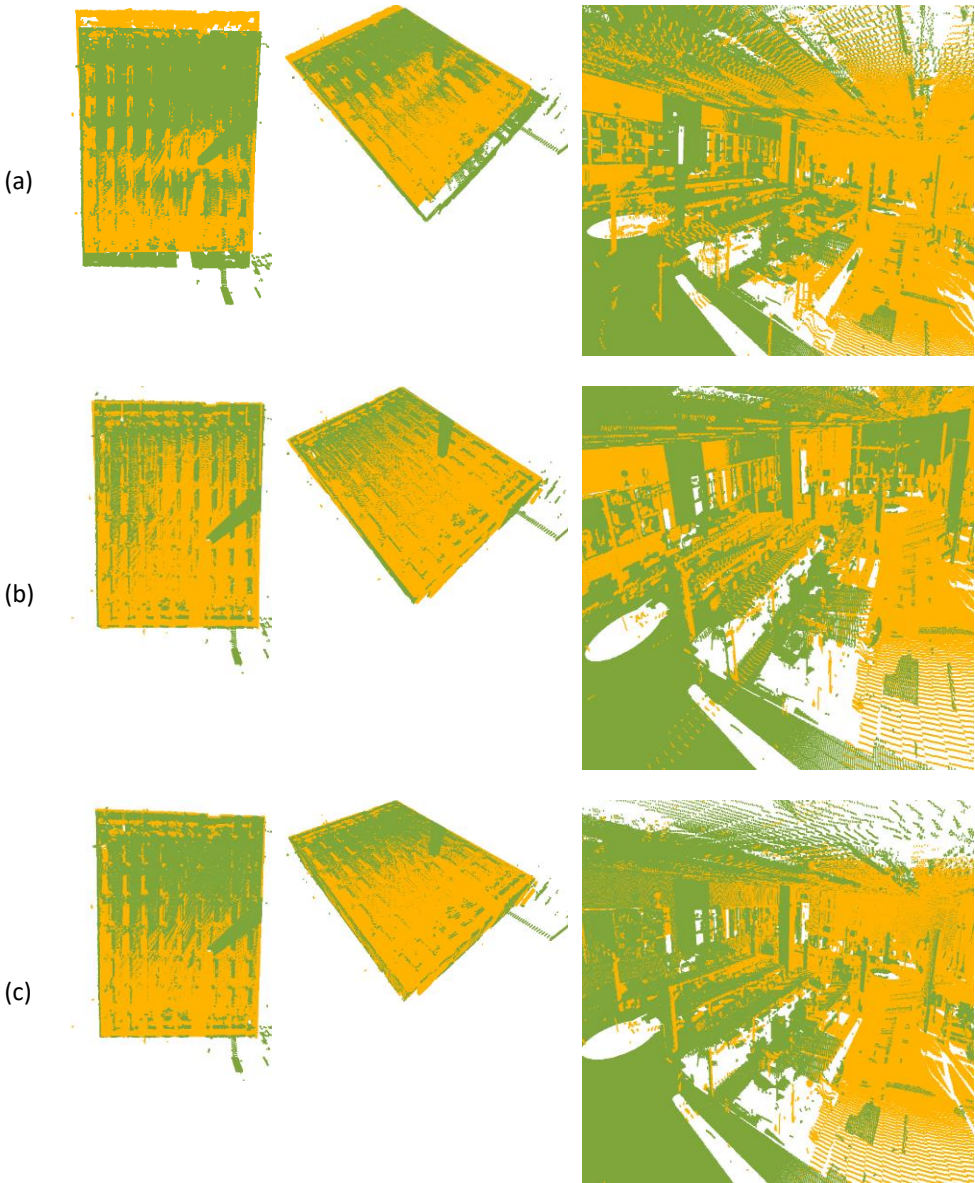
Apart from testing the six datasets, another real life dataset having occlusions was also tested to analyze the occlusion effect on the proposed method. This new dataset represents a large furnished room with both scan models, instead of scan and BIM, having intense occlusions in their point clouds. Both of the scan models in the dataset were collected with different position in the presence of numerous objects, as the missing points as clearly evident in **Figure 2.17**. Although the overall research is focused on registration of as-built model (scan) with their corresponding as-planned model, however this new dataset as opposed contain both as-built models

and tested only to confirm the reliability of proposed plane-based method at higher difficulty. Both the scan models contain plane models but highly affected due to different errors.



*Figure 2.17.* Visualization of point cloud in different views from (a) scan model 1, and (b) scan model 2.

Normally, the occlusion in the point cloud affects the centroid due to the unequal distribution of 3D points. Therefore, it can also influence the proposed method due to its dependence on centroid during translation assessment. The results demonstrate that the proposed method successfully registered the highly occluded scan models by diminishing the effect of occlusions. The underlying reason for the precise registration can be attributed to the fact that the proposed method calculates the centroids of plane segments from scan model that are calculated from their bounding boxes, instead of their individual point clouds, to get more accurate registration as evident in *Figure 2.18a* and *Figure 2.18b*. Similarly, the registration results of the proposed method, as shown in *Figure 2.18b*, are later refined with ICP registration, as shown in *Figure 2.18c*, which validates that the results of the proposed method are accurate enough for fine registration.



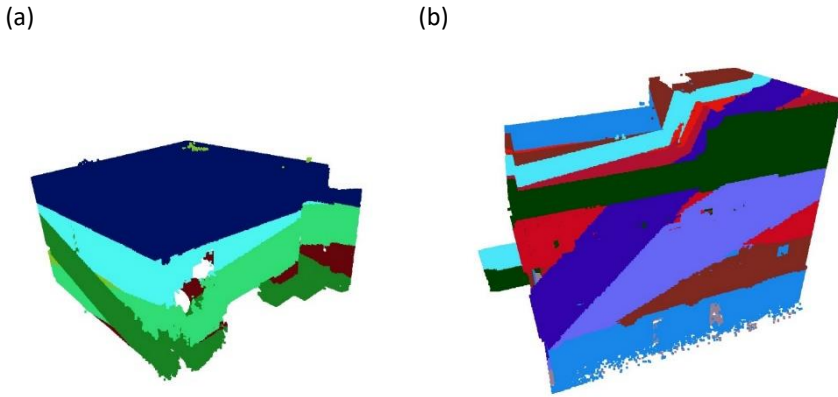
*Figure 2.18.* Visualization of registered scans in three different views after applying the (a) proposed method with the centroid of plane segments calculated from point clouds (b) proposed method (c) proposed method and then fine registration

### 2.5.6 Limitation

As emphasized frequently, the proposed method is totally dependent on extracted plane segments. These plane segments are obtained through a RANSAC-based plane segmentation technique that computes the same parameters but ends up with



different plane parameters every time. Hence, the plane parameters may change slightly which also affects the registration accuracy. In the worst case, it is also possible that the incorrect plane segments may be extracted, as shown in Figure 2.19 which will eventually affect the success of the proposed method leading it to the failure. The estimation of incorrect plane segments may occur due to numerous reasons including complex point cloud model, improper segmentation parameters, and the segmentation technique itself. This limitation was very much evident in the case of dataset R4 (Figure 2.19b) that contains most plane segments which are located very close to each other along with the presence of intense noise and occlusion, eventually leading to difficulty in obtaining accurate plane segments. The registration success was only achieved in this case after the successful extraction of plane segments from the model. It is worth mentioning here that the current research focuses on the novel utilization of plane segments to obtain successful registration, however, the way these plane segments are obtained is out of scope.



*Figure 2.19.* An example visualization the incorrect plane segments extracted in different colors from as-built point cloud of (a) dataset R1 and, (b) dataset R3.

## 2.6 Conclusions

Construction project monitoring includes the registration of as-built models with their as-planned model followed by the analysis of the aligned models to infer progress information. Normally, the registration process involves two steps: (1) coarse registration, in which both models are almost aligned to each other, and (2) fine registration, which involves an improvement of the coarse registration and augments the registration accuracy. This research presented in the current chapter addressed the coarse registration problem in detail and proposed a new automated method to align the as-built and as-planned building models using their geometric features in a highly robust and accurate way. Most building structures have an orthogonal geometry that consists primarily of plane segments. The extraction of these planar features is only slightly affected by the presence of noise or minor outliers; therefore, the proposed technique employs these features for the automated registration of building models for project monitoring. The technique

first utilizes the directions of the planes from the building models to determine the possible rotations for the registration. Then, it measures the matching between all the plane segments to recognize the rotation with the best match. Consequently, the translation is calculated from the best-matched plane segments. Along with the transformation parameters, the proposed method also has the ability to identify the matching plane segments between corresponding models. The identification of plane segments, representing the building components, can further aid in their individual inspection during project monitoring.

Experimentation was performed on building datasets with different geometries to evaluate the performance of the proposed method. The results demonstrated that the proposed method successfully registered all the building models with a high rotation and translation accuracy in a fully automated way. The presence of noise or occlusions only slightly affected the success of registration. The proposed method also proved to be robust in terms of computation time; however, the processing time was highly dependent on the number of plane segments.

Overall, the proposed method in this chapter exhibits reliable results for both complete and incomplete buildings, which makes it useful for progress monitoring as long as at least three identical plane segments with distinct directions are present in both models. From the perspective of construction management, the automated registration of scan models of partially completed as-built situations with their BIM model is a big step forward in the development of an automated system for project monitoring. Further research is necessary to enhance the applicability of the proposed method in complex buildings with a high number of planes and/or curved elements.

## 2.7 References

1. Bosché, F. Automated recognition of 3D CAD model objects in laser scans and calculation of as-built dimensions for dimensional compliance control in construction. *Adv. Eng. Inform.* **2010**, *24*, 107–118.
2. Navon, R. Research in automated measurement of project performance indicators. *Autom. Constr.* **2007**, *16*, 176–188.
3. Zhang, X.; Bakis, N.; Lukins, T.C.; Ibrahim, Y.M.; Wu, S.; Kagioglou, M.; Aouad, G.; Kaka, A.P.; Trucco, E. Automating progress measurement of construction projects. *Autom. Constr.* **2009**, *18*, 294–301.
4. Han, K.K.; Golparvar-Fard, M. Automated monitoring of operation-level construction progress using 4D BIM and daily site photologs. In Proceedings of the Construction Research Congress 2014: Construction in a Global Network, Atlanta, GA, USA, 19–21 May 2014; pp. 1033–1042.
5. Omar, T.; Nehdi, M.L. Automated Data Collection for Progress Tracking Purposes: A Review of Related Techniques. In Proceedings of the International Congress and Exhibition “Sustainable Civil Infrastructures: Innovative Infrastructure Geotechnology”, Sharm El Sheikh, Egypt, 15–20 July 2017; pp. 391–405.
6. Fang, J.; Li, Y.; Liao, Q.; Ren, Z.; Xie, B. Construction Progress Control And Management Measures Analysis. *Smart Constr. Res.* **2018**, *2*. <http://dx.doi.org/10.18063/scr.v2i1.392>.
7. Golparvar-Fard, M.; Savarese, S.; Peña-Mora, F. Interactive Visual Construction Progress Monitoring with D4 AR—4D Augmented Reality—Models. In Proceedings of Construction Research Congress 2009: Building a Sustainable Future, Seattle, WA, USA, 5–7 April 2009; pp. 41–50.
8. Braun, A.; Tuttas, S.; Borrmann, A.; Stilla, U. A concept for automated construction progress monitoring using BIM-based geometric constraints and photogrammetric point clouds. *J. Inf. Technol. Constr. (ITcon)* **2015**, *20*, 68–79.
9. Omar, H.; Dulaimi, M. Using BIM to automate construction site activities. *Build. Inf. Model. (BIM) Des. Constr. Oper.* **2015**, *149*, 45.
10. Pučko, Z.; Šuman, N.; Rebolj, D. Automated continuous construction progress monitoring using multiple workplace real time 3D scans. *Adv. Eng. Inform.* **2018**, *38*, 27–40.
11. Rebolj, D.; Pučko, Z.; Babič, N.Č.; Bizjak, M.; Mongus, D. Point cloud quality requirements for Scan-vs-BIM based automated construction progress monitoring. *Autom. Constr.* **2017**, *84*, 323–334.
12. Khairadeen Ali, A.; Lee, O.J.; Lee, D.; Park, C. Remote Indoor Construction Progress Monitoring Using Extended Reality. *Sustainability* **2021**, *13*, 2290.
13. Fathi, H.; Dai, F.; Lourakis, M. Automated as-built 3D reconstruction of civil infrastructure using computer vision: Achievements, opportunities, and challenges. *Adv. Eng. Inform.* **2015**, *29*, 149–161. <https://doi.org/10.1016/j.aei.2015.01.012>.
14. Golparvar-Fard, M.; Pena-Mora, F.; Savarese, S. Monitoring changes of 3D building elements from unordered photo collections. In Proceedings of the Computer Vision Workshops (ICCV Workshops), 2011 IEEE International Conference, Barcelona, Spain, 6–13 November 2011; pp. 249–256.



15. Golparvar-Fard, M.; Peña-Mora, F.; Savarese, S. Automated progress monitoring using unordered daily construction photographs and IFC-based building information models. *J. Comput. Civil. Eng.* **2012**, *29*, 04014025.
16. Han, K.; Degol, J.; Golparvar-Fard, M. Geometry-and Appearance-Based Reasoning of Construction Progress Monitoring. *J. Constr. Eng. Manag.* **2017**, *144*, 04017110.
17. Tuttas, S.; Braun, A.; Borrmann, A.; Stilla, U. Acquisition and consecutive registration of photogrammetric point clouds for construction progress monitoring using a 4D BIM. *PFG–J. Photogramm. Remote Sens. Geoinf. Sci.* **2017**, *85*, 3–15.
18. Bosche, F.; Haas, C.T. Automated retrieval of 3D CAD model objects in construction range images. *Autom. Constr.* **2008**, *17*, 499–512.
19. Kim, C.; Son, H.; Kim, C. Automated construction progress measurement using a 4D building information model and 3D data. *Autom. Constr.* **2013**, *31*, 75–82. <https://doi.org/10.1016/j.autcon.2012.11.041>.
20. Tang, P.; Huber, D.; Akinci, B.; Lipman, R.; Lytle, A. Automatic reconstruction of as-built building information models from laser-scanned point clouds: A review of related techniques. *Autom. Constr.* **2010**, *19*, 829–843.
21. Turkan, Y.; Bosche, F.; Haas, C.T.; Haas, R. Automated progress tracking using 4D schedule and 3D sensing technologies. *Autom. Constr.* **2012**, *22*, 414–421. <https://doi.org/10.1016/j.autcon.2011.10.003>.
22. Brilakis, I.; Lourakis, M.; Sacks, R.; Savarese, S.; Christodoulou, S.; Teizer, J.; Makhmalbaf, A. Toward automated generation of parametric BIMs based on hybrid video and laser scanning data. *Adv. Eng. Inform.* **2010**, *24*, 456–465.
23. El-Omari, S.; Moselhi, O. Integrating 3D laser scanning and photogrammetry for progress measurement of construction work. *Autom. Constr.* **2008**, *18*, 1–9.
24. Shahi, A.; Aryan, A.; West, J.S.; Haas, C.T.; Haas, R.C. Deterioration of UWB positioning during construction. *Autom. Constr.* **2012**, *24*, 72–80.
25. Besl, P.J.; McKay, N.D. Method for registration of 3-D shapes. In Proceedings of the Sensor Fusion IV: Control Paradigms and Data Structures, Boston, MA, USA, 12–15 November 1991; pp. 586–606.
26. Zhang, Z. Iterative point matching for registration of free-form curves and surfaces. *Int. J. Comput. Vis.* **1994**, *13*, 119–152.
27. Chen, Y.; Medioni, G. Object modelling by registration of multiple range images. *Image Vis. Comput.* **1992**, *10*, 145–155.
28. Rusinkiewicz, S.; Levoy, M. Efficient variants of the ICP algorithm. In Proceedings of the international conference on 3D digital imaging and modeling, Quebec, Canada, 28 May–1 June 2001; IEEE Computer Society Press: Quebec, QC, Canada, 2001.
29. Hattab, A.; Taubin, G. 3D rigid registration of cad point-clouds. In Proceedings of 2018 International Conference on Computing Sciences and Engineering (ICCSE), Kuwait, Kuwait, 11–13 March 2018; pp. 1–6.
30. Bueno, M.; Bosché, F.; González-Jorge, H.; Martínez-Sánchez, J.; Arias, P. 4-Plane congruent sets for automatic registration of as-is 3D point clouds with 3D BIM models. *Autom. Constr.* **2018**, *89*, 120–134.
31. Anil, E.B.; Tang, P.; Akinci, B.; Huber, D. Assessment of the quality of as-is building information models generated from point clouds using deviation

- analysis. In *Proceedings of Three-Dimensional Imaging, Interaction, and Measurement*, San Francisco, CA, USA, 24–27 January 2011; p. 78640F.
32. Bassier, M.; Vergauwen, M.; Poux, F. Point Cloud vs. Mesh Features for Building Interior Classification. *Remote Sens.* **2020**, *12*, 2224.
  33. Li, J.; Hu, Q.; Ai, M. GESAC: Robust graph enhanced sample consensus for point cloud registration. *ISPRS J. Photogramm. Remote Sens.* **2020**, *167*, 363–374.
  34. Zong, W.; Li, M.; Zhou, Y.; Wang, L.; Xiang, F.; Li, G. A Fast and Accurate Planar-Feature-Based Global Scan Registration Method. *IEEE Sens. J.* **2019**, *19*, 12333–12345.
  35. Xu, Y.; Boerner, R.; Yao, W.; Hoegner, L.; Stilla, U. Automated Coarse Registration of Point Clouds in 3D Urban Scenes Using voxel based plane constraint. *ISPRS Ann. Photogramm. Remote Sens. Spat. Inf. Sci.* **2017**, *4*, 185.
  36. Bolles, R.C.; Fischler, M.A. A RANSAC-based approach to model fitting and its application to finding cylinders in range data. In *Proceedings of IJCAI*, Vancouver, BC, Canada, 24–28 August 1981; pp. 637–643.
  37. Chen, C.-S.; Hung, Y.-P.; Cheng, J.-B. RANSAC-based DARCES: A new approach to fast automatic registration of partially overlapping range images. *IEEE Trans. Pattern Anal. Mach. Intell.* **1999**, *21*, 1229–1234.
  38. Fontanelli, D.; Ricciato, L.; Soatto, S. A fast ransac-based registration algorithm for accurate localization in unknown environments using lidar measurements. In *Proceedings of 2007 IEEE International Conference on Automation Science and Engineering*, Xi'an, China, 22–25 September 2007; pp. 597–602.
  39. Theiler, P.W.; Wegner, J.D.; Schindler, K. Keypoint-based 4-points congruent sets—automated marker-less registration of laser scans. *ISPRS J. Photogramm. Remote Sens.* **2014**, *96*, 149–163.
  40. Mellado, N.; Aiger, D.; Mitra, N.J. Super 4pcs fast global pointcloud registration via smart indexing. In *Computer Graphics Forum*; Wiley: Hoboken, NJ, USA, 2014; Volume 33, pp. 205–215.
  41. Aiger, D.; Mitra, N.J.; Cohen-Or, D. 4-points congruent sets for robust pairwise surface registration. In *ACM SIGGRAPH 2008 Papers*; ACM: New York, NY, USA, 2008; pp. 1–10.
  42. Xu, Y.; Boerner, R.; Yao, W.; Hoegner, L.; Stilla, U. Pairwise coarse registration of point clouds in urban scenes using voxel-based 4-planes congruent sets. *ISPRS J. Photogramm. Remote Sens.* **2019**, *151*, 106–123.
  43. Böhm, J.; Becker, S. Automatic marker-free registration of terrestrial laser scans using reflectance. In *Proceedings of the 8th Conference on Optical 3D Measurement Techniques*, Zurich, Switzerland, 9–12 July 2007; pp. 9–12.
  44. Weinmann, M.; Weinmann, M.; Hinz, S.; Jutzi, B. Fast and automatic image-based registration of TLS data. *ISPRS J. Photogramm. Remote Sens.* **2011**, *66*, S62–S70.
  45. Theiler, P.; Schindler, K. Automatic registration of terrestrial laser scanner point clouds using natural planar surfaces. *ISPRS Ann. Photogramm. Remote Sens. Spat. Inf. Sci.* **2012**, *3*, 173–178.
  46. Weber, T.; Hänsch, R.; Hellwich, O. Automatic registration of unordered point clouds acquired by Kinect sensors using an overlap heuristic. *ISPRS J. Photogramm. Remote Sens.* **2015**, *102*, 96–109.

47. Yang, B.; Dong, Z.; Liang, F.; Liu, Y. Automatic registration of large-scale urban scene point clouds based on semantic feature points. *ISPRS J. Photogramm. Remote Sens.* **2016**, *113*, 43–58.
48. Mahmood, B.; Han, S.; Lee, D.-E. BIM-Based Registration and Localization of 3D Point Clouds of Indoor Scenes Using Geometric Features for Augmented Reality. *Remote Sens.* **2020**, *12*, 2302.
49. Li, Z.; Zhang, X.; Tan, J.; Liu, H. Pairwise Coarse Registration of Indoor Point Clouds Using 2D Line Features. *ISPRS Int. J. Geo-Inf.* **2021**, *10*, 26.
50. Habib, A.; Ghanma, M.; Morgan, M.; Al-Ruzouq, R. Photogrammetric and LiDAR data registration using linear features. *Photogramm. Eng. Remote Sens.* **2005**, *71*, 699–707.
51. Al-Durgham, M.; Habib, A. A framework for the registration and segmentation of heterogeneous LiDAR data. *Photogrammetric Eng. Remote Sens.* **2013**, *79*, 135–145.
52. Yang, B.; Zang, Y. Automated registration of dense terrestrial laser-scanning point clouds using curves. *ISPRS J. Photogramm. Remote Sens.* **2014**, *95*, 109–121.
53. Xiao, J.; Adler, B.; Zhang, J.; Zhang, H. Planar segment based three-dimensional point cloud registration in outdoor environments. *J. Field Robot.* **2013**, *30*, 552–582.
54. Dold, C.; Brenner, C. Registration of terrestrial laser scanning data using planar patches and image data. *Int. Arch. Photogramm. Remote Sens. Spat. Inf. Sci.-ISPRS Arch.* **2006**, *36*, 78–83.
55. Ge, X.; Wunderlich, T. Surface-based matching of 3D point clouds with variable coordinates in source and target system. *ISPRS J. Photogramm. Remote Sens.* **2016**, *111*, 1–12.
56. Xu, Y.; Hoegner, L.; Tuttas, S.; Stilla, U. Voxel-and Graph-based point cloud segmentation of 3d scenes using perceptual grouping laws. *ISPRS Ann. Photogramm. Remote Sens. Spat. Inf. Sci.* **2017**, *4*, 43–50. <https://doi.org/10.5194/isprs-annals-IV-1-W1-43-2017>.
57. Pavan, N.L.; dos Santos, D.R.; Khoshelham, K. Global Registration of Terrestrial Laser Scanner Point Clouds Using Plane-to-Plane Correspondences. *Remote Sens.* **2020**, *12*, 1127.
58. Li, L.; Yang, F.; Zhu, H.; Li, D.; Li, Y.; Tang, L. An improved RANSAC for 3D point cloud plane segmentation based on normal distribution transformation cells. *Remote Sens.* **2017**, *9*, 433.
59. Schnabel, R.; Wahl, R.; Klein, R. Efficient RANSAC for point-cloud shape detection. *Comput. Graph. Forum* **2007**, *26*, 214–226.
60. Nurunnabi, A.; Belton, D.; West, G. Robust segmentation in laser scanning 3D point cloud data. In Proceedings of the 2012 International Conference on Digital Image Computing Techniques and Applications (DICTA), Fremantle, WA, Australia, 3–5 December 2012; pp. 1–8.
61. Li, M.; Gao, X.; Wang, L.; Li, G. Automatic registration of laser-scanned point clouds based on planar features. In Proceedings of the 2nd ISPRS International Conference on Computer Vision in Remote Sensing (CVRS 2015), Xiamen, China, 28–30 April 2015; p. 990103.
62. Grant, W.S.; Voorhies, R.C.; Itti, L. Finding planes in LiDAR point clouds for real-time registration. In Proceedings of the 2013 IEEE/RSJ International Conference

on Intelligent Robots and Systems, Tokyo, Japan, 3–7 November 2013; pp. 4347–4354.

63. Poppinga, J.; Vaskevicius, N.; Birk, A.; Pathak, K. Fast plane detection and polygonalization in noisy 3D range images. In Proceedings of the 2008 IEEE/RSJ International Conference on Intelligent Robots and Systems, Nice, France, 22–26 September 2008; pp. 3378–3383.
64. Zhang, D.; Huang, T.; Li, G.; Jiang, M. Robust algorithm for registration of building point clouds using planar patches. *J. Surv. Eng.* **2012**, *138*, 31–36.
65. He, W.; Ma, W.; Zha, H. Automatic registration of range images based on correspondence of complete plane patches. In Proceedings of the Fifth International Conference on 3-D Digital Imaging and Modeling (3DIM'05), Ottawa, ON, Canada, 13–16 June 2005; pp. 470–475.
66. Brenner, C.; Dold, C.; Ripperda, N. Coarse orientation of terrestrial laser scans in urban environments. *ISPRS J. Photogramm. Remote Sens.* **2008**, *63*, 4–18.
67. Pavan, N.L.; dos Santos, D.R. A global closed-form refinement for consistent TLS data registration. *IEEE Geosci. Remote Sens. Lett.* **2017**, *14*, 1131–1135.
68. Zhang, C.; Arditi, D. Automated progress control using laser scanning technology. *Autom. Constr.* **2013**, *36*, 108–116.
69. Kim, C.; Son, H.; Kim, C. Fully automated registration of 3D data to a 3D CAD model for project progress monitoring. *Autom. Constr.* **2013**, *35*, 587–594.
70. Liu, Y.-S.; Ramani, K. Robust principal axes determination for point-based shapes using least median of squares. *Comput.-Aided Des.* **2009**, *41*, 293–305.
71. Fitzgibbon, A.W. Robust registration of 2D and 3D point sets. *Image Vis. Comput.* **2003**, *21*, 1145–1153.
72. Chen, J.; Cho, Y.K. Point-to-point comparison method for automated scan-vs-bim deviation detection. In Proceedings of the 17th International Conference on Computing in Civil and Building Engineering, Tampere, Finland, 5–7 June 2018.
73. Wand, M.; Berner, A.; Bokeloh, M.; Jenke, P.; Fleck, A.; Hoffmann, M.; Maier, B.; Staneker, D.; Schilling, A.; Seidel, H.-P. Processing and interactive editing of huge point clouds from 3D scanners. *Comput. Graph.* **2008**, *32*, 204–220.
74. Medioni, G.; Lee, M.-S.; Tang, C.-K. *A Computational Framework for Segmentation and Grouping*; Elsevier: Amsterdam, The Netherlands, 2000.
75. Bassier, M.; Vergauwen, M. Clustering of wall geometry from unstructured point clouds using conditional random fields. *Remote Sens.* **2019**, *11*, 1586.
76. Bassier, M.; Vergauwen, M. Unsupervised reconstruction of Building Information Modeling wall objects from point cloud data. *Autom. Constr.* **2020**, *120*, 103338.

---

# 3

---

## 3. REGISTRATION BASED ON CORNER POINTS

*This chapter is an adapted version from the following original publication:*

Sheik, N. A., Veelaert, P., & Deruyter, G. (2022). Registration of Building Scan with IFC-Based BIM Using the Corner Points. *Remote Sensing*, 14(20), 5271. <https://doi.org/10.3390/rs14205271>

Sheik, N. A., Deruyter, G., Veelaert, P., & De Wulf, A. (2022). A first step towards automatic construction progress monitoring. In XXVII FIG Congress 2022.

## Abstract

Progress monitoring is an essential part of large construction projects. As manual progress monitoring is time-consuming, the need for automation emerges, especially as, nowadays, BIM for the design of buildings and laser scanning for capturing the as-built situation have become well adopted. However, to be able to compare the as-built model obtained by laser scanning to BIM design, both models need to use the same reference system, which often is not the case. Transforming the coordinate system of the as-built model into the BIM model is a specialist process that is pre-requisite in automated construction progress monitoring. The research described in this chapter is aimed at the automation of this so-called registration process and is based on the dominant planar geometry of most buildings with evident corner points in their structures. After extracting these corner points from both the as-built and the design model, a RANSAC-based pairwise assessment of the points is performed to identify potential matching points in both models using different discriminative geometric invariants. Next, the transformation for the potential matches is evaluated to find all the matching points. In the end, the most accurate transformation parameter is determined from the individual transformation parameters of all the matching corner points. The proposed method was tested and validated with a range of both simulated and real-life datasets. In all the case studies including the simulated and real-life datasets, the registration was successful and accurate. Furthermore, the method allows for the registration of the as-built models of incomplete buildings, which is essential for effective construction progress monitoring. As the method uses the standard IFC schema for data exchange with BIM, there is no loss of geometrical information caused by data conversions and it supports the complete automation of the progress-monitoring process. The current chapter also compares the proposed method (detailed in current chapter) with the plane-based registration method (provided in previous chapter) and describes their merits and de-merits in the end.

**Keywords:** BIM, point cloud, registration, buildings, automated, IFC, corner points.

### 3.1 Introduction

The accurate and efficient progress monitoring of under-construction buildings is a prerequisite for effective project management [1–5]. Current methods of progress monitoring are based on manual measurements and extensive processing performed by construction staff. The manual process with a dominant human presence consumes a lot of time and labor and can lead to inaccurate or missing information; therefore, accurate automated alternatives should be pushed forward [6–8].

Recently, several studies have been performed on automated progress monitoring through a model-based assessment where the as-built model of the building is compared with its as-planned model [1]. A three-dimensional (3D) point cloud of the building, acquired through reconstruction technologies such as laser scanning, image-based reconstruction, or the integration of both, represents the as-built model. This model is compared to its design state (as-planned model) in a suitable format that is usually obtained from a Building Information Model (BIM), a rich digital representation of the building comprising the 3D geometrical and semantic information [5]. The comparison of the as-built and as-planned model, termed “Scan-vs-BIM”, enables the accurate automated progress monitoring of buildings [1]. However, effective progress monitoring using Scan-vs-BIM requires an accurate alignment through a fundamental task of registration [9].

Registration is an active research area, with most efforts focused on the alignment of point clouds and less on the alignment of point clouds with BIM. In the latter case, BIM can be converted into a point cloud or some other suitable format like a mesh, although the conversion process can result in loss of geometrical details. The registration problem involves finding the rigid rotation and translation transformation parameters to overlap the as-built model onto the as-planned model. Normally, a coarse-to-fine strategy is applied in which coarse (or global) registration procedure is initially applied to obtain the approximate overlapping of the models, followed by a fine registration procedure using the iterative closest point (ICP) algorithm to improve the initial coarse registration. The results of the fine registration are highly dependent on the success of the coarse registration; hence, this first registration step requires a lot of attention. In this coarse registration, the extraction of geometric features and identifying their match are the critical steps. The features can be either points or primitives such as lines, planes, and curves. Furthermore, the application of registration methods can also be limited to specific scenarios based on their approach [10]. As a lot of building structures are dominated by planar features, approaches utilizing the planar features can be considered a suitable solution for registration. Methods employing the planar features are primarily dependent only on plane parameters, contrary to complete point clouds, and this makes them more robust in identifying their matching and less affected by outliers [10,11]. However, the identification of matching planes in these methods is

highly challenging [10,12–15]. Therefore, a plane-based method is required that infers the discriminative information from buildings to differentiate the matching features for registration.

Apart from registration, another challenge faced in Scan-vs-BIM is the direct extraction of geometrical details from BIM as an as-planned model. After the registration process, the aligned models are compared in Scan-vs-BIM to infer the progress information. Later, the progress information needs to be updated into a suitable catalog that can be later utilized in schedule planning, continuous updating of progress information, visualization, and communication of as-built progress [16]. To effectively perform these tasks, BIM integration with the construction schedule is required. Few researchers manually performed the exchange of progress information using software solutions, against the notion of automated progress monitoring [5,17–19]. In contrast, some studies performed the automated updating of progress data in BIM by directly accessing the relevant information using an Industry foundation classes (IFC)-based BIM [16,20]. IFC is a no-proprietary file exchange format for BIMs that provides a common solution to exchange intense information between stakeholders. The application of IFC-based BIMs in Scan-vs-BIM ensures a consistent information format and facilitates the thorough automation of all stages of progress monitoring, including registration. However, there is no registration attempt that directly utilizes the IFC-based BIM as an as-planned model. This demands a registration method that, instead of manually converting BIM into another format before use, directly extracts the geometrical information from BIM in an automated way.

The corner points, corresponding to three intersecting planes, are identifiable 3D points in the Euclidean scale. These corner points can be exploited for geometric invariants for matching to compute the transformation for building models. The current research detailed in the current chapter proposes a novel registration technique that makes use of the distinct corner points defined as the intersection points of three intersecting planes extracted from the model. A series of geometric discriminative invariants are used as matching constraints to prune the corner points in combination with the semantic information of their parent plane to find an accurate match. The method is made robust by applying Random Sample Consensus (RANSAC) during the initial identification of matching pairs to solve the combinatorial problem and then clustering the potential matching points with similar transformations. Similarly, the method also identifies the most optimal transformation from the clustered matched corner points. Another contribution of the current research is that it translates the geometrical information directly from the IFC-based BIM during the processing.

In Section 3.2, related works on registration, particularly on features-based registration, are reviewed to gain an insight into the problem. Section 3.3 details the stages of the proposed methodology. Experimentation results with simulated and



real-life datasets followed by a discussion are presented in Section 3.4. Finally, the conclusions are outlined in Section 3.5.

It is important to mention here that the detailed literature review focused on studies related to plane-based structural features is already elaborated in the previous chapter (Section 2.2). The literature discussed in the current chapter focuses on other aspects, challenges, and studies that are more related to point-based features.

## 3.2 Related Work

Registration is a widely studied research problem with the aim to align datasets in a common coordinate system. Registration methods often apply a coarse-to-fine strategy where an initial alignment is obtained by a coarse registration, after which it is improved by fine registration algorithms. [21] The quality of the coarse registration determines the success of the fine registration [21], which is mostly obtained by means of the well-established ICP algorithm [22] and its variants [23–25] or the normal distribution transformation (NDT) and its variants [26–29]. Hence, coarse registration remains the area of greater challenge, with numerous studies attempting to address this challenge.

Generally, the coarse registration method involves extracting geometric features from models and then identifying the matching features between them to compute the transformation. The main idea is that, instead of using all the 3D points in the models, the selection of key points or primitives formed by the points as a distinct feature is established for computational relief and improved matching [30]. The features are based on geometric characteristics such as fast point feature histograms (FPFHs) [31], semantic feature lines [32], intersecting lines [33], planes [34], curves [35], patches [36], or adaptive covariance [37]. Similarly, the identification of matching features is performed through different techniques including Random sample consensus (RANSAC) [38], inliers search [39], fast-matching pruning (FMP) [40], geometric consistency constraints [41], and non-cooperative game [37]. The approach of the feature-based registration method is widely adopted due to the practical effectiveness of geometric characteristics in various scenes. Approaches based on point features such as scale-invariant feature transform (SIFT) key points [42,43], virtual intersection points [12], Difference-of-Gaussian (DoG) points [44], FPFH key points [45], SURF key points [46], and semantic feature points [32,47] have registered the point clouds, but their success is sensitive to noise and varying point density. Furthermore, they are inefficient in the case of large datasets [13]. In contrast to the point-based features, approaches that use primitives such as lines, planes, and curved surfaces as features are more robust in identifying the features that can be matched [30]. Some studies used line features such as a linear invariant [48,49], the intersection of neighboring planes [33], and the footprint from a building [50] for registration. Similarly, curved surfaces [36,51] are also reported to be used as matching features. Additionally, a plane surface as a geometric feature for

matching has also been studied by numerous researchers [9,11,13,34,52–55]. These plane-feature-based approaches fail in rural landscapes, but they can achieve good performance in urban infrastructures as urban structures have plenty of these features [21].

Buildings in particular have abundant planar features that can be extracted for registration. The registration approaches with plane features primarily process the plane parameters, instead of complete point clouds, to reduce the computation time. Furthermore, these approaches are less affected by the outliers; hence, the accuracy can be increased [11]. The efficiency of these approaches also depends on the quality of the extracted planes. The extraction of planes from a point cloud can be performed with segmentation techniques such as RANSAC segmentation [56–58], region growing [59], Hough transform [60], dynamic clustering [55], and voxel-based growing [13]. Generally, high numbers of similar planar surfaces extracted from the large-scale point clouds increases the difficulty in identifying matching plane segments. Additionally, the lack of discriminative geometric primitives and distinct invariants remains a challenge for reliable identification of matching pairs. Consequently, some authors manually identify matching planes [14], although research efforts to automate this process are emerging. He, Ma, and Zha [15] performed the matching of complete plane patches through interpretation trees where the area, normal angles, and centroid were used for tree pruning. Although the computation complexity was reduced, employing only complete planes lowered the probability of determining the correct transformation because of varying overlap and occlusion conditions. Pavan and dos Santos [61] introduced the non-iterative global refinement step utilizing the local consistency of the plane. The identification of matching planes uses the plane similarity properties and the geometric constraint formed by the surfaces of planes. This method exploits the properties of quaternions to place the rotation matrices into the same coordinate system. Similarly, the use of 4-plane congruent sets (4-PCS), which inputs the pair of planar patches from voxelized point clouds to find their matching, is proposed [30]. Furthermore, many studies have attempted to solve the registration problem using geometric information obtained from the combination of three planes. For example, Dol and Brenner [52] conducted a search process with a triple product of plane normals to find their matching pairs with acceptable results. The number of combinations in the matching process was reduced using geometrical constraints such as area, boundary length, bounding box, and mean intensity values. However, the related practical details were not published [10]. Similarly, Brenner, et al. [62] used the intersecting angles formed by three planes for matching as geometrical constraints. Theiler and Schindler [12] tackled the correspondence problem by identifying the matching virtual tie points of three planes with the assistance of specialized descriptors (intersection quality, angles, smoothness, segment extent) to describe the geometrical characteristics of the planes. The distance between the tie points was employed as the matching constraint and a specific threshold was introduced to limit

the number of compatible candidates and reduce the exponential complexity. This method is not reliable, as additional virtual tie points at symmetrical distances can be obtained for planes that are not physically intersecting or are located near to each other, in which case the distance constraint is not enough to differentiate them. In addition, the success rate is also sensitive to high noise and occlusions. The matching problem was also approached through the utilization of three planes, in which the coordinate frame was estimated from the set of normal planes obtained from randomly selected non-parallel planar patches [13]. This method adopted the RANSAC-based strategy where transformation parameters from the coordinate frame of potential matching patches are computed and then assessed according to the number of coplanar patches. The parameter with the highest number of coplanar patches is considered the final transformation parameter. This method considers all tie points from planar patches of both models as their potential matching pairs without any initial scrutiny and applies the RANSAC-based selection that may not always select the matching points. Furthermore, the application of coplanar criteria as the only matching constraint may result from the incorrect transformation in datasets with many parallel planes. Moreover, Li, Gao, Wang, and Li [55] proposed an automated registration method to identify matching planes using only the relative angles of three planes with two strategies. The first strategy finds the potential correspondence for those three planes intersecting at one point with different relative angles with each other and the second strategy finds the correspondence for three planes having at least one perpendicular relative angle. The matching constraint marks the method as unreliable, as employing only angle constraints limits the practicality if there are a high number of planes. Kim, et al. [63] proposed to use a plane-matching algorithm in which three plane correspondences are identified by comparing their normal vectors. The rotation is computed from the identified corresponding planes and the translation is determined from the tie point of the corresponding planes. The method uses plane matching as an alternative if the primary method doesn't find sufficient initial alignment based on extracted common features from the RGB-fused point cloud. Similarly, the identification of matching planes is not explained nor is any evaluation performed to verify the transformation. Apart from the limitations of all these mentioned methods, none of them performed the registration from the perspective of construction progress monitoring in which the as-built point cloud is registered with its as-planned BIM model.

In studies focused on Scan-vs-BIM, Kim, et al. [64] proposed an automated method in which the 3D CAD model of a building converted into a point cloud is used as an as-planned model to register it with an as-built point cloud obtained from the construction site using a coarse-to-fine strategy. The coarse registration was performed with Principal component analysis (PCA) [65] with rotation determined from the bases formed by principal components of both models while the translation was computed from the centroids of the models. This method is not applicable in real-life scenarios involving occlusion, noise, or missing data as the method assumes

that the principal components of both models have the same direction and centroid, which is only possible if both models are duplicates. Recently, Bueno, Bosché, González-Jorge, Martínez-Sánchez, and Arias [9] performed Scan-vs-BIM registration in planar patches extracted from the as-built point cloud and BIM converted mesh model that were processed as 4-PCS to compute the possible transformation. The transformation was later evaluated using plane and centroid support. In the end, top-five ranked transformations are obtained, instead of top-only, based on the challenge that the presence of extreme self-similarity and symmetry in building structures can lead to several incorrect transformations. Although the correct transformation for the given simulated datasets was ranked first, the method ranked the correct transformation in second place for provided real datasets. Hence, none of these methods proved to be reliable in the construction environment. Nevertheless, registration methods involving Scan-vs-BIM may have mentioned BIM or CAD model but none of them directly extracted the geometrical information from them because all of them converted the model into a point cloud or mesh for compatible processing. Recently, Sheik, et al. [66] performed the registration of building models (Scan-vs-BIM) in which the geometrical parameters from the plane segments were processed through a rotational and translational assessment using a minimization process. Their method was able to successfully perform the registration for the partially built building models provided the minimum of three matching plane segments with distinct directions were present in both models. This chapter proposes an improved method that focuses on the utilization of corner points to perform the accurate registration of the scan model of the partially built building acquired from a construction site with its corresponding IFC-based BIM model.

In automated progress monitoring with Scan-vs-BIM, the aligned models are compared to infer the as-built progress information that ultimately needs to be updated in BIM. This demands the utilization of IFC-based BIMs as the common solution to allow exchange of information including the geometrical information of the as-planned model (before registration) and the communication of progress information (after registration). IFC is a platform-neutral and open data file exchange format for BIMs. This non-proprietary format, introduced by BuildingSMART International Ltd. (Camberly, UK) [67], allows the collaborative and interoperable use of BIMs at various stages of building projects between different stakeholders. Its applications include schedule planning, continuous updating of progress information, visualization, and communication of as-built progress [16,17,20]. There are some attempts that performed the IFC-based BIM updating using proprietary software such as Synchro [68] and Vico Office [69] by manually inputting the required information [5,17–19]. However, in compliance with automation, some efforts performed the direct exchange of progress information to the IFC-based BIM using the IFC schema. For example, Hamledari, McCabe, Davari, and Shahi [16] developed a method to update the progress information into IFC2X3 BIM by modifying the

schedule hierarchy, updating the progress ratios, and then color-coding the building elements. Apart from IFC support for schedules, other progress information such as facility inspection data including as-built details, images, notes, and changes were also reported to be updated in the IFC-based BIM [20]. Although these studies employed the IFC-based BIM to update progress information, its utilization as an as-planned model by accessing the 3D geometrical information using the standard IFC schema for registration still needs to be explored.

## 3.3 Methodology

### 3.3.1 Overview

Building structures have evident corners due to the dominant planar structures, such as walls, roofs, etc., in their geometry. The study detailed in this chapter 3, a corner point is defined as the intersection point of three plane segments, referred to as parent plane segments. Similar to the Cartesian points in the 3D Euclidean space, the geometrical information of these corner points, along with their parent plane segments, follows the geometric invariants; hence, they can be employed for geometrical computations.

The proposed method in this chapter employs corner points as points of interest to solve the registration problem of the building scan with its BIM model. The method can be divided in four consecutive stages: (1) extraction of the corner points from both models, (2) identification of the potential matching corner points through geometric invariants, (3) evaluation of the transformations of potential matching corner points, and (4) calculation of the most optimal transformation. Overall Methodology of the proposed method is also presented in Appendix 1.

### 3.3.2 Extracting Corner Points

The corner points are extracted from both models using their plane segments. However, the models may not be in their best form to obtain the plane segments from them; therefore, pre-processing might be necessary.

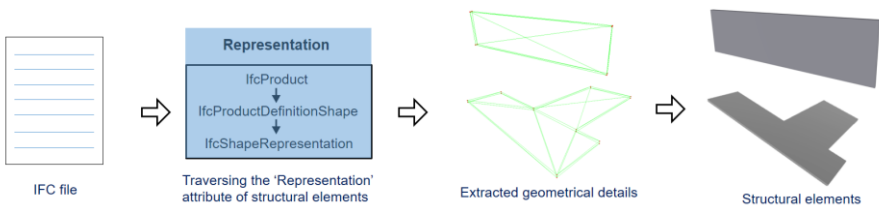
The as-built model obtained by laser scanning can contain millions of unevenly distributed points contaminated with noise and occlusions. Huge number of points will increase the computation time, while noise and occlusions affect the accuracy of extracted geometrical parameters. Therefore, pre-processing will consist of down-sampling the point cloud using octree-based voxelization, with voxel sizes as a function of the desired level of detail (LoD), after removal of noise based on existing algorithms. After that, plane segmentation is performed on the model to detect the plane segments from it.

Similarly, the as-planned model is assumed to be a BIM model of the building. Usually, the BIM model is converted into a point cloud before use for a compatible comparison with the as-built point cloud model. However, the conversion may limit the details in the model and causes the loss of quality in its extracted geometrical

parameters. Therefore, the current study directly extracts the geometrical details from an IFC-based BIM. The Industry Foundation Classes (IFC) data model follows a neutral and open file format, registered as an official international standard ISO 16739:2013. The file format is object-oriented and commonly used for Building information modelling. Objects have an accurate position in space that are distinguished by categories, characteristics, and function. IFC models include geometric and non-geometric entities: the building geometry and data associated with its elements. The IFC data schema assigns a name to, and relationships between, objects. It describes identity and semantics (ID, object, name, function), characteristics (material, properties, color), relationship between objects (e.g., walls, slabs, windows), abstract concepts (e.g., performance, costing), processes (e.g., installation, assembly), and people (e.g., owners, managers, designers, contractors). **Figure 3.1** shows an example of the IFC data format in plain text form that contains different entities exchanging various types of information related to building components. To obtain the plane segments from the as-planned model, the mesh model is constructed according to the geometrical details of structural elements from the IFC-based BIM in an automated way, as shown in **Figure 3.2**. The required geometrical shape information, including the vertices and faces from the planar structural elements, like walls and roofs, are taken out from each element by processing their geometric information. The elements are stored in IFC schema under the entity 'IfcProduct' with the inheritance (IfcRoot → IfcObjectDefinition → IfcObject → IfcProduct). The geometric information (such as shape, position, direction etc.) of the elements is obtained by traversing the representation attributes. The processed information of these elements in the form of vertices and faces is then used to create their mesh for further processing. Later, the required plane parameters can be directly acquired from the mesh in an accurate and efficient way, without any need of point cloud conversion. In comparison to other methods, we construct a mesh from the BIM model directly rather than a CAD model.

```
#165= IFCPRESENTATIONSTYLEASSIGNMENT(#163);
#167= IFCSTYLEDITER(#160,#165,$);
#170= IFCSHAPEREPRESENTATION(#101,'Body','SweptSolid',(#160));
#173= IFCPRODUCTDEFINITIONSHAPE($,$,#152,#170);
#177= IFCWALLSTANDARDCASE('3zv05uuRX5rhB2K73V3BRr',#41,'Basic Wall:Generic - 200mm:354100',$,'Basic Wall:Generic - 200mm',#146,#173,'354100');
#186= IFCMATERIAL('Default Wall');
#189= IFCPRESENTATIONSTYLEASSIGNMENT(#163);
#191= IFCSTYLEDITER($,#189,$);
#193= IFCSTYLEDREPRESENTATION(#96,'Style','Material',(#191));
#196= IFCMATERIALDEFINITIONREPRESENTATION($,$,#193,#186);
#199= IFCMATERIALLAYER(#186,0.2,$);
#201= IFCMATERIALLAYERSET((#199),'Basic Wall:Generic - 200mm');
#204= IFCMATERIALLAYERSETUSAGE(#201,.AXIS2.,.NEGATIVE.,.0.1);
```

**Figure 3.1.** An example of IFC content.

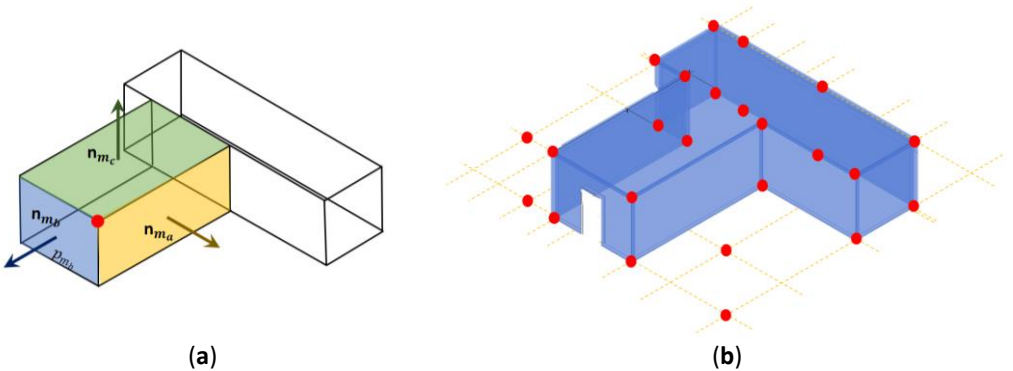


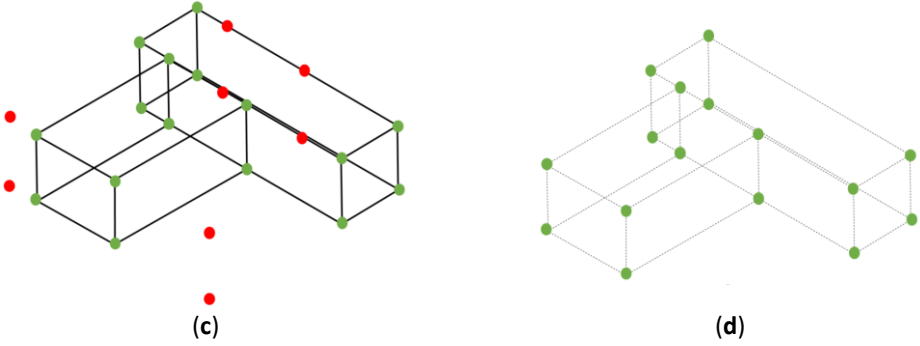
**Figure 3.2.** Extracting the geometric details of building components from IFC to construct their structural mesh model.

After acquiring the plane segments from both models, all the possible corner points are extracted. The corner point is the unique intersection point between three non-parallel plane segments. For the given plane segments  $p_{m_a}$ ,  $p_{m_b}$ , and  $p_{m_c}$ , with their respective normal vectors  $\vec{n}_{m_1}(a_1, b_1, c_1, d_1)$ ,  $\vec{n}_{m_2}(a_2, b_2, c_2, d_2)$ , and  $\vec{n}_{m_3}(a_3, b_3, c_3, d_3)$ , the coordinates of their intersection point (**Figure 3.3a**) can be computed using the given formula:

$$\begin{bmatrix} x \\ y \\ z \end{bmatrix} = \begin{bmatrix} a_1 & b_1 & c_1 \\ a_2 & b_2 & c_2 \\ a_3 & b_3 & c_3 \end{bmatrix}^{-1} \begin{bmatrix} -d_1 \\ -d_2 \\ -d_3 \end{bmatrix} \quad (1)$$

Equation (1) generates the intersection points for the given plane segments based on their plane directions, even if those segments are not actually intersecting. (**Figure 3.3b**) Accordingly, false corner points are also generated that not only increase the quantity of extracted corner points, but, due to the equidistant placement of these additional points, can also affect the reliability of the invariant-based matching step. Therefore, a verification is performed that confirms the intersection of the calculated corner point to the actual surface of all three parent plane segments (**Figure 3.3c**). In this study, a k-d tree nearest-neighbor search algorithm is used to verify the corner points are contained within their respective parent planes with a suitable tolerance radius to accommodate the errors in plane segments. In the end, only the points at the actual corners contained in their respective intersecting planes (**Figure 3.3d**) are extracted along with the geometrical information of their parent planes. Appendix 8 contains a pseudocode detailing the program developed to extract corner points from the plane segments, while pseudocode in Appendix 9 details the additional process to filter the actual corner points from extracted ones.





**Figure 3.3.** Visualization of (a) a single corner point generated from three parent planes; (b) all the possible corner points generated from a model, including the false points; (c) differentiation of false corner points (red color) from others (green) after verification; and (d) final corner points (green) in the model.

### 3.3.3 Identifying the Potential Matching Corner Points through Geometric Invariants

To identify the matching points between both models, the corner points are pruned using geometric matching criteria to reject the non-matching points based on distance, angle, rotation, and translation invariants. The remaining points that comply with all geometric criteria are termed ‘potential matching points’. These potential matching points are later evaluated in the next step to sort out the matching points.

If the corner points extracted from the as-planned and as-built model are  $M = \{\mathbf{m}_i\}_{i=1}^p$  and  $D = \{\mathbf{d}_i\}_{i=1}^q$ , with  $\mathbf{m}_i, \mathbf{d}_i \in \mathbb{R}^3$ , then their matching corner points can be identified as:

$$\mathbf{m}_i = \mathbf{R}\mathbf{d}_i + \mathbf{t} + \mathbf{e}_i \quad (2)$$

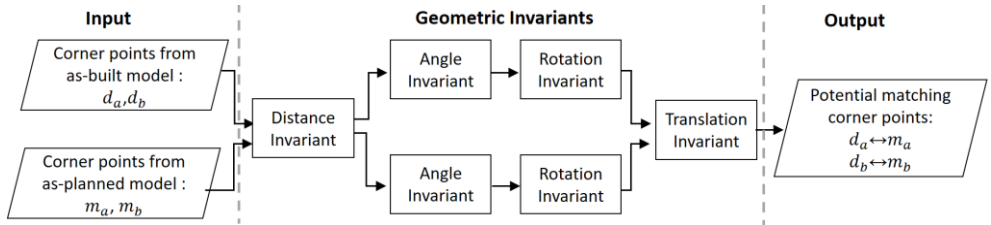
where  $p$  is the number of corner points in the as-planned model,  $q$  is the number of points in the as-built model,  $\mathbf{R} \in SO(3)$ , and  $\mathbf{t} \in \mathbb{R}^3$  are rotation and translation, respectively. Similarly,  $\mathbf{e}_i$  is the error in the as-built corner point as a result of the presence of noise and occlusions in the as-built model. In Equation (2),  $\mathbf{m}_i$  is the matching point of  $\mathbf{d}_i$  with an error  $\mathbf{e}_i$  in the  $i$ -th correspondence according to the rigid transformation parameters  $\mathbf{R}$  and  $\mathbf{t}$ .

The identification of matching points is performed in a cycle where the two corner points from both models are assessed for matching simultaneously through a series of different geometric invariants in a specified combination. For example, two corner points  $\{\mathbf{d}_a, \mathbf{d}_b\}$  from the as-built model are compared with the respective corresponding corner points  $\{\mathbf{m}_a, \mathbf{m}_b\}$  from an as-planned model in a particular cycle, and if they are congruent to all the invariants, only then they are withheld as potentially matching; otherwise, they are rejected. In the next cycle, two different



corner points from both models are compared. Each cycle can either reject or withhold the pairs of two corner points as potential matching corner points to eventually identify the possible pairs in the end. An algorithmic description in the form of pseudocode outlining the procedural steps utilizing diverse geometric invariants is presented in Appendix 10.

**Figure 3.4** shows the processing flow for the assessment of the geometric invariants for one cycle. The processing of two sets of corner points, instead of one, gives the opportunity to individually compare both sets with each other (in the first and last step) in addition to analyzing the match of corresponding points in each set (in the second and third step) in each scrutiny-based cycle. Overall, this pairwise processing of corner points in an invariant-based step-wise combination is designed to increase the prospects of identifying the matching corner points in a highly optimized way. The flowchart describing the processing using a series of geometric invariants to identify potential matching points is also shown in Appendix 2, with further details of these invariants provided below:



**Figure 3.4.** The processing sequence of geometric invariants to identify the potential matching corner points in a cycle.

### 3.3.3.1 Distance Invariant

The distance invariant is based on the characteristic that, if the two particular points from both models are matching points, then the distance between them should also be the same. A graphical example to understand the invariant is also provided in Appendix 3. Mathematically, given any two points  $\{m_a, m_b\}$  in M and their matching points  $\{d_a, d_b\}$  in D, where  $a \neq b$ , the relative distance of these two points and their matching points from Equation (1) becomes:

$$(m_a - m_b) = R \cdot (d_a - d_b) + (e_a - e_b) \quad (3)$$

$$\|m_a - m_b\| \leq \|d_a - d_b\| + \|e_a - e_b\| \quad (4)$$

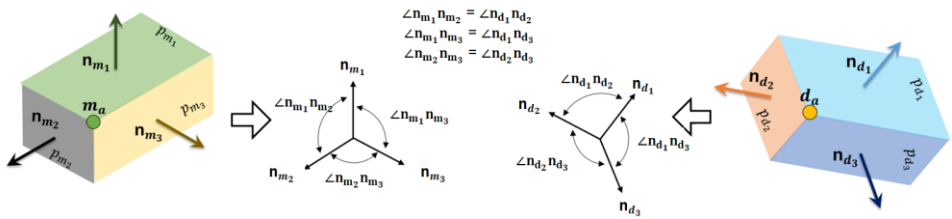
In above equations,  $\|\cdot\|$  denotes the Euclidean norm in  $\mathbb{R}^3$ . If  $c$  is the constant that represents the maximum allowed error on the distance, hence that  $c > \|e_a - e_b\|$ , then the Equation (4) can be written to reject the non-matching points:

$$\|m_a - m_b\| - \|d_a - d_b\| \leq c \quad (5)$$

As the relative distance between corner points is invariant with respect to rotation ' $R$ ' and translation ' $t$ ', it provides the possibility to initially probe the pair of corner points for matching without computing their transformation parameters.

### 3.3.3.2 Angle Invariant

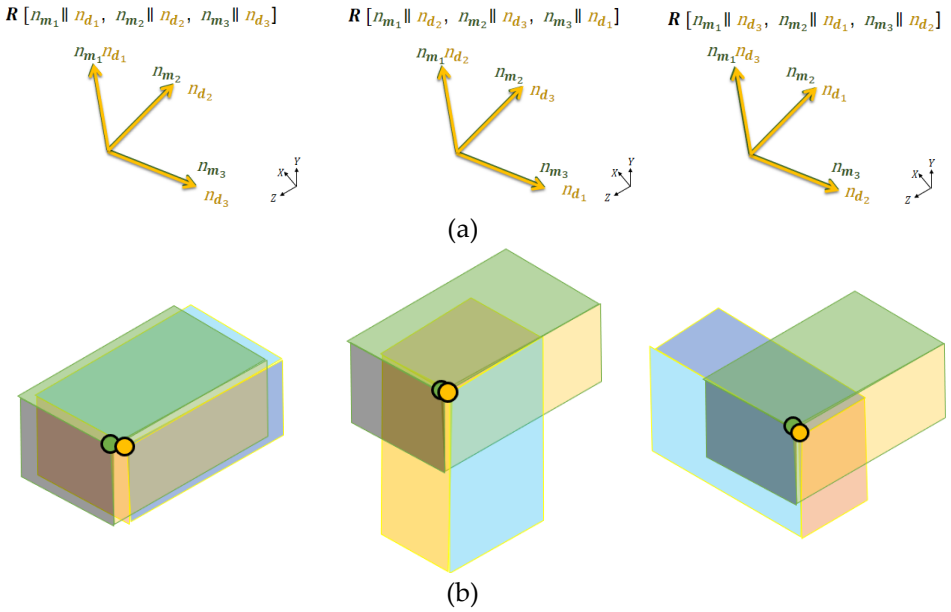
The angle invariant is based on the geometric invariant that the corresponding parent plane segments of matching corner points should have the same relative angles with each other. Each corner point is constructed from three parent plane segments with their respective normals. With a suitable tolerance, the angles between the corresponding parent plane segments for both potential matching corner points are probed using their plane normals, as demonstrated in **Figure 3.5**.



**Figure 3.5.** Verification of the relative angles between the parent planes of two potential matching corner points using their normals.

### 3.3.3.3 Rotation Invariant

If not rejected in the previous steps, both pairs of potential points are assessed to find their corresponding transformation with the correct rotation. It is based on the invariant that the transformation obtained from potential matching corner points with correct rotation should fit their respective corresponding parent plane segments.



**Figure 3.6.** Visualization of (a) rotation matrices obtained after alignment of the corresponding plane normal in different combinations and, (b) their respective rotation effect on the as-built model relative to an as-planned model.

To find the transformation of any potential matching corner points, the direction of their corresponding parent plane segments can be utilized to find out the rotation matrix and then the translation can be computed directly from the points. However, the estimation of correct transformation demands the determining the correct rotation matrix and this requires the identification of the respective corresponding segments. Most buildings have orthogonal geometries with perpendicular plane segments; therefore, the correspondence of plane segments cannot be truly determined based solely on their relative angles. To illustrate this, some examples of rotation matrices ( $\mathbf{R}_r$ ) resulting from the alignment of the corresponding plane's normal in different combinations 'r' are shown in **Figure 3.6a** while the visualization of the transformation obtained from the respective rotation matrices on the as-built model relative to the as-planned model is shown in **Figure 3.6b**.

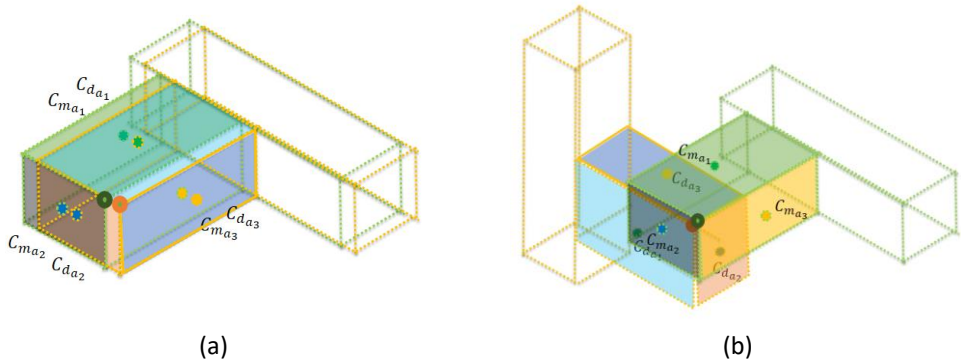
To solve this issue, transformation is determined for potential matching points with possible rotation matrices according to all the corresponding combination of parent plane segments and then evaluated in terms of their plane segment centroids to confirm their geometrical coincidence after transformation. For example, the rotation matrix ( $\mathbf{R}_{a,r}$ ) is determined for individual potential matching corner points ( $\mathbf{m}_a, \mathbf{d}_a$ ) by aligning the corresponding direction of plane segments based on the

correspondence combination ‘ $r$ ’ while the translation ( $\mathbf{t}_{a_r} = \mathbf{m}_a - \mathbf{R}_{a_r} \mathbf{d}_a$ ) is computed from the corner points. For all the possible rotation matrices with their respective translations for all the combinations, the projection of the average centroid of the parent plane segments from the as-planned and transformed as-built corner points are compared using Equations (6) and (7) for both pairs of points, respectively.

$$\mathbf{R}_a, \mathbf{t}_a = \operatorname{argmin}_{\mathbf{R}_{a_r}, \mathbf{t}_{a_r}} \sum_{r=1}^r \min(\|C_{m_a} - (\mathbf{R}_{a_r} \cdot C_{d_a} + \mathbf{t}_{a_r})\|^2) \quad (6)$$

$$\mathbf{R}_b, \mathbf{t}_b = \operatorname{argmin}_{\mathbf{R}_{b_r}, \mathbf{t}_{b_r}} \sum_{r=1}^r \min(\|C_{m_b} - (\mathbf{R}_{b_r} \cdot C_{d_b} + \mathbf{t}_{b_r})\|^2) \quad (7)$$

In the ideal case, the average centroids  $\{C_m, C_d\}$  of the plane segment from both models should project into each other with the correct rotation  $\mathbf{R}_a$  (**Figure 3.7a**) as compared to the incorrect rotations (**Figure 3.7b**). However, due to errors in the as-built plane segments, the projections may have slight deviations. Therefore, the rotation matrix allowing the projections to be nearest to each other is considered to be the most likely rotation matrix among the other matrices. The underlying reason is that it is the only rotation matrix obtained with the correspondence which permits the simultaneous fitting/coincidence of all the matching plane segments with each other. At the end of this step, the individual rotation matrices ( $\mathbf{R}_a, \mathbf{R}_b$ ) for both pairs of potential matching points that are later processed in next stage are computed.



**Figure 3.7.** Visualization of as-planned model and transformed as-built model with transformations aligning the (a) corresponding plane segments with centroids nearest to each other and, (b) non-corresponding plane segments with centroids relatively far from each other.

#### 3.3.3.4 Translation Invariant

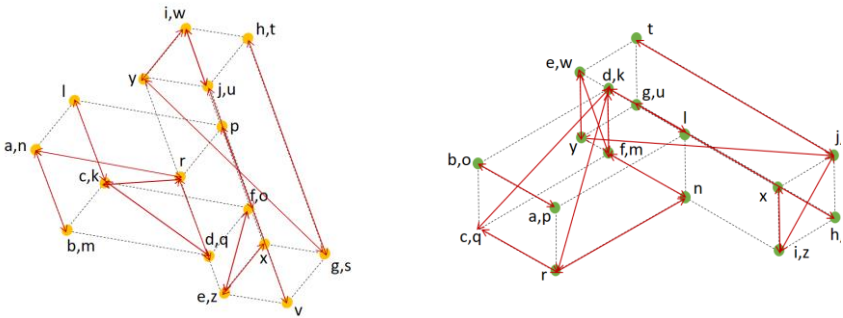
Finally, the transformation parameters calculated from both potential matching points are compared. It is based on the invariant that all the matching points should have the same rotation matrix and translation. If any of the transformation

parameters from both pairs of potential matchings points are not the same, then they are rejected.

Mathematically, any corner point  $m_i$  corresponding to its matching point  $d_i$  rotated with rotation matrix  $R_i$  has the translation  $t_i = m_i - R_i \cdot d_i$ . Similarly, in the case of potential matching corner points, the two corner points  $\{m_a, m_b\}$  in M corresponding to their matching points  $\{d_a, d_b\}$  in D, with respective rotation matrices  $\{R_a, R_b\}$ , should have the same rotation, such that  $R_a \cdot R_b^T = I_3$ , and the same translation, which satisfies the following:

$$\|(m_a - R_a \cdot d_a) - (m_b - R_b \cdot d_b)\| \leq c \quad (8)$$

In the above equation,  $c$  is the constant confirming  $c > \|e_a - e_b\|$  with a suitable value assigned according to the errors in as-built plane segments. Figure 3.8 indicates the potential matching corner points, indicated with same label in both models, obtained after consenting to all the geometrical invariants.



**Figure 3.8.** The identification of potential matching corner points from the as-built (**left**) and the as-planned model (**right**). The edges of the arrow with the same labels  $[a,b,c,\dots,y,z]$  in both models represent the potential matching points.

The combinations of invariants that sequentially process the pairs of candidate corner points for matching are arranged to identify the potential matching corner points with less possible computation. The first step rejects the non-matching pairs without the need to calculate other parameters, thus reducing the processing time of the succeeding steps. The non-rejected pairs are further probed in a step-wise arrangement using the required parameters that were computed in the preceding step. Furthermore, the identification of potential corner points can be performed using all the extracted corner points from both models. However, the processing time can be increased exponentially in the case of a high number of corner points and can affect the time efficiency. Therefore, the two corner points from both models are randomly picked in each cycle using RANSAC with a defined number of

cycles to ensure robustness during the current stage of identifying the potential matching points using geometric invariants.

### 3.3.4 Evaluating the Transformations of Potential Matching Corner Points

The identified potential matching corner points include the matching corner points with correct transformation, but there is a possibility that some non-matching points with incorrect transformation may be included as well, as evident in **Figure 3.8**. Non-matching corner points may have passed the identification due to the possible symmetries in the models. Therefore, all the remaining potential matching points are re-evaluated to find the correct or most likely matching corner points and transformations in two steps: (1) removal of duplicates and clustering of the remaining potential matching points according to their transformation parameters and (2) selection of the cluster with the correct transformation parameters.

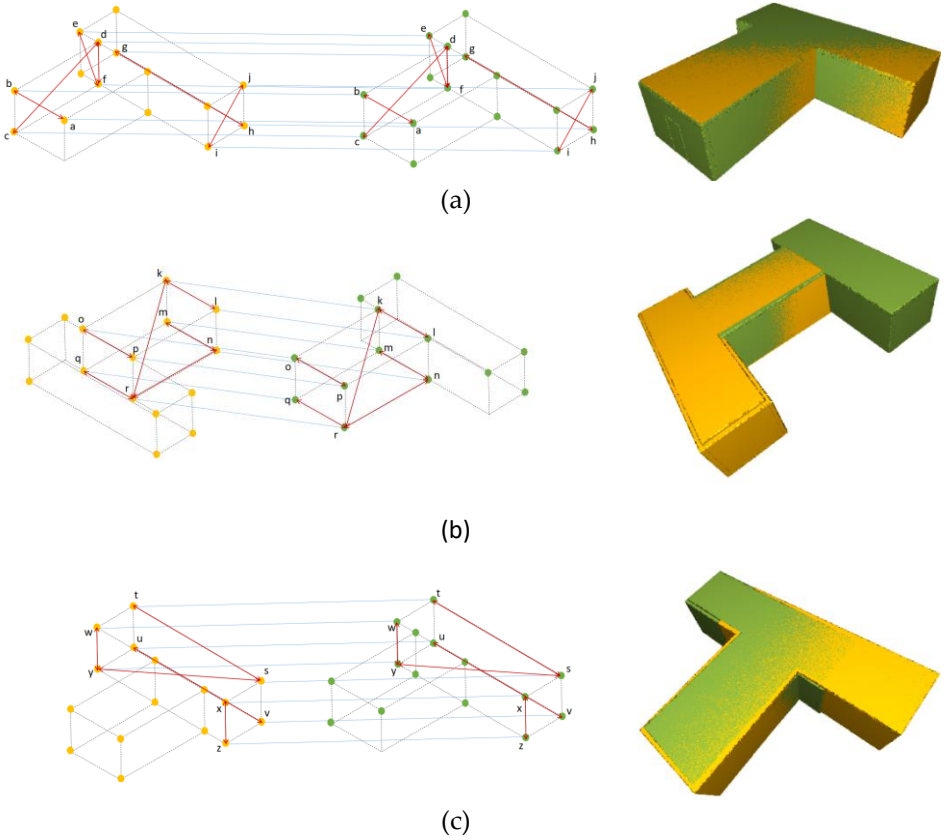
#### 3.3.4.1 Removing the Duplicates and Clustering the Potential Matching Corner Points

The potential matching corner points, identified in the last step, may contain duplicates due to the possibility of their identification in many pairs as a result of the RANSAC pairwise processing. There is a possibility that the duplicate pairs of potential corner points can be picked during RANSAC random selection. These duplicates are discarded by removing the other potential matching corner points having the same parent planes.

After removing the duplicates, potential matching corner points are grouped according to their transformation parameters. The translation vector  $\mathbf{t}_i = \mathbf{m}_i - \mathbf{R}_i \cdot \mathbf{d}_i$  is dependent on the rotation matrix; hence, it is unlikely that potential matching points with different rotation matrices have the same translation vectors. Therefore, the translation vectors of the points can be utilized to differentiate their transformation parameters. To allocate potential matching corner points to a cluster with translation  $\mathbf{t}_o$ , the candidate potential matching corner points with  $\mathbf{t}_i$  should have the same translation with a suitable tolerance  $c$ , as represented in Equation (9).

$$\|(\mathbf{m}_o - \mathbf{R}_o \cdot \mathbf{d}_o) - (\mathbf{m}_i - \mathbf{R}_i \cdot \mathbf{d}_i)\|^2 \leq c^2 \quad (9)$$

**Figure 3.9** represents the different potential matching points [a, b, c, ..., y, z], clustered according to their transformations where it is apparent that the potential matching points in each cluster have the same translations (blue line).



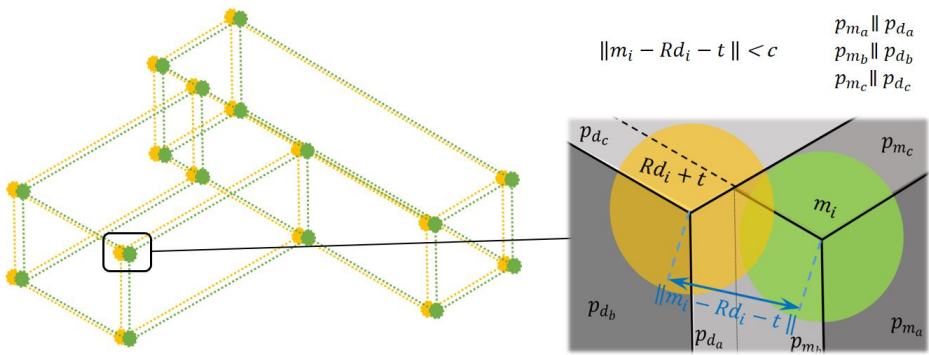
**Figure 3.9.** Potential matching points in the as-built (**left model**) and as-planned model (**right model**), clustered according to respective transformation parameters visualized next to them in terms of their corner points and 3D models (a–c).

### 3.3.4.2 Finding the Cluster with the Correct Transformation

To reduce computation time—instead of evaluating the individual potential matching corner points—the evaluation is performed directly on the clusters based on the two invariants to allow the simultaneous identification of the matching corners. According to the first invariant, the correct transformation aligns all (or the majority of) the corner points from both models. The second invariant advances that, if the aligned corner points in the correct transformation are matching, their corresponding parent planes should be parallel as well. Based on these two invariants as indicators of the correct registration, all the clusters, with their transformations, are evaluated.

Initially, all the corresponding corner points according to each transformation from the clusters are recognized. The transformation parameters from the respective clusters are applied to the original as-built corner points to project them into as-planned points. Ideally, corresponding points with the same parent plane segments

from both models should be aligned with each other in the case of correct transformations. However, due to the presence of errors in the as-built plane segments, the projection of corresponding corner points may not be exactly aligned but located near to each other. Therefore, neighboring corner points from both models having corresponding parallel parent plane segments are determined with a suitable tolerance, by means of k-d tree and the angles between the normals of the corresponding parent plane segments. **Figure 3.10** shows a corner point  $d_i$  from the as-built model transformed with rotation  $R_i$  and translation  $t_i$ . Its distance to a neighboring point  $m_i$  from the as-planned model is less than the tolerance  $c$ , and both points have parallel parent plane segments after transformation; hence, they are considered to be aligned corner points.



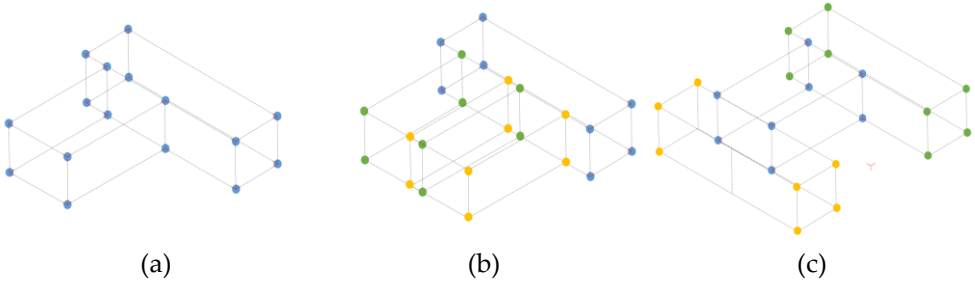
**Figure 3.10.** An example of neighbor corner points with parallel parent planes.

It is obvious in Figure 3.10 that some of the aligned corner points with parallel corresponding parent plane segments, according to the transformation of each cluster, are already present in the cluster along with other additional aligned corner points. The additional points are the potential matching points that have a similar transformation if computed. However, they were not identified previously due to the random selection of corner points from both models using RANSAC. Therefore, the current procedure enables their complete detection. The additional potential matching points  $m_i$  are detected at the current stage because the complete identification of all the potential matching points in the previous stage is computationally expensive. The random identification ensures the minimum computation and outputs sufficient potential matching points that include at least one matching point whose transformation is enough to detect the other matching points at this present stage. Overall, this approach allows the robustness in the proposed method with high reliability.

Finally, the cluster with the transformation having the highest number of aligned corner points is considered to be the correct transformation while the respective aligned points are finalized as matching corner points. **Figure 3.11** demonstrates the aligned points in both models according to the transformation of different clusters.



The cluster transformation in **Figure 3.11a** has the highest aligned points as compared to others; hence, it is finalized as a cluster with matching corner points having correct transformation.



**Figure 3.11.** Visualization of the corner points from the as-built (yellow) and transformed as-planned model (green) resulting in aligned corner points (blue) according to each cluster transformation (a–c).

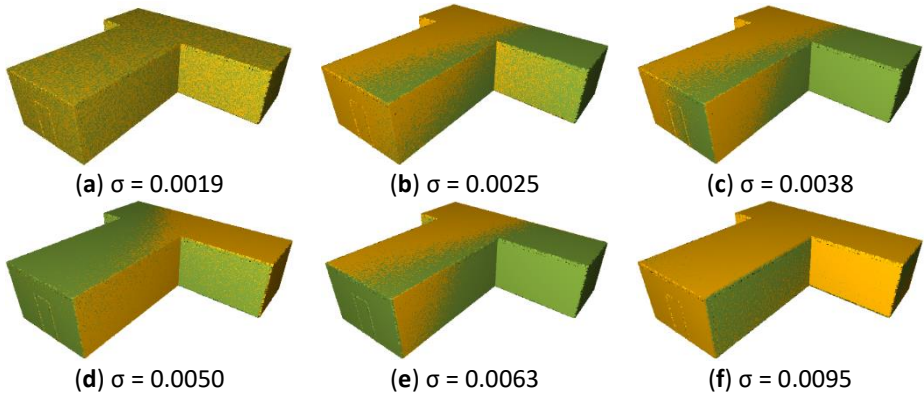
### 3.3.5 Calculating the Most Optimal Transformation from Matching Corner Points/Cluster

After sorting out the cluster with highest number of matching corner points, the individual transformation parameters of each corner point are assessed to find the most optimal transformation. The rotation  $\hat{\mathbf{R}}$  and translation  $\hat{\mathbf{t}}$  among the other respective rotation  $\{\mathbf{R}_1, \mathbf{R}_2 \dots \mathbf{R}_c\}$  and translation  $\{\mathbf{t}_1, \mathbf{t}_2 \dots \mathbf{t}_c\}$  parameters of clusters that align the corner points from both models with relatively more precise fitting, e.g., with less error, are finalized as the optimal transformation parameter, using Equations (10) and (11).

$$\sigma(\mathbf{R}, \mathbf{t}) = \sqrt{\frac{\sum_{i=1}^n \|\mathbf{m}_i - \mathbf{R} \cdot \mathbf{d}_i - \mathbf{t}\|^2}{n}} \quad (10)$$

$$\hat{\mathbf{R}}, \hat{\mathbf{t}} = \underset{\mathbf{R}, \mathbf{t}}{\operatorname{argmin}} \sigma(\mathbf{R}, \mathbf{t}) \quad \mathbf{R} \in \{\mathbf{R}_1, \mathbf{R}_2 \dots \mathbf{R}_c\}, \mathbf{t} \in \{\mathbf{t}_1, \mathbf{t}_2 \dots \mathbf{t}_c\} \quad (11)$$

In **Figure 3.12**, the models registered with transformation parameters corresponding to their error values are shown and **Figure 3.12a** indicates the optimal transformation (lowest error). It is evident that the optimal transformation parameter offers the relatively highest overlapping of models.



**Figure 3.12.** Visualization of as-built (yellow) and as-planned (green) registered according to the different transformation parameters with respective error values in ascending order (a–f).

### 3.3.6 Identifying the Matching Planes from Matching Corner Points (Optional)

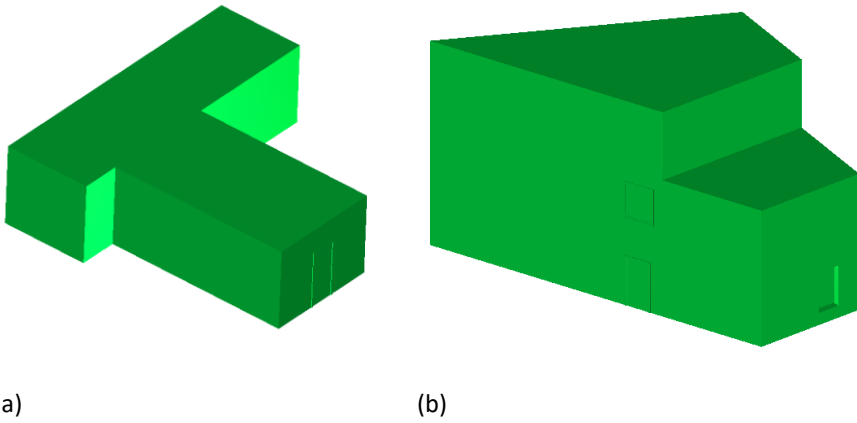
The construction project monitoring requires the progress estimation of building components that are represented by plane segments. The individual identification of matching plane segments is essential for an effective monitoring process. Normally, the matching planes can be easily identified using the criteria that the matching plane segments are parallel and fit with each other after registration. As an additional and reliable alternative, the utilization of corner points along with the semantic information of their parent plane segments in the proposed method enables the identification of plane segments as well. Generally, each plane segment is present as a parent plane segment in more than one corner point, with a maximum of four corner points. Therefore, after computing the transformation from the matched corner points, likewise, the matching plane segments can also be obtained by verifying their required presence in their corresponding multiple matching points.

## 3.4 Results and Discussion

The methodology was tested on different datasets presenting various challenges based on their geometrical shape. The datasets include two simulated (A1 and A2) and two real-life datasets (R1 and R2). It is important to mention here that the simulated datasets (A1 and A2) are the same that are also used in previous chapter but with different names (S1 and S3).

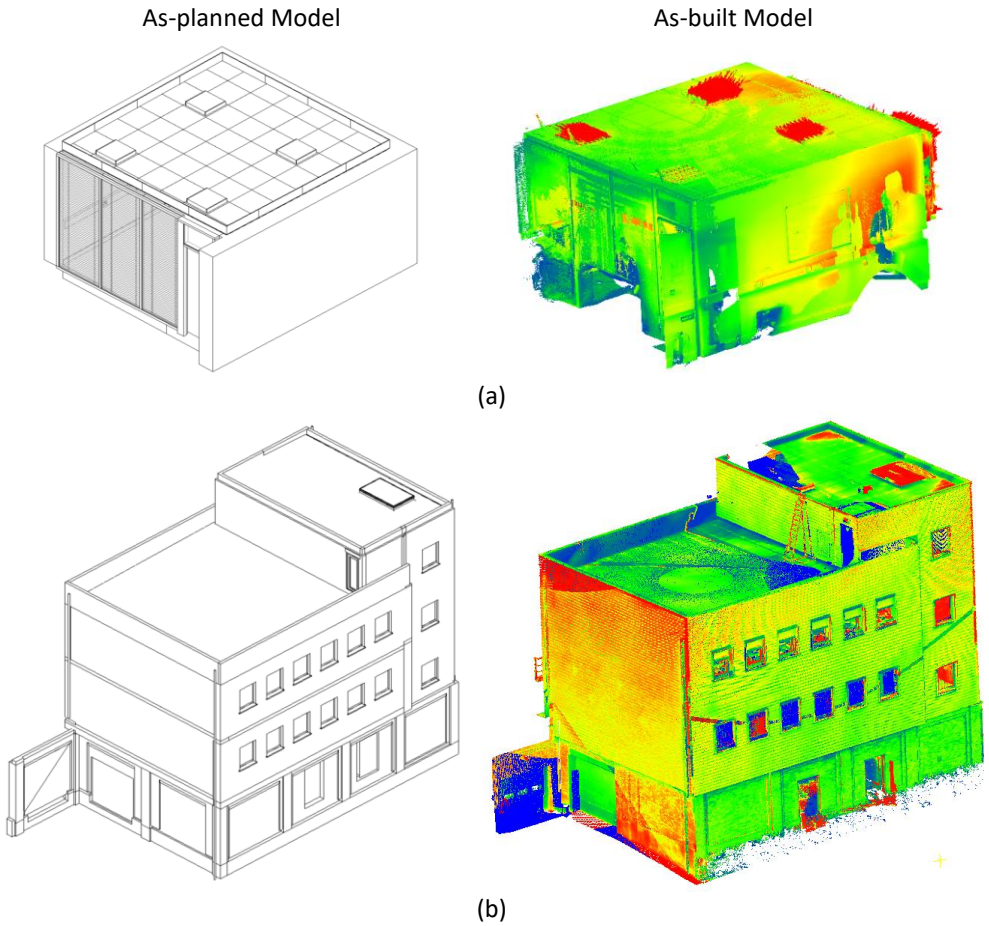
The simulated datasets were artificially designed to represent the building models with different structural compositions for testing, as shown in **Figure 3.13**. Using such datasets allowed for the assessment of the theoretical foundation of the proposed method, without effect of errors typical for real life situations. BIM models in IFC format were used as as-planned models, whereas randomly transformed models in point cloud format was used as as-built models. Both simulated models

have nine plane segments; however, the first model represents a single-floor building while the second one represents a triple-floor building.



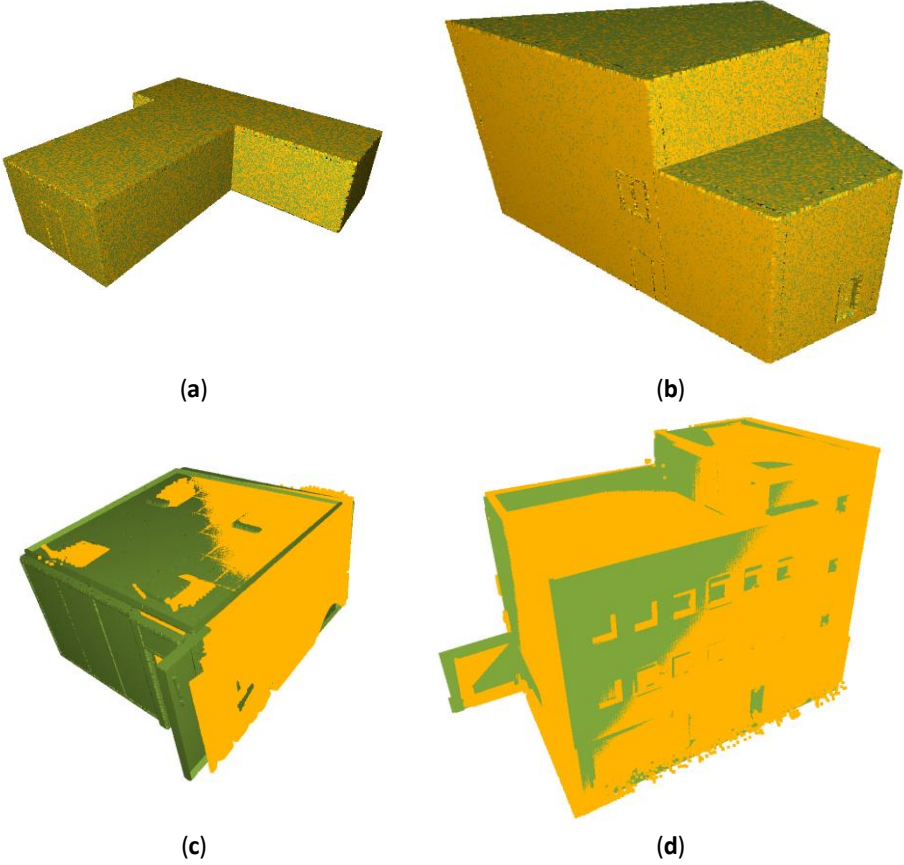
*Figure 3.13.* Visualization of models for (a) dataset A1 and (b) dataset A2.

The real-life datasets contain BIM and as-built models of two building projects. The as-built models were acquired by means of laser scanning. The datasets represent a conference room (R1) and a large educational building (R2), as shown in **Figure 3.14a,b**, respectively. The real-life dataset R1 represents a point cloud scan of an office space acquired using a Faro Focus 120 scanner. It comprises approximately seventy nine million 3D points and includes six plane segments structurally. The second real-life dataset, R2, is a point cloud scan of a four-storey structure captured with a terrestrial laser scanner. A comprehensive collection effort, involving 53 scans, yielded a densely populated dataset exceeding 500 million points. It is worth noting that both the real-life datasets were already used in other research [70–72]. Using these real-life datasets to assess the proposed method allows the evaluation of its performance and robustness in the case of the presence of occlusions, noise, and other errors typically present in as-built point clouds.



**Figure 3.14.** Visualization of as-planned and as-built models for (a) dataset R1 and (b) dataset R2.

The proposed method was implemented in the Python language, and all processing was conducted on a laptop equipped with an Intel i7-8850H CPU and 16 GB RAM. During the testing, the initial down-sampling of the as-built models was performed with a voxel size of 0.2 m and, later, RANSAC-based-plane segmentation was performed to obtain as-built plane segments. Similarly, the number of RANSAC iterations to randomly select the two corner points from both models for identification of potential matching points was limited to 5000. Furthermore, according to errors in the as-built model of each dataset, a suitable tolerance value was used to verify the geometric invariants. The proposed method successfully registered all the datasets, as shown in **Figure 3.15**. A detailed analysis was also performed to evaluate the registration accuracy and explore the limitations.



*Figure 3.15.* Visualization of registered as-built (yellow) and as-planned (green) models of (a) dataset A1, (b) dataset A2, (c) dataset R1, and (d) dataset R2.

To evaluate the registration accuracy of method, the root-means-square errors (RMSE) were computed. Furthermore, the transformed models were also compared with their ground truth models as RMSE is not sufficient as an indicator of registration accuracy [10]. The ground truth models were the same as the as-planned models for the simulated datasets; however, in the case of the real-life datasets, the transformed models after fine registration were used as ground truth. The rotation error in degrees and the translation error in mm for each dataset were calculated as additional evaluating metrics using Equations (12) and (13), respectively.

$$\epsilon_R = |\theta^{GT} - \theta^T| \quad (12)$$

$$\epsilon_t = \|\mathbf{t}^{GT} - \mathbf{t}^T\| \quad (13)$$

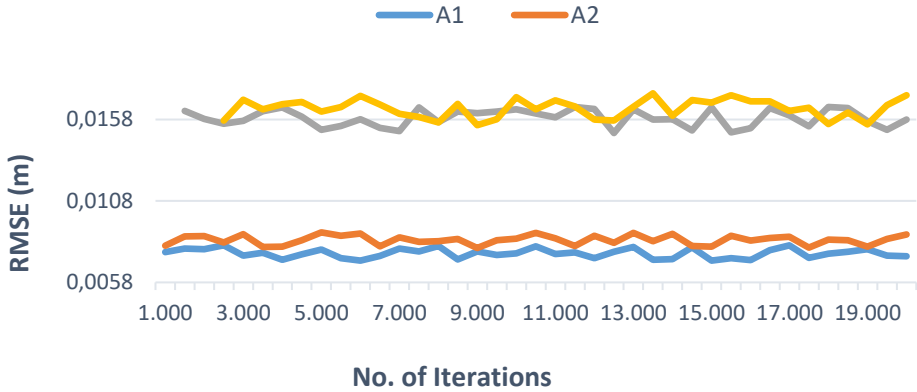
In the above equations,  $\theta^{GT}$  and  $\mathbf{t}^{GT}$  represent the quaternion rotation angles and translation vector of ground truth, whereas  $\theta^T$  and  $\mathbf{t}^T$  are the quaternion rotation

angles and translation vector of the transformed model. The evaluation parameters, listed in the **Table 3.1**, indicate an overall good accuracy as a coarse registration method. The method registered not only the simulated datasets but also the real-life datasets with higher accuracy. Furthermore, the registration results were also compared with our previous plane-based method [66] which is described in chapter 2, as shown in the **Table 3.1**, where it is evident that the proposed method registered all the datasets with more accuracy. The higher accuracy can be attributed to the approach of the proposed method that ensures the detection of all the matching corner points to compute the most accurate transformation parameter from them.

**Table 3.1.** Details of simulated datasets.

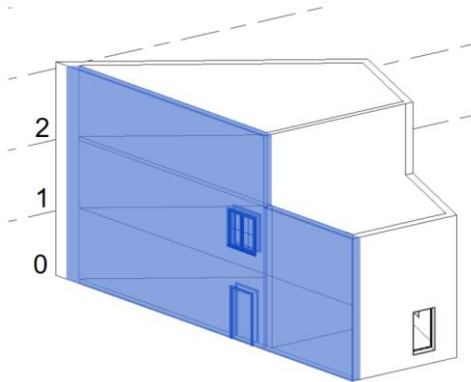
Datasets	Plane-Based Method			Proposed Method		
	RMSE (mm)	$\epsilon_R$ (°)	$\epsilon_t$ (mm)	RMSE (mm)	$\epsilon_R$ (°)	$\epsilon_t$ (mm)
A 1	7.186	0.007	29.164	7.519	0.002	4.036
A 2	8.792	0.005	35.385	8.485	0.003	7.821
R 1	18.119	0.027	94.267	15.884	0.015	37.649
R 2	17.781	0.021	107.142	16.139	0.007	31.224

The proposed method is RANSAC-dependent to ensure robustness, so the number of iterations could have an influence on the success. Although increasing the number of iterations results in more potential matching points with a cost of higher processing, this does not improve the registration accuracy (as shown in **Figure 3.16**) as the method already ensures the highest accuracy by detecting the remaining matching points after selecting the most optimal cluster in the third step. Generally, the method can only fail if the potential matching corner points obtained in stage 2 do not include any actual matching point, which can happen if the number of RANSAC iterations is too low. During testing, the method failed for dataset R1 and R2 prior to a number of iterations of 1500 and 2500, respectively. By increasing the number of iterations, this problem was resolved. In our results, 5000 iterations were found to be sufficient for both robustness and successful execution of the proposed method for all tested datasets.



**Figure 3.16.** Graph showing the effect on RMSE of increasing the number of RANSAC iterations.

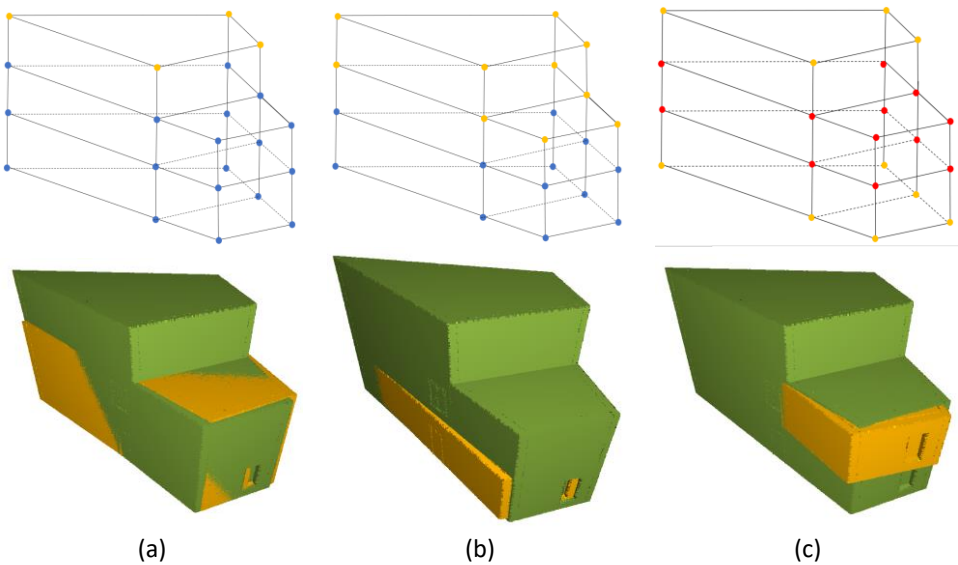
The potential matching points are identified using a series of geometric invariants to try to ensure that only the actual matching corner points are detected; however, geometrical symmetry in the building can still lead to the selection of non-matching points. To further explore this problem concerning construction progress monitoring, the proposed method was also tested for partially built buildings to analyze its success. For this purpose, two additional as-built models derived from dataset A2 (**Figure 3.17**), representing the completion of the first and second floor, were created.



**Figure 3.17.** Visualization of the dataset A2 model with different floors utilized to create incomplete as-built models.

The experimentation validated the successful registration of the as-built model with two floors completed as shown in **Figure 3.18a**; however, the registration success of the remaining model with the single model was inconsistent. Sometimes registration was successful, but other times there was some translation error, as shown with the

registered models in **Figure 3.18b,c**. The reason can be attributed to the fact that there was a lack of distinct points in both models. Hence, the proposed methodology finalized the two transformation clusters with equal number of corresponding corner points due to symmetrical positions of corner points at ground zero, first, and second, as demonstrated with the corner points in **Figure 3.18b,c**. However, in the case of the as-built model with two floors completed, the points are also the same and symmetrical, but the transformation cluster with maximum corresponding points is identified. The same happened with the fully completed as-built model (dataset A2). Therefore, it can be concluded that the proposed method works well for incomplete buildings not only with non-symmetric corner points but also with symmetric points if not all the as-built points form the symmetry with additional as-planned points.



**Figure 3.18.** Visualization of registered incomplete as-built (yellow) with as-planned (green) models according to their respective extracted corner points shown above.

The presence of symmetrical corner points in the building models challenges the registration due to similar geometrical parameters. However, the presence of a few discriminatory corner points can support the identification of correct transformation. Hence, the proposed method may fail in buildings with a symmetrical geometry; however, the presence of few distinct planar structures in the buildings can resolve this limitation. To solve this limitation in future research, the same matching strategy for complicated structures in the building can be developed if required.

It is important to mention here that the current research make use of the BIM model and extensively leverages its semantic information within the BIM model across all



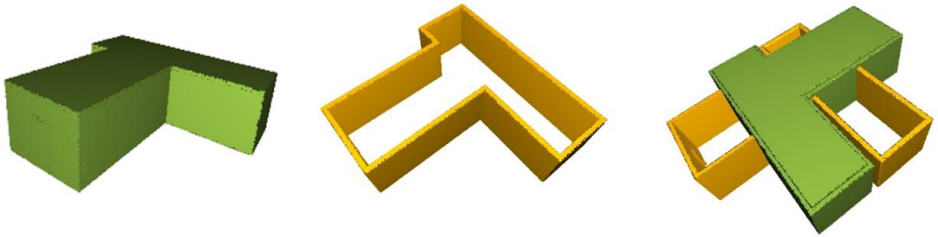
the phases. For example, geometric data from BIM is utilized in the current phase for the registration process (as detailed in chapter 2 and chapter 3), while subsequent phases involve estimating and storing as-built completion information in BIM (as detailed in chapter 4). Additionally, semantic parameters related to time, cost, and progress are utilized for storing, retrieving, modifying, and reporting construction progress monitoring data (as detailed in chapter 5). In addition, using BIM as the as-planned model also opens up a multitude of opportunities to address various limitations effectively, as BIM's ability to incorporate semantic information provides a powerful tool for overcoming the limitations. In the limitation scenario described above, such as when faced with the challenge of symmetric building shapes, we can supplement the semantic information with geo-referencing data. This enables us to provide detailed floor-level information during scan acquisition, augmenting the robustness of our methodology and surpassing the symmetric limitation.

### Comparison with plane-based registration

The current corner-based registration method is also compared with the plane-based registration method, which is detailed in (previous) chapter 2. From the results as indicated in Table 3.1 it is evident that the current corner point-based method is relatively more accurate although both are coarse registration methods that only aim to roughly align the models. This higher accuracy of current method can be explained as the plane-based method directly utilizing the centroid of plane segments, however, the presence of point cloud errors such as noise or occlusion can slightly affect the centroid parameters eventually influencing the registration accuracy. In contrast, the corner point-based method, dependent on corner points, computes the accurate corner point from the intersection of the plane segment using their normal values and the presence of noise or occlusion doesn't affect significantly the precision of corner points if the plane segments are detected. Therefore, the dependency of the second point on corner points, as compared to plane segments, doesn't compromise considerably on registration accuracy. Apart from that, the corner point-based method selects the most accurate rotation and translation parameter among the pool of correct parameters obtained from all the matched corner points. Overall, these measures give the second method an upper hand in terms of accuracy. Both methods were also tested with simulated datasets representing an under-construction building for registration. The results demonstrate that both methods successfully registered the scan model of an under-construction building if their respective conditions were met.

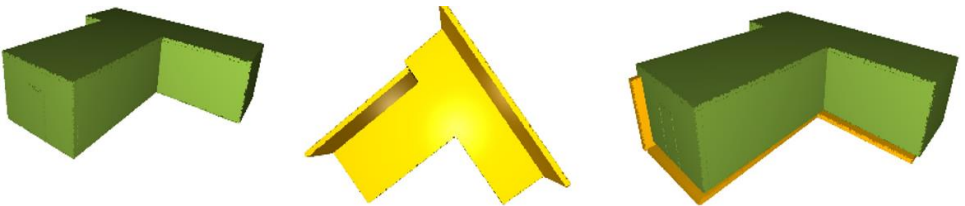
If we discuss their boundary conditions for success, the plane-based method requires two conditions. The first condition is the scan model should have at least three plane segments in a distinct direction so that the rotation matrix can be correctly computed. The second condition is that the size of most plane segments in the scan model should correspond to their matching plane segments so that the minimization process can accurately find out the correct transformation. For example, Figure 3.19

shows a simulated dataset in which the partially built model contains all the segments except the segments in one direction (horizontal). As there are two distinct directions of plane segments instead of three, the plane-based method incorrectly computed the transformation parameters. It is important to mention here that the proposed corner point method is also a plane dependent method hence it also fail if the plane segments are not obtained correctly as described in section 2.5.6



*Figure 3.19.* Visualization of the unsuccessful registration of the dataset with a partially built scan model using the plane-based method.

In contrast, the simulated model shown in **Figure 3.20** contains a partially built model with only three plane segments. Although there are only three segments all of them are in distinct directions, hence, the plane-based method registered the model successfully.



*Figure 3.20.* Visualization of the successful registration of the dataset with partially built scan model using the plane-based registration method.

As compared to the plane-based method, the corner point-based method requires at least two corner points in the scan model, otherwise, the method will fail due to not having enough points for processing. As the extraction of corner points commits the presence of three plane segments in distinct directions, this necessitates more than three corresponding plane segments for a minimum of two corner points. However, the registration still may fail relatively because of the reason that demands a matching pair of corner points from both models during processing to confirm the geometric invariants. Furthermore, at least one corner point, in terms of its position with others, should be non-symmetric as well. **Figure 3.21** demonstrates that if all the corner points extracted from the dataset (**Figure 3.21a**) of the partially built building model are positioned symmetric then the incorrect transformation (**Figure**

3.21b) can be computed based on the correspondence to non-matching points (Figure 3.21c). Therefore, the corner point-based method demands the presence of at least one asymmetric position of the corner point among the other symmetric points to accurately identify the correct transformation.

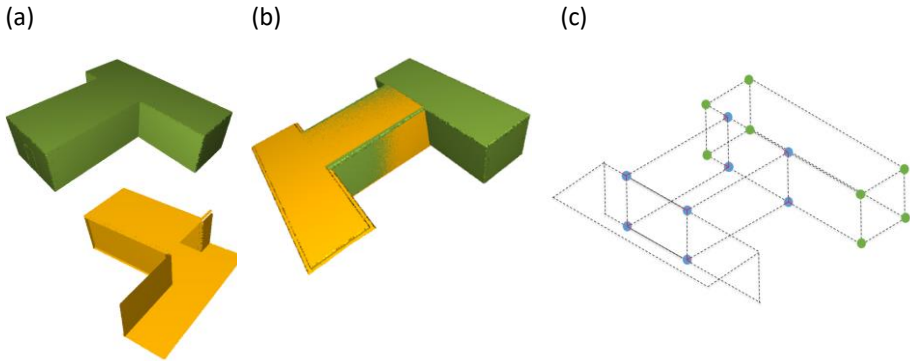


Figure 3.21. Visualization of (a) Models before registration, (b) Incorrectly registered models, and (c) Corner points of Incorrectly registered models

To sum up, the corner point-based method is relatively more accurate, however, the plane-based method is more suitable for datasets with scan models having less no. of structural components constructed.

### 3.5 Conclusions

A novel method is proposed in the current chapter for registration that utilizes corner points as the distinct feature to perform the accurate alignment of building scans with their BIM model to facilitate construction progress monitoring using Scan-vs-BIM. To ensure a consistent information format in automated progress monitoring, the study utilized an IFC-based BIM to directly extract the lossless geometrical details using the IFC schema, instead of converting BIM into another format. Buildings have evident corner points due to the dominant planar features in their structures. The method extracts those corner points from both models and then identifies their matching to eventually compute the most precise transformation parameters from them. The matching corner points are identified after RANSAC-based geometric pruning through a series of different geometric invariants. The results demonstrated that the proposed method successfully registered all the datasets, both the simulated and real-life datasets, with a high level of accuracy in a fully automated way. Apart from registering the scan models of completed buildings with their respective BIM models, the proposed method also proved its ability to register the scan model of the under-construction building as well, if a distinct corner point is present.

In terms of model-based construction progress monitoring, the research study in the current chapter adds a significant contribution by introducing a another fully automated and accurate point-based registration technique that utilizes IFC-based BIMs, identifies the matching structural features, and is capable of performing the registration of under-construction buildings. Further research is aimed to refine the proposed method to upgrade its application in complex buildings through additional geometric invariants.

### 3.6 References

1. Rebolj, D.; Pučko, Z.; Babič, N.Č.; Bizjak, M.; Mongus, D. Point cloud quality requirements for Scan-vs-BIM based automated construction progress monitoring. *Autom. Constr.* **2017**, *84*, 323–334.
2. Arditi, D.; Gunaydin, H.M. Total quality management in the construction process. *Int. J. Proj. Manag.* **1997**, *15*, 235–243.
3. Zhang, C.; Arditi, D. Automated progress control using laser scanning technology. *Autom. Constr.* **2013**, *36*, 108–116.
4. Bosché, F. Automated recognition of 3D CAD model objects in laser scans and calculation of as-built dimensions for dimensional compliance control in construction. *Adv. Eng. Inform.* **2010**, *24*, 107–118.
5. Golparvar-Fard, M.; Pena-Mora, F.; Savarese, S. Automated progress monitoring using unordered daily construction photographs and IFC-based building information models. *J. Comput. Civ. Eng.* **2014**, *29*, 04014025.
6. Tuttas, S.; Braun, A.; Borrmann, A.; Stilla, U. Acquisition and consecutive registration of photogrammetric point clouds for construction progress monitoring using a 4D BIM. *PFG–J. Photogramm. Remote Sens. Geoinf. Sci.* **2017**, *85*, 3–15.
7. Omar, H.; Dulaimi, M. Using BIM to automate construction site activities. *Build. Inf. Model. BIM Des. Constr. Oper.* **2015**, *149*, 45.
8. Golparvar-Fard, M.; Savarese, S.; Peña-Mora, F. Interactive Visual Construction Progress Monitoring with D4 AR—4D Augmented Reality—Models. In Proceedings of the Construction Research Congress 2009: Building a Sustainable Future, Washington, DC, USA, 5–7 April 2019; pp. 41–50.
9. Bueno, M.; Bosché, F.; González-Jorge, H.; Martínez-Sánchez, J.; Arias, P. 4-Plane congruent sets for automatic registration of as-is 3D point clouds with 3D BIM models. *Autom. Constr.* **2018**, *89*, 120–134.
10. Zong, W.; Li, M.; Zhou, Y.; Wang, L.; Xiang, F.; Li, G. A Fast and Accurate Planar-Feature-Based Global Scan Registration Method. *IEEE Sens. J.* **2019**, *19*, 12333–12345.
11. Pavan, N.L.; dos Santos, D.R.; Khoshelham, K. Global Registration of Terrestrial Laser Scanner Point Clouds Using Plane-to-Plane Correspondences. *Remote Sens.* **2020**, *12*, 1127.
12. Theiler, P.; Schindler, K. Automatic registration of terrestrial laser scanner point clouds using natural planar surfaces. *ISPRS Ann. Photogramm. Remote Sens. Spat. Inf. Sci.* **2012**, *3*, 173–178.
13. Xu, Y.; Boerner, R.; Yao, W.; Hoegner, L.; Stilla, U. Automated coarse registration of point clouds in 3d urban scenes using voxel based plane constraint. *ISPRS Ann. Photogramm. Remote Sens. Spat. Inf. Sci.* **2017**, *4*, 185.
14. Zhang, D.; Huang, T.; Li, G.; Jiang, M. Robust algorithm for registration of building point clouds using planar patches. *J. Surv. Eng.* **2012**, *138*, 31–36.
15. He, W.; Ma, W.; Zha, H. Automatic registration of range images based on correspondence of complete plane patches. In Proceedings of the Fifth International Conference on 3-D Digital Imaging and Modeling (3DIM'05), Ottawa, ON, Canada, 13–16 June 2005; pp. 470–475.
16. Hamledari, H.; McCabe, B.; Davari, S.; Shahi, A. Automated schedule and progress updating of IFC-based 4D BIMs. *J. Comput. Civ. Eng.* **2017**, *31*, 04017012.

17. Son, H.; Kim, C.; Kwon Cho, Y. Automated schedule updates using as-built data and a 4D building information model. *J. Manag. Eng.* **2017**, *33*, 04017012.
18. Pučko, Z.; Šuman, N.; Rebolj, D. Automated continuous construction progress monitoring using multiple workplace real time 3D scans. *Adv. Eng. Inform.* **2018**, *38*, 27–40.
19. Turkan, Y.; Bosche, F.; Haas, C.T.; Haas, R. Automated progress tracking using 4D schedule and 3D sensing technologies. *Autom. Constr.* **2012**, *22*, 414–421.
20. Hamledari, H.; Rezazadeh Azar, E.; McCabe, B. IFC-based development of as-built and as-is BIMs using construction and facility inspection data: Site-to-BIM data transfer automation. *J. Comput. Civ. Eng.* **2017**, *32*, 04017075.
21. Dong, Z.; Liang, F.; Yang, B.; Xu, Y.; Zang, Y.; Li, J.; Wang, Y.; Dai, W.; Fan, H.; Hyyppä, J. Registration of large-scale terrestrial laser scanner point clouds: A review and benchmark. *ISPRS J. Photogramm. Remote Sens.* **2020**, *163*, 327–342.
22. Besl, P.J.; McKay, N.D. Method for registration of 3-D shapes. In Proceedings of the Sensor Fusion IV: Control Paradigms and Data Structures, Boston, Massachusetts, USA, 12–15 November 1991; pp. 586–606.
23. Yang, J.; Li, H.; Jia, Y. Go-icp: Solving 3d registration efficiently and globally optimally. In Proceedings of the IEEE International Conference on Computer Vision, Sydney, NSW, Australia, 1–8 December 2013; pp. 1457–1464.
24. Pavlov, A.L.; Ovchinnikov, G.W.; Derbyshev, D.Y.; Tsetserukou, D.; Oseledets, I.V. AA-ICP: Iterative closest point with Anderson acceleration. In Proceedings of the 2018 IEEE International Conference on Robotics and Automation (ICRA), Brisbane, QLD, Australia, 21–25 May 2018; pp. 3407–3412.
25. Tazir, M.L.; Gokhool, T.; Checchin, P.; Malaterre, L.; Trassoudaine, L. CICP: Cluster Iterative Closest Point for sparse-dense point cloud registration. *Robot. Auton. Syst.* **2018**, *108*, 66–86.
26. Biber, P.; Straßer, W. The normal distributions transform: A new approach to laser scan matching. In Proceedings of the 2003 IEEE/RSJ International Conference on Intelligent Robots and Systems (IROS 2003) (Cat. No. 03CH37453), Las Vegas, NV, USA, 27–31 October 2003; pp. 2743–2748.
27. Magnusson, M. The Three-Dimensional Normal-Distributions Transform: An Efficient Representation for Registration, Surface Analysis, and Loop Detection. Doctoral Dissertation, Örebro universitet, Örebro, Sweden, 2009.
28. Das, A.; Waslander, S.L. Scan registration with multi-scale k-means normal distributions transform. In Proceedings of the 2012 IEEE/RSJ International Conference on Intelligent Robots and Systems, Vilamoura-Algarve, Portugal, 7–12 October 2012; pp. 2705–2710.
29. Takeuchi, E.; Tsubouchi, T. A 3-D scan matching using improved 3-D normal distributions transform for mobile robotic mapping. In Proceedings of the 2006 IEEE/RSJ International Conference on Intelligent Robots and Systems, Beijing, China, 9–15 October 2006; pp. 3068–3073.
30. Xu, Y.; Boerner, R.; Yao, W.; Hoegner, L.; Stilla, U. Pairwise coarse registration of point clouds in urban scenes using voxel-based 4-planes congruent sets. *ISPRS J. Photogramm. Remote Sens.* **2019**, *151*, 106–123.
31. Rusu, R.B.; Blodow, N.; Beetz, M. Fast point feature histograms (FPFH) for 3D registration. In Proceedings of the 2009 IEEE International Conference on Robotics and Automation, Kobe, Japan, 12–17 May 2009; pp. 3212–3217.

32. Yang, B.; Dong, Z.; Liang, F.; Liu, Y. Automatic registration of large-scale urban scene point clouds based on semantic feature points. *ISPRS J. Photogramm. Remote Sens.* **2016**, *113*, 43–58.
33. Stamos, I.; Leordeanu, M. Automated feature-based range registration of urban scenes of large scale. In Proceedings of the 2003 IEEE Computer Society Conference on Computer Vision and Pattern Recognition, 2003. Proceedings., Madison, WI, USA, 18–20 June 2003; pp. II–li.
34. Xiao, J.; Adler, B.; Zhang, J.; Zhang, H. Planar segment based three-dimensional point cloud registration in outdoor environments. *J. Field Robot.* **2013**, *30*, 552–582.
35. Yang, B.; Zang, Y. Automated registration of dense terrestrial laser-scanning point clouds using curves. *ISPRS J. Photogramm. Remote Sens.* **2014**, *95*, 109–121.
36. Ge, X.; Wunderlich, T. Surface-based matching of 3D point clouds with variable coordinates in source and target system. *ISPRS J. Photogramm. Remote Sens.* **2016**, *111*, 1–12.
37. Zai, D.; Li, J.; Guo, Y.; Cheng, M.; Huang, P.; Cao, X.; Wang, C. Pairwise registration of TLS point clouds using covariance descriptors and a non-cooperative game. *ISPRS J. Photogramm. Remote Sens.* **2017**, *134*, 15–29.
38. Bolles, R.C.; Fischler, M.A. A RANSAC-based approach to model fitting and its application to finding cylinders in range data. In Proceedings of the IJCAI, Vancouver, BC, Canada, 24–28 August 1981; pp. 637–643.
39. Glent Buch, A.; Yang, Y.; Kruger, N.; Gordon Petersen, H. In search of inliers: 3d correspondence by local and global voting. In Proceedings of the IEEE Conference on Computer Vision and Pattern Recognition, Columbus, OH, USA, 23–28 June 2014; pp. 2067–2074.
40. Cai, Z.; Chin, T.-J.; Bustos, A.P.; Schindler, K. Practical optimal registration of terrestrial LiDAR scan pairs. *ISPRS J. Photogramm. Remote Sens.* **2019**, *147*, 118–131.
41. Tombari, F.; Salti, S.; Di Stefano, L. Unique signatures of histograms for local surface description. In Proceedings of the European Conference on Computer Vision, Berlin, Heidelberg, 5 September 2010; pp. 356–369.
42. Böhm, J.; Becker, S. Automatic marker-free registration of terrestrial laser scans using reflectance. In Proceedings of the 8th Conference on Optical 3D Measurement Techniques, Zurich, Switzerland, 9–12 July 2007; pp. 9–12.
43. Weinmann, M.; Weinmann, M.; Hinz, S.; Jutzi, B. Fast and automatic image-based registration of TLS data. *ISPRS J. Photogramm. Remote Sens.* **2011**, *66*, S62–S70.
44. Theiler, P.W.; Wegner, J.D.; Schindler, K. Keypoint-based 4-points congruent sets-automated marker-less registration of laser scans. *ISPRS J. Photogramm. Remote Sens.* **2014**, *96*, 149–163.
45. Weber, T.; Hänsch, R.; Hellwich, O. Automatic registration of unordered point clouds acquired by Kinect sensors using an overlap heuristic. *ISPRS J. Photogramm. Remote Sens.* **2015**, *102*, 96–109.
46. Knopp, J.; Prasad, M.; Willems, G.; Timofte, R.; Van Gool, L. Hough transform and 3D SURF for robust three dimensional classification. In Proceedings of the European Conference on Computer Vision Berlin, Heidelberg, 5 September 2010; pp. 589–602.

47. Ge, X. Automatic markerless registration of point clouds with semantic-keypoint-based 4-points congruent sets. *ISPRS J. Photogramm. Remote Sens.* **2017**, *130*, 344–357.
48. Al-Durgham, M.; Habib, A. A framework for the registration and segmentation of heterogeneous LiDAR data. *Photogramm. Eng. Remote Sens.* **2013**, *79*, 135–145.
49. Habib, A.; Ghanma, M.; Morgan, M.; Al-Ruzouq, R. Photogrammetric and LiDAR data registration using linear features. *Photogramm. Eng. Remote Sens.* **2005**, *71*, 699–707.
50. Cheng, X.; Cheng, X.; Li, Q.; Ma, L. Automatic registration of terrestrial and airborne point clouds using building outline features. *IEEE J. Sel. Top. Appl. Earth Obs. Remote Sens.* **2018**, *11*, 628–638.
51. Angjeliu, G.; Cardani, G.; Coronelli, D. A parametric model for ribbed masonry vaults. *Autom. Constr.* **2019**, *105*, 102785.
52. Dold, C.; Brenner, C. Registration of terrestrial laser scanning data using planar patches and image data. *Int. Arch. Photogramm. Remote Sens. Spat. Inf. Sci.-ISPRS Arch.* **2006**, *36*, 78–83.
53. Von Hansen, W. Robust automatic marker-free registration of terrestrial scan data. *Proc. Photogramm. Comput. Vis.* **2006**, *36*, 105–110.
54. Khoshelham, K. Automated localization of a laser scanner in indoor environments using planar objects. In Proceedings of the 2010 International Conference on Indoor Positioning and Indoor Navigation, Zürich, Switzerland, 15–17 September 2010; pp. 1–7.
55. Li, M.; Gao, X.; Wang, L.; Li, G. Automatic registration of laser-scanned point clouds based on planar features. In Proceedings of the 2nd ISPRS International Conference on Computer Vision in Remote Sensing (CVRS 2015), Xiamen, China, 28–30 April 2015; p. 990103.
56. Li, L.; Yang, F.; Zhu, H.; Li, D.; Li, Y.; Tang, L. An improved RANSAC for 3D point cloud plane segmentation based on normal distribution transformation cells. *Remote Sens.* **2017**, *9*, 433.
57. Schnabel, R.; Wahl, R.; Klein, R. Efficient RANSAC for point-cloud shape detection. *Comput. Graph. Forum* **2007**, *26*, 214–226.
58. Nurunnabi, A.; Belton, D.; West, G. Robust segmentation in laser scanning 3D point cloud data. In Proceedings of the 2012 International Conference on Digital Image Computing Techniques and Applications (DICTA), Fremantle, Australia, 3–5 December 2012; pp. 1–8.
59. Poppinga, J.; Vaskevicius, N.; Birk, A.; Pathak, K. Fast plane detection and polygonalization in noisy 3D range images. In Proceedings of the 2008 IEEE/RSJ International Conference on Intelligent Robots and Systems, Nice, France, 22–26 September 2008; pp. 3378–3383.
60. Grant, W.S.; Voorhies, R.C.; Itti, L. Finding planes in LiDAR point clouds for real-time registration. In Proceedings of the 2013 IEEE/RSJ International Conference on Intelligent Robots and Systems, Tokyo, Japan, 3–7 November 2013; pp. 4347–4354.
61. Pavan, N.L.; dos Santos, D.R. A global closed-form refinement for consistent TLS data registration. *IEEE Geosci. Remote Sens. Lett.* **2017**, *14*, 1131–1135.
62. Brenner, C.; Dold, C.; Ripperda, N. Coarse orientation of terrestrial laser scans in urban environments. *ISPRS J. Photogramm. Remote Sens.* **2008**, *63*, 4–18.



63. Kim, P.; Chen, J.; Cho, Y.K. Automated point cloud registration using visual and planar features for construction environments. *J. Comput. Civ. Eng.* **2018**, *32*, 04017076.
64. Kim, C.; Son, H.; Kim, C. Fully automated registration of 3D data to a 3D CAD model for project progress monitoring. *Autom. Constr.* **2013**, *35*, 587–594.
65. Liu, Y.-S.; Ramani, K. Robust principal axes determination for point-based shapes using least median of squares. *Comput.-Aided Des.* **2009**, *41*, 293–305.
66. Sheik, N.A.; Deruyter, G.; Veelaert, P. Plane-Based Robust Registration of a Building Scan with Its BIM. *Remote Sens.* **2022**, *14*, 1979.
67. BuildingSMART International. Available online: <https://www.buildingsmart.org/> (accessed on 1 December 2021).
68. Bentley Synchro. Available online: <https://www.bentley.com/en/products/brands/synchro> (accessed on 1 December 2021).
69. Trimble Vico Office. Available online: <https://vicooffice.dk/> (accessed on 1 December 2021).
70. O’Keeffe, S.; Hyland, N.; Dore, C.; Brodie, S.; Hore, A.; McAuley, B.; West, R. Automatic Validation of As-Is and As-Generated IFC BIMs for Advanced Scan-to-BIM Methods. In Proceedings of the CitA BIM Gathering, Croke Park, Dublin, Ireland, 23-24 November, 2017.
71. Bassier, M.; Vergauwen, M. Clustering of wall geometry from unstructured point clouds using conditional random fields. *Remote Sens.* **2019**, *11*, 1586.
72. Bassier, M.; Vergauwen, M. Unsupervised reconstruction of Building Information Modeling wall objects from point cloud data. *Autom. Constr.* **2020**, *120*, 103338.



---

# 4

---

## 4. IMPROVING THE CONSTRUCTION PROGRESS MONITORING THROUGH DETECTION ANALYSIS

## Abstract

Accurate and reliable construction progress monitoring plays a critical role in ensuring successful project outcomes. Recently, Scan-vs-BIM comparison methods have been increasingly employed for automated progress monitoring that mainly consists of the geometrical comparison between the as-built scan model and the corresponding as-planned model. Despite the capability to estimate the progress, these methods suffer from inaccuracies mainly due to the presence of occlusions along with other errors in the as-built scan, resulting in unreliable progress estimation. The current research detailed in this chapter is an effort to address these challenges and improve the Scan-vs-BIM comparison process through new innovative advancements. The proposed method initially integrates reasoning measures to reduce the progress error based on the execution sequence of building components. Later, a geometric analysis is performed to develop a suitable surface model from as-planned BIM, for its compatible comparison with as-built scan. The surface model is then classified to provide the as-built coverage information of the building structure according to data-capturing equipment and external objects present at the scene. Subsequently, the classified surface model is utilized in comparison to accurately detect the exposed and non-exposed potential as-built surfaces in the scan model. Finally, progress information along with additional information is obtained that allows the comprehensive understanding and meaningful insights in the building progress. This novel method is evaluated and validated through both simulated and real-life datasets, which demonstrates its preciseness in measuring the partial completion of building components and its ability to deliver valuable comprehension of progress through supplementary information.

**Keywords:** Scan-vs-BIM comparison, progress monitoring, as-built detection, progress estimation, IFC-based BIM.

## 4.1 Introduction

Recently, there has been a significant advancement in automated progress monitoring using model based-assessment, which mainly involves the geometrical comparison of the as-built and as-planned three-dimensional (3D) information of the building. The as-built information includes the 3D point cloud, mostly obtained through reconstruction technologies like laser scanning, image-based reconstruction, or their integration. Similarly, the as-planned information involves a geometrical design model extracted from the BIM model in a suitable 3D format. These assessment techniques initially register both models (as-built scan and as-planned BIM) ultimately to perform their comparison to find out the progress information that is then updated back into BIM model.

The comparison is the core part of the process that identifies and estimates the progress by examining the as-built 3D geometry from the point cloud in contrast with BIM information, hence also referred to as Scan-vs-BIM comparison. Although Scan-vs-BIM comparison has been increasingly used for automated progress monitoring of construction projects, the accuracy of this technique heavily relies on the scan-vs-BIM comparison preciseness, which is often affected by occlusions and other errors. As a result, the reliability of the overall progress monitoring process can be compromised. The as-built model obtained from the construction site includes numerous errors which may compromise the accuracy of the scan-vs-BIM comparison. For example, occlusions caused by already constructed components, the presence of construction materials, labor, machinery, or other obstacles, can make certain areas of the building inaccessible to the data acquisition instrument, resulting in incomplete scans. Hence, scan-vs-BIM comparison can fail to identify occluded surfaces in the captured as-built scan and assumes that it covers the entire surface of the structure, resulting in inaccurate estimations. In addition, the point cloud generated from the as-built model may contain errors, such as noise and outliers. Another source of error arises from inaccuracies in the alignment of the as-built and as-planned models, which can affect the comparison process. All these errors increase false positives or false negatives in the built scan, thus influence its comparison with the as-planned model.

Despite the significance of these issues, there is a paucity of research that focuses on addressing the challenges associated with as-built data acquisition and alignment for Scan-vs-BIM. As such, there is a pressing need to explore new approaches that can improve the accuracy and reliability of Scan-vs-BIM for progress monitoring by addressing these issues. The proposed research in this current chapter aims to improve the Scan-vs-BIM comparison process by developing a comparison model derived from the as-planned BIM model, detecting occlusions and other possible errors in the as-built data, performing their precise comparison while utilizing semantic information to optimize the process through reasoning.

The structure of this research study described in this chapter 4 is as follows. Section 2 presents a comprehensive review of the relevant literature, followed by Section 3 that explains the problem statement. Section 4 details the proposed methodology and Section 5 showcases the results obtained from the experiments and includes a detailed discussion of the findings. Finally, a concise conclusion summarizing the key contributions of the research and its potential implications is outlined in Section 6.

## 4.2 Related Work

The development of infrastructure, housing, and other physical structures is dependent on the construction industry, which is facing numerous challenges, including the critical issue of construction progress monitoring. Monitoring practices entail tracking the progress of a under-construction project to identify any variances or divergences from the scheduled plan (or design), thereby allowing early detection of potential issues. This early detection through construction progress monitoring enables prompt remediation, ultimately resulting in significant time and resource savings [1,2]. Regardless of its importance, a majority of construction projects, numbering over 53%, experience delays, and over 66% exceed their original cost [3,4]. Hence, research has highlighted the critical importance of efficient and precise monitoring of the as-built status of constructions as a prerequisite for effective project management [5-14].

The traditional monitoring methods involve manual measurement techniques with substantial processing carried out by construction staff which is time-consuming, error-prone, and labor-intensive, resulting in serious flaws, such as missing and imprecise as-built information [15-18]. Additionally, they have been found to be costly, ineffective [7,19], complex [20], and non-systematic [21-23]. Eventually, this created a critical demand for automated progress monitoring in the construction industry that has the ability to produce accurate, efficient, and reliable progress information. However, despite the strong necessity, automated progress monitoring is still in its early development stage and lacks the desired level of efficiency and reliability [5,24,25]. As a result, there is a significant research gap that requires the development of approaches aimed towards automated construction progress monitoring [26-28].

As the technology has rapidly advanced, there have been numerous research studies that investigated potential solutions for automating construction progress monitoring by using various technologies including the radio frequency identification (RFID) [29-33], ultra-wideband (UWB) [34-36], barcodes[37], and global positioning systems (GPS) [38]. Although, these technologies are primarily focused on monitoring materials or labor, however, they has limitations in providing the comprehensive as-built information required to accurately identify the progress in terms of the geometrical structure of the building [39]. To overcome these issues, advanced reconstruction technologies were introduced in the construction industry

to capture the as-built geometry and spatial information of structures through millions of 3D points to create their respective as-built model. This is achieved through methods such as laser-based scanning [40-43], image-based reconstruction [3,11,15,17,44-47], or their integration [34,48,49]. Normally, laser-based scanning, being a modern surveying technology, is more accurate and dense than image-based reconstruction for capturing as-built geometry, but the devices are also more expensive [50]. The reconstruction technologies are non-contact and non-destructive, and offer significant advantages as compared to traditional techniques, in terms of accuracy, time, and automation. However, these technologies are limited by their dependence on a clear line of sight range, which can adversely affect the accuracy of the as-built capturing process at the construction site and result in undetected points in certain areas of the structure that are obstructed or have limited access [5,41].

While the reconstruction technologies enable the capture of as-built geometry, the as-planned geometry of the building is represented through various 3D models such as computer-aided design (CAD) [51] or mesh format [7,43,52] in the construction industry. With the recent digitization, BIM models are increasingly being employed as as-planned models, because they comprise not only the 3D geometry of the building, but also semantic information, enabling the detailed representation of the building [9,53]. The semantic information in BIM allows for the inclusion of additional information such as time-related schedules, costs, and any other relevant data, which expands the opportunities for construction management and improves decision-making throughout the project lifecycle [54,55]. Recently, Industry Foundation Classes (IFC) have emerged as a widely recognized open standard for information exchange in Building Information Modeling (BIM). It provides a standardized digital description of the built asset industry released by BuildingSMART, enabling data exchange and collaboration among stakeholders in a consistent and compatible manner, facilitating the integration of various data sources, and allowing for real-time updates on project progress [26,56-58]. As a result of the standardized and compatible nature of IFC-based BIM facilitating automation, it has become a popular choice for construction progress monitoring, with many research studies utilizing its capabilities [9,26,27,54,55,59,60].

Construction progress monitoring has been extensively studied with the advancement in technologies, resulting in a proliferation of proposed methods [61]. Kopsida, Brilakis and Vela [2] reviewed several methods in terms of data acquisition, progress estimation, information retrieval, and visualization capabilities while assessing their usefulness, precision, degree of automation, necessary preparation, time effectiveness, training needs, expense, and mobility. The study found that no single method is superior in all aspects, and the optimal method depends on the specific circumstances, such as whether the application is indoor or outdoor, the

type of building structure being monitored, the available cost, and the desired level of precision.

In recent times, research studies have utilized a model-based assessment technique for construction progress monitoring in which BIM (as-planned) model is geometrically compared with its corresponding aligned laser scanned (as-built) model to obtain progress information of a building, also known as a Scan-vs-BIM comparison [5,62]. This technique requires the initial alignment of both models in the same coordinate system, which is accurately established through the registration process, either manually [7,63], semi-automated [64,65], or fully automated [3,8,56,57,66]. The Scan-vs-BIM comparison involves the analysis and inference of 3D surfaces of the as-built model, relative to the as-planned model, to determine the completion of building components, providing a valuable tool for construction progress monitoring. Technically, the as-planned surface of the component structure is regarded as constructed when corresponding as-built points are present, allowing for an estimation of overall completion. Despite the usefulness of this technique, the manual implementation of the comparison is often hindered by its time-consuming, labor-intensive, and expensive nature, making it unreliable for comprehensive applications on construction sites [8]. Hence, numerous studies have been performed to automate the Scan-vs-BIM comparison, but the effectiveness of these automated techniques is heavily reliant on resolving several challenges encountered.

In these studies, the geometrical comparison of the 3D points from the as-built scan is performed either with the points extracted from the as-planned surface [67,68] or with the as-planned surface itself [8,26,27,69]. Some of the earliest Scan-vs-BIM approaches, introduced by Bosche and Haas [40] and Bosché [8], involved object detection in the laser-scanned as-built point cloud which was subsequently extended by, Turkan, *et al.* [70] to track the temporary and secondary objects such as formwork, shoring and rebars in concrete works. Turkan, Bosche, Haas and Haas [43] also used the object detection approach [8] to monitor the progress of structural building objects in construction projects in which an additional metric for recognizable objects was introduced to reduce the false positives and false negatives in the result. However, this metric is dependent on a fixed threshold value representing the minimum recognizable surface, making it prone to occlusion errors [9], and therefore requires proper estimation instead of a fixed threshold. Kim, Son and Kim [41] employed a Lalonde features-based supervised classification approach to identify targeted building component types in the as-built model by matching them with their counterparts in the as-planned model, both of which were in point cloud form. Similarly, Zhang and Arditi [7] developed a method by analyzing the point distribution in relation to the enlarged and shrunken boundaries of the objects to determine the object's presence, its completeness, or any deviation from the expected object. However, the method was evaluated in a simplified, simulated environment, which may not fully reflect the complexity and difficulties inherent in



analyzing data from actual construction sites. Similarly, Tuttas, *et al.* [71] utilized a voxelized octree to validate the existence of points in cells. Another technique proposed by Pučko, Šuman and Rebolj [24] involves constantly updating the as-built model using small low-precision scanning devices, attachable to safety helmets or machinery, to allow the identification of deviations and differences from the planned schedule. Limitations of this technique, which was tested on a testbed, include manual simulation of some activities, manual registration of various partial point clouds for comparison, and successful object detection during comparison only when at least one-third of the surface is covered, while a commercial software was used for model comparison.

Normally, the effectiveness of reliable automated progress monitoring through Scan-vs-BIM heavily relies on the accuracy of the comparison, which encounters several challenges that must be actively addressed. One of the significant challenges in the Scan-vs-BIM is the occlusion in the as-built model, which arises when some parts of a building are obstructed from the view of the data acquisition instrument. These obstructions can occur due to various physical blockages such as construction materials, equipment, labor, or other objects present at the construction site [9]. As a consequence, it creates missing points or inaccuracies in the as-built model, which in turn can lead to difficulties in the geometric comparison process and ultimately impact the reliability of the results [26,60,72,73]. Several studies have considered occlusion in the scan-vs-BIM comparison, such as the method proposed by Golparvar-Fard, Pena-Mora and Savarese [9] that leverage unstructured site photographs to generate their dense point cloud using structure-from-motion and multi-view stereo. To facilitate the comparison between as-planned and as-built geometries, the scene is discretized into a voxel grid while a probabilistic approach was employed to determine construction progress, with threshold parameters for detection determined through supervised learning. Another study utilized the inverse photogrammetric approach to project building elements into corresponding site photographs for automated labeling based on semantic information provided by BIM model, subsequently training a neural network for reliable detection rates [74]. Although these image-based reconstruction approaches somewhat consider occlusion, they may not be applicable for laser-based as-built scans. While occlusion in the as-built scan can be addressed with new data acquisition, identifying the occluded surfaces is necessary to plan for the new location [75]. Despite efforts, occlusion continues to pose a challenge in Scan-vs-BIM [26,76]. In addition to occlusion, the as-built scans obtained from construction sites may include noise due to the presence of moving objects during laser scanning, resulting in measurement errors that can impact object detection [9,26,76]. Furthermore, the precision of registration is critical for Scan-vs-BIM techniques, as even minor registration errors can significantly impact the comparison's accuracy [77].

In construction projects, the time-related schedule provides information about the time information of components such as the start and finish time, duration, completion, etc. As the BIM model can store additional semantic information including the time-related schedule, hence, many studies also utilized the schedule-integrated BIM in Scan-vs-BIM by providing the geometry of the as-planned model based on the planned progress dates [9,24,74]. Moreover, the schedule-integrated BIM has been utilized for the completion reasoning of components by exploiting their precedence relationship for construction [41,60,78,79]. The precedence relationship plays a critical role in determining technological dependencies between building objects by establishing which object cannot be built until a preceding object is completed. Therefore, identifying and analyzing precedence relationships is crucial in ensuring the accurate and timely completion of construction projects through Scan-vs-BIM comparison. However, the implementation of this approach using the latest IFC4 schema has not been detailed in any study.

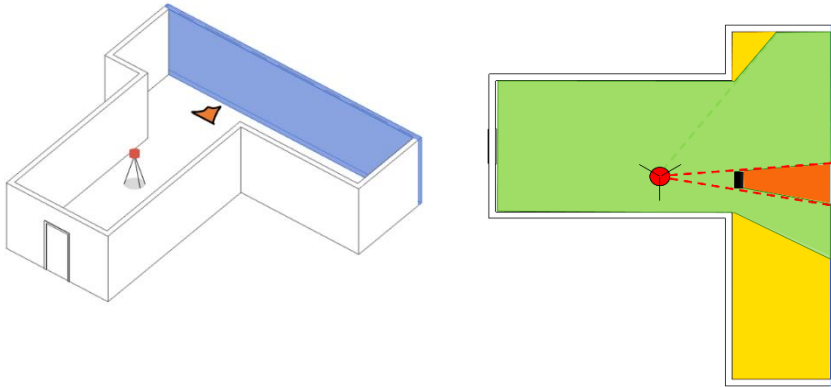
### 4.3 Problem Statement

It is a challenge for data acquisition instruments to actually capture all the surfaces of the building structure ideally in the as-planned model as some of their surface may not be structurally exposed to the instrument for coverage. In real-life, joined surfaces of building components are sandwiched, making their unexposed surface undetectable during scanning. For example, a beam could be potentially obscure a portion of joined roof, or the edge surface of one wall might conceal a section of another wall. Consequently, the employment of these raw as-planned models having complete surfaces for comparison can affect the scan-vs-BIM comparison, mainly due to the lack of benchmark parameters defining the expected detection of built surface and ultimately impact the comparison accuracy. Therefore, this requires the identification of detectable surfaces of as-planned BIM that can be utilized for comparison during Scan-vs-BIM instead of comparing the complete surface that may affect the Scan-vs-BIM accuracy. This identification process involves converting the as-planned model into a detectable model that can be used as a benchmark for comparison.

Similarly, the captured as-built point cloud in an ideal Scan-vs-BIM comparison should also truly represent the actually built component in a perfect scenario and must contain only 3D points that completely cover the surface of that built structure. However, in actual cases that may not be possible. In real life, the acquired as-built scan  $S$  of a building component captured at the construction site may not fully comprise points covering the as-built surface (referred to as detected as-built  $D$ ) as some as-built points may be missing (referred to as undetected points  $O$ ). The detected as-built  $D$  are the points that perfectly represent the as-built surface for precise scan-vs-BIM comparison. Similarly, the undetected points  $O$  are those assumed points that are not present in the as-built scan  $S$  due to occlusion as the built component may not have been fully captured by the data acquisition

instrument due to various reasons. Eventually, these occluded or undetected points  $O$  coupled with the inadequate number of detected as-built points  $D$  in the as-built scan  $S$  create uncertainty about the percent completion of building components and increase the false negatives during scan-vs-BIM comparison, ultimately reducing the accuracy. Although, these undetected points  $O$  cannot be determined without another data acquisition round, identifying the occluded surfaces, where these undetected points  $O$  were assumed to be present, can aid in improving the scan-vs-BIM comparison. This can help in better understanding the obtained results, enhancing the accuracy further, and estimating the space required for the next data acquisition.

**Figure 4.1a** illustrates a data collection instrument scanning a wall component. Occlusions caused by other building components and external obstacles at the scene limit the laser scanner's exposure, as shown in yellow and orange in **Figure 4.1b**.



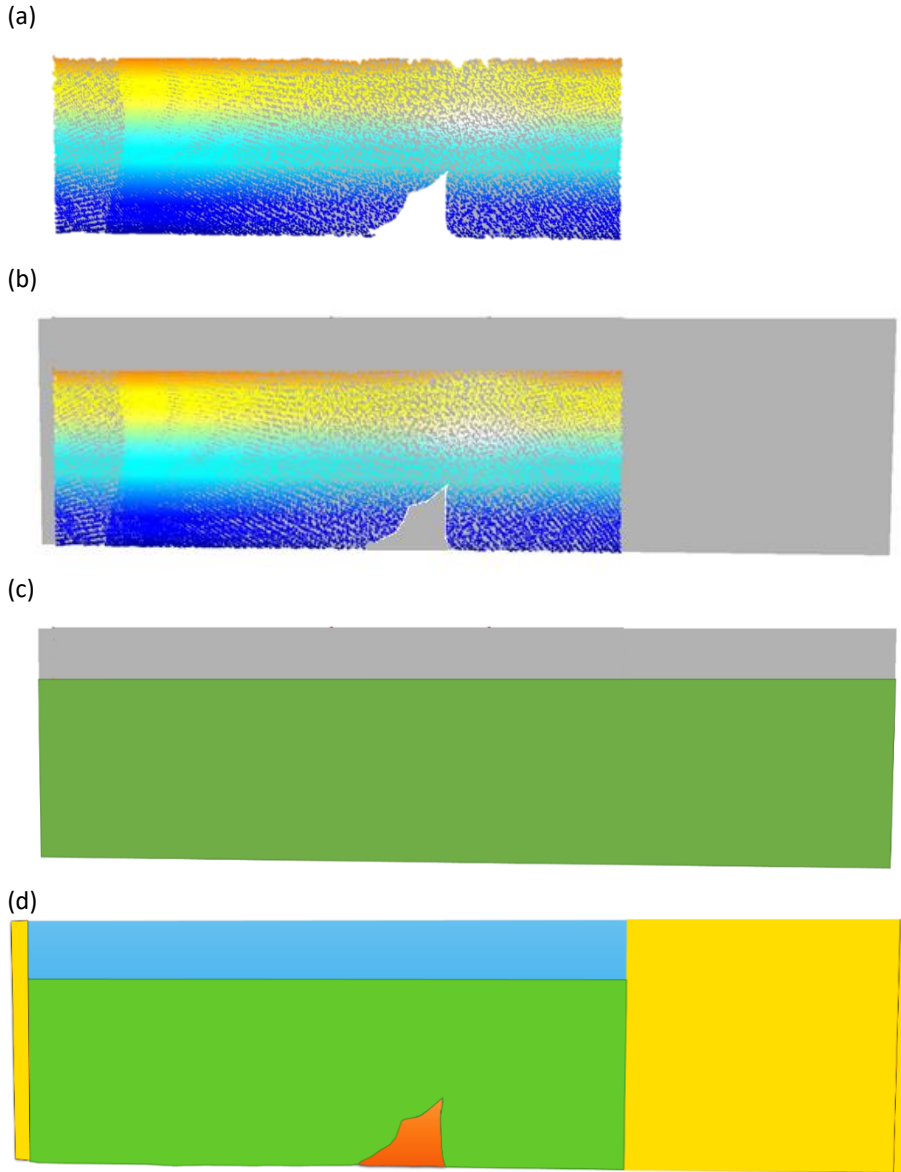
**Figure 4.1.** Visualization of building with data acquisition instrument placed to scan the wall component (in blue) along with obstacle in (a) 3D view, and (b) top view highlighting the detectable coverage (green), and non-detectable coverage due to building component (yellow) and external occluder (orange).

The non-exposure of the surface creating the occlusion in an as-built scan  $S$  is categorized into two main types based on the type of obstacle/occluder:

- 1) A (major) part of the surface may not be directly visible to the line of sight of data acquisition instruments (such as laser scanners) due to the presence of other building components that are already built, as highlighted with yellow in **Figure 4.1b**. In this case, already built components block the surface exposure, thus acting as occluders.
- 2) The presence of material, laborers, or machinery located between the data acquisition instrument and required building component may hinder the surface exposure of building components, in which case these external

obstacles act as occluders. The orange-highlighted area in **Figure 4.1b** illustrates the blockage due to this type of occlusion.

In traditional Scan-vs-BIM comparison, the completion ratio of as-built components is calculated based on the (acquired) detected points only, without accounting for the presence of occluded or undetected points. This can lead to a significant difference between the reported and actual completion ratios, as illustrated in **Figure 4.2(a-d)**, which shows an example of an as-built point cloud of a wall component captured in the presence of occlusions, while **Figure 4.2b** represents its aligned comparison with the corresponding as-planned surface. The surface occupied by as-built point cloud through the traditional method is 56% of the as-planned surface. However, the actual as-built surface, as depicted in **Figure 4.2c**, along with the as-planned surface, indicates an actual completion ratio of 80%. This difference is primarily attributed to the presence of undetected points  $O$ , represented by undetectable surfaces ( $\sigma_{Un-detectable}$ ) which include the occluded surface due to internal building components ( $\sigma_{Un-detectable}^{As-planned}$ ) and external obstacle ( $\sigma_{Un-detectable}^{As-built}$ ) in as-built scan, classified with yellow and orange respectively, as shown in **Figure 4.2d**. Together, these undetectable surface account for 30% of the total surface area. Therefore, the measured completion ratio can also be reported as 56% of the total surface, but with only 70% detectable surface or overall 80% (=56%/70%) of the complete surface. This highlights the limitations of the traditional Scan-vs-BIM method and the importance of considering the coverage as an additional parameter in progress reporting. By accounting for the presence of occluded or undetected points, this approach can provide a more accurate and reliable representation of the actual conditions, leading to better decision-making in construction projects.



**Figure 4.2.** Visualization of the: (a) acquired as-built scan colored using scalar fields, (b) as-built scan with corresponding as-planned surface (grey), (c) surface of the actual as-built wall (green) as compared to the as-planned surface (grey), and (d) provides a classification of different surfaces in which the detectable surface is highlighted with green while the occluded surfaces  $\{(\sigma)_{Un-detected}\}$  due to building component and external occluder are represented with yellow and orange respectively.

Furthermore, it is important to consider potential challenges that could influence the accuracy of the Scan-vs-BIM comparison. Here are some of the key factors that play significant roles in this regard:

- Some error points  $E$ , mostly attributed to 3D noise and outliers, present in the captured as-built scan  $S$  may result in an increase in the false positive in the Scan-vs-BIM comparison.
- Registration errors, caused by inaccurate registration between different as-built scans or between the as-built scan and BIM, can also affect the scan-vs-BIM comparison.
- The traditional Scan-vs-BIM comparison doesn't consider the occluded surfaces while performing the comparison, which also affects the accuracy of the obtained progress.

These errors can limit the ability of points in the as-built to represent their corresponding surface in BIM during the comparison, highlighting the importance of addressing these errors in Scan-vs-BIM to minimize their impact.

During the continuous Scan-vs-BIM comparison being performed after each data acquisition, it is possible to mistakenly identify a fully built building component as non-completed as the currently acquired as-built point cloud may not have full coverage of its surface although the same component was identified as completed in previous comparison phase. The comparison may yield a different result with each iteration and requires sound reasoning to be incorporated into the process. Additionally, time-related information defined in the construction schedule specifies the completion sequence of building components. For example, walls cannot be constructed until preceding components, such as the foundation, are completed, and successor components, such as the roof, depending on the completion of all preceding components (walls and foundation). This time-related information can be integrated into BIM (also known as 4D BIM) which can be exploited to further improve the Scan-vs-BIM comparison.

The challenges concerning the as-planned model (lack of suitable detectable model), as-built model (errors including occlusions, outlier, registration, etc.) and then their imprecision comparison in the scan-to-BIM process that can significantly affect the accuracy and reliability of progress monitoring in the construction projects. Therefore, there is a strong need for a method that addresses these challenges and improves the Scan-vs-BIM process. Specifically, this method should be able to provide a suitable detectable model for comparison (as an alternate to the as-planned BIM) and identify the occlusion in the captured as-built scan  $S$  (by classifying the surfaces). Furthermore, it should also perform the precise comparison of detected as-built with the detectable as-planned model while reducing the possible errors  $E$  and considering the possible as-built in the occluded surfaces. Additionally, it should also introduce some measures to assist the Scan-vs-BIM comparison for

improvement by utilizing the semantic information from as-planned BIM through possible reasoning. Addressing these challenges will enable a more comprehensive and accurate Scan-vs-BIM comparison between the as-built scan and as-planned BIM, ultimately improving the reliability of progress monitoring in construction projects. Eventually, it will lead to better decision-making and more efficient resource allocation, which can positively impact the success of construction projects.

#### 4.4 Methodology

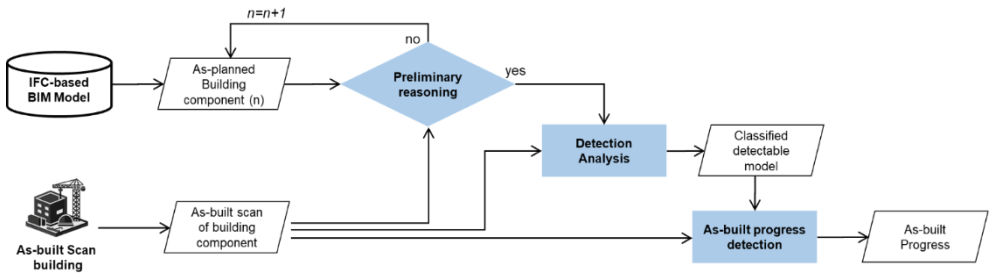
The current research aims to propose an automated and improved method for enhancing the accuracy and reliability of progress monitoring in construction projects through the scan-vs-BIM comparison. The proposed mechanism aims to address the challenges by accurately identifying and predicting the detected and non-detected as-built points while reducing error points eventually to improve the comparison between the as-built scan and as-planned BIM. To achieve this goal, the proposed novel approach focuses on processing each individual component of the building model through different stages to ensure overall accuracy in the Scan-vs-BIM comparison. By proposing a more improved and automated method, the proposed approach can enhance construction progress monitoring and improve the reliability of the scan-vs-BIM comparison.

Ideally, the highest accuracy in Scan-vs-BIM comparison can be ensured if the total as-built scan  $S$  consists completely of all the as-built points  $D$  that is not possible in real life. The research study conducted in the current chapter, we define the undetected points  $O$  as points that have not been captured (by data acquisition instrument) but are intended to represent the surface actually constructed/built structure; once captured, they become detected as-built points  $D$ . In actuality, the captured as-built scan  $S = \{s_i\}_{i=1}^n$  with 'n' no. of 3D points ( $s_i$ ) acquired from the construction site may include the detected as-built points  $D$  along with error points  $E$  but also lacks (undetected) points  $O$ . The direct comparison of the captured as-built scan with BIM may not yield the optimum results due to error points  $E$  and undetected points  $O$ . Mathematically, the detected as-built  $D$ , to be used for ideal Scan-vs-BIM comparison, can be written using equation 1 where all these 3D points are representing their respective types.

$$D = [S - E] + O \quad (1)$$

In the above equation, detected as-built  $D$  consist of captured as-built scan  $S$  along with undetected points  $O$  but without the error points  $E$ . To improve the accuracy and reliability of the scan-vs-BIM comparison, the proposed approach is an effort to identify the most likely detected as-built  $D$  in the captured as-built scan  $S$ , by reducing the error points  $E$ , and predicting the undetected points  $O$ , along with other reasoning measures.

To accomplish this, the proposed novel method involves three main stages to process the building components individually, beginning with a preliminary assessment to determine the need for comparison based on different logic and processing measures. In the next stage, detection analysis is performed to identify the detection model for comparison and classify the non-exposed surfaces that contain the undetected as-built points  $O$ . The final stage utilizes the surface classification information to perform the accurate estimation of the as-built progress through identification and prediction of detected as-built points  $D$  and un-detected as-built points  $O$ , respectively. The stages of the proposed method are illustrated in **Figure 4.3** while their details are as follows:



**Figure 4.3.** The overall workflow of the proposed three-stage methodology.

#### 4.4.1 Preliminary Reasoning

The proposed method performs the preliminary evaluation by utilizing the semantic time-related information of the BIM model through reasoning measures to improve progress monitoring. The time-related information includes the schedule of building components having their execution sequencing, dates, duration, and other related progress information related. The current stage relies on provided time-related information to carry out logical reasoning which allows the Scan-vs-BIM of only those components whose progress needs to be updated. By adopting this approach, the method enhances the understanding of the construction process and enables the detection of errors and inconsistencies in the construction progress monitoring, while reducing overall processing.



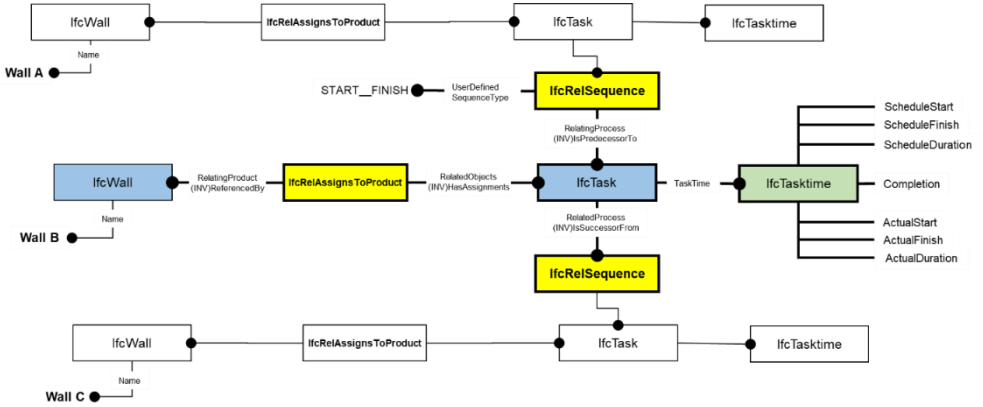


Figure 4.4. An example of time-related IFC entities associated with three walls having a sequential relationship with each other in IFC-based BIM model information.

In IFC-based BIM, the time-related information is usually present in the ‘IfcTaskTime’ entity which is linked through a defined task entity ‘IfcTask’ that can be eventually linked to its corresponding building component through a representative entity under ‘IfcBuiltElement’ (like IfcWall). The ‘IfcTaskTime’ entity contains the time-based attributes that describe the planned and actual schedule information while the ‘IfcRelSequence’ provides the relationship between entities. An example of three building components (Wall A, B, and C) connected to their respective time-related entity along with their sequencing relationship with each other using IFC4 schema, are shown in **Figure 4.4**.

---

### Algorithm 4.1: Preliminary Reasoning

---

*Input: IFC-based BIM, As-built Scan*

- 1 Extract building components information from *IFC-based BIM*  $\rightarrow C_i$
  - 2 Sort all building components according to their planned start date  $\rightarrow C^{Sorted}_i$
  - 3 **for every**  $C^{Sorted}_i$  **do**
  - 4     **if**  $Scan^{Sorted}_i$  exists and  $Completion^{Sorted}_i < 1$  **then**
  - 5         **do** Schedule reasoning
  - 6         **Proceed** Scan-vs-BIM
- 

The current stage initially sorts the building components for processing based on their planned start dates and then applies reasoning based on some invariants for each component before proceeding to the Scan-vs-BIM comparison. The first reasoning ensures the obvious that the building component’s comparison is only performed if it is not completely built and it’s as-built scan is present, eventually reducing the processing. The next reasoning relies on the construction schedule invariant that the required building component can only begin if the preceding

components are already built, assuming the construction is being performed according to the planning schedule. The overall algorithm to perform the current stage based on the IFC schema is outlined in following algorithm (Algorithm 4.1) and the relevant details are as follows:

At the start, the planned start dates of all building components are extracted using the relevant IFC entities (IfcBuiltElement → IfcRelAssignsToProduct → IfcTask → IfcTaskTime.ScheduleStart), and the components are sorted accordingly (line 2). The processing of components begins based on their planned start dates by performing two initial checks (line 4). The first check ensures that the as-built scan of the corresponding under-processed building component is available. If the dedicated point cloud of the required component is not provided, then the as-built scan is probed by cropping the relevant part using the oriented bounding box of the required component structurally covering in the as-planned BIM. The second check confirms whether the required building component has been built or not, based on the 'Completion' attribute of the IfcTaskTime entity linked to the required component (IfcBuiltElement → IfcRelAssignsToProduct → IfcTask → IfcTaskTime.Completion). If both checks are true, the building component progress is assessed using schedule reasoning (line 5) to ensure the completion of preceding building components based on time-related schedule information. For example, the construction of a structural roof can commence only after the completion of underlying walls or columns. This reasoning involves identifying the preceding building components and verifying their actual completion. The preceding components can be explored using the 'IfcRelSequence' entity (IfcBuiltElement→IfcRelAssignsToProduct→IfcTask→IfcRelSequence) to identify the other building components having a sequential relationship with the required building components through their tasks. After identification, the completion of all the preceding components is confirmed through the 'Completion' attribute of their 'IfcTaskTime' entity. An example with technical details is visualized in **Figure 4.5** in which 'Wall 6' is the successor building component to 'Wall 5' with a finish-to-start relationship, indicating that the construction of 'Wall 6' requires the completion of 'Wall 4'. If all preceding building components (Wall 4, 5 & Floor) are already built, the required building component (wall 6) is further processed in the next stages for comparison to measure its progress. It is pertinent to mention here that the proposed schedule reasoning only uses schedule connectivity, not structural connectivity since the construction schedule follows structural connectivity. All those components that didn't qualify the reasoning are not processed for Scan-vs-BIM based on the reasons that they are already built, or they didn't start as either their corresponding as-built scan is not provided, or their preceding components are not constructed.

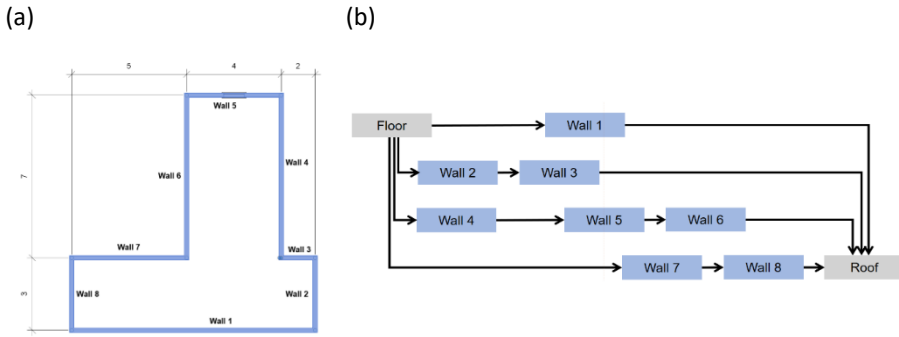


Figure 4.5. Visualization of (a) Building 2D plan view and (b) Construction schedule.

#### 4.4.2 Detection analysis

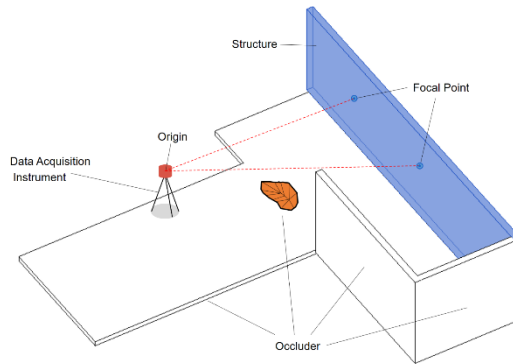
The objective of this stage is to transform the as-planned BIM model (Figure 4.6a) into a detectable model (Figure 4.6b) that represents the possible exposed surface of building components for comparison and then classifying those not exposed surfaces according to data acquisition and possible occlusion present at site eventually to obtain a classified detectable model (Figure 4.6c). The detectable model provides the compatible surface of the as-planned BIM for accurate comparison with the corresponding as-built scan while the classification enables a better understanding of the as-built information by providing an additional parameter that defines the coverage for effective progress monitoring. Furthermore, the classification surfaces also play their part in the minimization of errors in the as-built scan during comparison. Additionally, these classified surfaces can also aid the data acquisition process in the future by highlighting the surfaces where acquisition is required.



Figure 4.6. The 3D visualization of the (a) geometrical model from as-planned BIM, (b) detectable model, (c) classified detectable model.

The detection analysis simulates the scene using the geometrical information from BIM and the captured as-built scan through the ray-casting approach. It is assumed in the simulation that the laser scanner is capturing the building structure in the

presence of other building structures as well as the external objects that are acting as obstacles or occluders. In the simulation, perspective-based multiple rays are cast in presence of the scene (obstacle) from the laser scanner location (origin) towards the surface of the required building component structure. The surfaces of the required structure where the rays intersect are identified. The standardized procedure of ray casting for the simulation in the proposed methodology is given in following algorithm (Algorithm 4.2), while the involved elements are demonstrated in **Figure 4.7** respectively. Furthermore, the details about how this simulation is utilized to develop the detectable model and then perform the classification of its surfaces are summarized in the following sub-sections.



**Figure 4.7.** Illustration of different elements involved in a ray casting scene.

---

**Algorithm 4.2:** Simulation to find the detectable surface of structure

---

**Input:** *Origin, Structure, Occluder(s)*

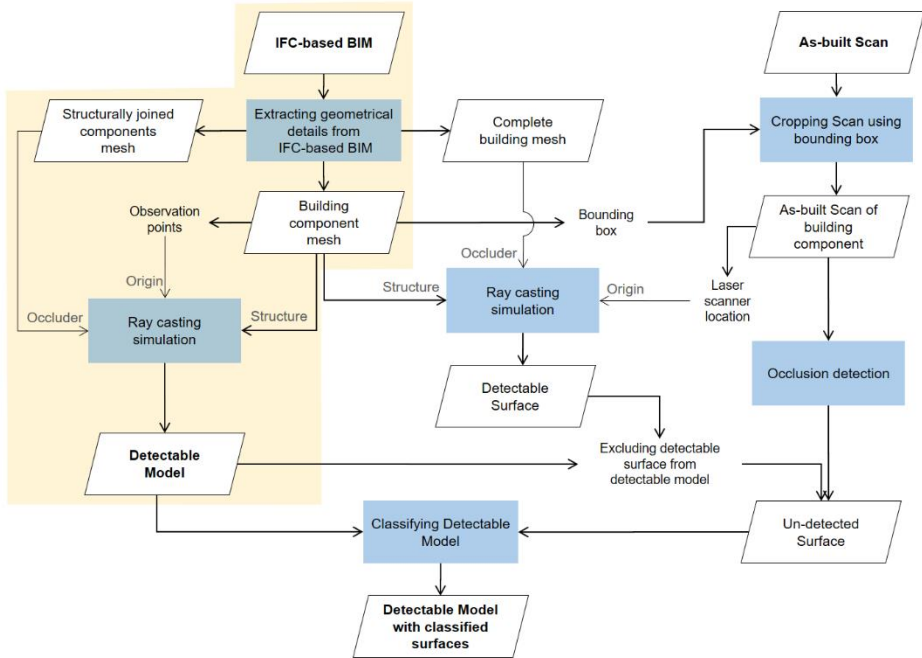
**Output:** *Detectable Surface(s)*

- 1 Create scene with *Structure* and *Occluder(s)*
  - 2 Find *Focal Point(s)* from *Structure*
  - 2 **for** every *Focal point(s)* **do**
  - 3     Project multiple rays from *Origin* to *Focal Point* through ray casting
  - 4     Identify the ray intersecting surfaces of *Structure*
  - 5     Include the identified surfaces of *Structure* into the *Detectable surface(s)*
  - 6 **end for**
- 

*4.4.2.1 Detectable Model*

The detectable model in this study is defined as the suitable 3D model having the possible exposed surface of as-planned BIM that can be used later for accurate comparison with the captured as-built scan. It is developed by analyzing the geometrical information from BIM to include only surfaces that are detectable to data acquisition instrument and remove those that are completely hidden (or

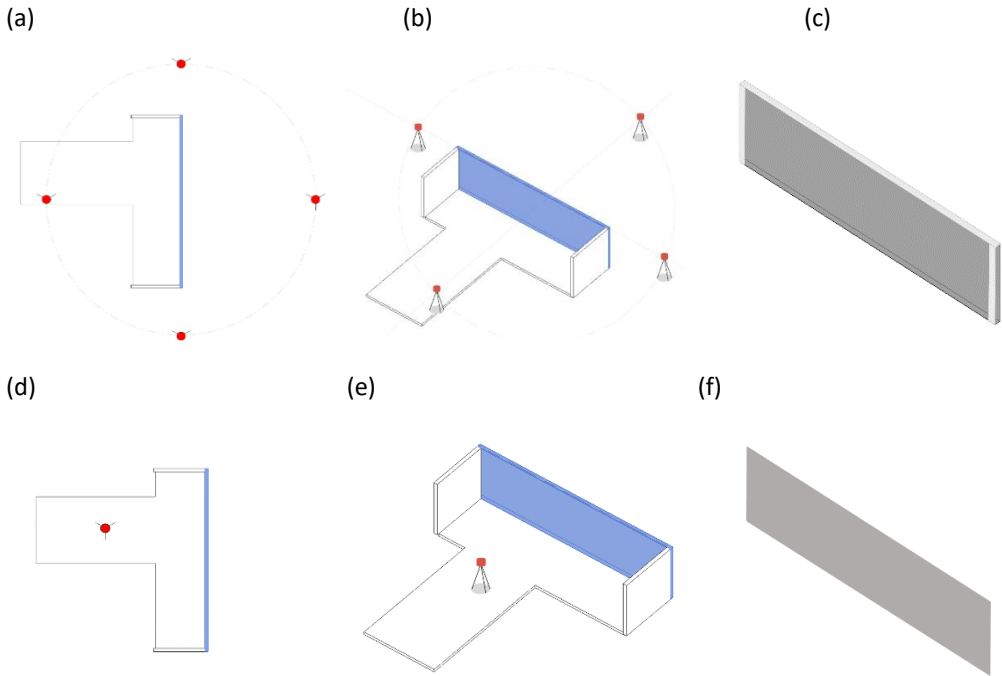
sandwiched) due to other building components. The flowchart to create the detectable model is highlighted (with yellow background) in **Figure 4.8**.



**Figure 4.8.** Flowchart of the detection analysis stage outlining the steps for developing and classifying a detection model.

To create a detectable model, ray casting simulation, as outlined in the Algorithm 4.2, is performed to find the detectable surface of any building component. For simulation, the building component whose detectable model is required is utilized as a structure while the other building component components that are structurally joined with the required component (structure) are used as occluders. The other building components (occluder) are extracted from the IFC-based BIM by exploring the 'IfcRelConnectsElements' entity of the required element (structure) that contains information about its structural connectivity with other elements. The mesh models of these other building components are utilized in the simulation which is created by processing their respective geometrical details from the IFC-based BIM. Similarly, different data acquisition locations in 3D space are used as origin at a suitable distance and height set according to the laser scanner to make sure that the simulated data acquisition is performed. The location can be selected either around the required structure to ensure the coverage from every possible side (different angles) or only inside the building in case the data acquisition is performed indoors, as demonstrated in **Figure 4.9(a-c)** and around **Figure 4.9(d-f)** respectively. The various points uniformly distributed on the surface of the required component are

used as focal points for organizing rays, ensuring that the possible maximum surface is covered according to the dimensions of casted rays.



**Figure 4.9.** An example of placing the scanner either around the required structure (a-b) or only indoors (d-e) to obtain the respective detectable model (grey) of the required building component (structure) after ray casting simulation.

**Figure 4.9** illustrates the ray casting simulation used to obtain the detectable model of a wall. The resulting detectable model obtained for a scanner location placed around the structure includes both surfaces except for the joint part at the edges part that joins with other structures, as shown in **Figure 4.9(c)**. However, when the laser scanner is placed only inside the structure, the resulting detectable model includes one inside surface as shown in **Figure 4.9(f)**. This process is repeated for each building component to obtain its corresponding detectable model ( $\sigma_{comparison}$ ).

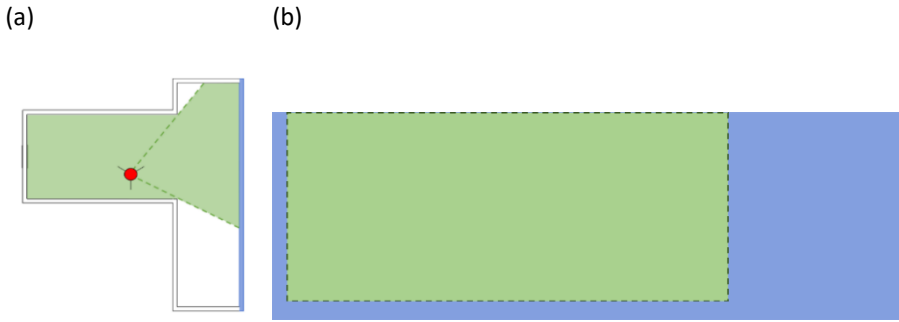
#### 4.4.2.2 Classification of surfaces

After obtaining the detectable model, the identification of exposed and non-exposed surfaces is performed for classification according to the data acquisition instrument by examining both models e.g. as-built scan and BIM model. First, the BIM model is utilized by extracting geometrical information of all the building components for simulation to estimate the non-exposed surface ( $\sigma_{Un-detected}^{As-planned}$ ). Later, the as-built scan surface is analyzed for identification of possible occlusion ( $\sigma_{Un-detected}^{As-built}$ ). Based on the information from both models, the detectable ( $\sigma_{Detectable}$ ) and undetectable

surfaces ( $\sigma_{Un-detectable}$ ) are classified. The technique is designed to determine the level of exposure of a particular building component in the presence of other components and objects at the scene. The classification process is outlined in **Figure 4.8** through a flow chart.

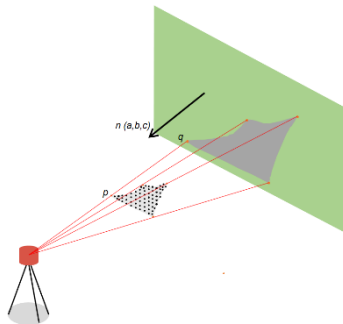
The classification using BIM information to determine the non-detectable surfaces for a required building component involves obtaining the detectable surface using the ray-casting simulation and then excluding that surface from the detectable model to obtain the un-detectable surfaces. The simulation, as described in Algorithm 4.2 and **Figure 4.8**, is performed while assuming that the data acquisition is performed for a specified location (origin) in the presence of other building components (occluders) to find the detectable surface of the required component (structure). The 3D origin point of the as-built scan is used as the location for the ray casting simulation. In the case of multiples scans registered together, their transformed origin are used. Once the simulation is performed, the detectable model of each building component is obtained with its surfaces classified based on the laser scanner location and possible occlusion present in the scene. In the end, the obtained surface is classified as the detectable surface ( $\sigma_{Detectable}^{As-planned}$ ) while all the surfaces of detectable models ( $\sigma_{Comparison}$ ) obtained earlier except the detectable surface itself are classified as the un-detectable surfaces ( $\sigma_{Un-detectable}^{As-planned} = \sigma_{Comparison} - \sigma_{Detectable}^{As-planned}$ ) where  $\sigma_{Un-detectable}^{As-planned}, \sigma_{Detectable}^{As-planned} \subseteq \sigma_{Comparison}$ . **Figure 4.10** illustrates the classification of detectable surfaces based on scanner location (**Figure 4.10a**), where the surfaces are classified (**Figure 4.10b**) into detectable and remaining (non-detectable), represented in green and blue, respectively. The lower and side portions of the component surface are mainly classified as undetectable due to being sandwiched between other components that are joined.

This is performed for each building component in the presence of other components, that were supposed to be built, to classify their respective surfaces based on a given location. In the case that there are multiple scans at different locations, then the same procedure is repeated with the respective locations of their scans. Please note that running the procedure for every targeted building component separately could result in redundant raycasts, however, this approach is adopted to ensure precision in the methodology.



**Figure 4.10.** Visualization of (a) detectable coverage of laser scanner from the top view, and (b) classification of building component surfaces into detectable (green) and non-detectable (blue).

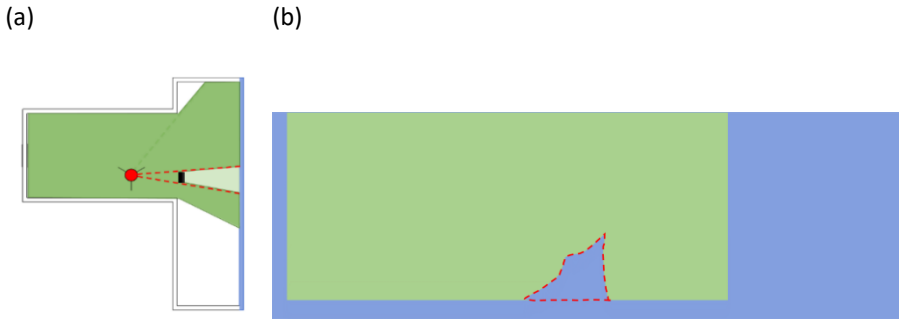
After estimating the undetectable surfaces using the as-planned BIM model, its corresponding scan is analyzed for identification of the possible occlusion in it to verify the presence of different objects such as construction material, labor, or machinery at the construction site. The corresponding as-built scan is initially obtained by cropping its specified part according to the bounding box of the undetectable surface with some tolerance. The building consists of planar building components, hence, this property is being exploited in this step to identify the occlusion possibly present within the scan point cloud. This assumes that if there is a gap within the scan point cloud then there is a possibility that either that gap is due to the occlusion because of any occluder object at the site, or the building component is not built at that particular gap. Hence, the occlusion is being identified to further confirm the built surface, eventually increasing the accuracy. The process of occlusion detection is demonstrated in **Figure 4.11** and implementation details are as follows:



**Figure 4.11.** Illustration of occlusion in as-built scan caused by obstacles in the scene, resulting in occluded point clouds of planar building component.



For occlusion detection, the cropped scan point cloud according to the detectable surface is being verified whether it contains any gap or not with some threshold. In the case that there is a gap, all the points present between the laser scanner location and the gap are projected into that gap based along the plane normal of the building component surface. If the projected points fill the gap then it means that there was an occlusion and that particular part was not directly exposed to the scanner due to occlusion, hence, that occluded part is classified as an un-detectable surface ( $\sigma_{Un-detectable}^{As-built}$ ). **Figure 4.1a** shows a building scene with a laser scanner placed inside to scan a specific building component (highlighted in blue) in the presence of 3D obstacle/occluder (highlighted in orange). In **Figure 4.12a**, the same scene is displayed in a plan view to demonstrate how external obstacles affect the laser scanner's detectable coverage. After scanning, **Figure 4.12b** illustrates the classification of building component surfaces into detectable (green) and non-detectable (blue), with red markings indicating occluded surfaces due to the obstacle.



**Figure 4.12.** Visualization of (a) detectable coverage of laser scanner from top view in the presence of an external obstacle, and (b) classification of building component surfaces into detectable surface (green) and non-detectable surface (blue) including the occluded surfaces marked in red due to the obstacle.

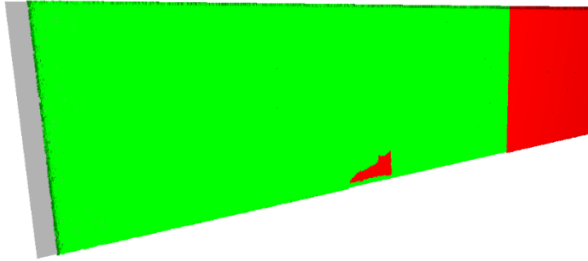
In the final step, the undetectable surfaces obtained from the as-built scan (where external objects are occluder) are combined with the undetectable surfaces obtained from BIM simulation (where other building components are occluder) to obtain the final undetectable surface ( $\sigma_{un-detectable}$ ) of the component detection model using equation 2 and 3.

$$\sigma_{Un-detectable} = \sigma_{Un-detectable}^{As-planned} \cup \sigma_{un-detectable}^{As-built} \quad (2)$$

$$\sigma_{Detectable} = \sigma_{Comparison} - \sigma_{Un-detectable} \quad (3)$$

In the above equations,  $\sigma_{Detectable}, \sigma_{Un-detectable} \subseteq \sigma_{Comparison}$  and  $\cup$  denotes the set union operation, whereas  $\sigma_{un-detectable}^{As-built}$  represents the set of undetectable surfaces obtained from the as-built scan,  $\sigma_{un-detectable}^{As-planned}$  represents the set of undetectable surfaces obtained from BIM simulation, and  $\sigma_{Detectable}$  is the set of

detectable surfaces in the detectable model ( $\sigma_{Comparison}$ ). **Figure 4.13** illustrate the obtained classified detectable model of wall component in which the surfaces  $\sigma_{Detectable}$  and  $\sigma_{Un-detectable}$  are highlighted in green and red respectively, as compared to their original as-planned surface (in grey).



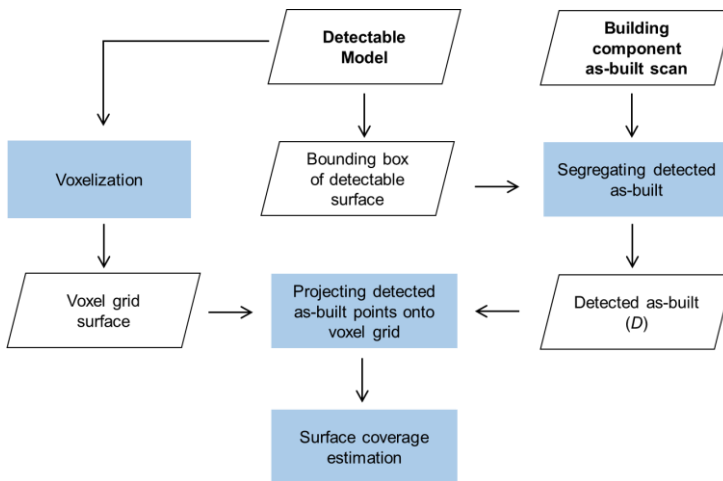
**Figure 4.13.** Visualization of obtained detectable model of building component classified with detectable surface (green) and un-detectable surface (in red).

#### 4.4.3 As-built Progress Detection

The current stage initially performs the precise estimation of exposed as-built surfaces through their geometrical comparison with the as-planned model and then predicts the overall as-built surface by combining the information from the recently developed detectable model with classified surfaces. This approach enables the accurate estimation of as-built completion of buildings, considering both the exposed and non-exposed surfaces. The implementation details are as follow:

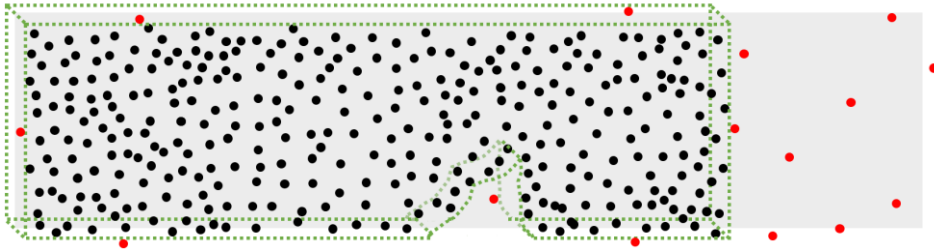
##### 4.4.3.1 Exposed as-built surface estimation

As-built surface detection mainly involves the accurate comparison of captured as-built scan with the as-planned detectable model by removing the possible errors. The flowchart for this comparison step is shown in **Figure 4.14**.



**Figure 4.14.** Workflow for as-built surface detection.

The captured as-built scan of a building component consists of unclassified points, including both detected as-built  $D$  points and error points  $E$  caused by outliers or noise. As an optional preliminary step, the as-built scan can be down-sampled to ease the processing while the noise-reducing algorithm can also be applied to minimize the noise. On the other hand, the detectable model ( $\sigma_{Comparison}$ ) includes classified surfaces designating the detectable ( $\sigma_{Detectable}$ ) and undetectable ( $\sigma_{Un-detectable}$ ) areas. We can also represent this in set operations:  $\sigma_{Detectable}, \sigma_{Un-detectable} \subseteq \sigma_{Comparison}$ . However, the undetectable surfaces ( $\sigma_{Un-detectable}$ ) in the detectable model represent the confirmed occluded areas in terms of laser scanner coverage and occluder object presence. Any points (if present) in these undetectable surfaces ( $\sigma_{Un-detectable}$ ) may belong to the errors ( $E$ ) due to outliers or noise in the overall scan. Therefore, the corresponding as-built points of these confirmed undetectable surfaces are removed to diminish the error points  $E$  while retaining the as-built  $D$  points. To achieve this, a bounding box is created using the classified detectable surfaces ( $\sigma_{Detectable}$ ) of the detectable model with some suitable tolerance to accommodate the 3D points parallel to the surface. Subsequently, the as-built point cloud is cropped by filtering out the points outside the box, resulting in the remaining points that lie inside the detectable area representing the detected as-built  $D$  points, as shown in **Figure 4.15**. Optionally, Iterative-closest-point [80] (ICP) algorithm can also be applied to accurately align the both models before creating bounding box to accommodate the registration error and ensure that the segregated points are accurately representing the detected as-built  $D$ .



**Figure 4.15.** An illustration of removing the most likely error points (red) by cropping the as-built scan of a wall component using a detectable surface bounding box (green) to retain the detected as-built points (black).

Later, the cropped scan points are further processed for comparison with surface of (as-planned) detectable model and the points nearest to the surface are identified. To do that, the surface is voxelized into a voxel grid for accurate and efficient computation of the total surface coverage is performed, as demonstrated in **Figure 4.16**.

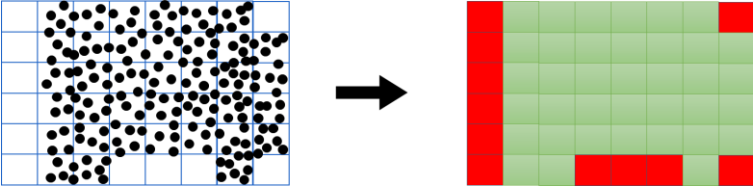


Figure 4.16. Surface coverage determination based on 3D points within voxel grids.

It involves computing the number of occupied voxels compared to the total number of voxels in the detectable model using the equation 4. This calculation takes into account the principle that the structure of a building component can be inferred from the surfaces that can be detected from any side.

$$Completion_{Detected} = \frac{\text{Covered voxels in detectable model } i}{\text{Total no. of voxels in detectable model } i} \quad (4)$$

The above equation provides information on the surface area covered by the as-built scan, which in turn indicates the extent to which the building component has been constructed. This parameter can be utilized for the progress estimation of building components, combined with classification data, to facilitate effective progress monitoring. **Figure 4.17** demonstrate the obtained as-built surface detected (in blue color) in the detectable model of a wall component relative to original as-planned surface (grey). This gives a visual breakdown about the surfaces, which can be detected along with the actual as-built surface.

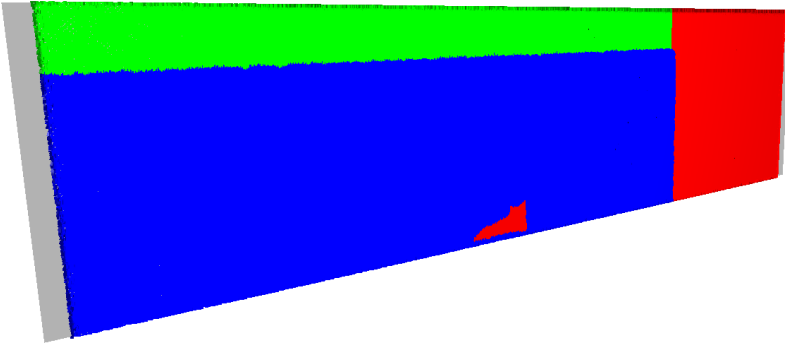


Figure 4.17. Visualization of as-built surface detected (blue) on a classified detectable model having detectable surface (green) and un-detectable surface (red).

#### 4.4.3.2 Non-exposed as-built surface prediction

Traditionally, the as-built surface coverage, computed in equation (4), is generally utilized as the parameter for the progress estimation parameter, representing the obtained completion ratio of the building structure. This as-built surface actually corresponds to the detected surface which is a percentage  $\rho_{Detectable} (= \frac{\sigma_{Detectable}}{\sigma_{Comparison}}$

) of the total surface of the detectable model. However, its direct adoption without considering the occluded surface/un-detectable surface ( $\sigma_{Un-detectable}$ ) may not be accurate as compared to actual progress. Therefore, the proposed method also calculates the predicted completion ratio based on the as-built surface of both detectable and un-detectable surfaces.

The predicted values include the minimum, maximum, and expected value for the completion ratio corresponding to the possible status of the undetectable surface which can either be completely built, not built at all, or have a surface coverage similar to detectable surfaces. Taking these possibilities into account, the potential completion ratio of each building component is calculated by adding the potential completion of the un-detectable surface into the already calculated as-built (of the detectable surface). For any building component, the minimum predicted value would be equal to the as-built surface detectable ( $Completion^{Minimum}_{Predicted} = Completion_{Detected}$ ) while the maximum predicted value can be calculated using the following equation (5) which assume that the undetectable surfaces are representing as-built surface.

$$Completion^{Maximum}_{Predicted} = Completion_{Detected} + \rho_{Detected} \quad (5)$$

Similarly, the projected predicted completion ratio, representing the equivalent completion as-built coverage in both detectable and non-detectable surfaces, can be calculated through equation 6.

$$\begin{aligned} Completion^{Projected}_{Predicted} &= Completion_{Detected} + \frac{Completion_{Detected} \cdot (1 - \rho_{Detected})}{\rho_{Detected}} \\ &= \frac{Completion_{Detected}}{\rho_{Detected}} \end{aligned} \quad (6)$$

Later, the overall progress of the building is estimated for each type of completion (detected and predictive) through the weighted average of the completion ratios of individual building components according to their surfaces, using equation 7.

$$Completion^{Total} = \frac{\sum_{i=1}^n Completion_i \cdot \sigma_{Comparison_i}}{\sum_{i=1}^n \sigma_{Comparison_i}} \quad (7)$$

## 4.5 Results and Discussion

To comprehensively evaluate the proposed method, a combination of simulated (S1) and real-life datasets (R1, R2, R3) were employed. The simulated data was primarily used to validate the theoretical framework, while the real-life datasets provided an understanding of the practical challenges and limitations of implementing the proposed method in real-world building projects. This facilitated a thorough analysis of the proposed method's performance and its potential for practical applications in the construction progress monitoring of buildings. The proposed methodology was

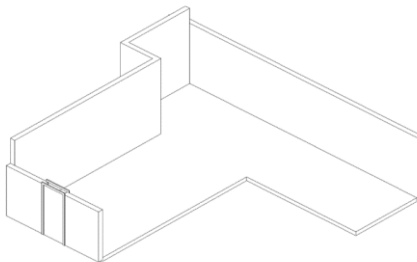
implemented using a Python-based program all the processing was conducted on a laptop with an Intel i7-8850H CPU and 16 GB RAM.

The proposed method utilized the IFC schema to process the as-planned BIM in the IFC4.x version format and performed the analysis of geometrical structures in the form of point clouds. The progress information obtained from the as-built surface coverage was integrated back into the BIM model using IFC schema as detailed in the next chapter 5.

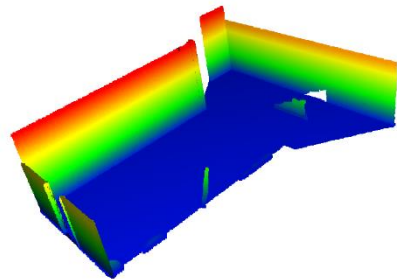
### 1. Simulated dataset

The simulated dataset was designed to represent a challenging building model with various structural compositions that can allow a comprehensive assessment of the proposed method, as depicted in **Figure 4.6**. The same standard simulated dataset has also been utilized in all preceding and subsequent chapters throughout the thesis. Geometrically, it comprises 8 walls and 2 slabs (floor and roof), representing the main structural building components. **Figure 4.5** shows the plan view of the simulated dataset, illustrating the positions, names, and dimensions (in meters) of the wall components while **Figure 4.5b** is demonstrating their schedule timeline providing insights into their construction order with the finish-start relationship. The as-planned BIM model was created in IFC format, while another modified model was developed from the as-planned model to represent the actually built condition of building construction as shown in **Figure 4.18a**. This as-built progress of the building components indicates the longest (front) wall of the building is partially constructed (80% complete), while all three walls on the left side are completely built and the three walls on the right side are not started yet, and the remaining wall with the attached door is partially built (50%). Later, the as-built scan model (as illustrated in **Figure 4.18b**) was generated from this model, which was then processed to demonstrate the indoor point cloud of the building coupled with a variety of errors while replicating real-life conditions.

(a)

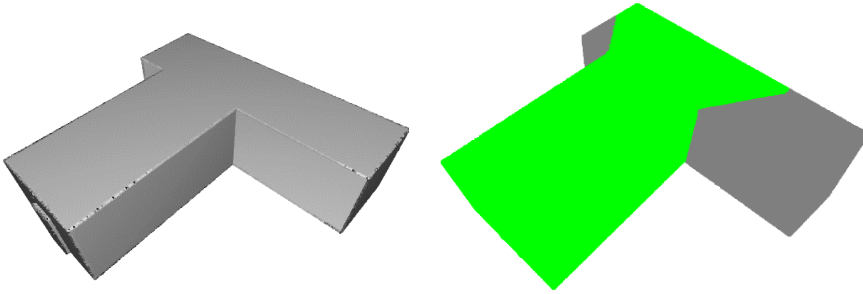


(b)



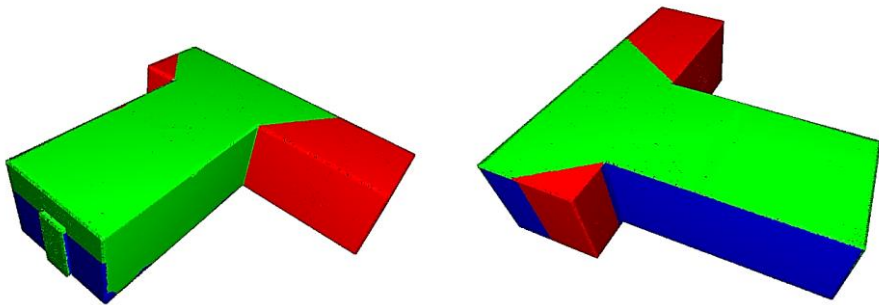
**Figure 4.18.** The 3D visualization from the simulated dataset demonstrates the geometrical difference between (a) a 3D model representing actual built components at the site, and (b) a 3D as-built scan model (colorized based on scalar fields) representing the actual conditions at the site according to laser scanner range.

During the testing, the developed detectable model of the simulated dataset mainly representing the indoor surface of the building is shown in **Figure 4.19**. Similarly, the classified detectable model highlighting the detectable surfaces is shown in **Figure 4.20**, which is based on the data acquisition location illustrated in **Figure 4.1**.



**Figure 4.19.** 3D visualization of (a) detectable model and (b) Classified detectable model with highlighted detectable surface (green) of the simulated dataset.

Later, the as-built surface was detected through the comparison of obtained classified detectable model with the as-built scan. The comparison result is 3D demonstrated in **Figure 4.20** through different visual perspectives in which the detectable model is marked with different colors representing the surface status. Surfaces marked with green and red color are representing the detectable and un-detectable surfaces according to the given laser scanner location while the blue color is representing the detected surfaces being identified as as-built.



**Figure 4.20.** 3D visualization of surfaces highlighting the as-built (blue) from detectable (green), and un-detectable (red).

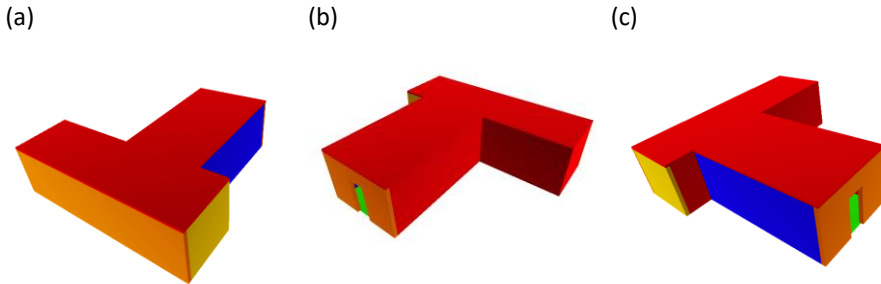
In the end, the as-built covered surfaces were quantified to estimate the progress of the building components and overall building structure. The obtained results of the simulated dataset through the proposed method are summarized in **Figure 4.21**.

According to the results, estimated building progress based on the weighted completion ratios of individual building components according to provided as-built scan is ( $Completion^{Total} =$ ) 37.59%, while the predicted progress, with the prediction range of ( $Completion^{Minimum\ Predicted} =$ ) 37.59% to ( $Completion^{Maximum\ Predicted} =$ ) 52%, is more likely to be around ( $Completion^{Projected\ Predicted} =$ ) 50%. Regarding the individual building component, wall 1 has achieved a completion ratio of ( $Completion_{Detected} =$ ) 56.26% with a detectable surface of ( $\rho_{Detectable} =$ ) 70.42%. It is predicted that if its complete surface is scanned, the completion ratio can attain a maximum of ( $Completion^{Maximum\ Predicted} =$ ) 85.83% while the expected completion is around ( $Completion^{Projected\ Predicted} =$ ) 79.89% based on the given detectable surface and completion ratio.

Building Component Name	Building Component GlobalID	Classified Detectable Surface	Completion Ratio Obtained	Predicted Completion Ratio	
				Projected	Maximum
Wall 1	3zv0SsuRX5rhB2K73V3BRr	0.704225352112676	0.5626106364965751	0.7989071038251366	0.858385284383899
Wall 2	3zv0SsuRX5rhB2K73V3B8Xu	0.3759742004837409	0.3679481322225208	0.9786526090064331	0.9919739317387799
Wall 4	3zv0SsuRX5rhB2K73V3B8Kc	1	0.9857440508827723	0.9857440508827723	0.9857440508827723
Wall 5	3zv0SsuRX5rhB2K73V3B8tT	1	0.5053037608486017	0.5053037608486017	0.5053037608486017
Wall 6	3zv0SsuRX5rhB2K73V3B8sb	0.9355192455313083	0	0	0
Wall 3	3zv0SsuRX5rhB2K73V3B8wQ	0.04629137529137528	0.035186480186480185	0.7601087668059823	0.9888951048951049
Floor	3zv0SsuRX5rhB2K73V3A50	0.7355134127563011	0.7274061917497365	0.9889774668062365	0.9918927789934354
Roof	3zv0SsuRX5rhB2K73V3A0K	0.7439266739668249	0	0	0
Wall 7	3zv0SsuRX5rhB2K73V3B07	0.03325072221377527	0	0	0
Wall 8	3zv0SsuRX5rhB2K73V3B21	0	0	0	0
Overall Building	-	0.6887699062944611	0.3759460334592552	0.5069635047711925	0.5205538438895158

**Figure 4.21.** Estimated and predicted completion ratios for building components and the overall building structure.

The progress achieved by individual components is also visualized through color-coding in **Figure 4.22**, represented by five levels. According to their obtained completion rates, the components are highlighted as follows: 90-100% in blue (Wall 4), 70-90% in green (Floor), 50-70% in orange (Wall 1 & 5), 30-50% in yellow (Wall 2), and less than 30% in red (Wall 3, 6, 7, 8, and roof).



**Figure 4.22.** Progress visualization of building components classified with four different colors (blue, green, orange, red) representing different ranges of respective completion ratio percentages (100-90, 90-70, 70-50, 50-30, 30-0).

From the results, it is evident that the obtained completion ratios are accurate according to the given point cloud of the as-built scan (**Figure 4.18b**). The building components with fully visible surfaces to the laser scanner (including Wall 4, 5, 6)



have reported the completion ratios that accurately reflect their as-built status, as demonstrated in **Figure 4.18a**. However, the remaining components with surfaces not completely exposed, have a completion that is different from their as-built. For example, Wall 1 has its surfaces partially exposed to a laser scanner which is evident in its classified detectable model, illustrated in **Figure 4.13**, and when it is compared with the corresponding as-built scan, the identified as-built surface is shown in **Figure 4.17**. Similarly, the building components: wall 2, 3, and floor, are actually completely built but their surfaces are not fully detected, hence respective completion ratios are not adhering to that. Although, it is invariant that their accurate completion ratios can only be computed if their as-built scan model contained the complete as-built surface and that is only possible with another laser scan. If we assess the completion ratio of building components against their actual progress then it is apparent that relying solely on the completion ratio is insufficient progress due to limited coverage of as-built surfaces which is evident in wall 1, 2, 3, and floor.

Similarly, the predicted completion ratios for all of these affected building components through the proposed method are very much accurate which is quite apparent in the results detailed in **Figure 4.21**. All of these components have precisely reported their projected completion ratio except Wall 3 whose projected parameter is relatively not accurate (76%). In this case, wall 3 has a very small percentage of the surface being exposed ( $\sigma_{Detectable} = 4.6\%$ ) which leads to projected ( $Completion^{Projected}_{Predicted} =$ ) 76% completion, however, the maximum predicted value is ( $Completion^{Maximum}_{Predicted} =$ ) 98.8%, which is almost equivalent to its actual status being completely as-built, that confirmed the utility of prediction range. Overall, the predicted results of the simulated dataset clearly demonstrate that as the classified detectable surface completion increases, the accuracy of the prediction improves and the results bracket narrows, eventually assisting the progress monitoring process.

It is pertinent to mention here that the built scan corresponding to wall 6 contains certain 3D points there that may be associated with different errors, while the wall component itself is not actually built at all, as shown in **Figure 4.18**. These points can be recognized as the as-built surface in traditional Scan-vs-BIM comparison and contribute to the false positives in the results. However, the proposed method didn't determine the the inaccurate as-built completion corresponding to these error points mainly due to the preliminary reasoning stage, as this component was intended to be start after the completion of the preceding wall component (wall 5) which is still not completed (50%).

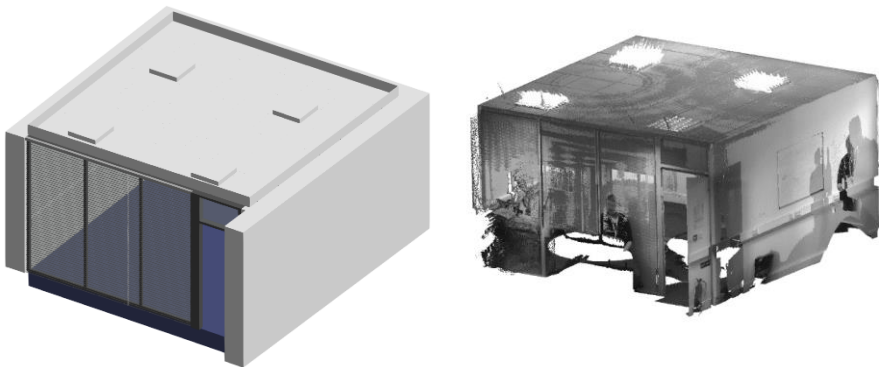
## 2. Real-life datasets

To further assess the proposed method, testing was also performed on the real-time datasets to see how the method could aid current practices where extensive data acquisition is normally performed. Two real-life datasets representing a hall (R1) and a conference room (R2) were processed. The as-planned BIM and as-built scans of these two datasets are shown in **Figure 4.23**. The as-built scans for dataset R1 and R2, which contains 3,580,303 and 79,537,667 3D points, were captured through indoor laser scanning. The dataset R1 is a geometrically distinctive gabled roof structure that covers an area of 84.2 square meters per floor. Similarly, real-life dataset R2, whose as-built scan was captured through a Faro Focus 120 scanner, covers an area of 18.7 meters square. These scans exhibit slight geometric variations from their corresponding BIM models, thus providing an intriguing testing scenario for the proposed method.

(a)

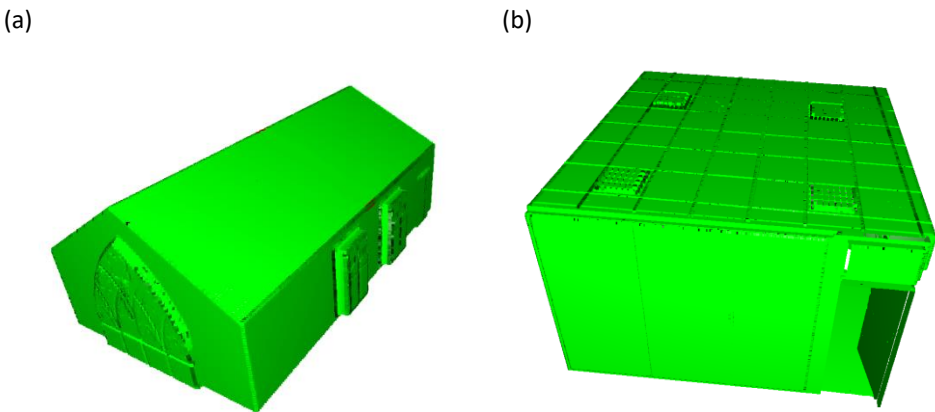


(b)



**Figure 4.23.** 3D Visualization of as-planned BIM and as-built scan for real-time datasets: (a) RT-1 and, (b) RT-2.

The classified detectable models obtained from these two datasets are shown in **Figure 4.24**. Both models represent small-scale indoor spaces that can be captured with good coverage, which is also confirmed through their detectable models. The large glass window at the front of dataset R2 is visible in the classified detectable model. Generally, the scan point cloud obtained from the windows may not be accurate due to their reflective surface, hence, resulting in incorrect as-built information regardless of the comparison approach. Consequently, this particular component, using its IFC entity (*IfcWindow*) was excluded from the proposed method. It is important to mention here that the occlusion projection, to determine the undetectable surface ( $\sigma_{un-detected}^{As-built}$ ) in as-built scan, which is very minor fraction of complete undetectable surface ( $\sigma_{Un-detectable}$ ), was not performed during the classification of the detectable model for real-life datasets. The underlying reason is that the projection approach is not refined to a sufficient level as the determined undetectable surfaces through projection was not giving desired results. Hence, the occluded surfaces due to external objects present at the scene were not identified. Furthermore, the IFC-based BIM models of the real-time datasets did not include the time-related information, hence the schedule reasoning was not performed during processing in stage 1.



**Figure 4.24.** 3D visualization of classified detectable model obtained for dataset (a) RT-1 and, (b) RT-2.

The results of these two datasets, as summarized in **Table 4.1**, shows the precise as-built computation of the as-built surface. In actuality, both building structures are completely constructed which is also evident from their as-built scan models. The obtained completion ratio of dataset R-1 demonstrates the almost completion of building structures where the slight difference can be attributed to a few surface areas of as-built scan that are geometrically different from their corresponding surfaces of as-planned BIM, hence, they were not recognized. Similarly, dataset R-2 demonstrates nearly 90% completion which has a moderate difference from the

actual 100% that can be associated with the occlusion in its as-built scan which was mainly present due to the presence of different external objects (including human personnel) at the site, also evident in corresponding as-built scan (**Figure 4.23b**). Furthermore, both datasets have fully detectable surfaces in their detectable model, hence their projected and maximum completion ratios are not changed.

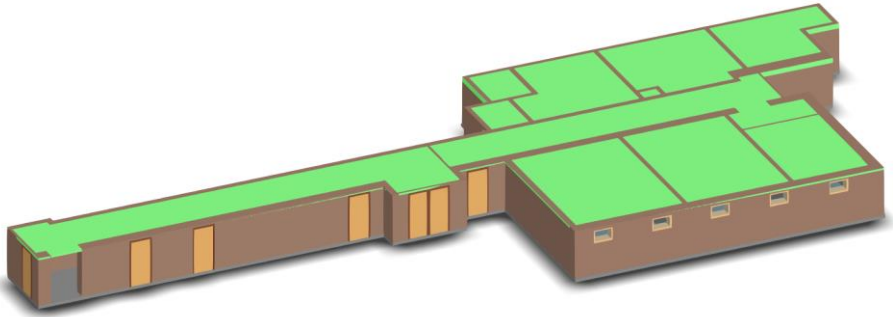
Additionally, a large real-time dataset (R-3) was also analyzed for the as-built progress estimation through Scan-vs-BIM comparison. This is a publically available ISPRS benchmark dataset [81] that has been used in numerous studies [82-85]. The as-built scan model is an indoor point cloud of the building captured through a mobile laser scanner, containing 32,597,694 3D points. Similarly, the corresponding as-planned IFC-based BIM model containing 69 IFC elements was modeled by experts on Autodesk Revit™ software. As compared to other datasets, this dataset contains many structural components. The as-built BIM and as-built scan model utilized for testing are shown in **Figure 4.25a** and **Figure 4.25b**, respectively.

*Table 4.1.* Summary of results for simulated and real-life datasets.

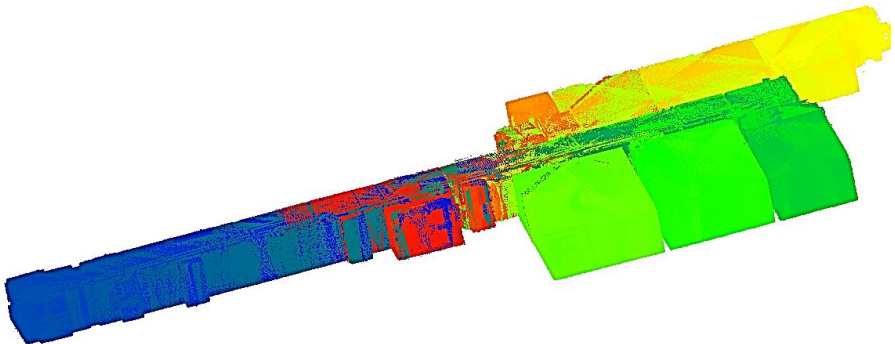
Dataset	Classified detectable Surface (%)	Completion Ratio Obtained (%)	Predicted Completion Ratio	
			Projected (%)	Maximum (%)
S	68.87	37.59	50.69	52.05
R-1	100	98.13	98.13	98.13
R-2	100	89.81	89.81	89.81
R-3	94.26	93.98	96.73	96.78

The trajectory of the mobile scanner during data acquisition is shown in **Figure 4.26a**, while the classified detectable model developed according to the data acquisition trajectory with observation points all around the model, is shown in **Figure 4.26b**. From the classified detectable model (**Figure 4.26b**) and classified surface detection parameter (Table 4.1), it is obvious that the data acquisition trajectory route was remarkably effective as it successfully captured the possibly exposed surfaces of all the building components, except those that are situated outside the indoor area with surfaces inaccessible for scanning. This also confirmed that the as-built scan of this ISPRS benchmark dataset is comprehensive enough to benchmark indoor modeling.

(a)



(b)

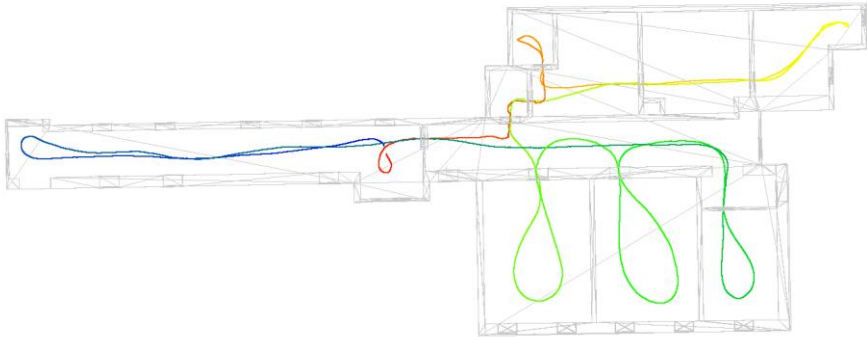


*Figure 4.25.* 3D Visualization of as-planned BIM (a) and as-built scan (b) for real-time datasets RT-3.

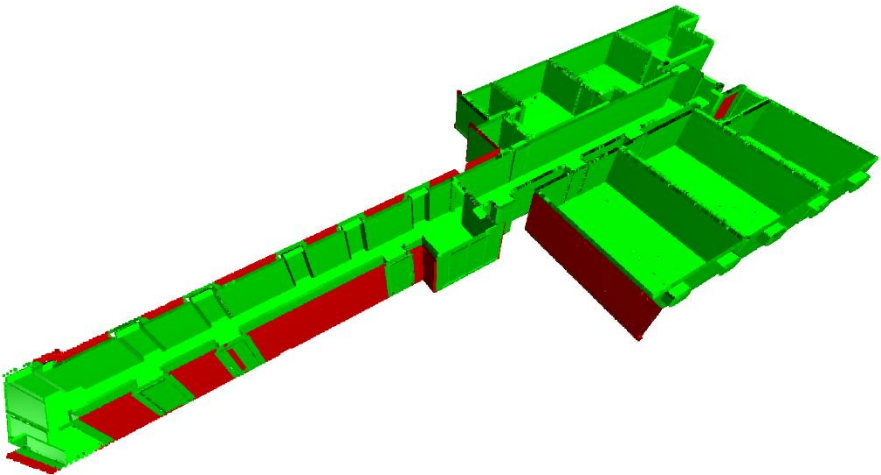
While processing the dataset R-3, it was also observed that the method took a relatively higher time as compared to other datasets and the reason can be linked to the higher number of IFC elements present in it. The proposed method employed a component-based approach in which each IFC element is individually processed and undergoes iterative ray-casting during detection analysis which eventually increased the processing time. If we analyze the results for dataset R3, then it is apparent that the proposed method successfully recognized all the as-built surfaces of all the component structures with precision. Apart from the accurate results, it is interesting to observe that the reporting of detectable surfaces along with its 3D

visualization combined with completion ratios is offering insight for the progress monitoring team. The absence of this additional information in traditional Scan-vs-BIM may lead to poor understanding and a misleading impression of achieved progress. In addition, the classification of undetected surfaces, as highlighted for RT-3 in **Figure 4.26b**, can also serve as a valuable input for the data acquisition process in the future.

(a)



(b)



**Figure 4.26.** Visualization of the (a) Data acquisition trajectory in plan view and, (b) Classified detectable model representing detectable and non-detectable surfaces, for real-time datasets RT-3.

## 4.6 Conclusion

The Scan-vs-BIM comparison has been extensively explored for automated construction monitoring of building projects. However, the reliability of the traditional methods is often compromised by imprecise results, primarily attributed to various errors, especially the occluded surfaces, in the as-built scan. The method proposed in the current chapter is an effort to improve the Scan-vs-BIM comparison by addressing these challenges. First, reasoning measures are introduced that leverage the semantic information in the IFC-based BIM to detect progress errors and inconsistencies. Later, a detectable is developed from the geometrical information of IFC-based BIM, which provides a suitable surface for a more precise comparison with the as-built scan. The surfaces of the detectable model are then classified according to their exposure to data acquisition instrument and occlusion, eventually to identify the possible as-built coverage. The additional coverage information is further utilized during comparison to not only identify the accurate as-built exposed surface but also predict the non-exposed surface. Through these significant advancements, the proposed novel method provides a more accurate computation of as-built detection with additional parameters, enabling reliable progress monitoring of building projects.

The novel method is tested on a range of simulated and real-time datasets. The experimental results highlight its capability in the accurate detection of as-built structures with their precise estimation of their progress. Moreover, the incorporation of additional progress parameters has allowed valuable insights and a more comprehensive understanding of progress information, surpassing the limitation of traditional comparison methods that lack these enhancements. This also serves as the perfect example of how BIM can be effectively utilized for the accurate detection of as-built progress from error-prone scans of buildings. Overall, the research study conducted in the current chapter contributes to the advancement of construction progress monitoring techniques, offering significant potential to improve the accuracy and success of construction projects. The findings of this study pave the way for further advancements in construction monitoring techniques, ultimately leading to improved efficiency and better decision-making in the construction industry.

## 4.7 References

1. Yang, J.; Park, M.-W.; Vela, P.A.; Golparvar-Fard, M. Construction performance monitoring via still images, time-lapse photos, and video streams: Now, tomorrow, and the future. *Advanced Engineering Informatics* **2015**, *29*, 211-224.
2. Kopsida, M.; Brilakis, I.; Vela, P.A. A review of automated construction progress monitoring and inspection methods. In Proceedings of Proc. of the 32nd CIB W78 Conference 2015; pp. 421-431.
3. Han, K.; Degol, J.; Golparvar-Fard, M. Geometry-and Appearance-Based Reasoning of Construction Progress Monitoring. *Journal of Construction Engineering and Management* **2017**, *144*, 04017110.
4. Bevan, M.; Steve, J. LCI National Webinar: Preliminary findings from national project performance research. 2016.
5. Rebolj, D.; Pučko, Z.; Babič, N.Č.; Bizjak, M.; Mongus, D. Point cloud quality requirements for Scan-vs-BIM based automated construction progress monitoring. *Automation in Construction* **2017**, *84*, 323-334.
6. Arditi, D.; Gunaydin, H.M. Total quality management in the construction process. *International Journal of Project Management* **1997**, *15*, 235-243.
7. Zhang, C.; Arditi, D. Automated progress control using laser scanning technology. *Automation in construction* **2013**, *36*, 108-116.
8. Bosché, F. Automated recognition of 3D CAD model objects in laser scans and calculation of as-built dimensions for dimensional compliance control in construction. *Advanced engineering informatics* **2010**, *24*, 107-118.
9. Golparvar-Fard, M.; Pena-Mora, F.; Savarese, S. Automated progress monitoring using unordered daily construction photographs and IFC-based building information models. *Journal of Computing in Civil Engineering* **2014**, *29*, 04014025.
10. Navon, R. Research in automated measurement of project performance indicators. *Automation in Construction* **2007**, *16*, 176-188.
11. Zhang, X.; Bakis, N.; Lukins, T.C.; Ibrahim, Y.M.; Wu, S.; Kagioglou, M.; Aouad, G.; Kaka, A.P.; Trucco, E. Automating progress measurement of construction projects. *Automation in Construction* **2009**, *18*, 294-301.
12. Han, K.K.; Golparvar-Fard, M. Automated monitoring of operation-level construction progress using 4D BIM and daily site photologs. In Proceedings of Construction Research Congress 2014: Construction in a Global Network; pp. 1033-1042.
13. Omar, T.; Nehdi, M.L. Automated Data Collection for Progress Tracking Purposes: A Review of Related Techniques. In Proceedings of International Congress and Exhibition " Sustainable Civil Infrastructures: Innovative Infrastructure Geotechnology"; pp. 391-405.
14. Fang, J.; Li, Y.; Liao, Q.; Ren, Z.; Xie, B. Construction Progress Control And Management Measures Analysis. *Smart Construction Research* **2018**.
15. Tuttas, S.; Braun, A.; Borrmann, A.; Stilla, U. Acquisition and consecutive registration of photogrammetric point clouds for construction progress monitoring using a 4D BIM. *PFG-journal of photogrammetry, remote sensing and geoinformation science* **2017**, *85*, 3-15.



16. Omar, H.; Dulaimi, M. Using BIM to automate construction site activities. *Building Information Modelling (BIM) in Design, Construction and Operations* **2015**, *149*, 45.
17. Golparvar-Fard, M.; Savarese, S.; Peña-Mora, F. Interactive Visual Construction Progress Monitoring with D4 AR—4D Augmented Reality—Models. In *Proceedings of Construction Research Congress 2009: Building a Sustainable Future*; pp. 41-50.
18. Braun, A.; Tuttas, S.; Borrmann, A.; Stilla, U. A concept for automated construction progress monitoring using BIM-based geometric constraints and photogrammetric point clouds. *Journal of Information Technology in Construction (ITcon)* **2015**, *20*, 68-79.
19. Braun, A.; Tuttas, S.; Stilla, U.; Borrmann, A. Towards automated construction progress monitoring using BIM-based point cloud processing. *eWork Ebus. Archit. Eng. Constr. ECPPM* **2014**, *2014*.
20. Kerzner, H. *Project management: a systems approach to planning, scheduling, and controlling*; John Wiley & Sons: 2017.
21. Meredith, J.R.; Mantel Jr, S.J. *Project management: A managerial approach: A managerial approach*; Wiley Global Education: 2011.
22. Song, K.; Pollalis, S.N.; Peña-Mora, F. Project dashboard: Concurrent visual representation method of project metrics on 3D building models. In *Computing in Civil Engineering (2005)*, 2005; pp. 1-12.
23. Alizadehsalehi, S.; Yitmen, I. A concept for automated construction progress monitoring: technologies adoption for benchmarking project performance control. *Arabian Journal for Science and Engineering* **2019**, *44*, 4993-5008.
24. Pučko, Z.; Šuman, N.; Rebolj, D. Automated continuous construction progress monitoring using multiple workplace real time 3D scans. *Advanced Engineering Informatics* **2018**, *38*, 27-40.
25. Khairadeen Ali, A.; Lee, O.J.; Lee, D.; Park, C. Remote Indoor Construction Progress Monitoring Using Extended Reality. *Sustainability* **2021**, *13*, 2290.
26. Kavaliauskas, P.; Fernandez, J.B.; McGuinness, K.; Jurelionis, A. Automation of Construction Progress Monitoring by Integrating 3D Point Cloud Data with an IFC-Based BIM Model. *Buildings* **2022**, *12*, 1754.
27. Erdélyi, J.; Honti, R.; Funtík, T.; Mayer, P.; Madiev, A. Verification of Building Structures Using Point Clouds and Building Information Models. *Buildings* **2022**, *12*, 2218.
28. Li, H.; Zhang, C.; Song, S.; Demirkesen, S.; Chang, R. Improving tolerance control on modular construction project with 3D laser scanning and bim: A case study of removable floodwall project. *Applied Sciences* **2020**, *10*, 8680.
29. Akinci, B.; Kiziltas, S.; Ergen, E.; Karaesmen, I.Z.; Keceli, F. Modeling and analyzing the impact of technology on data capture and transfer processes at construction sites: a case study. *Journal of construction engineering and management* **2006**, *132*, 1148-1157.
30. Ergen, E.; Akinci, B. An overview of approaches for utilizing RFID in construction industry. In *Proceedings of 2007 1st Annual RFID Eurasia*; pp. 1-5.

31. Kiziltas, S.; Akinci, B.; Ergen, E.; Tang, P.; Gordon, C. Technological assessment and process implications of field data capture technologies for construction and facility/infrastructure management. *Journal of Information Technology in Construction (ITcon)* **2008**, *13*, 134-154.
32. Akinci, B.; Boukamp, F.; Gordon, C.; Huber, D.; Lyons, C.; Park, K. A formalism for utilization of sensor systems and integrated project models for active construction quality control. *Automation in construction* **2006**, *15*, 124-138.
33. Fang, Y.; Cho, Y.K.; Zhang, S.; Perez, E. Case study of BIM and cloud-enabled real-time RFID indoor localization for construction management applications. *Journal of Construction Engineering and Management* **2016**, *142*, 05016003.
34. Shahi, A.; Aryan, A.; West, J.S.; Haas, C.T.; Haas, R.C. Deterioration of UWB positioning during construction. *Automation in Construction* **2012**, *24*, 72-80.
35. Shahi, A.; West, J.S.; Haas, C.T. Onsite 3D marking for construction activity tracking. *Automation in construction* **2013**, *30*, 136-143.
36. Furlani, K.M.; Pfeffer, L.E. Automated tracking of structural steel members at the construction site. *Proceedings of 17th ISARC* **2000**, 1201-1206.
37. Navon, R.; Sacks, R. Assessing research issues in automated project performance control (APPC). *Automation in construction* **2007**, *16*, 474-484.
38. Caldas, C.H.; Torrent, D.G.; Haas, C.T. Using global positioning system to improve materials-locating processes on industrial projects. *Journal of Construction Engineering and Management* **2006**, *132*, 741-749.
39. Hamledari, H.; McCabe, B.; Davari, S. Automated computer vision-based detection of components of under-construction indoor partitions. *Automation in Construction* **2017**, *74*, 78-94.
40. Bosche, F.; Haas, C.T. Automated retrieval of 3D CAD model objects in construction range images. *Automation in Construction* **2008**, *17*, 499-512.
41. Kim, C.; Son, H.; Kim, C. Automated construction progress measurement using a 4D building information model and 3D data. *Automation in construction* **2013**, *31*, 75-82.
42. Tang, P.; Huber, D.; Akinci, B.; Lipman, R.; Lytle, A. Automatic reconstruction of as-built building information models from laser-scanned point clouds: A review of related techniques. *Automation in construction* **2010**, *19*, 829-843.
43. Turkan, Y.; Bosche, F.; Haas, C.T.; Haas, R. Automated progress tracking using 4D schedule and 3D sensing technologies. *Automation in construction* **2012**, *22*, 414-421.
44. Fathi, H.; Dai, F.; Lourakis, M. Automated as-built 3D reconstruction of civil infrastructure using computer vision: Achievements, opportunities, and challenges. *Advanced Engineering Informatics* **2015**, *29*, 149-161, doi:10.1016/j.aei.2015.01.012.
45. Golparvar-Fard, M.; Pena-Mora, F.; Savarese, S. Monitoring changes of 3D building elements from unordered photo collections. In Proceedings of

- Computer Vision Workshops (ICCV Workshops), 2011 IEEE International Conference on; pp. 249-256.
46. Golparvar-Fard, M.; Peña-Mora, F.; Savarese, S. Automated progress monitoring using unordered daily construction photographs and IFC-based building information models. *Journal of Computing in Civil Engineering* **2012**, *29*, 04014025.
  47. Golparvar-Fard, M.; Peña-Mora, F.; Savarese, S. Automated Progress Monitoring Using Unordered Daily Construction Photographs and IFC-Based Building Information Models. *Journal of Computing in Civil Engineering* **2015**, *29*, 04014025, doi:10.1061/(asce)cp.1943-5487.0000205.
  48. Brilakis, I.; Lourakis, M.; Sacks, R.; Savarese, S.; Christodoulou, S.; Teizer, J.; Makhmalbaf, A. Toward automated generation of parametric BIMs based on hybrid video and laser scanning data. *Advanced Engineering Informatics* **2010**, *24*, 456-465.
  49. El-Omari, S.; Moselhi, O. Integrating 3D laser scanning and photogrammetry for progress measurement of construction work. *Automation in construction* **2008**, *18*, 1-9.
  50. Kükenbrink, D.; Marty, M.; Bösch, R.; Ginzler, C. Benchmarking laser scanning and terrestrial photogrammetry to extract forest inventory parameters in a complex temperate forest. *International Journal of Applied Earth Observation and Geoinformation* **2022**, *113*, 102999.
  51. Kim, C.; Son, H.; Kim, C. Fully automated registration of 3D data to a 3D CAD model for project progress monitoring. *Automation in Construction* **2013**, *35*, 587-594.
  52. Turkan, Y.; Bosche, F.; Haas, C.T.; Haas, R. Automated progress tracking of erection of concrete structures. In Proceedings of Annual Conference of the Canadian Society for Civil Engineering; pp. 2746-2756.
  53. Yin, X.; Liu, H.; Chen, Y.; Al-Hussein, M. Building information modelling for off-site construction: Review and future directions. *Automation in Construction* **2019**, *101*, 72-91.
  54. Hamledari, H.; McCabe, B.; Davari, S.; Shahi, A. Automated schedule and progress updating of IFC-based 4D BIMs. *Journal of Computing in Civil Engineering* **2017**, *31*, 04017012.
  55. Hamledari, H.; Rezazadeh Azar, E.; McCabe, B. IFC-based development of as-built and as-is BIMs using construction and facility inspection data: Site-to-BIM data transfer automation. *Journal of Computing in Civil Engineering* **2017**, *32*, 04017075.
  56. Sheik, N.A.; Veelaert, P.; Deruyter, G. Registration of Building Scan with IFC-Based BIM Using the Corner Points. *Remote Sensing* **2022**, *14*, 5271.
  57. Sheik, N.A.; Deruyter, G.; Veelaert, P. Plane-Based Robust Registration of a Building Scan with Its BIM. *Remote Sensing* **2022**, *14*, 1979.
  58. Söbke, H.; Peralta, P.; Smarsly, K.; Armbruster, M. An IFC schema extension for BIM-based description of wastewater treatment plants. *Automation in Construction* **2021**, *129*, 103777.

59. Yang, B.; Dong, M.; Wang, C.; Liu, B.; Wang, Z.; Zhang, B. IFC-based 4D construction management information model of prefabricated buildings and its application in graph database. *Applied Sciences* **2021**, *11*, 7270.
60. Braun, A.; Tuttas, S.; Borrmann, A.; Stilla, U. Improving progress monitoring by fusing point clouds, semantic data and computer vision. *Automation in Construction* **2020**, *116*, 103210.
61. Yalcinkaya, M.; Singh, V. Patterns and trends in building information modeling (BIM) research: A latent semantic analysis. *Automation in construction* **2015**, *59*, 68-80.
62. Bosché, F.; Ahmed, M.; Turkan, Y.; Haas, C.T.; Haas, R. The value of integrating Scan-to-BIM and Scan-vs-BIM techniques for construction monitoring using laser scanning and BIM: The case of cylindrical MEP components. *Automation in Construction* **2015**, *49*, 201-213.
63. Memon, Z.A.; Majid, M.Z.A.; Mustaffar, M. An automatic project progress monitoring model by integrating auto CAD and digital photos. In *Computing in Civil Engineering (2005)*, 2005; pp. 1-13.
64. Golparvar-Fard, M.; Peña-Mora, F.; Savarese, S. Integrated sequential as-built and as-planned representation with D 4 AR tools in support of decision-making tasks in the AEC/FM industry. *Journal of Construction Engineering and Management* **2011**, *137*, 1099-1116.
65. Bosché, F. Plane-based registration of construction laser scans with 3D/4D building models. *Advanced Engineering Informatics* **2012**, *26*, 90-102.
66. BuildingSMART International. Available online: <https://www.buildingsmart.org/> (accessed on Dec 01, 2021).
67. Bosche, F.; Haas, C.T.; Akinci, B. Automated recognition of 3D CAD objects in site laser scans for project 3D status visualization and performance control. *Journal of Computing in Civil Engineering* **2009**, *23*, 311-318.
68. Chen, J.; Cho, Y.K. Point-to-point comparison method for automated scan-vs-bim deviation detection. In Proceedings of 17th International Conference on Computing in Civil and Building Engineering.
69. Tuttas, S.; Braun, A.; Borrmann, A.; Stilla, U. Validation of BIM components by photogrammetric point clouds for construction site monitoring. *ISPRS Annals of the Photogrammetry, Remote Sensing and Spatial Information Sciences* **2015**, *2*, 231-237.
70. Turkan, Y.; Bosché, F.; T. Haas, C.; Haas, R. Tracking of secondary and temporary objects in structural concrete work. *Construction Innovation* **2014**, *14*, 145-167.
71. Tuttas, S.; Braun, A.; Borrmann, A.; Stilla, U. COMPARISON OF PHOTOGRAMMETRIC POINT CLOUDS WITH BIM BUILDING ELEMENTS FOR CONSTRUCTION PROGRESS MONITORING. *International Archives of the Photogrammetry, Remote Sensing & Spatial Information Sciences* **2014**.
72. Meyer, T.; Brunn, A.; Stilla, U. Change detection for indoor construction progress monitoring based on BIM, point clouds and uncertainties. *Automation in Construction* **2022**, *141*, 104442.

73. Pexman, K.; Lichti, D.D.; Dawson, P. Automated Storey Separation and Door and Window Extraction for Building Models from Complete Laser Scans. *Remote Sensing* **2021**, *13*, 3384.
74. Braun, A.; Borrmann, A. Combining inverse photogrammetry and BIM for automated labeling of construction site images for machine learning. *Automation in Construction* **2019**, *106*, 102879.
75. Frías, E.; Díaz-Vilariño, L.; Balado, J.; Lorenzo, H. From BIM to scan planning and optimization for construction control. *Remote Sensing* **2019**, *11*, 1963.
76. Kopsida, M.; Brilakis, I. Real-time volume-to-plane comparison for mixed reality-based progress monitoring. *Journal of Computing in Civil Engineering* **2020**, *34*, 04020016.
77. Bueno, M.; Bosché, F.; González-Jorge, H.; Martínez-Sánchez, J.; Arias, P. 4-Plane congruent sets for automatic registration of as-is 3D point clouds with 3D BIM models. *Automation in Construction* **2018**, *89*, 120-134.
78. Han, K.K.; Cline, D.; Golparvar-Fard, M. Formalized knowledge of construction sequencing for visual monitoring of work-in-progress via incomplete point clouds and low-LoD 4D BIMs. *Advanced Engineering Informatics* **2015**, *29*, 889-901.
79. Wu, I.-C.; Borrmann, A.; Beißert, U.; König, M.; Rank, E. Bridge construction schedule generation with pattern-based construction methods and constraint-based simulation. *Advanced Engineering Informatics* **2010**, *24*, 379-388.
80. Besl, P.J.; McKay, N.D. Method for registration of 3-D shapes. In Proceedings of Sensor fusion IV: control paradigms and data structures; pp. 586-606.
81. Khoshelham, K.; Vilariño, L.D.; Peter, M.; Kang, Z.; Acharya, D. The ISPRS benchmark on indoor modelling. *Int. Arch. Photogramm. Remote Sens. Spat. Inf. Sci* **2017**, *42*, W7.
82. Cui, Y.; Li, Q.; Yang, B.; Xiao, W.; Chen, C.; Dong, Z. Automatic 3-D reconstruction of indoor environment with mobile laser scanning point clouds. *IEEE Journal of Selected Topics in Applied Earth Observations and Remote Sensing* **2019**, *12*, 3117-3130.
83. Tran, H.; Khoshelham, K. Procedural reconstruction of 3D indoor models from lidar data using reversible jump Markov Chain Monte Carlo. *Remote Sensing* **2020**, *12*, 838.
84. Previtali, M.; Díaz-Vilariño, L.; Scaioni, M. Indoor building reconstruction from occluded point clouds using graph-cut and ray-tracing. *Applied Sciences* **2018**, *8*, 1529.
85. Tran, H.; Khoshelham, K.; Kealy, A. Geometric comparison and quality evaluation of 3D models of indoor environments. *ISPRS journal of photogrammetry and remote sensing* **2019**, *149*, 29-39.



---

# 5

---

## 5. EXCHANGING PROGRESS INFORMATION USING IFC- BASED BIM

*This chapter is an adapted version from the following original publication:*

Sheik, N. A., Veelaert, P., & Deruyter, G. (2023). Exchanging Progress Information Using IFC-Based BIM for Automated Progress Monitoring. *Buildings*, 13(9), 2390. <https://doi.org/10.3390/buildings13092390>

## Abstract

BIM has become an intrinsic tool in managing building projects due to its ability to comprehensively represent information in digital form. However, using BIM as an information exchange tool is still in its infancy, particularly with regard to construction progress monitoring beyond time schedule information. The current chapter describes the thorough research which focuses on the development of an automated progress monitoring framework based on an IFC-based BIM and provides an extensive methodology based on a structured task-based approach in accordance with the latest IFC4.x schema in four stages. The first stage creates the appropriate IFC entities, which are then enriched with their values in the second stage. The third stage integrates the actual progress information, which requires regular updating from the construction site. Finally, the fourth stage enables the retrieval of progress information, which is then reported in a user-friendly format along with the estimation of additional progress indicators. The proposed method successfully integrated the progress information into their IFC-based BIM models, demonstrating its practical use for monitoring construction progress. In the end, a web-based application was also developed that made use of progress information stored within the standardized hierarchy of the updated IFC-based BIM to facilitate efficient reporting.

**Keywords:** BIM updating, progress monitoring, IFC-based BIM, automation, Building Information Model, scheduling



## 5.1 Introduction

Effective project management is crucial for the timely completion of building projects within schedule, budget, and quality requirements, and it necessitates constant monitoring and control of construction progress. Precise and efficient monitoring of the as-built status of construction has been widely recognized as a critical component of the building process [1-4]. It not only ensures adequate project management but also enables the early detection of deviations from the plan, providing opportunities to adopt early stage remedial actions, which can result in precious time and cost saving [5-7]. Hence, accurate and efficient tracking of the as-built status of under-construction buildings is critical for successful project control. To address this need, Building Information Modeling (BIM), with the capability of facilitating communication and collaboration among project stakeholders, has evolved as a valuable tool for construction project management [8-11].

BIM is a comprehensive and precise representation of a building in digital form. It includes information related to geometry, spatial relationships, and non-graphical information such as cost and schedule data. The application of BIM in the construction process, particularly in the design and planning phases, has improved accuracy, reduced errors, and increased efficiency. The construction industry has undergone significant changes with the adoption of Building Information Modeling (BIM) technology, which has allowed effective project management through enhanced collaboration, communication, and project control [2,12-14]. However, despite the benefits and advancements of BIM, its full potential has yet to be realized in construction progress monitoring and reporting [15]. A major challenge in this regard is the effective exchange and management of information throughout the entire construction process.

Consequently, there is a strong need to explore BIM for communicating progress information during construction monitoring eventually unlocking its potential for effective project management. The study in this chapter aims to do so by investigating the use of Industry Foundation Classes (IFC), an open standard to exchange BIM data, as a means of effectively communicating progress information through BIM during construction progress monitoring. The IFC is a widely recognized open and neutral file format for standardized BIM data and acknowledged by prominent international standardization organizations, including the International Organization for Standardization (ISO), the European Committee for Standardization (CEN), and the German Institute for Standardization (DIN) [16-19]. The IFC standard is maintained by the non-profit entity BuildingSMART [20] that facilitates the interoperability of BIM software applications. It is described by a general schema, also known as the IFC schema, which is used to formally describe the semantic information related to buildings and infrastructure [21]. The implementation of IFC-based BIM models requires the extraction of relevant information through the IFC schema while updating the model involves creating, modifying, or updating IFC

entities [3]. However, this process can be challenging to perform, especially given the complexity of the data and the specific objectives required.

Recent studies have highlighted the potential of IFC-based BIM for various purposes [22-32] including the domain of construction monitoring [2,3,5,33-35]. However, there is a gap in the research when it comes to utilizing IFC-based BIM for updating progress information beyond just schedule updates. Furthermore, there is a need for a comprehensive approach to exchanging progress information using IFC-based BIM, leveraging the latest IFC4 schema.

In comparison to the outdated IFC2×3 schema, the IFC4.x [36] schema represents a significant advancement in BIM technology due to several improvements and new features; hence, it is a more suitable schema for progress monitoring. One major difference is that IFC4.x now uses the ISO 8601 string format for date and time definitions, reducing the model footprint. In addition, time-related information such as schedule or actual Start/finish/duration, completion, status time, etc. are stored in the 'IfcTaskTime' entity in IFC4.x, while in IFC2×3, they were stored in 'IfcScheduleTimeControl'. Furthermore, the definitions for construction resources have been reworked and now include the notion of resource types, which has improved the assignment of resources to schedules and costs. Similarly, the concept of a process type and relevant subtypes has been introduced, allowing for the sequencing of tasks. The new process and cost definitions in IFC4.x significantly reduce the model footprint when capturing the geometrical details along with time, cost, and other information, making it a more effective schema for progress monitoring in BIM projects.

The research detailed in this chapter focuses on the development of an automated progress monitoring framework that adopts a structured task-based approach and utilizes the IFC-based BIM to exchange progress information (independent of data collection technique), including time, cost, and other additional progress parameters for construction progress monitoring. This framework leverages the latest IFC4 data to ensure standardized and consistent progress monitoring without any software dependency, providing project stakeholders with up-to-date and accurate insights into the project's status. The aim is to improve the accuracy and efficiency of progress monitoring and control in construction projects. The methodology presented in this chapter involves four main steps: (1) integration of progress-related entities with the IFC-BIM; (2) inputting planned parameters according to progress information obtained from construction; (3) updating actual progress into the IFC-based BIM model; and (4) reporting progress information directly from the updated BIM. The updated (obtained) IFC-based BIM model reflects both the as-planned and as-built progress information, which provides a comprehensive and up-to-date view of the project status. In addition, this also allows the progress information to be reported with additional progress parameters, such as earned value, estimated completion time, and inspection comments, providing a detailed and holistic

understanding of the project progress, and ultimately facilitating effective project tracking.

The chapter is organized as follows: Section 2 provides a literature review of the existing research on construction progress monitoring related to IFC-based BIM and focuses on the methodologies used and the progress parameters monitored. The proposed methodology for automated progress monitoring using IFC-based BIM is detailed in the Section 3 while the Section 4 presents the results and related discussion of the implementation of methodology. Finally, Section 5 concludes the chapter by summarizing the key contributions of the study and highlighting its significance for the field of construction progress monitoring.

## 5.2 Literature Review

Efficient progress monitoring and control are critical elements of successful construction project management [4,6,37-40]. Numerous studies have expressed the significance of accurate monitoring in the field of construction management by highlighting its pivotal role in ensuring project completion within specified timelines and budgets, while also emphasizing its ability for the timely identification of any potential issues that may arise during the construction process [3,5,41-43].

Efficient construction progress monitoring requires up-to-date and accurate as-built progress information. However, the traditional methods for collecting and processing this information are time-consuming and labor-intensive, leading to the possibility of missing or inaccurate information [42,44-48]. Although automated progress monitoring systems are being developed with time to address this issue, there are still significant challenges in performing the exchange of progress information in terms of automation, accuracy, standardization, and interoperability [33]. This highlights the necessity for a proficient solution that allows the automated exchange of progress information from a construction site into a centralized digital platform, such as BIM. The current research exploits the use of BIM to facilitate information exchange for automated construction progress monitoring.

To achieve this goal, it is important to understand the potential benefits of BIM in the construction industry. BIM is positioned at the forefront of digitization initiatives in the construction industry and is becoming progressively integrated with other digital technologies as part of the broader Industry 4.0 framework [49-51]. There are numerous studies demonstrating the transformative impact of Building Information Modeling (BIM) on the design, construction, and operation of buildings, where it serves as a valuable repository of information to enhance these processes [8,52-54]. Moreover, digital planning and construction supported by BIM have the potential to yield significant cost reductions of 13% to 21%, while the operation phase may see cost reductions ranging from 10% to 17% [19,55]. Additionally, BIM integration with other technologies also presents an opportunity to revolutionize infrastructure construction and maintenance [56].

Consequently, BIM has gained popularity in construction projects, with several countries mandating its use in large projects. In Europe, there has been a substantial increase in BIM applications from 2012 to 2017 [57,58]. Therefore, it is essential to explore the potential of integrating BIM with automated progress monitoring systems to optimize the construction progress monitoring process, which can result in better project outcomes and increased efficiency.

Building Information Modeling (BIM) is a digital representative of a construction project, providing comprehensive information about its physical and functional characteristics. The information content of BIM is diverse and tailored to specific project requirements, implying that it is not standardized. BIM encompasses both 3D geometry and semantics, where the former provides the cornerstone for consistent technical drawings and enables clash detection [59] and collision resolution during the design phase [60]. On the other hand, semantics complements the meaning of objects by providing alphanumeric data, including mechanical and thermal properties, associations, materials, aggregation, and other relationships between objects in the model [61]. Consequently, various analyses, simulations, and advanced controls can be performed on BIM model, facilitating effective collaboration, coordination, and decision-making throughout the project lifecycle [52].

In the realm of construction management, 4D BIM (BIM with time-related schedule information) has improved project management efficiency. It has been utilized for progress monitoring through comparison with 3D scan models [43,62,63]. Other studies have demonstrated its use in quality monitoring and project scheduling improvements by combining it with quality information models and tabu-search algorithms, respectively [64,65]. Although 4D BIM offers benefits for on-site construction management, it also poses challenges such as labor-intensive and time-consuming updating of models to reflect as-built conditions during construction [33,66] and difficulties in interoperability between stakeholders, phases, and BIM software [67,68]. Additionally, 4D BIM models rely on specific software, which can make information inaccessible once separated from the software, leading to inefficiencies in managing buildings and creating a dependence on specific tool vendors [69,70].

To address these challenges, it is vital to establish standardized BIM content with comprehensive guidelines and standards to govern BIM content across the construction industry. However, the successful adoption of BIM relies heavily on integrating mono-discipline BIM models into a cohesive, multi-disciplinary model. This demands the development of standardized and interoperable information exchange between individual models using specialized BIM software tools to achieve a neutral and universal data format [52,71]. This challenge can also be addressed using the IFC data format, which is globally recognized as the standard for BIM data exchange and sharing.

IFC is an internationally accepted standard for data sharing in construction and facility management. It allows BIM data to be exchanged and shared between various software applications used in construction and facility management for both buildings and infrastructure. For the purpose of information exchange and data sharing, the IFC standard serves as the basis and provides a universal and consistent file format. IFC is an open and non-proprietary schema based on the EXPRESS language for data specifications, ensuring a consistent approach to data transfer. This eventually enables some certified BIM software applications to convert their BIM models into the neutral IFC model, facilitating interoperability and collaboration among different stakeholders in the construction industry [16,52]. Despite some drawbacks, such as the incomplete association of modeled elements with semantics and potential loss of information during export to the IFC format [42,72,73], the IFC-based BIM schema continues to be enhanced and is widely employed in contemporary construction projects. The IFC standard has been widely utilized and studied in various areas of the construction industry, such as data standards for facilities management classes [22], energy consumption [23,24], virtual construction [25,26], and project performance evaluation [27]. In addition, several scholars have extended the IFC standard for construction management information, including the integration of completion and design information [28], plan information storage [29], quantity take-off [30,31], GIS integration [74], and daily 4D BIM visualization [32].

In the field of construction progress monitoring, Golparvar-Fard, Pena-Mora and Savarese [2] and Son, Kim and Kwon Cho [35] employed the IFC-based BIM, with manually integrated time-related schedule information, for progress detection by comparing it with reconstructed as-built point cloud obtained from photographs and laser scans, respectively. Similarly, there are some studies [3,5] that performed the registration of an as-built model with the IFC-based BIM model where geometrical details were extracted from the latter to obtain matching features for alignment. Although these methods utilized the IFC-based BIM as the as-planned model, they did not address the exchange of progress information using IFC-based BIM models. In addition, Hamledari, McCabe, Davari and Shahi [33] developed an automated method using the IFC-based BIM for updating time-related schedule information. This method involved adjusting the task-object relationship based on the level of progress details, updating actual progress entities according to their completion ratios, and estimating the non-completed planned entities based on actual progress. Although this method automates the updating process, it is limited in its scope as it only focuses on time-related schedule information and does not incorporate cost or other crucial factors for effective progress monitoring. Furthermore, the method was based on the IFC2x3 schema, which may not be compatible with the latest IFC4.x schema as the latter schema natively supports progress information with new entities and different approaches. This highlights a research gap that demands the development of a comprehensive and integrated approach that leverages the full

potential of BIM for construction progress monitoring. It also requires the investigation of BIM as an information exchange tool by incorporating different types of progress parameters such as time, cost, or any additional information using the latest IFC4.x schema.

The current study aims to address this gap and explores the application of IFC-based BIM models for construction progress monitoring. A methodology is proposed that the model with current progress information, including scheduling, cost, and other key performance indicators, to improve the accuracy and effectiveness of project monitoring. The proposed methodology not only enables the updating of progress information but also supports the addition of semantic information such as comments, notes, and delay reasons. In the end, the visualization and reporting of progress information from the updated IFC-based BIM model through the use of color-coded 3D models, graphs, and other critical information is also demonstrated. With these measures, the research aims to provide a comprehensive solution for information exchange to facilitate effective construction project monitoring.

### 5.3 Methodology

The proposed methodology presents a systematic approach that mainly consists of four stages, as shown in Figure 5.1. The first stage involves the integration of progress-related entities with the IFC-BIM according to progress information obtained from construction. In the second stage, the planned parameters are inputted into the relevant entities of the IFC-based BIM while the third stage allows the updating of actual progress into the IFC-based BIM model. Finally, the last stage details the reporting of progress information directly from the updated BIM to provide stakeholders with up-to-date and accurate insights into the project’s status. Using these different stages, the proposed methodology enables the effective communication of progress information between IFC-based BIM and construction sites for efficient and accurate construction progress monitoring.

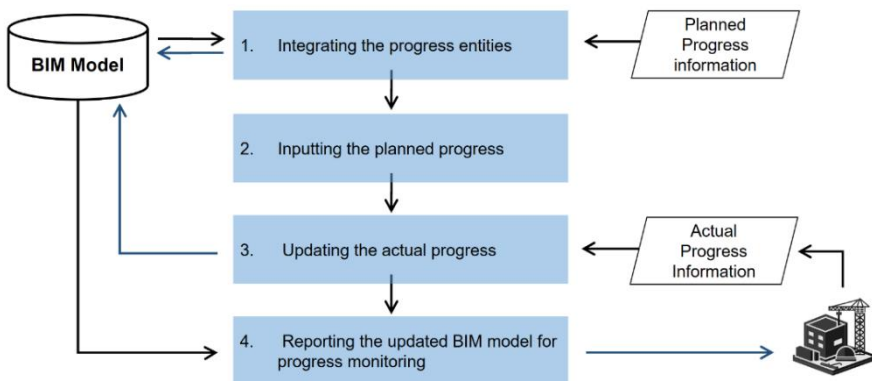


Figure 5.1. Flowchart of the proposed methodology.

The proposed methodology requires the input of planned and actual progress from the construction site. The planned progress comprises the IFC-based BIM model, the planned progress schedule, and the budgeted cost schedule. Similarly, the actual information includes the actual progress, actual cost information, and comments related to individual building components obtained from the construction site.

The construction of a building includes various physical components such as walls, doors, slabs, etc. The overall completion of the building depends on the individual progress of each of these components so that any delays or cost overruns can be traced back to their performance. These building components are constructed through a set of different work activities (or tasks), and the completion status of the component is signified by the advancement of these tasks. For example, the construction of a wall may involve tasks such as layout, bricklaying, and plastering, which together determine the completion status of the wall. An effective and accurate approach to monitoring construction progress requires a framework that is centered around the individual tasks of the building components. In all stages of the proposed methodology, a task-based approach is adopted in which the progress entities for tasks, building components, and the overall project are designed accordingly.

### IFC schema for progress monitoring

The proposed methodology leverages the IFC schema for exchanging progress information during construction monitoring. This IFC schema [75] follows an object-oriented data model that organizes concepts into four layers: core, interoperability, domain, and resource. The (first) core layer includes the most general classes, such as `IfcRoot`, `IfcRelationship`, and `IfcObject`, that are used to define objects, relationships, and properties. Similarly, the interoperability layer includes classes that specialize in the product extension schema and provide more detailed information. The domain-specific layer describes classes for particular domains, while the resource layer further describes objects at other levels. A key feature of the schema is inheritance between classes, with the `IfcRoot` class serving as the initial root class from which other classes are derived in three directions: conceptual and physical objects (`IfcObjectDefinition`), relations a objects (`IfcRelationships`), and object properties (`IfcPropertyDefinition`). The schema is organized in a hierarchy, with layers grouped according to their function and specialization.

An IFC entity consists of attributes and their corresponding values. The attributes represent the type of information, while its corresponding values provide specific details about the object being represented. This allows for a standardized and structured way of representing building information throughout the construction process, making it easier to exchange and interpret data between different software applications and stakeholders. The proposed method is in line with the IFC4.3 schema, and the IFC entities used in the method are shown in **Figure 5.2** with their hierarchy.

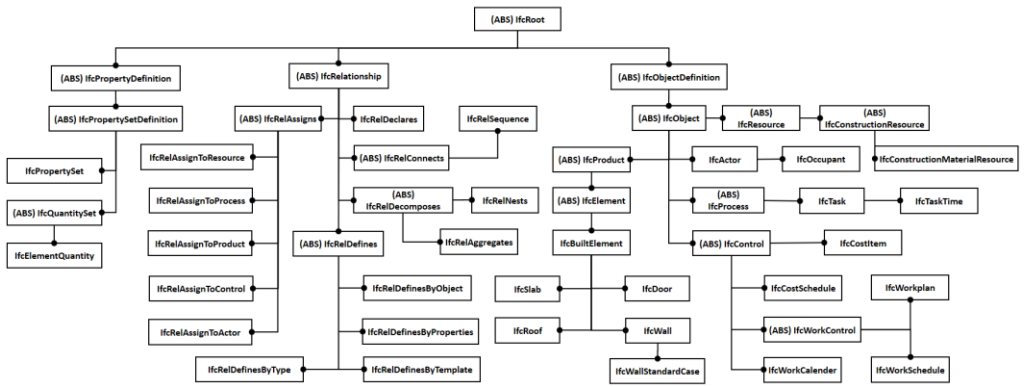
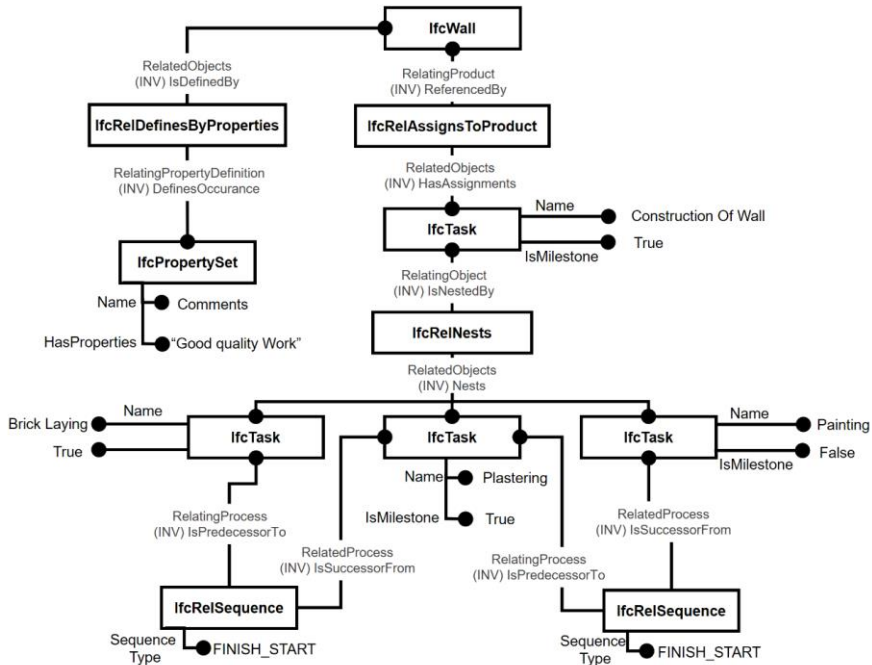


Figure 5.2. IFC entities related progress information in hierarchy.

In the IFC-based BIM model, building components such as walls, slabs, columns, and doors can be represented by corresponding subtype IFC entities of 'IfcBuiltElement', such as 'IfcWall', 'IfcSlab', 'IfcColumn', and 'IfcDoor', respectively. The work tasks involved in the construction of these components are represented by the 'IfcTask' entity. Furthermore, a suitable relationship entity such as 'IfcRelAssignsToProduct' is used to express their association between entities. In cases where there are multiple activities or tasks, additional 'IfcTask' entities can be assigned and linked to the main task entity through a nest relationship 'IfcRelNests' entity. Furthermore, property entities can also be linked to store additional information. An example of the IFC representation of tasks with their defined sequences involved in the construction of the wall is illustrated in **Figure 5.3**.





**Figure 5.3.** An example of entities associated with a building component in the IFC-based BIM model.

The utilization of IFC-based BIM not only enables the updating of the progress entities related to schedule, cost, and other indicators but also other semantic information such as comments, important notes, delay reasons, etc. Furthermore, it is not necessary for the planned information, such as the planned schedule or cost schedule, to be integrated into the IFC-based BIM model beforehand, as the proposed method deals with this challenge (stages 1 and 2) in an automated way. Similarly, the proposed method not only updates the IFC-based BIM with progress information (stages 2 and 3) but also enables the retrieval of progress information in the form of progress indicators for construction progress monitoring in the last stage.

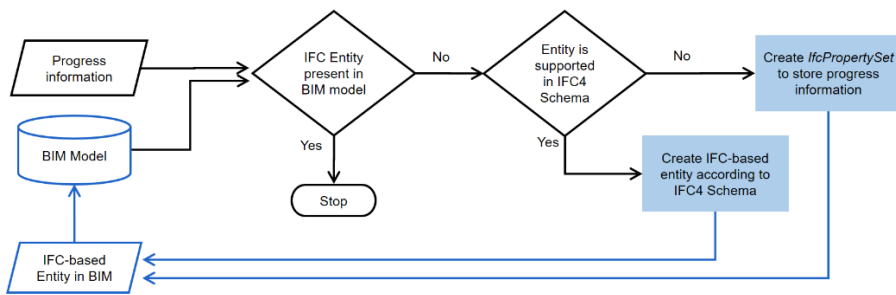
### 5.3.1 Integrating the Progress Entities into IFC-Based BIM

The first stage of the proposed methodology involves upgrading the IFC-based BIM by integrating additional IFC entities to accommodate progress information related to time, cost, and other relevant data. The original BIM model may lack the necessary progress entities; hence, the model is adapted by automating the creation process of standardized progress entities using the IFC4 schema. The resulting BIM model incorporates these IFC entities to comprehensively represent planned and actual progress information.

In this stage, the IFC-based BIM and planned progress information are processed to output a revised BIM model that includes progress-related entities. The aim is to

minimize the overall size of the output IFC BIM and prevent an increase in the complexity of IFC entities. To achieve this goal, the process is formulated to create only the necessary IFC entities for adjusting the maximum progress information into the suitable IFC4 entities without any duplication.

To include any progress information in BIM, the appropriate IFC entities are created along with their linkage with other entities within an IFC-based BIM. A verification step has been implemented to establish that the appropriate IFC entity, preferably an IFC4 native entity, is opted for specific progress information while preventing the duplicate creation of that entity. This step determines the presence of the entity responsible for storing the specific information in the input BIM model. In the event that the entity is absent, the process of its creation is initiated that utilizes the native IFC4-based entities, as demonstrated in **Figure 5.4**.



**Figure 5.4.** Flowchart of verification step to create an IFC entity based on progress information.

The proposed method, through this approach, facilitates the creation of progress entities within any IFC-based BIM, regardless of the presence of an integrated time or cost schedule. Additionally, the method remains effective irrespective of whether the IFC-based BIM model is being processed for the first time or not. For example, in the case when the same BIM model is again processed for updating or retrieval of progress information, the proposed method will skip this creation stage as all the required entities were already created during the first processing. In this way, the creation of progress entities is standardized and efficient while ensuring compliance with the IFC4 schema at all stages.

The proposed method utilizes the IFC4 schema to store progress information in the IFC model by creating appropriate IFC entities and linking them with other organized entities in the hierarchical structure. Each IFC entity has a defined number of IFC attributes and may have additional IFC properties. The IFC attributes, with their fixed names defined by buildingSMART, play an important role in the identification of the entities. The IFC entities inherit attributes from their supertype or parent entities in the hierarchy (demonstrated in **Figure 5.5**), in addition to their directly attached entity attributes. This hierarchical organization of information ensures consistency

while maintaining data integrity in the IFC model. By following this standardized structure, the creation and retrieval of progress entities can be streamlined and automated, making the process more efficient and accurate.

**Figure 5.5** highlights the hierarchy of some object classes. The object classes `IfcSlab` and `IfcWall` are the subtypes of `IfcBuiltElement` and thus share the common attributes (highlighted in green and blue) between them, with the exception of their direct attributes. In contrast, `IfcTask` also shares some attributes (highlighted in green) with both `IfcSlab` and `IfcWall`; however, only up to the `IfcObject` level. As a result, `IfcTask` has the same initial attributes as the other two classes, while the remaining attributes differ based on their position in the hierarchical structure.

	IfcSlab	IfcWall	IfcTask
<b>IfcBut</b>	1 GlobalId 2 OwnerHistory 3 Name 4 Description	IfcGloballyUniqueId IfcOwnerHistory IfcLabel IfcText	
<b>IfcObjectDefinition</b>	HasAssignments Nests IsNestOf HasContext IsDecomposedBy Decomposes HasAssociations	IfcRelAssigns IfcRelNests IfcRelNests IfcRelDeclares IfcRelAggregates IfcRelAggregates IfcRelAssociates	
<b>IfcObject</b>	5 ObjectType IsDeclaredBy Declares IsTypedBy IsDefinedBy	IfcLabel IfcRelDefinesByObject IfcRelDefinesByObject IfcRelDefinesByType IfcRelDefinesByProperties	
<b>IfcProduct</b>	6 ObjectPlacement 7 Representation ReferencedBy PositionedRelativeTo ReferencedStructures	IfcObjectPlacement IfcProductRepresentation IfcRelAssignsToProduct IfcRelPositions IfcRelReferencedInSpatialStructure	<b>IfcProcess</b> 8 Identification 7 LongDescription IsPredecessorTo IsSuccessorFrom OperatesOn
<b>IfcElement</b>	8 Tag FillsVoids ConnectedTo IsInterferedByElements InterferesElements HasProjections HasOpenings IsConnectionRealization ProvidesBoundaries ConnectedFrom ContainedInStructure HasCoverings	IfcIdentifier IfcRelFillsElement IfcRelConnectsElements IfcRelInterferesElements IfcRelInterferesElements IfcRelProjectsElement IfcRelVoidsElement IfcRelConnectsWithRealizingElements IfcRelSpaceBoundary IfcRelConnectsElements IfcRelContainedInSpatialStructure IfcRelCoversBldgElements	<b>IfcTask</b> 8 Status 9 WorkMethod 10 IsMilestone 11 Priority 12 TaskTime 13 PredefinedType
<b>IfcBuiltElement</b>	(Nil)		
<b>IfcSlab</b>	9 PredefinedType IfcSlabTypeEnum	<b>IfcWall</b> 9 PredefinedType IfcWallTypeEnum	

**Figure 5.5.** IFC entities `IfcSlab`, `IfcWall`, `IfcTask` having common attributes based on their hierarchical structure.

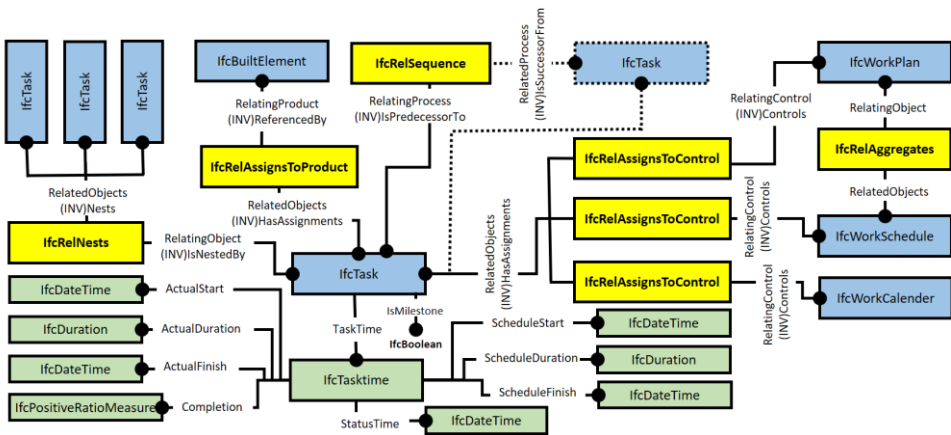
To add new information to the IFC-based BIM, it is necessary to create a new entity with the appropriate IFC subtype. This defines the set of attributes and properties applicable to the entity. The entity can be linked to other entities using required relationship classes, such as ‘`IfcRelAssignsToControl`’, allowing the establishment of relationships between entities and ultimately enabling the organization of information using the IFC schema. Compliance with the IFC schema is critical while creating new entities to ensure that the correct attributes and properties are included and the relationship with other entities is established correctly, which in turn facilitates the organization of information using the IFC schema.

The IFC-based entities in the proposed method are always created with *IfcRoot* attributes, such as *GlobalId*, *Name*, and *Description*. The *GlobalId* attribute is populated with a 22-character string based on the *IfcGloballyUniqueId* type. The *OwnerHistory* attribute records the identification details of the person responsible for creating the entities and is populated using the *IfcOwnerHistory* entity. The *Name* and *Description* attributes are filled with relevant information pertaining to the entity.

The process of integrating progress information into the IFC-based BIM requires a specific approach to ensure that the relevant entities are created and linked appropriately. This involves creating separate IFC entities for time, cost, and other information and establishing the necessary connections between them. The detailed procedures outlined below for each type of information are essential for ensuring that the resulting BIM model comprehensively represents progress information.

### 5.3.1.1 Time-Related Entities

The IFC4 schema already supports scheduling information for individual building components. Hence, the proposed method creates appropriately supported entities to store the relevant information as per IFC standards. The inclusion of time-related information into BIM includes creating native entities such as *IfcTask*, *IfcTaskTime*, *IfcWorkPlan*, *IfcWorkSchedule*, *IfcWorkCalendar*, etc. for each building component ‘*IfcBuiltElement*’ along with their respective relationships, as shown in **Figure 5.6**.



**Figure 5.6.** Structure of IFC-based entities created to include time-related progress information.

The proposed method is a task-based approach; hence, the entities are created accordingly. The Algorithm 5.1, as shown below, outlines the steps to create time-related IFC entities in a Building Information Model (BIM) to include information on planned and actual scheduling parameters. It inputs the IFC-based BIM and the planned work schedule to output an updated BIM with the necessary schedule

entities created in accordance with the work activities or tasks. The algorithm creates entities for ( $i$ -th) work main tasks and their ( $n$ -th) sub-tasks under each building component, establishes their sequential relationship, and links them with relevant time-related schedule entities such as task time, work plan, schedule, and calendar.

---

**Algorithm 5.1:** Creating time-related IFC entities into IFC-based BIM model

---

**Input:** IFC-based BIM, Planned Time-related Schedule  
**Output:** Updated IFC-based BIM

- 1 **for** each '*IfcBuiltElement*  $i$ ' in IFC-based BIM **do**
- 2     create an '*IfcTask*  $i$ ' entity
- 3     create an '*IfcTaskTime*  $i$ ' entity
- 4     link '*IfcTask*  $i$ ' with '*IfcTaskTime*  $i$ ' as *TaskTime*
- 5     create relationship '*IfcRelAssignsToProduct*' to assign '*IfcTask*  $i$ ' with '*IfcBuiltElement*  $i$ '
- 6     **if** sub-activities exist **then**
- 7         create relationship '*IfcRelnests*' to assign '*IfcTask*  $i$ ' as *RelatingObject*
- 8         **for** each sub-activity **do**
- 9             create '*IfcTask*  $n$ ' entity
- 10            create '*IfcTaskTime*  $n$ ' entity
- 11            link '*IfcTask*  $n$ ' with '*IfcTaskTime*  $n$ ' as *TaskTime*
- 12            link '*IfcRelnests*' with '*IfcTask*  $n$ ' as *RelatedObjects*
- 13         **end for**
- 14     **end if**
- 15 **end for**
- 16 create relationship '*IfcRelSequence*' to establish sequential relationship between all '*IfcTask*' entities
- 17 create '*IfcWorkSchedule*'
- 18 create relationship '*IfcRelassignsToControl*' to assign '*IfcWorkSchedule*' with all '*IfcTask*' entities
- 19 create '*IfcWorkPlan*'
- 20 create relationship '*IfcRelassignsToControl*' to assign '*IfcWorkPlan*' with all '*IfcTask*' entities
- 21 create relationship '*IfcRelAggregates*' to assign '*IfcWorkPlan*' with '*IfcWorkSchedule*'
- 22 create '*IfcWorkCalender*'
- 23 create relationship '*IfcRelassignsToControl*' to assign '*IfcWorkCalender*' with all '*IfcTask*' entities

---

The workflow of the algorithm is briefly explained below.

The algorithm starts by looping through each '*IfcBuiltElement*' in the IFC-based Building Information Model (BIM). For each *i*-th building component represented by the '*IfcBuiltElement*' entity, the algorithm creates an '*IfcTask*' entity that represents a specific piece of work that is to be accomplished. The attribute '*IsMilestone*' of '*IfcTask*' represents whether the particular task is critical for completion; it is not optional, and it is initially set to '*False*' with the intention to revise it at the final updating stage. To associate the time-relation information with the task, a new entity '*IfcTaskTime*' is created and linked to the '*IfcTask*' through the *TaskTime* attribute such that *IfcTask.Tasktime = IfcTaskTime*. Through this linkage, the time-related information of tasks, including their start and end dates as well as duration, is stored in the attributes of '*IfcTaskTime*' that are illustrated in **Figure 5.6**. The '*IfcRelAssignsToProduct*' relationship entity is then created to assign the '*IfcTask*' to the '*IfcBuiltElement*' through the attributes in such a way that *IfcRelAssignsToProduct.RelatingProduct = IfcBuiltElement* and *IfcTask.HasAssignments = IfcRelAssignsToProduct*.

Next, if there are multiple sub-tasks present under the main task in planned information, then the already created '*IfcTask*' acts as the main task, and the sub-tasks are created separately. The algorithm creates another loop to go through each sub-task. For each *n*-th sub-task, the algorithm creates a new '*IfcTask*' and '*IfcTaskTime*' entity and links the '*IfcTaskTime*' to the '*IfcTask*'. The algorithm then creates the '*IfcRelNests*' relationship entity to assign the sub-task to the main task of the building component.

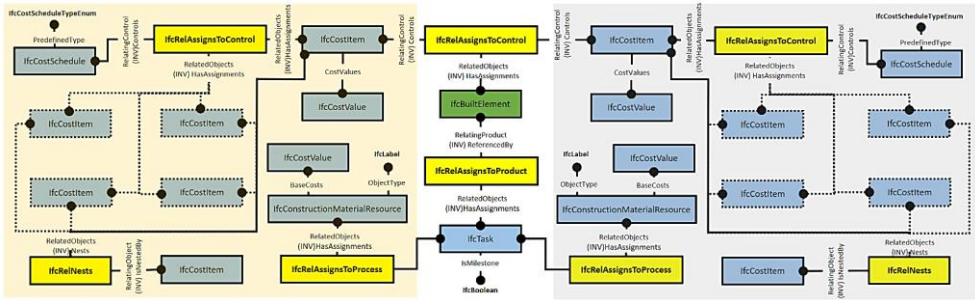
After creating all the entities for '*IfcBuiltElement*', the algorithm creates the '*IfcRelSequence*' relationship entity to establish the sequential relationship between '*IfcTask*' entities according to planned tasks using the attributes *RelatingProcess* and *RelatedProcess* that represent the predecessor and successor tasks, respectively. To manage the work schedule, the algorithm creates an '*IfcWorkSchedule*' entity and assigns it to all '*IfcTask*' using the '*IfcRelAssignsToControl*' relationship entity, linking the entities through relationship *IfcRelAssignsToControl.RelatingControl = IfcWorkSchedule*. Similarly, an '*IfcWorkPlan*' entity is then created to represent the detailed plan of the work schedule, assigns it to all '*IfcTask*' using the '*IfcRelAssignsToControl*' relationship entity, and aggregates it to the '*IfcWorkSchedule*' using the '*IfcRelAggregates*' relationship entity. Finally, the algorithm concludes by creating an '*IfcWorkCalender*' entity to represent the working days and hours and assigning it to all '*IfcTask*' entities in the same way, using the '*IfcRelAssignsToControl*' relationship entity.

The algorithm creates the time-related information for tasks (under the building component) and sub-tasks (under the main tasks) with appropriate entities in a standardized form. However, the project-based time-related entities are not created

as they already exist in IFC-based BIM through a project-related `IfcPropertySet` (`Pset_ConstructionResource`) and are updated based on tasks and subtasks in the later stage.

### 5.3.1.2 Cost-Related Entities

The proposed method creates cost-related entities in the form of resources and cost items. The resource entities, such as `IfcConstructionMaterialResource` are assigned for the cost of tasks, while the `IfcCostItem` entities are employed to represent the costs of building components and the overall project. **Figure 5.7** illustrates the structure of IFC entities being created to represent the cost parameters for construction progress monitoring.



**Figure 5.7.** The Structure of IFC-based entities was created to include cost-related progress information. Entities on the left and right sides representing the planned and actual cost information.

Algorithm 5.2, as shown below, creates the appropriate cost-related entities along with the corresponding relationships to retain the clearly defined cost information of each work task, building component, and overall project in a standardized form. The algorithm is processed in two phases to create IFC entities, both for planned and actual progress, respectively. In each phase, the 'PredefinedType' attribute of the 'IfcCostSchedule' entity is set to 'Budget' and 'USERDEFINED' to specify the cost of planned or actual work, respectively. Hence, two entities, indicating the cost associated with planned and actual work, will be created in the end for each task or building component, as shown in **Figure 5.7**, where the left and right sides, respectively, represent the planned and actual entities created to represent the cost. Additionally, the program assumes that the input IFC-based BIM has already been processed with the previous algorithm (Algorithm 5.1) and therefore contains the relevant 'IfcTask' entities that will be further utilized in this algorithm.

---

**Algorithm 5.2:** Creating cost-related entities into IFC-based BIM model

---

**Input:** IFC-based BIM, Planned Cost-Related Schedule

**Output:** Updated IFC-based BIM

```
1 create an 'IfcCostSchedule' entity
2 create an 'IfcRelAssignsToControl' entity
3 link 'IfcRelAssignsToControl' with 'IfcCostSchedule' as RelatingControl
4 create an 'IfcCostValue  $t$ ' entity
5 create an 'IfcPhysicalQuantity  $t$ ' entity
6 create an 'IfcCostItem  $t$ ' entity
7 link 'IfcCostItem  $t$ ' entity with 'IfcCostValue  $t$ ' and 'IfcPhysicalQuantity  $t$ ' entity
8 create a relationship 'IfcRelNests' entity to assign 'IfcCostItem  $t$ ' as RelatingObject
9 for each 'IfcBuiltElement  $i$ ' in IFC-based BIM do
10     create an 'IfcCostValue  $i$ ' entity
11     create an 'IfcPhysicalQuantity  $i$ ' entity
12     create an 'IfcCostItem  $i$ ' entity
13     link 'IfcCostItem  $i$ ' entity with 'IfcCostValue  $i$ ' and 'IfcPhysicalQuantity  $i$ ' entity
14     create a relationship 'IfcRelAssignsToControl' entity to assign 'IfcCostItem  $i$ '
        with 'IfcBuiltElement  $i$ '
15     link 'IfcRelAssignsToControl' with 'IfcCostItem  $i$ ' as RelatedObjects
16     link 'IfcRelNests' entity with 'IfcCostItem  $i$ ' as RelatedObjects
17     if sub-activities exist then
18         for each sub-activity do
19             create an 'IfcCostValue  $n$ ' entity
20             create an 'IfcPhysicalQuantity  $n$ ' entity
21             create an 'IfcConstructionMaterialResource  $n$ ' entity
22             link 'IfcConstructionMaterialResource  $n$ ' with 'IfcCostValue  $n$ ' and
                'IfcPhysicalQuantity  $n$ ' entity
23             create a relationship 'IfcRelAssignsToProcess  $n$ ' entity to assign
                'IfcTask  $n$ ' with 'IfcConstructionMaterialResource  $n$ '
18         end for
24     else
25         create an 'IfcCostValue  $i$ ' entity
26         create an 'IfcPhysicalQuantity  $i$ ' entity
27         create an 'IfcConstructionMaterialResource  $i$ ' entity
28         link 'IfcConstructionMaterialResource  $i$ ' with 'IfcCostValue  $i$ ' and
            'IfcPhysicalQuantity  $i$ ' entity
29         create a relationship 'IfcRelAssignsToProcess  $i$ ' entity to assign 'IfcTask  $i$ '
            with 'IfcConstructionMaterialResource  $i$ '
30 end for
```

---



The details of this algorithm are as follows.

The algorithm begins by creating an 'IfcCostSchedule' entity with a value of a 'Pre-defined Type' attribute, which has the type of 'IfcCostScheduleTypeEnum', set at 'Budget' or 'USERDEFINED' corresponding to the planned or actual type of information, respectively.

Subsequently, the relationship entity 'IfcRelAssignsToControl' is established for the connection of the 'IfcCostSchedule' entity ( $\text{IfcRelAssignsToControl.RelatingControl} = \text{IfcCostSchedule}$ ) with the cost item entities that will be created for each building component. Next, the algorithm creates an 'IfcCostItem' entity and links it with the 'IfcCostValue' entity to represent the total cost of the building. Later, an 'IfcCostItem' entity along with 'IfcCostValue' are created to represent the cost information for each 'IfcBuiltElement'. This 'IfcCostItem' is then assigned to 'IfcBuiltElement' using the relationship 'IfcRelAssignsToControl' entity such that  $\text{IfcRelAssignsToControl.RelatingControl} = \text{IfcCostItem}$  and  $\text{IfcBuiltElement.HasAssignments} = \text{IfcRelAssignsToControl}$ .

Later in the algorithm, for each work activity, the 'IfcTask' entity linked to the 'IfcBuiltElement', resource entities are created. The process begins by creating the 'IfcConstructionMaterialResource' entity along with the linked 'IfcCostValue' and 'IfcPhysicalQuantity' entities. This entity is then linked with 'IfcTask' using the relationship 'IfcRelAssignsToProcess' entity, where  $\text{IfcRelAssignsToProcess.RelatingProcess} = \text{IfcTask}$  and  $\text{IfcConstructionMaterialResource.HasAssignments} = \text{IfcRelAssignsToProcess}$ .

Finally, all the individual 'IfcCostItem<sub>i</sub>' entities of building components are nested with the 'IfcCostItem<sub>t</sub>' to ensure their linkage for the representation of the total building cost. Similarly, these entities are linked with the initially created 'IfcCostSchedule' using the relationship 'IfcRelAssignsToControl'. In this way, all the required cost-related entities are created either for cost, planned, or actual progress.

#### 5.3.1.3 Additional Information

During construction progress monitoring, it is common to collect additional information that may not fit into standard IFC entities. This information, such as progress-related comments and non-standard progress parameters, can be stored in customized 'IfcPropertySets' to accommodate project-specific data. This approach allows construction stakeholders to ensure that valuable project information is not overlooked or lost and can be utilized for progress tracking and analysis.

To enable the communication of additional progress information, such as textual comments and estimated finish dates, IfcPropertySets can be created using Algorithm 3. The name, description, and value of the IfcPropertySets can be customized for the specific types of information being stored. For example, an IfcPropertySet can be created for progress comments with the name 'Progress

Comments' and a value in the *IfcText* type. Similarly, an *IfcPropertySet* can be created for estimated finish dates with the name 'EstimatedFinish' and a nominal value (e.g., 2022-12-27T14:57:48.803492) set as a normal date in the *IfcDateTime* representation.

---

**Algorithm 5.3:** Creating IFC-based entities for additional progress information into IFC-based BIM

---

**Input:** IFC-based BIM, Additional information details (Name, Description and Value)

**Output:** Updated IFC-based BIM

```
1 for each 'IfcBuiltElement'  $i$  in IFC-based BIM do
2     create an 'IfcPropertySingleValue' entity
3     Input Name, Description and Value into 'IfcPropertySingleValue' attributes
4     Name, Description, Nominal Value
5     create an 'IfcPropertySet' entity
6     link 'IfcPropertySet' with 'IfcPropertySingleValue' as HasProperties
7     create relationship 'IfcRelDefinesByProperties' to assign 'IfcPropertySet' with
8     'IfcBuiltElement'
9 end for
```

---

The algorithm creates an '*IfcPropertySingleValue*' entity with attributes such as name, description, and *NominalValue* to store additional information associated with it and later assign it to the building components. This allows for any information that is not represented in the native IFC schema to be stored in the *IfcPropertySets* of the required components. By utilizing *IfcPropertySets* and *IfcPropertySingleValues*, all relevant progress-related information can be accurately documented and made available for analysis in BIM models.

### 5.3.2 Inputting the Planned Progress Information into IFC-Based BIM

Once the progress-related entities are created and linked in the IFC-based BIM model, the proposed method inputs the planned information into the task and the building component-based entities of BIM model. The planning information mainly includes the time and cost schedules of planned tasks. To achieve this, the planned parameters of tasks are stored in the relevant entities, followed by the estimation and updating of relevant building components. This process enables the updating of building component parameters, which are essential for tracking project progress. The current stage is designed to only enrich those planned entities that do not require regular updating. These entities, which are also shown in **Figure 5.6** and **Figure 5.7**, are detailed in **Table 5.1**.

*Table 5.1.* Details of planned progress entities.

<b>Level of Information</b>	<b>IFC Entity</b>	<b>Attribute/Property</b>	<b>Data Type</b>	<b>Decription</b>
Task(s)/ SubTask(s)	IfcTaskTime	ScheduleStart	IfcDateTime	Schedule start time of the task/subtask
		ScheduleFinish	IfcDateTime	Schedule finish time of the task/subtask
		ScheduleDuration	IfcDuration	Schedule duration of the task/subtask
		StatusTime	IfcDateTime	Time at which the status of the task/subtask was last updated
	IfcConstructionMaterialResource	BaseCosts	IfcMonetary Measure	Planned cost of the task
Building Component	IfcTaskTime	ScheduleStart	IfcDateTime	Schedule start time of the building component
		ScheduleFinish	IfcDateTime	Schedule finish time of the building component
		ScheduleDuration	IfcDuration	Schedule duration of the building component
		StatusTime	IfcDateTime	Time at which the status of the building component was last updated
	IfcCostItem	CostValues	IfcMonetary Measure	Planned cost of building component

To perform this, the required planning information from the construction site is acquired in the form of a list that includes the respective schedule information. The time-related planned information includes the start and finish dates of tasks along with their duration, while the cost-related information lists the total cost planned for the completion of the tasks.

This information is then inputted into BIM using the appropriate IFC type through a program that identifies the tasks from the list using the name and then enriches the corresponding entities or attributes of the corresponding task present in BIM with the planned information. From the corresponding task in the schedule list, the program later infers all the 'IfcTaskTime' and IfcContructionMaterialResource' that are the sub-types of the 'IfcTask' entity and inputs their attributes.

The algorithm for the enrichment of planned entities is explained in Algorithm 5.4. Initially, the task-level entities are inputted from the given planned information, i.e., time and cost-related parameters of the task from the schedule list. The start date, finish date, and duration of each task are enriched into the relevant attributes (ScheduleStart, ScheduleFinish, ScheduleSDuration) of the 'IfcTaskTime' entity under the corresponding 'IfcTask'. Similarly, the task cost is stored in the attribute (AppliedValues) of the 'BaseCosts' entity under 'IfcConstructionMaterialResource', which is linked with the corresponding 'IfcTask'. The information regarding the task is critical for the timely completion of the building and is directly stored in the corresponding 'IfcTask' entity. In the case of building components containing several subtasks, the main task duration is also updated based on the attributes of the sub-task by using the following Equations (1)–(3):

---

**Algorithm 5.4:** Inputting planned information into IFC-based BIM

---

**Input:** IFC-based BIM, Planned time-related Schedule, Planned cost Schedule

**Output:** Updated IFC-based BIM

```

1 for each 'IfcBuiltElement i' in IFC-based BIM do
2   if sub-activities exist then
3     for each sub-activity do
4       Input the attributes of 'IfcTaskTime n' entity under 'IfcTask n' entity
5       Input the attributes of 'IfcCostValue n' entity under
        'IfcConstructionMaterialResource nPlanned' entity
6     end for
7     Update the attributes of 'IfcTaskTime i' entity under 'IfcTask i' entity
8   else
9     Input the attributes of 'IfcTaskTime i' entity under 'IfcTask i' entity
10    Input the attributes of 'IfcCostValue i' entity under
        'IfcConstructionMaterialResource iPlanned' entity
11  end if
12  Update the attributes of 'IfcCostValue i' entity under 'IfcCostItem iPlanned'
    entity
13 end for

```

---

$$IfcTaskTime_i.ScheduleStart = \min[ IfcTaskTime_n.ScheduleStart ]_{n=1,2,3,..N} \quad (10)$$

$$IfcTaskTime_i.Schedulefinish = \max[ IfcTaskTime_n.ScheduleStart ]_{n=1,2,3,..N} \quad (2)$$

$$IfcTaskTime_i.ScheduleDuration = IfcTaskTime_i.Schedulefinish - IfcTaskTime_i.ScheduleStart \quad (3)$$

In the above equations,  $IfcTaskTime_n$  and  $IfcTaskTime_i$  represent the 'IfcTaskTime' entity of sub-task 'n' and main task 'i' associated with the building component, respectively, while min and max are the minimum and maximum parameters from the N number of total sub-tasks having attributes: *ScheduleStart*, *ScheduleFinish*, and *ScheduleDuration*.

In the end, the 'IfcCostItem' entity representing the cost of the building component is also estimated for updating using Equation (4). It is based on the total costs of all the task(s) that are required for the completion of a building component, and the task costs are stored under the 'IfcConstructionMaterialResource' entity.

$$\begin{aligned}
 & IfcCostItem_i^{Planned}.CostValues \\
 = & \begin{cases} \sum_{n=1}^N (IfcConstructionMaterialResource_n^{Planned}.BaseCosts) & \text{if subactivity exist} \\ IfcConstructionMaterialResource_i^{Planned}.BaseCosts & \text{else} \end{cases} \quad (4)
 \end{aligned}$$

In the above equation,  $IfcConstructionMaterialResource_i^{Planned}$  and  $IfcConstructionMaterialResource_n^{Planned}$  are the planned resource entities of i-th task and the n-sub task respectively whereas  $IfcCostItem_i^{Planned}$  is the entity representing the total planned cost of the i-th building component.

The values of the progress parameters are stored in their relevant entities in the form of suitable data types. For example, 'ScheduleStart' and 'ScheduleFinish' attributes should be updated with values having the IfcDateTime data type, which has the representation of YYYY-MM-DDThh:mm:ss defined by ISO 8601. The data types of other planned entities are given in the column 'Data type' of **Table 5.1**.

These entities are those that do not update regularly. Hence, the current stage is only performed if these entities are empty, which is possible for the first time. This stage is designed to only input the planned entities and does not need to be executed every time if the planned entities are already there.

### 5.3.3 Updating the Actual Progress into IFC-Based BIM

The objective of this stage is to enrich the actual progress-related IFC entities in the BIM model based on the progress information obtained from the construction site. It not only updates the task and building component-based entities according to the given actual progress but also revises the project-based entities to express the overall building progress, as shown in **Figure 5.8**. The updating stage mainly involves inferring the required entities, estimating their values, and then adding progress values to them.

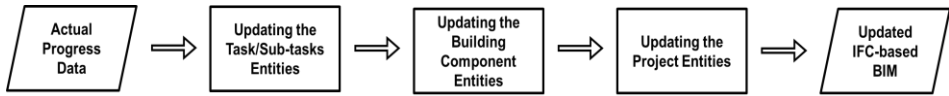


Figure 5.8. An example of IFC content.

The actual information includes the progress of completion (or completion ratios) and the actual cost of the tasks that are either under progress or completed, along with the inspection date. This actual information is sufficient to estimate the concerned attributes and the respective entities that are being updated. The details of the actual progress-related entities, also shown in **Figure 5.6** and **Figure 5.7**, are given in **Table 5.2**.

The procedure to update the IFC-based BIM model in this stage is outlined in Algorithm 5.5, while the estimation required for this updating, along with the procedure for all three steps, is detailed below:

---

**Algorithm 5.5:** Updating actual information into IFC-based BIM

---

**Input:** IFC-based BIM, Actual progress Information

**Output:** Updated IFC-based BIM

```

1  for each 'IfcBuiltElementi' in IFC-based BIM do
2    if sub-activities exist then
3      for each sub-activity do
4        Update the attributes of 'IfcTaskTimen' entity under 'IfcTaskn' entity
5        Update the attributes of 'IfcCostValuen' entity under
6        'IfcConstructionMaterialResourcenActual' entity
7      end for
8      Update the attributes of 'IfcTaskTimei' entity under 'IfcTaski' entity
9    else
10     Update the attributes of 'IfcTaskTimei' entity under 'IfcTaski' entity
11     Update the attributes of 'IfcCostValuei' entity under
12     'IfcConstructionMaterialResourceiActual' entity
13   end if
14   Update the attributes of 'IfcCostValuei' entity under 'IfcCostItemiPlanned' entity
15   Update the attributes of 'IfcCostValuei' entity under 'IfcCostItemiActual' entity
16   Update the attributes 'IfcTaski' entity
17   Update the propertyset 'EstimatedFinishDatei' entity
18 end for
19 Update the propertyset 'Pset_ConstructionResource' entity
  
```

---

Table 5.2. Details of actual progress entities.

Level of information	IFC Entity	Attribute/Property	Data Type	Description	
Task(s)/ SubTask(s)	IfcTaskTime	Completion	IfcPositiveRatioMeasure	Completion ratio of the task/subtask	
		ActualStart	IfcDateTime	Actual start time of the task/subtask	
		ActualFinish	IfcDateTime	Actual finish time of the task/subtask	
		ActualDuration	IfcDuration	Actual duration of the task/subtask	
		StatusTime	IfcDateTime	Time at which the status of the task/subtask was last updated	
	IfcConstructionMaterialResource*	BaseCosts	IfcMonetaryMeasure	Planned cost of the construction material resource	
	IfcConstructionMaterialResource*	BaseCosts	IfcMonetaryMeasure	Base cost of the construction material resource	
	Building Component	IfcTaskTime	Completion	IfcPositiveRatioMeasure	Completion ratio of the building component
			ActualStart	IfcDateTime	Actual start time of the building component
			ActualFinish	IfcDateTime	Actual finish time of the building component
ActualDuration			IfcDuration	Actual duration of the building component	
StatusTime			IfcDateTime	Time at which the status of the building component was last updated	
IfcTask		IsMilestone	IfcBoolean	Indicates if the task is a milestone	
		Status	IfcLabel	Status of the task (NOTSTARTED/ STARTED/ COMPLETED)	
IfcPropertySet		EstimatedFinish	IfcDateTime	Estimated finish time of the property set	
IfcCostItem*		CostValues	IfcMonetaryMeasure	Cost value of the cost item	
Overall Project		Pset_ConstructionResource	ScheduleCompletion	IfcNormalisedRatioMeasure	Planned completion ratio of the overall project
	ActualCompletion		IfcNormalisedRatioMeasure	Actual completion ratio of the overall project	

---

<i>ScheduleCost</i>	<i>IfcMonetaryMeasure</i>	To-date scheduled cost of the overall project
<i>ActualCost</i>	<i>IfcMonetaryMeasure</i>	To-date actual cost of the overall project

---

### 5.3.3.1 Tasks/Sub-Task

As the planned information for tasks/subtasks is already inputted into the IFC-based BIM, the actual progress entities are estimated based on actual progress to update fully completed or partially completed tasks. For time-related updates, the 'IfcTaskTime' entity is updated with different attributes related to actual progress, such as 'Completion', 'ActualStart', and 'ActualFinish', while the resource entity 'IfcConstructionMaterialResource' with attribute *ObjectType* = 'Actual' is designated for the actual cost. Algorithm 5.6, as shown below, estimates the actual attributes based on the completion ratio of each task using their 'IfcTaskTime' entity.

---

#### **Algorithm 5.6:** Updating *IfcTaskTime* entity using actual progress information

---

**Input:** 'IfcTaskTime' entity, Time-related progress information

**Output:** Updated IFC-based BIM

```

1 if IfcTask.Tasktime.ActualStart = Nil then
2     if IfcTask.Tasktime.Completion > 0 and IfcTask.Tasktime.Completion < 1 then
3         IfcTask.Tasktime.ActualStart = InspectionDate
4         IfcTask.Tasktime.Statustime = InspectionDate
5     end if
6 end if
7 if IfcTask.Tasktime.ActualFinish = Nil then
8     if IfcTask.Tasktime.Completion = 1 then
9         IfcTask.Tasktime.ActualFinish = InspectionDate
10        IfcTask.Tasktime.ActualDuration = IfcTask.Tasktime.ActualFinish -
11        IfcTask.Tasktime.ActualStart
12        IfcTask.Tasktime.Statustime = InspectionDate
13    end if
14 end if

```

---

### 5.3.3.2 Building Components

After updating the entities of individual tasks, the progress entities of individual building components are processed. This includes updating the 'IfcTaskTime' and 'IfcCostItem' entities associated with each component according to the estimated parameters from tasks. If that building component contains only one task, then this task will act as the main task, having attributes already updated in the last step. However, if there are subtasks in the building component, then the actual attributes of the 'IfcTasktime' entity will be estimated. The actual start, finish, and duration attributes are estimated similarly to the planned attributes in Equations (1)–(3).



Later, the completion of the building component is estimated using the following Equation (5), which takes the weighted average of the included tasks based on their schedule duration:

$$\text{Completion}_i^{\text{Actual}} = \frac{\sum (\text{IfcTaskTime}_n \cdot \text{Completion}_n \times \text{IfcTaskTime}_n \cdot \text{ScheduleDuration}_n)}{\sum (\text{IfcTaskTime}_n \cdot \text{ScheduleDuration}_n)} \quad (5)$$

In the above equation,  $\text{Completion}_i^{\text{Actual}}$  is the actual completion ratio of particular building component 'i' whereas  $\text{Completion}$  and  $\text{ScheduleDuration}$  are representing the completion ratio and schedule duration of sub-task 'n', respectively. Based on the estimated completion value, the 'Status' attribute of 'IfcTask' associated with the building component is also updated. It is set as 'NOTSTARTED' and 'COMPLETED' for completion values of 0 and 1, respectively, while "STARTED" is for values in between. In the end, the critical path method is performed using all the time-related information about building components to calculate the building components that are critical for completion. Correspondingly, these building components were marked as critical by updating the "IsMilestone" of their associated 'IfcTask' entity to "True" and the non-critical components are marked as "False".

Regarding the cost of a building component, already created entities 'CostItem' for actual progress under each 'IfcBuiltElement' are updated based on the cost values of individual tasks represented with the 'IfcConstructionMaterialResource'. The actual cost is estimated using the following Equation (6):

$$\text{IfcCostItem}_i^{\text{Actual}}.\text{CostValues} = \sum_{n=1}^N (\text{IfcConstructionMaterialResource}_n^{\text{Actual}}.\text{BaseCosts} \times \text{Completion}_n) \quad (6)$$

In the above equation,  $\text{IfcCostItem}_i^{\text{Actual}}$  Represents the actual cost of building component 'i' that has been spent to date, whereas  $\text{IfcConstructionMaterialResource}_n^{\text{Actual}}$  represents the actual cost of sub-task 'n' in that component with a completion ratio  $\text{Completion}_n$ . The attributes  $\text{CostValues}$  and  $\text{BaseCost}$  of both entities are linked to 'IfcCostValue' to represent their cost.

In the end, the estimated finish date is also calculated for each building component 'i' using time attributes based on the actual progress rate of all the individual tasks involved in that component, using the following Equation (7):

$$\begin{aligned} \text{EstimatedFinishDate}_i &= \text{IfcTaskTime}_i.\text{ActualStart} \\ &+ \frac{(\text{InspectionDate} - \text{IfcTaskTime}_i.\text{ActualStart})}{\text{IfcTaskTime}_i.\text{Completion}} \end{aligned} \quad (7)$$

### 5.3.3.3 Project

After updating the entities of all the individual building components with progress information, the overall progress of the project is estimated for updating the supported IFC entity. It includes the up-to-date total completion and cost parameters for both planned and actual progress. These project-based parameters are updated in the native IFCPropertySet 'Pset\_ConstructionResource' defined for storing the parameters to track the project's progress over time. In this property, the to-date planned and actual completion progress is stored in properties 'ScheduleCompletion' and 'ActualCompletion', whereas the to-date total planned and actual cost are stored under 'ScheduleCost' and 'ActualCost', respectively.

Initially, the parameters for up-to-date planned and actual completion are estimated based on the individual progress parameters of building components. To date, actual completion of the project can be calculated using Equation (8), which considers the weighted average of individual completion ratios of building components for actual progress. Similarly, the to-date planned completion ratio of the project is calculated using Equation (9), which takes into account the overall time-related project parameters.

$$\begin{aligned} & \text{To – date Actual Completion} \\ & = \frac{\sum (IfcTaskTime_i.Completion \times IfcTaskTime_i.ActualDuration)}{\sum (IfcTaskTime_i.ActualDuration)} \end{aligned} \quad (8)$$

$$\begin{aligned} & \text{To – date Planned Completion} \\ & = \frac{(\text{InspectionDate} - \min[IfcTaskTime_i.ScheduleStart]_{i=1,2,3,..,I})}{\max[IfcTaskTime_i.ScheduleFinish]_{i=1,2,3,..,I} - \min[IfcTaskTime_i.ScheduleSt} \end{aligned} \quad (9)$$

In the above equations,  $IfcTaskTime_i$  is the time-related progress entity of building component 'i' having attributes  $ScheduleStart$ ,  $ScheduleStart$ ,  $ActualDuration$  whereas  $InspectionDate$  represents the date of progress inspection performed at the construction site.

After that, the to-date total planned and actual costs are estimated. The cost item entities are defined in the project  $IfcCostItem_t^{Planned}$  and  $IfcCostItem_t^{Actual}$  represent the sums of cost items of individual building components due to the nested relationship. As all the planned costs are already inputted while the actual costs are only added with time as per the actual progress, hence,  $IfcCostItem_t^{Planned}$  and  $IfcCostItem_t^{Actual}$  entities are representing the total planned cost and to-date actual cost (total), respectively. Therefore, the individually planned completion of building components until the inspection date is initially estimated using Equation (10), and then, based on that to-date total planned cost of the project, it is computed using Equation (11).

$$Completion_i^{Planned} = \begin{cases} \frac{(InspectionDate - IfcTaskTime_i.ScheduleStart)}{IfcTaskTime_i.ScheduleDuration} & \text{if } InspectionDate > IfcTaskTime_i.ScheduleFinish \\ 1 & \text{elif } InspectionDate > IfcTaskTime_i.ScheduleStart \\ 0 & \text{else} \end{cases} \quad (10)$$

$$To - date\ planned\ Cost = \sum (IfcCostItem_i^{Planned}.CostValue \times Completion_i^{Planned}) \quad (11)$$

$$To - date\ Actual\ Cost = IfcCostItem_t^{Actual}.CostValue \quad (12)$$

In the above equation, ScheduleStart, ScheduleFinish, and ScheduleDuration are the attributes of the 'IfcTaskTime' entity associated with the main task 'IfcTask' of building component 'i' to estimate its completion ratio  $Completion_i^{Planned}$  till inspection date, which is represented as *InspectionDate*. Similarly  $IfcCostItem_t^{Planned}$  and  $IfcCostItem_t^{Actual}$  are representing the cost item nest with the individual cost items of building component 'i'. It is pertinent to mention here that the proposed method does not create new entities for time- or cost-related information for the overall project as the project IfcPropertyset (Pset\_ConstructionResource) already has the entities of these project-based progress information.

After estimating all these parameters, they are updated into their respective entities with appropriate data types as given in **Table 5.2**. The use of proper and relevant data types and units of measure for each attribute is crucial in ensuring the accuracy of the information added to the IFC-based BIM model.

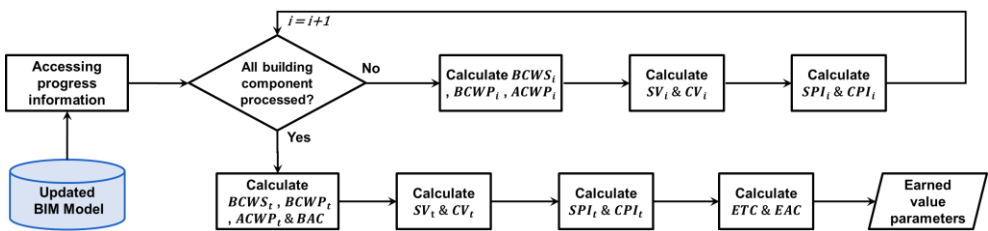
#### 5.3.4 Reporting the Progress from Updated IFC-Based BIM

The proposed method not only updates progress information in the BIM model but also extracts this information for efficient and user-friendly progress reporting. The extracted information can be used to assess progress by comparing the planned progress information with actual information. Additionally, the extracted progress parameters are processed based on their combination to find the earned value parameters for valuable insights about progress to ensure the project stays within budget and on schedule. Moreover, this stage makes use of BIM information to create more automated representations of extracted progress through 2D charts and 3D models, providing a clearer visualization of the project than traditional reporting. Overall, this approach enhances project monitoring by utilizing BIM technology to provide more accurate and detailed progress tracking.

The updated progress information is retrieved by accessing the corresponding IFC entities that were processed during the update. These entities are organized in the standard hierarchical structure of the IFC schema, which provides a clear path to access them. The proposed method links the progress-related entities to their corresponding building components. For example, for a particular building component 'IfcSlab', the time-related progress information is accessed through the

subtype 'IfcTaskTime' entity of 'IfcTask' with linkage (IfcTask → IfcRelAssignsToProduct → IfcSlab), while the cost information is accessed through the subtype entity 'IfcCostValue' of 'IfcCostItem' respectively with linkage (IfcCostItem → IfcRelAssignsToControl → IfcSlab). The building component entities (e.g., IfcSlab, IfcWall, IfcDoor, etc.) are the subtypes of 'IfcBuildingElement' that are present under the hierarchy ((IfcBuiltElement → IfcElement → IfcProduct → IfcObject → IfcObjectDefinition → IfcRoot) in the IFC schema. The extracted progress information from the entities is later used to report the progress monitoring of the construction project. In this way, information is directly retrieved from the concerned entities in the same way they were accessed to store information, which ultimately ensures the accurate and reliable communication of information within BIM.

The retrieved progress information can be further utilized to perform the earned value analysis, which is a well-accepted and common progress measurement in the construction industry [76]. The earned value analysis provides additional progress indicators that act as an early warning of performance problems. Integrating this analysis into the current method can facilitate the reporting stage. The updated BIM model contains both cost and schedule information, which is stored in the appropriate work breakdown structure in the BIM model being linked through the IFC schema. This presence of information entities in this standardized form enables the computation of earned value indicators such as variances (cost/schedule, variance at completion), performance indices (cost/schedule performance index), and forecasts (estimate at completion, estimate to completion). The proposed method also performs the earned value analysis of individual building components to analyze each component for comprehensive project tracking. The approach to performing the earned value analysis is illustrated in **Figure 5.9**.



**Figure 5.9.** Flowchart to estimate the earned value parameters.

Initially, the earned value measures are calculated, which include the budgeted cost of work scheduled (BCWS), the budgeted cost of work performed (BCWP), and the actual cost of work performed (ACWP). The formulas to calculate these measures for  $i$ -th building components using their IFC entities are given in Equations (13)–(15).

$$BCWS_i = IfcCostItem_i^{Planned}.CostValues \times Completion_i^{Planned} \quad (13)$$

$$BCWP_i = IfcCostItem_i^{Planned}.CostValues \times Completion_i^{Actual} \quad (14)$$

$$ACWP_i = IfcCostItem_i^{Actual}.CostValue \quad (15)$$

After calculating these measures, the variances and the performance indices are calculated. The variances, including the schedule variance ( $SV_i = BCWP_i - BCWS_i$ ) and cost variance ( $CV = BCWP_i - ACWP_i$ ) are calculated. Similarly, the performance indices including the schedule performance index ( $SPI_i = BCWP_i/BCWS_i$ ) and cost performance index ( $CPI_i = BCWP_i/ACWP_i$ ) are calculated.

After calculating the earned value parameters for the individual building components, earned value analysis at the project level is performed, which includes the calculation of earned value parameters based on the progress parameters of the overall project. The earned value measures for the project are computed by summing up all the measures of building components, including  $BCWS_t = \sum_{i=1}^I(BCWS_i)$ ,  $BCWP_t = \sum_{i=1}^I(BCWP_i)$ ,  $ACWS_t = \sum_{i=1}^I(ACWP_i)$ . Additionally, the budget at completion ( $BAC = \text{Total Planned Cost}$ ) is also calculated. After that, the variances and performance indices are calculated using these cumulative measures. Furthermore, the forecast parameters are also calculated, including the 'Estimate To Complete' ( $ETC = EAC - ACWP_t$ ) and 'EstimateAtCompletion' ( $EAC = ACWP_t + ((BAC - BCWP_t)/CPI_i)$ ) values describing the estimated cost to complete remaining works and the estimated total cost required for completion, respectively. These calculated earned value parameters can also be updated into an IFC-based BIM using `IfcPropertySet` if required.

The progress parameters extracted from the updated BIM model, along with the estimated additional parameters, can be utilized to report the construction progress of the project. However, additional efforts were made to further exploit the capabilities of the BIM model to facilitate the reporting process and make it more user-friendly. By leveraging BIM model's rich (non-progress-related) information, progress information can be reported more efficiently and accurately using various techniques such as bar charts, Gantt charts, and 3D model visualization. This approach not only enhances the visual presentation of the progress but also provides a better understanding of the project's status to all the stakeholders involved. **Table 5.3** provides details on the different types of reporting utilized for different types of progress information to report construction progress. It is worth noting that this is solely based on BIM information without relying on any third-party software.

*Table 5.3.* Details of different reporting types for different categories of progress information.

Category of Progress Information	Type of Reporting	Purpose
Time-related progress information	3D color-coded visualization	Provides a quick overview of time performance and highlights areas where the project is ahead/behind schedule for individual building components and the overall project.
	3D visualization of model	Allows for visual inspection of progress and identification of potential issues for individual building components and the overall project
	2D Gantt chart	Shows the overall project schedule, critical path, and delays for individual building components and the overall project
Cost-related progress information	3D color-coded visualization	Provides a quick overview of cost performance and highlights areas where costs are over/under budget for individual building components and the overall project
	2D bar chart	Allows for a detailed comparison of planned versus actual costs for individual building components and overall project
Earned value parameters	3D color-coded visualization	Provides a quick overview of earned value indicators and highlights components where indicators are over/under budget for individual building components
	Table form	Provides a detailed analysis of project performance by comparing planned versus actual costs and schedule for individual building components and overall project
	Line graph	Shows the trend of earned value parameters over time for individual building components and overall project
Additional information - estimated finish date	Textual form	Provides a simple and easy-to-understand summary of project status and estimated completion date for individual building components and overall project
	3D visualization of model	Shows the expected completion of activities in the coming week/month for individual building components
Additional information- textual comments	Textual form	Allows for a detailed explanation of project status and any issues that may be affecting progress for individual building components and overall project

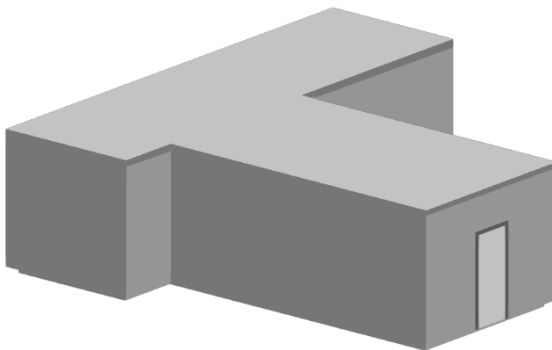
An automated program was developed to extract the necessary information on building components and generate the appropriate construction progress monitoring reports. Time-related progress information is extracted from the entities  $IfcTaskTime_i$ ,  $Pset\_ConstructionResource$ , and the cost-related information is extracted from entities  $IfcCostItem_i^{Planned}$ ,

$IfcCostItem_i^{Actual}$ ,  $Pset\_ConstructionResource$ . Earned value parameters and additional information are extracted from  $IfcPropertySet$ . To create the 2D charts, graphs, and textual information, the relevant progress parameters are extracted into a suitable arrangement accordingly. To perform the 3D visualization, the geometrical information of each building component is extracted from the BIM model using the different subtypes of geometrical entities such as 'IfcRepresentation', 'IfcGeometricRepresentationItem', 'IfcSpatialElement', and 'IfcOpeningElement'. Later, a 3D mesh model is developed using the geometrical information where the individual building components are color-coded according to their progress indicators obtained from comparison or earned value parameters. In addition, the mesh model can also be used to show only the planned or actual completed building components for more detailed understanding, if desired.

In the end, a web-based application was developed to allow for real-time reporting of all this progress information from the BIM model in the recommended format of texts, 2D charts, and 3D models. The application enables users to view the progress information of building components at any given time and to track the project's progress status efficiently. This approach enhances the visual presentation of progress information and provides stakeholders with a better understanding of the project's status.

#### 5.4 Result and Discussion

The proposed method was tested on several IFC-based BIM models to assess the exchange of progress information. A program was developed in Python language based on the proposed methodology which was tested on a laptop with an Intel i7-8850H CPU and 16 GB RAM. A BIM model, as shown in **Figure 5.10**, is a standard 3D BIM without any additional IFC entities, making it ideal for testing, which focuses on incorporating progress-related entities. This same building model is also used in all the previous chapters as well.



**Figure 5.10.** Geometrical visualization of an IFC-based BIM model illustrating various building components.





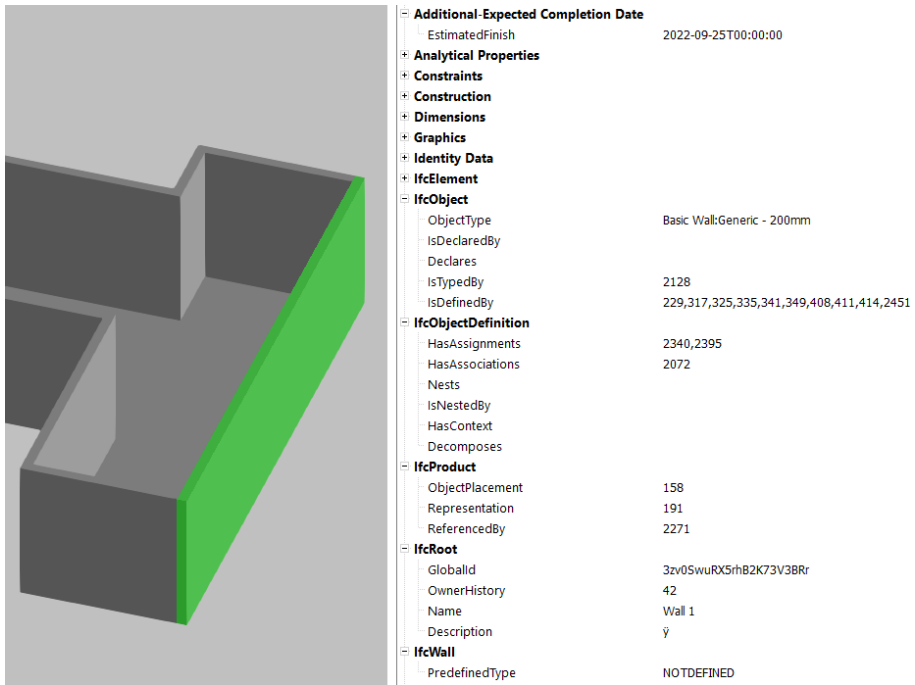
```

#197=IfcWall('3zv0SwuRX5rhB2K73V3BRr',#42,'Wall 1',$,'Basic Wall:Generic - 200mm',#158,#191,'354100',.NOTDEFINED.)
..... Extracting details .....
GlobalId:                3zv0SwuRX5rhB2K73V3BRr
Building Component Name: Wall 1
Schedule Start Date :    2022-09-12T00:00:00
Schedule Finish Date :   2022-09-16T00:00:00
Planned Cost :           264.00000000000364
Status Time :            2022-09-22T00:00:00
Completion Ratio :        0.5626106364965751
Actual Start Date :      2022-09-19T00:00:00
Actual Finish Date :     None
Expected Finish Date :   2022-09-25T00:00:00
Actual Cost               204.22766104825953
Schedule Performance Index (SPI):0.5626106364965751
Cost Performance Index (CPI):  0.7272727272727274

```

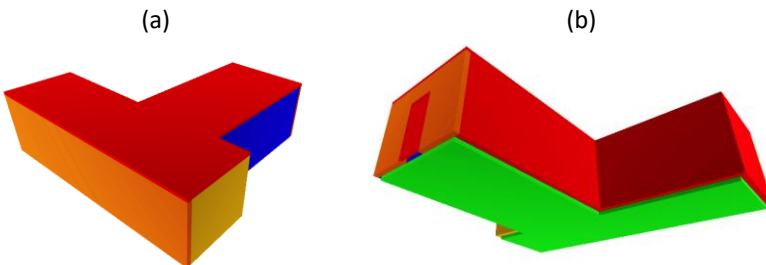
*Figure 5.12.* Retrieval of progress information for the building component (#197) using Python.

Furthermore, the same updated BIM file was exported into the external IFC-based software to confirm the successful storage and accessibility of information with the other applications. The building component (#197) along with its attributes are highlighted in *Figure 5.13*, where the BIM model was exported in ‘Open IFC Viewer version 23.3.0 [77], as also used in another study [78]. The parameter ‘EstimatedFinish’ is also noticeable, which was stored under the property set mainly because this additional information did not fit into the standard entities of the IFC schema. The successful export of the updated BIM model in the external software also confirms that the proposed method performed the successful update according to the IFC schema, as minor deviation while creating and updating IFC entities can corrupt the complete IFC file.



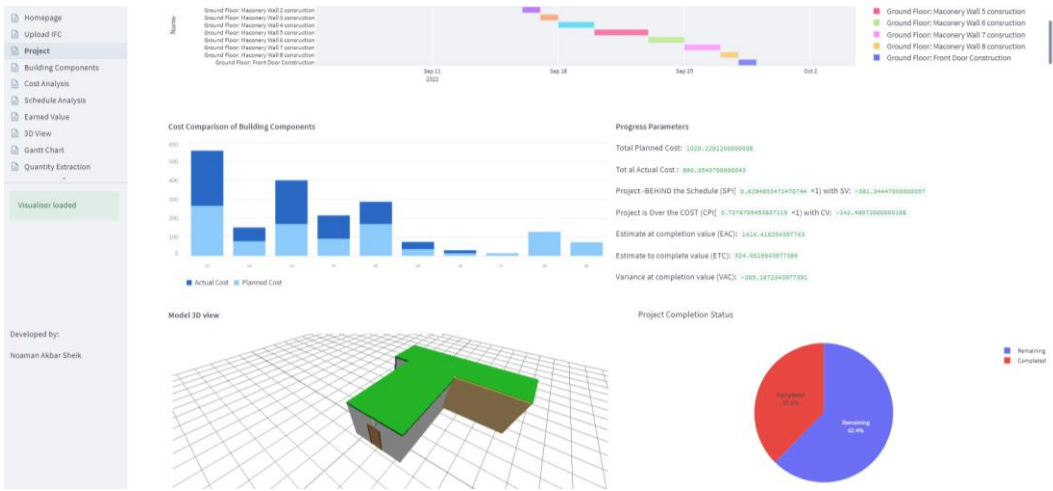
**Figure 5.13.** Building component (#197) highlighted in the exported BIM model, along with its attribute details, viewed in the external software (Open IFC Viewer, version 23.3.0).

In the end, the progress results were also color-coded according to the completion ratios of building components to assess the progress made. For this purpose, the geometrical information of the components is extracted into mesh form, and then four colors are assigned based on their completion ratios: 0–30% (red), 30–50% (yellow), 50–70% (orange), 70–90% (green), and 90–100% (blue). The color-coded models of the updated BIM model are illustrated in **Figure 5.14** from different viewpoints.



**Figure 5.14.** Visualization of building components using different colors (red, yellow, orange, green, and blue) corresponding to their respective completion ratios (0–30%, 30–50%, 50–70%, 70–90%, and 90–100%) in two different viewpoints.

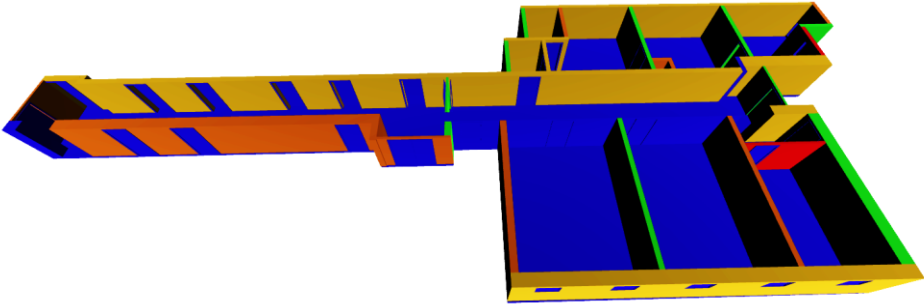
Furthermore, a web-based application was also developed to effectively report the progress information from the updated IFC-based BIM model. The application only requires the updated BIM model and then details all the progress-related information in real-time through the different types of reporting. A screenshot of the application is shown in **Figure 5.15**, displaying the project-level progress details of the updated BIM model in the form of charts, graphs, and 3D visualization. The developed application makes use of different progress parameters present within the standardized hierarchy of IFC-based BIM to facilitate reporting. It is pertinent to mention here that the proposed method does not store the individually earned parameter values, mainly to ensure a possible reduction of the IFC file size. The parameters are computed in real-time based on the already-stored schedule and cost parameters; however, they can be stored in a separate property set if required.



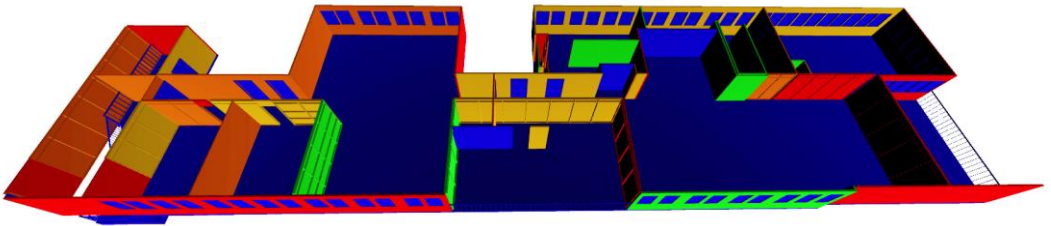
**Figure 5.15.** A screenshot of the developed web-based application demonstrating the project-level progress details of the updated BIM model.

The effectiveness of the proposed method was further evaluated by applying it to other IFC-based models, including the ISPRS model studies dataset [79]. These BIM models, as shown in Figure 5.16(a) and Figure 5.16(b), are representing a university and fire brigade building respectively. The IFC-based BIM model of first dataset contains 69 IFC elements while the second IFC-based BIM model contains 157 IFC elements. Both the model were modeled by experts on Autodesk Revit™ software. In the evaluation, random progress information was exchanged with BIM models to access its updating framework, as the proposed method enables the incorporation of input data from various sources. The method successfully updated the progress information for these models as well. **Figure 5.16** shows the visualization of the two ISPRS models, in which their building components are color-coded according to their time-related progress details after exchanging progress information.

(a)



(b)



**Figure 5.16.** Color-coded visualization of two different BIM models (a,b) highlighting the progress status of their building components: 0–30% (Red), 30–50% (Yellow), 50–70% (Orange), 70–90% (Green), and 90–100% (Blue).

From the results, it is evident that the proposed method is capable of updating IFC-based BIM models with progress information. The method processed the IFC models by creating the new entities, accurately estimating their progress parameters, updating existing entities, and then successfully reporting the progress information in a user-friendly manner. These IFC-based BIM models, updated with progress information, can be utilized for construction progress monitoring, facilitating the automated transfer of information in construction. Similarly, the development of a web-based application also proved that progress details can be effortlessly reported without any reliance on third-party commercial software if the information is stored in a structurally organized way through a standard framework, eventually leveraging the potential of BIM technology in construction projects. This proposed method holds significant potential for enhancing the efficacy of other construction progress monitoring studies [3,5,42,63] by providing them with a standardized solution for information exchange.

## 5.5 Conclusions

BIM provides an extensive and accurate digital representation of a building in the form of geometrical and semantic information that describes its physical and functional characteristics. However, its potential is not fully realized in construction progress monitoring and reporting. IFC is a widely recognized open standard for BIM exchange; however, its utility needs to be addressed for exchanging progress

information based on the latest IFC4.x schema, which encompasses not only time-related information but also cost and other non-standardized information. In the current chapter, a research study is presented that detailed a comprehensive methodology with a task-based approach to exchange the progress information of under-construction buildings with the BIM model using the latest IFC4 schema in four stages. The progress information is integrated into the BIM model through structural organization in the form of appropriate IFC entities. Apart from the standard progress information, including the time-related schedule or cost, the method also allows the integration of additional semantic information that may not fit into the defined IFC entities to ensure that valuable information is not overlooked. To enable effective progress monitoring, the method not only updates the BIM model but also allows the efficient retrieval of progress information, which is reported in the form of additional progress indicators, including earned value analysis, to offer valuable insights. Furthermore, it is also ensured that the estimated progress values of the building components and project are being revised according to their corresponding tasks or sub-tasks.

The testing demonstrated the successful updating of BIM models to accommodate the progress information while demonstrating a web-based application that reads the intricate information from the IFC entities and then reports it in a user-friendly format. The exchange of progress information using the IFC-based BIM is a significant step towards automation in construction progress monitoring that enables the ability to accurately track construction progress and timely identify deviations, which eventually improves decision-making, increases efficiency, and enhances project management.

## 5.6 References

1. Hamledari, H.; McCabe, B.; Davari, S. Automated computer vision-based detection of components of under-construction indoor partitions. *Autom. Constr.* **2017**, *74*, 78–94.
2. Golparvar-Fard, M.; Pena-Mora, F.; Savarese, S. Automated progress monitoring using unordered daily construction photographs and IFC-based building information models. *J. Comput. Civ. Eng.* **2014**, *29*, 04014025.
3. Sheik, N.A.; Veelaert, P.; Deruyter, G. Registration of Building Scan with IFC-Based BIM Using the Corner Points. *Remote Sens.* **2022**, *14*, 5271.
4. Bosché, F. Automated recognition of 3D CAD model objects in laser scans and calculation of as-built dimensions for dimensional compliance control in construction. *Adv. Eng. Inform.* **2010**, *24*, 107–118.
5. Sheik, N.A.; Deruyter, G.; Veelaert, P. Plane-Based Robust Registration of a Building Scan with Its BIM. *Remote Sens.* **2022**, *14*, 1979.
6. Mahami, H.; Nasirzadeh, F.; Hosseinaveh Ahmadabadian, A.; Nahavandi, S. Automated progress controlling and monitoring using daily site images and building information modelling. *Buildings* **2019**, *9*, 70.
7. Azhar, S.; Carlton, W.A.; Olsen, D.; Ahmad, I. Building information modeling for sustainable design and LEED® rating analysis. *Autom. Constr.* **2011**, *20*, 217–224.
8. Ghaffarianhoseini, A.; Tookey, J.; Ghaffarianhoseini, A.; Naismith, N.; Azhar, S.; Efimova, O.; Raahemifar, K. Building Information Modelling (BIM) uptake: Clear benefits, understanding its implementation, risks and challenges. *Renew. Sustain. Energy Rev.* **2017**, *75*, 1046–1053.
9. Doumbouya, L.; Gao, G.; Guan, C. Adoption of the Building Information Modeling (BIM) for construction project effectiveness: The review of BIM benefits. *Am. J. Civ. Eng. Archit.* **2016**, *4*, 74–79.
10. Nawari, N.O. BIM standard in off-site construction. *J. Archit. Eng.* **2012**, *18*, 107–113.
11. Lee, D.; Lee, S.H.; Masoud, N.; Krishnan, M.; Li, V.C. Integrated digital twin and blockchain framework to support accountable information sharing in construction projects. *Autom. Constr.* **2021**, *127*, 103688.
12. Eastman, C.; Teicholz, P.; Sacks, R.; Liston, K.; Handbook, B. A guide to building information modeling for owners, managers, designers, engineers and contractors. *BIM Handb.* **2011**, *2*, 147–150.
13. Arayici, Y.; Aouad, G. Building information modelling (BIM) for construction lifecycle management. *Constr. Build. Des. Mater. Tech.* **2010**, *2010*, 99–118.
14. Succar, B. Building information modelling framework: A research and delivery foundation for industry stakeholders. *Autom. Constr.* **2009**, *18*, 357–375.
15. Azhar, S.; Khalfan, M.; Maqsood, T. Building information modeling (BIM): Now and beyond. *Australas. J. Constr. Econ. Build.* **2012**, *12*, 15–28.
16. *ISO 16739-1: 2018*; Industry Foundation Classes (IFC) for Data Sharing in the Construction and Facility Management Industries—Part 1: Data Schema. ISO: Geneva, Switzerland, 2018.
17. Poljanšek, M. *Building Information Modelling (BIM) Standardization*; European Commission: Brussels, Belgium, 2017.
18. *ISO\_29481-1*; Building Information Models—Information Delivery Manual—Part 1: Methodology and Format. International Organization for Standardization: Geneva, Switzerland, 2016.

19. Söbke, H.; Peralta, P.; Smarsly, K.; Armbruster, M. An IFC schema extension for BIM-based description of wastewater treatment plants. *Autom. Constr.* **2021**, *129*, 103777.
20. BuildingSMART International. Available online: <https://www.buildingsmart.org/> (accessed on 1 December 2021).
21. BuildingSMART International. *IFC Overview Summary*; BuildingSMART International: Cambridge, UK, 2018.
22. Yu, K.; Froese, T.; Grobler, F. A development framework for data models for computer-integrated facilities management. *Autom. Constr.* **2000**, *9*, 145–167.
23. Lam, K.; Wong, N.; Shen, L.; Mahdavi, A.; Leong, E.; Solihin, W.; Au, K.; Kang, Z. Mapping of industry building product model for detailed thermal simulation and analysis. *Adv. Eng. Softw.* **2006**, *37*, 133–145.
24. Ma, Z.; Teng, M.; Ren, Y. Method of extracting static data for building energy consumption monitoring from BIM. *J. Harbin Inst. Technol.* **2019**, *51*, 187–193.
25. Zhang, J.; Yu, F.; Li, D.; Hu, Z. Development and implementation of an industry foundation classes-based graphic information model for virtual construction. *Comput. -Aided Civ. Infrastruct. Eng.* **2014**, *29*, 60–74.
26. Zhang, J.; Guo, J.; Wang, S.; Xu, Z. Intelligent facilities management system based on IFC standard and building equipment integration. *Tsinghua Univ.* **2008**, *48*, 940-942, 946.
27. Xu, Z.; Wang, X.; Xiao, Y.; Yuan, J. Modeling and performance evaluation of PPP projects utilizing IFC extension and enhanced matter-element method. *Eng. Constr. Archit. Manag.* **2020**, *27*, 1763–1794.
28. Akinci, B.; Boukamp, F. Representation and integration of as-built information to IFC based product and process models for automated assessment of as-built conditions. In Proceedings of the ISARC 2002: 19 th International Symposium on Automation and Robotics in Construction, Gaithersburg, MA, USA, 23–25 September 2002; pp. 543–549.
29. Seo, J.; Kim, I. Industry foundation classes-based approach for managing and using the design model and planning information in the architectural design. *J. Asian Archit. Build. Eng.* **2009**, *8*, 431–438.
30. Choi, J.; Kim, H.; Kim, I. Open BIM-based quantity take-off system for schematic estimation of building frame in early design stage. *J. Comput. Des. Eng.* **2015**, *2*, 16–25.
31. Akanbi, T.; Zhang, J.; Lee, Y.-C. Data-driven reverse engineering algorithm development method for developing interoperable quantity takeoff algorithms using IFC-based BIM. *J. Comput. Civ. Eng.* **2020**, *34*, 04020036.
32. Park, J.; Cai, H.; Dunston, P.S.; Ghasemkhani, H. Database-supported and web-based visualization for daily 4D BIM. *J. Constr. Eng. Manag.* **2017**, *143*, 04017078.
33. Hamledari, H.; McCabe, B.; Davari, S.; Shahi, A. Automated schedule and progress updating of IFC-based 4D BIMs. *J. Comput. Civ. Eng.* **2017**, *31*, 04017012.
34. Hamledari, H.; Rezazadeh Azar, E.; McCabe, B. IFC-based development of as-built and as-is BIMs using construction and facility inspection data: Site-to-BIM data transfer automation. *J. Comput. Civ. Eng.* **2017**, *32*, 04017075.
35. Son, H.; Kim, C.; Kwon Cho, Y. Automated schedule updates using as-built data and a 4D building information model. *J. Manag. Eng.* **2017**, *33*, 04017012.

36. IFC2x3 to IFC4. Available online: [https://standards.buildingsmart.org/IFC/DEV/IFC4\\_2/FINAL/HTML/annex/annex-f/ifc2x3-to-ifc4/index.htm](https://standards.buildingsmart.org/IFC/DEV/IFC4_2/FINAL/HTML/annex/annex-f/ifc2x3-to-ifc4/index.htm) (accessed on 1 March 2023).
37. Navon, R. Research in automated measurement of project performance indicators. *Autom. Constr.* **2007**, *16*, 176–188.
38. Zhang, X.; Bakis, N.; Lukins, T.C.; Ibrahim, Y.M.; Wu, S.; Kagioglou, M.; Aouad, G.; Kaka, A.P.; Trucco, E. Automating progress measurement of construction projects. *Autom. Constr.* **2009**, *18*, 294–301.
39. Yang, J.; Park, M.-W.; Vela, P.A.; Golparvar-Fard, M. Construction performance monitoring via still images, time-lapse photos, and video streams: Now, tomorrow, and the future. *Adv. Eng. Inform.* **2015**, *29*, 211–224.
40. Alizadehsalehi, S.; Yitmen, I. A concept for automated construction progress monitoring: Technologies adoption for benchmarking project performance control. *Arab. J. Sci. Eng.* **2019**, *44*, 4993–5008.
41. Fang, J.; Li, Y.; Liao, Q.; Ren, Z.; Xie, B. Construction Progress Control and Management Measures Analysis. *Smart Constr. Res.* **2018**, *2*.
42. Kavaliuskas, P.; Fernandez, J.B.; McGuinness, K.; Jurelionis, A. Automation of Construction Progress Monitoring by Integrating 3D Point Cloud Data with an IFC-Based BIM Model. *Buildings* **2022**, *12*, 1754.
43. Kim, C.; Son, H.; Kim, C. Automated construction progress measurement using a 4D building information model and 3D data. *Autom. Constr.* **2013**, *31*, 75–82.
44. Golparvar-Fard, M.; Savarese, S.; Peña-Mora, F. Interactive Visual Construction Progress Monitoring with D4 AR—4D Augmented Reality—Models. In Proceedings of the Construction Research Congress 2009: Building a Sustainable Future, Seattle, WA, USA, 5–7 April 2009; pp. 41–50.
45. Omar, H.; Dulaimi, M. Using BIM to automate construction site activities. *Build. Inf. Model. BIM Des. Constr. Oper.* **2015**, *149*, 45.
46. Braun, A.; Tuttas, S.; Borrmann, A.; Stilla, U. A concept for automated construction progress monitoring using bim-based geometric constraints and photogrammetric point clouds. *J. Inf. Technol. Constr.* **2015**, *20*, 68–79.
47. Carrera-Hernández, J.; Levresse, G.; Lacan, P. Is UAV-SfM surveying ready to replace traditional surveying techniques? *Int. J. Remote Sens.* **2020**, *41*, 4820–4837.
48. Abd-Elmaaboud, A.; El-Tokhey, M.; Ragheb, A.; Mogahed, Y. Comparative assessment of terrestrial laser scanner against traditional surveying methods. *Int. J. Eng. Appl. Sci* **2019**, *6*, 79–84.
49. Matarneh, S.; Elghaish, F.; Rahimian, F.P.; Dawood, N.; Edwards, D. Automated and interconnected facility management system: An open IFC cloud-based BIM solution. *Autom. Constr.* **2022**, *143*, 104569.
50. Shirowzhan, S.; Sepasgozar, S.M.; Edwards, D.J.; Li, H.; Wang, C. BIM compatibility and its differentiation with interoperability challenges as an innovation factor. *Autom. Constr.* **2020**, *112*, 103086.
51. Newman, C.; Edwards, D.; Martek, I.; Lai, J.; Thwala, W.D.; Rillie, I. Industry 4.0 deployment in the construction industry: A bibliometric literature review and UK-based case study. *Smart Sustain. Built Environ.* **2021**, *10*, 557–580.
52. Petronijević, M.; Višnjevac, N.; Prašević, N.; Bajat, B. The extension of IFC for supporting 3D cadastre LADM geometry. *ISPRS Int. J. Geo Inf.* **2021**, *10*, 297.



53. Bortoluzzi, B.; Efremov, I.; Medina, C.; Sobieraj, D.; McArthur, J. Automating the creation of building information models for existing buildings. *Autom. Constr.* **2019**, *105*, 102838.
54. Mihindu, S.; Arayici, Y. Digital construction through BIM systems will drive the re-engineering of construction business practices. In Proceedings of the 2008 International Conference Visualisation, London, UK, 9–11 July 2008; pp. 29–34.
55. Gerbert, P.; Castagnino, S.; Rothballer, C.; Renz, A.; Filitz, R. *Digital in Engineering and Construction*; The Boston Consulting Group: Boston, MA, USA, 2016; pp. 1–18.
56. Justo, A.; Soilán, M.; Sánchez-Rodríguez, A.; Riveiro, B. Scan-to-BIM for the infrastructure domain: Generation of IFC-compliant models of road infrastructure assets and semantics using 3D point cloud data. *Autom. Constr.* **2021**, *127*, 103703.
57. Kwon, T.H.; Park, S.I.; Jang, Y.-H.; Lee, S.-H. Design of railway track model with three-dimensional alignment based on extended industry foundation classes. *Appl. Sci.* **2020**, *10*, 3649.
58. Jones, S.; Laquidara-Carr, D.; Lorenz, A.; Buckley, B.; Barnett, S. The business value of BIM for infrastructure 2017. SmartMarket Report 2017. Available online: <https://www2.deloitte.com/content/dam/Deloitte/us/Documents/finance/us-fas-bim-infrastructure.pdf> (accessed on 1 December 2021).
59. Radke, A.; Wallmark, T.; Tseng, M. An automated approach for identification and resolution of spatial clashes in building design. In Proceedings of the 2009 IEEE International Conference on Industrial Engineering and Engineering Management, Hong Kong, China, 8–11 December 2009; pp. 2084–2088.
60. Borrmann, A.; Berkhahn, V. Principles of Geometric Modeling. In *Building Information Modeling: Technology Foundations and Industry Practice*; Springer: Cham, Switzerland, 2018; pp. 27–41.
61. Borrmann, A.; Beetz, J.; Koch, C.; Liebich, T.; Muhic, S. Industry foundation classes: A standardized data model for the vendor-neutral exchange of digital building models. In *Building Information Modeling: Technology Foundations and Industry Practice*; Springer: Cham, Switzerland, 2018; pp. 81–126.
62. Turkan, Y.; Bosche, F.; Haas, C.T.; Haas, R. Automated progress tracking using 4D schedule and 3D sensing technologies. *Autom. Constr.* **2012**, *22*, 414–421.
63. Pučko, Z.; Šuman, N.; Rebolj, D. Automated continuous construction progress monitoring using multiple workplace real time 3D scans. *Adv. Eng. Inform.* **2018**, *38*, 27–40.
64. Chen, L.; Luo, H. A BIM-based construction quality management model and its applications. *Autom. Constr.* **2014**, *46*, 64–73.
65. de Soto, B.G.; Rosarius, A.; Rieger, J.; Chen, Q.; Adey, B.T. Using a Tabu-search algorithm and 4D models to improve construction project schedules. *Procedia Eng.* **2017**, *196*, 698–705.
66. Lopez, R.; Chong, H.-Y.; Wang, X.; Graham, J. Technical review: Analysis and appraisal of four-dimensional building information modeling usability in construction and engineering projects. *J. Constr. Eng. Manag.* **2016**, *142*, 06015005.

67. Li, C.Z.; Xue, F.; Li, X.; Hong, J.; Shen, G.Q. An Internet of Things-enabled BIM platform for on-site assembly services in prefabricated construction. *Autom. Constr.* **2018**, *89*, 146–161.
68. Deng, Y.; Gan, V.J.; Das, M.; Cheng, J.C.; Anumba, C. Integrating 4D BIM and GIS for construction supply chain management. *J. Constr. Eng. Manag.* **2019**, *145*, 04019016.
69. Vieira, R.; Carreira, P.; Domingues, P.; Costa, A.A. Supporting building automation systems in BIM/IFC: Reviewing the existing information gap. *Eng. Constr. Archit. Manag.* **2020**, *27*, 1357–1375.
70. Yang, B.; Dong, M.; Wang, C.; Liu, B.; Wang, Z.; Zhang, B. IFC-based 4D construction management information model of prefabricated buildings and its application in graph database. *Appl. Sci.* **2021**, *11*, 7270.
71. Noardo, F.; Arroyo Otori, K.; Krijnen, T.; Stoter, J. An inspection of IFC models from practice. *Appl. Sci.* **2021**, *11*, 2232.
72. Noardo, F.; Wu, T.; Otori, K.A.; Krijnen, T.; Stoter, J. IFC models for semi-automating common planning checks for building permits. *Autom. Constr.* **2022**, *134*, 104097.
73. Koo, B.; Shin, B. Applying novelty detection to identify model element to IFC class misclassifications on architectural and infrastructure Building Information Models. *J. Comput. Des. Eng.* **2018**, *5*, 391–400.
74. Wang, N.; Issa, R.R. Ontology-based integration of BIM and GIS for indoor routing. In Proceedings of the Construction Research Congress 2020: Computer Applications, Tempe, AZ, USA, 8–10 March 2020; pp. 1010–1019.
75. BuildingSMART. Latest Available Documentation for IFC 4.3.x Specification. Available online: <https://ifc43-docs.standards.buildingsmart.org/> (accessed on 1 March 2023).
76. Aramali, V.; Sanboskani, H.; Gibson Jr, G.E.; El Asmar, M.; Cho, N. Forward-looking state-of-the-art review on earned value management systems: The disconnect between academia and industry. *J. Manag. Eng.* **2022**, *38*, 03122001.
77. Open IFC Viewer. Available online: <https://openifcviewer.com/> (accessed on 1 March 2023).
78. Li, H.; Zhang, J. Interoperability between BIM and BEM using IFC. In *Computing in Civil Engineering 2021*; American Society of Civil Engineers: Reston, VA, USA, 2021; pp. 630–637.
79. Khoshelham, K.; Vilariño, L.D.; Peter, M.; Kang, Z.; Acharya, D. The ISPRS benchmark on indoor modelling. *Int. Arch. Photogramm. Remote Sens. Spat. Inf. Sci.* **2017**, *42*, W7.

---

# 6

---

## 6. DISCUSSION AND CONCLUSION

## 6.1 Concluding Remarks

The dissertation focuses on improving automated construction progress monitoring by addressing the challenges during different phases of model-based assessment. The main contributions of the research are outlined as follows:

Chapter 2 presents a novel registration approach that aims to exploit the orthogonal geometry of building structures containing an abundance of plane segments with high robustness and accuracy. Initially, it extracts the plane segments from the models and then clusters them according to their directions, which are then processed to identify the possible rotation matrices for the registration of models. Later, the correspondence between potential plane segments in each rotation matrix is measured through directional and translational assessment to identify the matrix with the highest matching. In the end, the translation vector is calculated from the relatively best-matched plane segments.

This technique was tested with a variety of datasets that represented the different types of buildings. The results demonstrated the successful registration of all the datasets with a high degree of accuracy. The errors such as noise and occlusions were also analyzed and they slightly affected the registration success. During the testing, it was found that the technique is robust but the processing time is dependent on the plane segments present in the models. In the end, the incomplete as-built scan was also tested for registration to confirm its application for partially constructed buildings through model-based assessment. The method exhibited reliable results for incomplete models too with the only requirement that both models should have at least three non-parallel matching plane segments. From the standpoint of keeping track of the construction progress of under-construction buildings, this technique represents a significant advancement as it ensures their application in model-based assessment.

In the next chapter, another registration technique is developed that also makes use of the dominant planar geometry of building structures, similar to the earlier technique described in Chapter 2. The new approach instead of directly employing the plane segments of the building, leverages them to extract the evident corner points from both models. The procedure to extract plane segments from a BIM model is also detailed in which direct geometrical details from BIM are directly obtained using the IFC schema that is later processed to create the plane segments. The extracted corner points are then processed through a RANSAC-based pairwise assessment to identify their potential matching points. The assessment involves a pruning of the corresponding pair of corner points from the model through a sequence of discriminative geometric invariants concerning their distance, angle, rotation, and translation. The potential matching points are further evaluated through their transformations to identify the actual matching corner points. In the end, the most optimal rotation and translation parameters are estimated from the

transformation of matched corner points that offer the maximum overlap of both models. In addition, this technique also addressed the first research question (RQ 1) as it allows the application of a BIM model as an as-planned model and details the process of extracting lossless geometrical information to develop the respective 3D model using the IFC schema.

The method was also tested with numerous datasets having different geometries and it successfully validated the novel approach for registration. Results confirmed the method's high degree of precision, largely because it was possible to identify multiple matching corner points from which the most precise transformation parameter is estimated. The technique also proved to be capable of registering as-built scans of under-construction buildings with their BIM models with the exception that the models must have distinct corner points.

Chapter 3 also compares the corner point-based registration method to the plane-based method which is presented in Chapter 2. It is pertinent to mention here that both registration methods are accurate as their dependence on plane segments reduces their sensitivity to noise and outliers, however, the corner point-based method is slightly more accurate. Similarly, both methods also detect the matching plane segments leading towards the identification of the corresponding building components, eventually assisting their individual inspection during progress monitoring. Furthermore, the application of both methods in partially constructed building structures is also successful, provided some boundary conditions are met. The plane-based method requires the presence of at least three plane segments in distinct directions in the as-built and the surfaces of plane segments corresponding to their matching plane segments in the as-planned model. The corner point-based method demands at least two corner points with one point located at the asymmetric position should be present in the as-built scan for matching, hence, requires the presence of six plane segments in total.

In summary, the plane-based method is better suited for datasets having scan models that have a limited number of structural components, even though the corner point-based method is relatively more accurate. Chapters 2 and 3 addressed the second research question (RQ 2) by introducing the two successful techniques tailored for under-construction building structures.

Chapter 4 deals with the core phase of model-based assessment which involves the structural comparison of the as-built scan and BIM model to determine the as-built completion of the building. The overall comparison process is extensively analyzed in terms of construction progress monitoring to identify inaccuracies. Consequently, numerous improvements are introduced with the aim of increasing the overall accuracy without using external input. Initially, it employs the semantic information from BIM to perform the reasoning measures based on component sequencing and then performs in-depth detection analysis on the surfaces of models. The detection

analysis exploits the ray-tracing technique in combination with BIM geometrical information to develop a revised as-planned model for suitable comparison and then classify its surfaces according to the possible occlusion in the as-built scan. In the end, the as-built scan is compared with the classified revised as-planned model while reducing the effects of different errors along with the coverage information to precisely detect the exposed as-built surface. The approach measures the completion ratios of each building component, and then based on their weightage average according to their surface areas, it computes the overall completion ratio of the building.

This approach is tested successfully with different datasets, demonstrating its precise detection of as-built surfaces. It not only determined their accurate completion ratios but also the percentage of surfaces that were exposed to the data acquisition instrument have been quantified. The information about how much the surface of each building component can be scanned and how much of that scanned surface has been actually built enables the better realization of as-built progress. Apart from that, the overall completion ratios of those building components whose surfaces are not fully scanned, are also estimated by providing a range of predicted completion parameters including projected, minimum, and maximum values. This improved comparison process with significant advancements not only estimates the accurate completion ratios but also provides additional parameters that give valuable insights and a comprehensive understanding of as-built progress, surpassing the limitation of traditional comparison. This chapter particularly addressed the third research question (RQ 3) by exploring the challenge in the comparison phase and improving the accuracy of comparison for reliable construction progress monitoring.

The estimation of progress information and then performing it exchange in an automated way is presented in Chapter 5. This chapter is an effort to fully realize the potential of BIM for automated construction progress monitoring by allowing the effective and standardized exchange of progress information from construction sites to stakeholders. A four-step framework is presented that estimates the progress information, including the time-related schedule, cost, and other non-standard information such as inspection notes, particular dates, construction comments, etc., and makes use of the BIM model to update them in a structurally organized way. The framework utilizes a task-based approach in accordance with the latest IFC4.x schema to integrate the relevant IFC entities into the BIM model to accommodate the different types of progress information. Initially, the relevant entities are integrated into the BIM model according to the progress information, and then their planned values are enriched in the second stage. The third stage updates the actual values and the last stage enables the reporting of all the information in a user-friendly way accompanied with the additional progress indicators.

The method was tested with several BIM models and it successfully performed the automated exchange of as-planned and as-built progress information by incorporating the related native and non-native IFC entities in a standardized way. The automated method without any reliance on third-party commercial software created the IFC entities, estimated their progress parameters, and updated the existing entities while adhering to the IFC hierarchical structure. The accessibility of information in updated IFC-based BIM was also validated through the IFC-compatible program as well as the external IFC-based application. The method not only performed the updating of progress information but also efficiently retrieved them for progress reporting. For progress monitoring visualization, the models were also color-coded according to the completion ratios of their building components. Furthermore, a web-based application was also developed which presents overall progress information of buildings eventually to practically enable effective reporting and visualization using the only IFC-based BIM model. The formulation of a standard framework for automated updating and reporting of progress information from the construction site represents an accomplishment of a crucial milestone in construction monitoring using model-based assessment. This chapter completely addressed the last research question (RQ 4) by utilizing the BIM model as an information exchange tool with the capability to estimate and integrate different types of progress information.

To address the traditional manual progress monitoring methods at construction sites, which are inaccurate, time-consuming, and labor-intensive, this dissertation facilitates automated construction progress monitoring by providing significant improvements across all major phases of the model-based assessment method. It introduced the fully automated and precise registration techniques to achieve the alignment of models, improved the traditional comparison process to accurately estimate the as-built completion of the building and provide better valuable insights about the as-built with supplementary information, and developed an automated framework that supports the estimation and exchange of progress information. On top of that, the research utilizes a consistent BIM model throughout each phase to facilitate automation in model-based assessment while providing an outline for integration, updating, and retrieval of progress information. Improving the automated construction progress monitoring process can result in considerable savings in both cost and time for the construction industry, leading to improved efficiency and productivity.

These improvements and breakthroughs signal a meaningful advancement toward the practicality of automating progress monitoring in the construction industry, however, there is still a long way to go. The results of this dissertation open the door for further advancements in construction progress monitoring which will ultimately result in improved efficiency and better decision-making in the construction sector.

## 6.2 Discussion

### 6.2.1 Boundaries and Limitations

Efficient construction progress monitoring of buildings entails addressing a wide range of challenges. Therefore, this research domain is quite extensive. It is important to realize that the present study does not claim to solve all of these issues. This section discusses the main limitations of the proposed solutions.

The registration methods, as detailed in Chapters 2 and 3, are dependent on plane segments. The strategy of these methods is designed to make use of the orthogonal geometry of most building structures having the dominant planar features. However, it is imperative to acknowledge that there are some limitations associated as well due to this dependency which should also be considered. For example, these methods may fail if the building models do not have enough plane segments to be extracted which is possible when the building structure exhibits a non-planar or curved structural design. Similarly, the methods also require that the extracted plane segments should have distinct directions, and failure to this requirement is possible if all the extracted planes are parallel with no distinct direction. Apart from that, building models should not be completely symmetrical to each other otherwise the methods may fail due to difficulties in identifying the matching segments. For example, if rooms located on different floors of a building have symmetrical designs, registration may not be able to accurately identify the corresponding room in the BIM model based on a scan point cloud. However, this challenge can be addressed through necessary geo-referencing, specifying the floor information from which the scan was acquired. The geo-referencing data can provide information about the location of the scan model, which can later be used to differentiate the actual as-built part of the building from its symmetrical counterparts. In the future, it is planned to integrate the additional semantic information including the geo-referencing data to further increase the applicability of the proposed methods.

It is worth mentioning here that the proposed method identifies the building components requiring scanning as well as its exact non-scanned surface, as detailed in Chapter 4. However, it does not give any location information, including the viewpoint and optimal scanning location, for data acquisition, which is another broad research domain. Similarly, the current study doesn't address the quality monitoring. Consequently, if an as-built component is not constructed in its planned location, the proposed method will not be able to perform its surface comparison. In this particular situation, there will be no progress update, which will eventually alert the management to investigate the issue.

Although the current research work covers a large research area for progress monitoring using model-based assessment, however, there are still some challenges that need to be addressed. The first area is the exploration of the planar segmentation technique as the proposed registration methods are dependent on



that. The new segmentation techniques should be developed in context to progress monitoring taking into account the various errors present in point cloud data acquisition, inherent to construction environments.

Furthermore, the scalability of the proposed technique is a critical aspect to consider, especially when dealing with datasets featuring larger models. The detailed analysis of time efficiency conducted in this study sheds light on the significant impact of voxel size, the number of plane segments, and IFC elements in models, as well as the iterative nature of the methodology on computation time. The finding suggests that as datasets grow in size or complexity, the method's ability to handle them efficiently may be challenged. Hence, scalability may become a concern when dealing with large models or datasets with extensive plane segments. Therefore, future efforts aim to address this concern by optimizing the computational processes to minimize processing time. By doing so, we aim to enhance the method's suitability for broader applications, even in scenarios involving larger datasets and more complex project requirements.

It is pertinent to mention here that when discussing the minimum requirements for model representation, the current research requires that both models effectively represent the surface geometry. BIM, being used to accurately represent the design model of the building, can be sufficiently achieved with LOD 300. This level of detail is practically attainable, especially since progress monitoring occurs during the construction phase when the BIM model design is supposed to be developed up to LOD 400. Correspondingly, the as-built point cloud should also be having a quality that it must adequately represent the as-built surface for subsequent processing in registration and as-built detection. The current research mainly concentrates on employing the as-built point clouds obtained through laser scanning, as they tend to provide precise data. However, it is essential to delve deeper into the use of lower-quality point clouds obtained from image-based reconstruction or other methods. This investigation, planned for the future is vital for understanding the potential limitations and challenges in utilizing diverse point cloud data sources, particularly within Building Information Modeling (BIM) applications.

In practical terms, the research is structured around progress monitoring, an iterative method used to measure progress after following specific events in construction, such as completion or planned completion of a building component, or if there is a requirement for progress update after a certain time. The current study utilized a systematic approach to integrate this procedure into practical application, as detailed in the methodologies of chapters 4 and 5.

The research study divides the entire building based on its individual components to facilitate its accurate progress monitoring, aligning with the construction industry practices. It prioritizes building components based on their proximity to the expected completion date, a defined additional parameter, ensuring timely data collection.

When the expected completion date of a specific building component is reached, a call for data collection is initiated for that component. This involves performing a 3D scan of the component's current state, ensuring comprehensive coverage of its surface. If the initial scan does not adequately capture the as-built surface, additional scanning sessions may be required, focusing on surfaces where data collection was insufficient. Subsequently, the scanned surface is registered (chapters 2 and 3) and compared (chapter 4) with its corresponding BIM model to accurately measure the component's as-built completion status. Time-related and other progress information is then measured based on the completion status and later updated within the model, as detailed in Chapter 5. If the component is not completed, the expected completion date is re-calculated to determine when the component is supposed to be completed eventually to plan another scanning session. This iterative process continues until the building component achieves full completion, with overall progress monitoring concluding upon the completion of all components.

Additionally, the approach utilized in the current research study is highly flexible as it allows the processing of the entire point cloud against the BIM model to measure progress comprehensively. In this scenario, the as-built completion of all building components is estimated simultaneously.

## 6.2.2 Directions for Future Research

### *Improvement within scope*

In the comparison phase, the current research performed the detection analysis in which classification is performed according to occluded surfaces due to two cases. The first case involves occlusion caused by the presence of other building components, while the second case involves occlusion arising due to external objects placed at the scene. The current study presents and implements the solutions for identifying occluded surfaces for both cases for simulated datasets. For real-life datasets, only the solution for the first case was applied, but the second case was not implemented. The underlying reason is that during the testing it was found that the real-life datasets are complex enough for the identification of external objects placed on site. The proposed solution required some maturity and advancement, which in turn required a great deal of research. Therefore, it is planned to work in this particular case in the future to further develop it for practical application in real-life datasets for complete identification of all possible occluded surfaces.

The current doctoral research improves the construction progress monitoring by geometry analyzing the 3D as-built point cloud and BIM model in which the as-built is obtained after laser scanning the site. Although, the as-built model obtained from the image-based reconstructed 3D point cloud through photogrammetry can also be utilized in the current study, however, the accuracy of results may be affected as the laser-scanned as-built model is relatively more precise but lacks color information. In the future, another study will be performed which investigates the current

approaches implemented with image-based reconstructed as-built which aims to utilize their color information as well to further optimize the process.

Currently, there is an unavailability of standardized data for testing the model-based assessment techniques. It is planned to address this limitation in the future for the establishment of comprehensive standardized datasets for benchmarking purposes. The focus is to arrange the datasets that encompass diverse building models, including scans and their corresponding BIM models, augmented with essential planning information, particularly time-related data for components and their construction sequences. Efforts will be directed towards the collaborative endeavors to curate, share, and expand datasets, eventually to facilitate robust evaluations and advancements in model-based assessment techniques.

The detection analysis proposed in Chapter 5 identifies the building component whose as-built completion has to be determined and then classifies its surfaces based on exposure to the data acquisition equipment through simulation. This simulation can be further leveraged to estimate the optimum location for data acquisition based on their non-exposed surface. A potential approach involves dividing the floor into different zones for data acquisition and then measuring the exposure of each zone according to the classified non-exposed surfaces. Eventually, this process aims to determine the optimum zone with the most favorable location for accurate data collection. A conceptual demonstration of this approach is also presented in Appendix 4.

Chapter 6 of this dissertation introduced a comprehensive methodology for exchanging progress information using the collaborative and standardized open file format of IFC. This approach addressed the significant gap, as there was previously no solution available that presented how the IFC-based BIM model can be natively leveraged to perform the progress updating without relying on commercial software support. The proposed method effectively demonstrated how the progress information could be natively stored, and retrieved natively without requiring the support of any commercial software. However, integrating with the software poses a challenge due to the inherent mapping of data to their internal data structures, hindering interoperability. While some commercial software now supports exporting models as IFC, this process often involves conversion and can result in information loss. To overcome this limitation, future research should focus on accurately mapping data using linked data technology. Leveraging linked data technologies with standardized ontologies presents a promising avenue for achieving seamless integration, capitalizing on the interoperable nature of information in the IFC schema.

#### *New research directions*

Current research focuses mainly on building structures for progress monitoring. Future research will focus on other infrastructures such as roads, bridges, water

supply, etc. for their progress monitoring. In this respect, the approaches of all three phases will be modified to take into account their different geometric structure. Similarly, BIM information extraction approaches will be adapted according to the IFC hierarchy of these new structures.

There is another novel method planned for the future to perform the registration. The method involves the identification of potential matching plane components of building through machine learning. After that, the evaluation approaches and their combinations described in the current study, particularly in Chapters 2 and 3, can be exploited to find the confirmed matches of components which can be further processed to find registration. This new method requires the implementation of machine learning to identify the 3D planar objects from real-life as-built scans and computer-generated as-planned models of buildings and therefore presents unique challenges.

The current research already covers a wide spectrum within the field of construction progress monitoring and introduced several innovative methodologies. These methodologies not only enhance the scope of current research work but also benefit the related research areas, particularly in the field of data acquisition. Appendix 5 highlights the potential extension of the current research to contribute to the advancement of data acquisition research areas, thereby demonstrating the versatility and applicability of the methodologies developed herein. In the future, it is planned to integrate the data acquisition research with the current BIM-based study, with a specific focus on identifying the optimal data acquisition locations within construction constraints. This integration aims to enhance the efficacy and precision of data acquisition processes, ultimately contributing to more informed decision-making in construction projects.

In addition, it is also planned in the future to carry out detailed research with a new approach that performs the construction progress monitoring by using 2D images instead of the laser-scanned 3D point cloud. The reconstructed 3D point cloud obtained from the 2D images may not be as accurate as the laser-scanned point cloud, but it contains additional color information that can be used. Furthermore, the mass availability of mobile phones in today's working environment makes it quite convenient for construction workers to use them to capture images, as opposed to laser scanners which are very expensive and require adequate training to operate. The newly proposed technique will explore the photogrammetry techniques in combination with current registration approaches to register the images into the corresponding BIM model to capture the as-built surfaces. This technique will perform the registration and comparison simultaneously, instead of processing them in stages, and can facilitate the progress monitoring process with the captured images at the site.

In the future, a key focus will be on real-time implementation of the proposed methodologies. This involves the development of algorithms and technologies capable of processing and analyzing data in real-time by increasing the time efficiency thereby enabling continuous monitoring of construction progress. Achieving real-time implementation will not only enhance the efficiency of progress monitoring but also provide stakeholders with timely insights, facilitating prompt decision-making and intervention when necessary.

The future plans also include the further enhancement of the developed web-based application (mentioned in Chapter 5) by integrating it with other useful progress indicators and important information to practically normalize its utilization at construction sites. In addition, dedicated applications for hand-held smartphones can also be developed. The main aim improve the progress monitoring process using the web-based real-time application that effectively fulfills the needs of construction staff adequately and gives more insights for decision-making.



---

# 7

---

## 7. APPENDICES

# Appendix 1: Corner-Point Based Registration Workflow

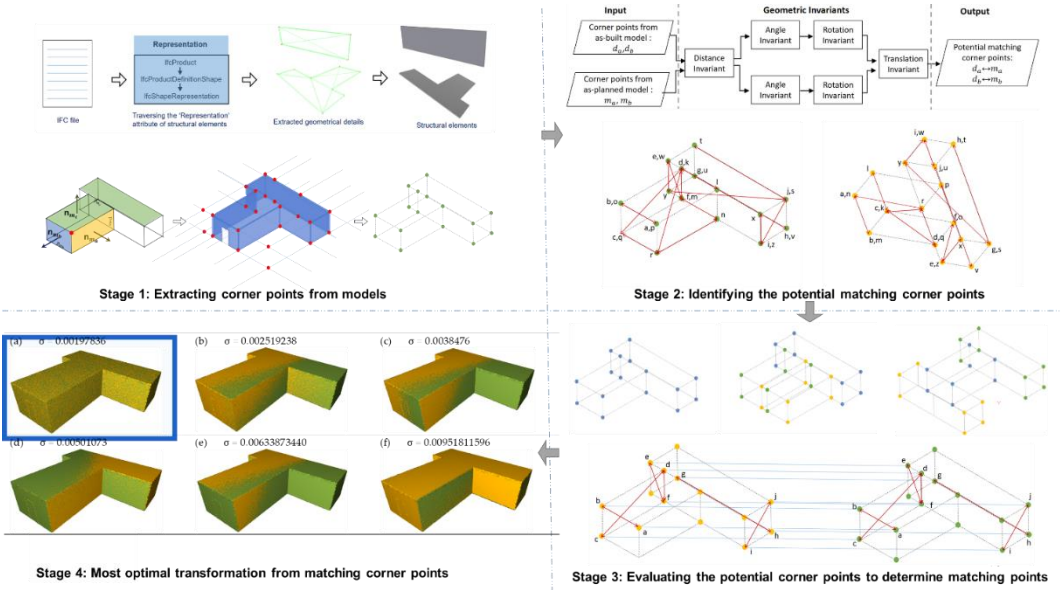
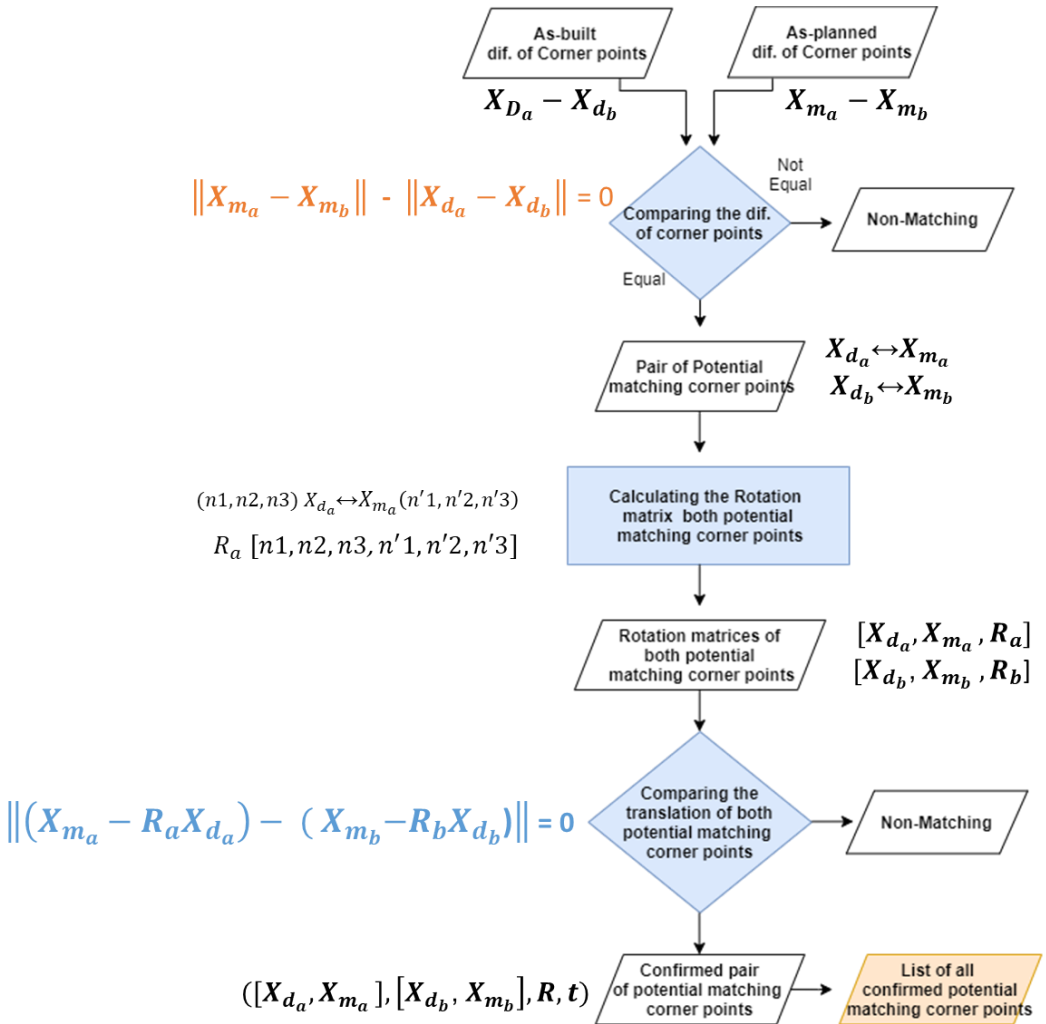


Figure 7.1. Overall workflow of Corner-point based registration method detailed in Chapter 3.



## Appendix 2: Corner Point Matching Process Flowchart



*Figure 7.2.* The Flowchart showing the process of identifying potential matches between pairs of corner points from as-built and as-planned models using various geometric invariants.

### Appendix 3: Corner Point Matching with Distance and Translation Invariants

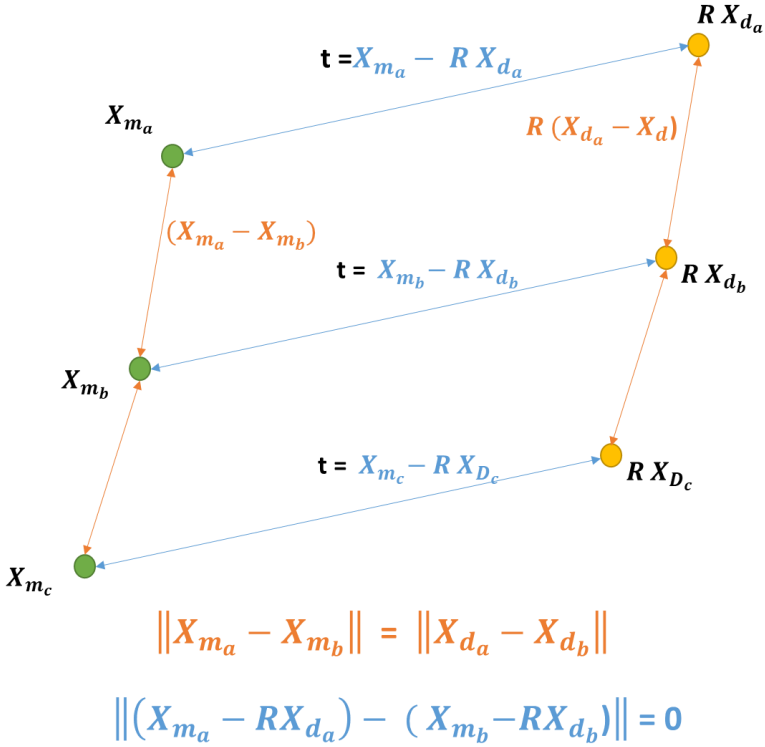
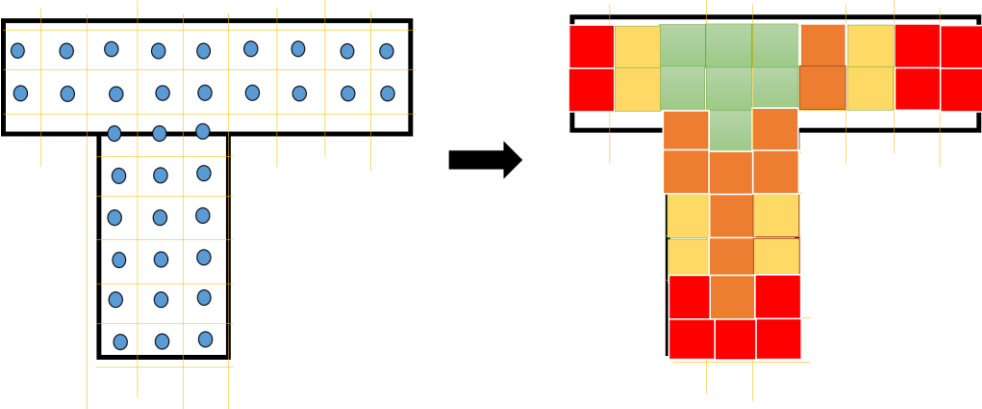


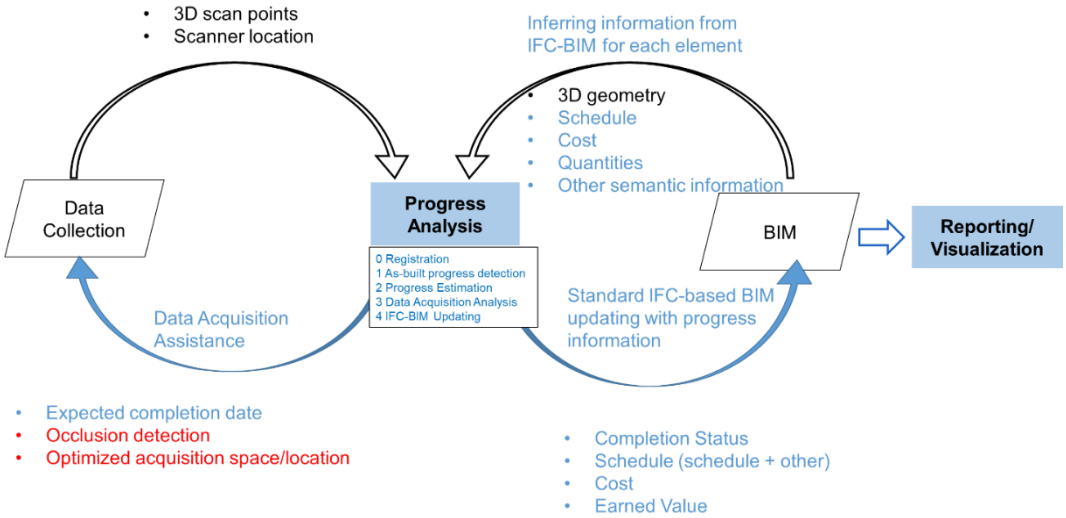
Figure 7.3. Demonstration of distance and translation invariants for matching corner points in as-built (highlighted in yellow) and as-planned (highlighted in green) models.

# Appendix 4: A Conceptual Illustration of Optimal Grid-Based Data Acquisition Analysis



*Figure 7.4.* A conceptual illustration showing the partitioning of a plane space of model into uniform grids, followed by the detection analysis of the grids with the eventual aim to identify the optimal location for data acquisition.

## Appendix 5: Graphical Representation of Extended Research Methodologies



*Figure 7.5.* Graphical representation highlighting the potential extension of current research methodologies with data acquisition domain, highlighting key parameters utilized in the current study (highlighted in blue) and those critical for future investigations (highlighted in red).

## Appendix 6: UML Representation of IFC Schema for IfcSlab, IfcWall, and IfcTask

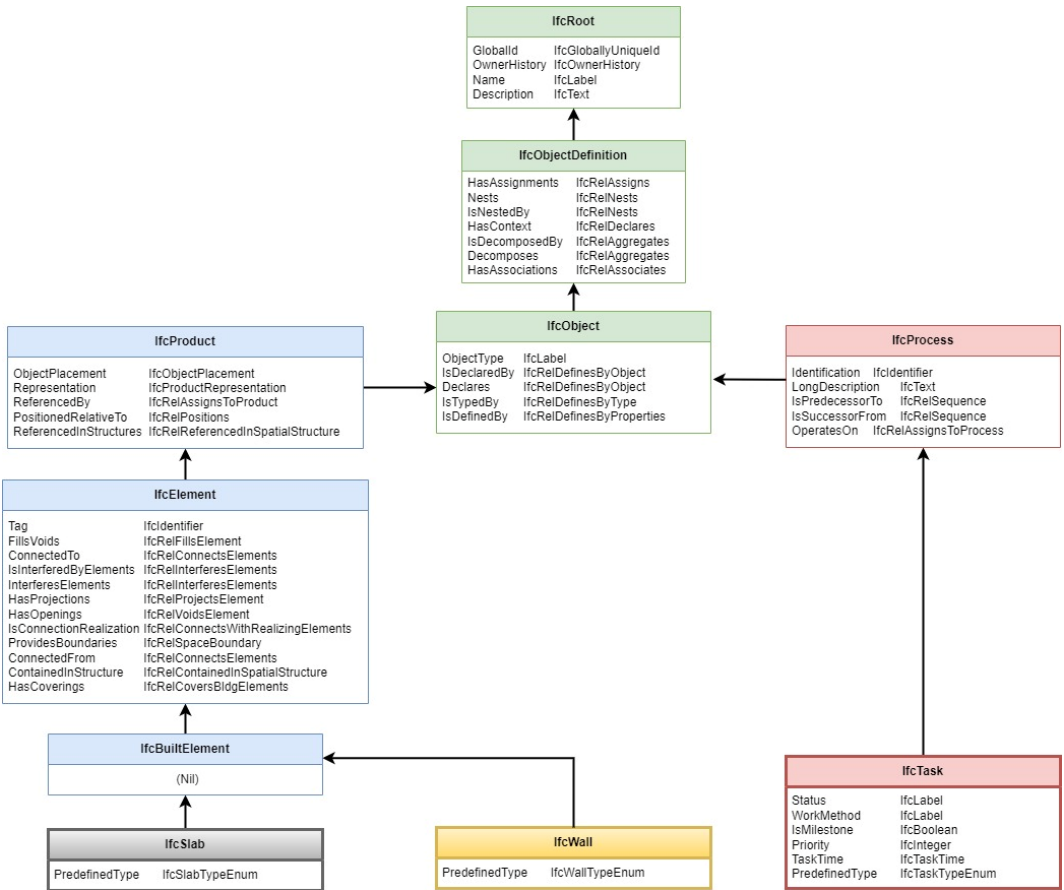


Figure 7.6. UML representation of the IFC schema for IfcSlab, IfcWall, and IfcTask.

## Appendix 7: Plane-Based Registration Methodology Algorithm

---

**Algorithm 7.1:** Methodology of plane-based registration

---

**Input:**

*As\_builtModel*: 3D geometrical as-built Model

*As\_plannedModel*: 3D geometrical as-planned Model

**Output:**

$R_o, T_o$ : Transformation parameters to register the as-built and as-planned models

- 1  $PSegments\_AsBuilt\_list = PlaneSegmentation(As\_builtModel)$
  - 2  $PSegments\_AsPlanned\_list = PlaneSegmentation(As\_plannedModel)$
  - 3  $Cl\_PSegments\_AsBuilt = ClusterSegment(PSegments\_AsBuilt\_list)$
  - 4  $Cl\_PSegments\_AsPlanned = ClusterSegment(PSegments\_AsPlanned\_list)$
  - 5  $possible\_R\_all = CalculatePossibleRotation(Cl\_PSegments\_AsBuilt, Cl\_PSegments\_AsPlanned)$
  - 6  $R_o, T_o = ComputeMostLikelyTransformation(possible\_R\_all)$
  - 7 **return**  $R_o, T_o$
-

## Appendix 8: Parallel Plane Segments Clustering Algorithm

---

**Algorithm 7.2: Clustering Parallel Plane Segments**

---

**Input:**

*PSegments\_list*: List of plane segments

*angle\_threshold*: Threshold angle for considering plane segments as parallel

**Output:**

*clustered\_segments\_list*: List of clustered parallel plane

```
1  for each plane_segment in PSegments_list do
2      cluster_total = 0
3      if clustered_segments_list != 0 then
4          for each existing_cluster in clustered_segments_list do
5              angle = ComputeAngle(plane_segment, existing_cluster)
6              if angle < angle_threshold then
7                  cluster_total = cluster_total + 1
8              end if
9          end for
10     end if
11     if cluster_total == 0 then
12         Add plane_segment to clustered_segments_list
13     end if
14 end for
15 return clustered_segments_list
```

---

## Appendix 9: Creating Corner points from Plane Segments Algorithm

---

**Algorithm 7.3:** Create Corner points from plane segments

---

**Input:**

*vab1*: Coefficients of the first plane segment ( $a1, b1, c1, d1$ )

*vab2*: Coefficients of the second plane segment ( $a2, b2, c2, d2$ )

*vab3*: Coefficients of the third plane segment ( $a3, b3, c3, d3$ )

**Output:**

CornerPoint: Computed corner point coordinates ( $x, y, z$ )

- 1 Unpack the coefficients from *vab1*, *vab2*, and *vab3*:  
 $(a1, b1, c1, d1) = vab1$   
 $(a2, b2, c2, d2) = vab2$   
 $(a3, b3, c3, d3) = vab3$
  - 2 Create 'matrix A' using the coefficients extracted from the plane segments:  
$$A = \begin{bmatrix} a1, & b1, & c1, \\ a2, & b2, & c2, \end{bmatrix}$$
  - 3 Calculate the inverse of 'matrix A' and store it as 'in\_matrixA':  
 $in\_matrixA = Inverse(A)$
  - 4 Create 'matrix B' using the negative of the coefficients  $d1, d2$ , and  $d3$ :  
$$matrix\_B = \begin{bmatrix} [-d1], \\ [-d2], \\ [-d3] \end{bmatrix}$$
  - 5 Compute the dot product of *in\_matrixA* and *matrix\_B* to obtain the corner point matrix:  $corner\_matrix = DotProduct(in\_matrixA, matrix\_B)$
  - 6 Extract the corner point coordinates ( $x, y, z$ ) from the 'corner\_matrix'
-



## Appendix 10: Corner Point Filtering Algorithm

---

**Algorithm 7.4:** Filtering the actual corner points

---

**Input:**

*list\_cornerpoints*: List of corner points with potential duplicates

*threshold*: Threshold distance for considering points near the surface

**Output:**

*verified\_list\_cornerpoints*: List of filtered corner points lying near the surface

```
1  for each corner_point in list_cornerpoints do
2      Extract the coordinates of the corner_point (c_point_coordinates).
3      Extract the corresponding parent plane segments of corner_point →
      (p_segment1, p_segment2, p_segment3).
4      Compute the distance between c_point_coordinates & p_segment1 →
      dist_segment1.
5      Compute the distance between c_point_coordinates & p_segment2 →
      dist_segment2.
6      Compute the distance between c_point_coordinates & p_segment3 →
      dist_segment3.
7      if dist_segment1 < threshold and dist_segment2 < threshold and
      dist_segment3 < threshold then
8          | Add corner_point to verified_list_cornerpoints
9      end if
10 end for
11 return verified_list_cornerpoints
```

---

## Appendix 11: Geometric Invariants-Based Corner Point Matching Algorithm

**Algorithm 7.5:** Identifying potential matching corner points through geometric invariants

**Input:**

*corner\_points\_asbuilt*: List of corner points from the as-built model  
*corner\_points\_asplanned*: List of corner points from the as-planned model  
*all\_thresholds*: Dictionary containing all threshold values for geometric invariants

**Output:**

*p\_matched\_corner\_pairs\_list*: List of potential matching corner point pairs from

```
1  for iterate from 0 to number of iterations do
2    [d_a, d_b] = RandomlySelect(corner_points_asbuilt)
3    [m_a, m_b] = RandomlySelect(corner_points_asplanned)
4    threshold_distance, threshold_angle, threshold_rotation, threshold_translation =
      all_thresholds ['distance', 'angle', 'rotation', 'translation']
5    distance = ComputeDistance([d_a, d_b], [m_a, m_b])
6    if distance < threshold_distance then
7      angle_a = ComputeAngle([d_a, m_a])
8      angle_b = ComputeAngle([d_b, m_b])
9      if angle_a < threshold_angle and angle_b < threshold_angle then
10       rotation_invariant_a = CheckRotationInvariant([d_a, m_a], threshold_rotation)
11       rotation_invariant_b = CheckRotationInvariant([d_b, m_b], threshold_rotation)
12       if rotation_invariant_a = True and rotation_invariant_b = True then
13         translation_invariant = CheckTranslationInvariant([d_a, d_b], [m_a,
14           m_b], threshold_translation)
15         if translation_invariant = True then
16           Add ([d_a, m_a], [d_b, m_b]) to p_matched_corner_pairs_list
17         end if
18       end if
19     end if
20 end for
21 return p_matched_corner_pairs_list
```